Black Holes and Chaos

Gustavo Joaquin Turiaci

A Dissertation

Presented to the Faculty

of Princeton University

in Candidacy for the Degree

of Doctor of Philosophy

Recommended for Acceptance

by the Department of

Physics

Adviser: Professor Herman Verlinde

September 2018

Abstract

We study some aspects of quantum chaos and its relation to scattering near the black hole event horizon, in the context of gauge/gravity dualities. Chaos is an important ingredient related to the onset of thermalization. A signal of chaos is given by the behavior of out-of-time-ordered correlators (OTOC) and exponential growth of commutators. In the gravity side this growth is controlled by a near-horizon high energy scattering, semiclassically described by a shockwave geometry.

A holographic quantum mechanical toy model was developed by Kitaev, the SYK model, consisting of a large number of interacting Majorana fermions without a quasi-particle description. At low temperatures, this system has an emergent conformal symmetry. The thermodynamics and chaos of the model are described by the Schwarzian mode associated to the pattern of breaking of the conformal symmetry, which is also equivalent to the boundary gravitons of dilaton-gravity in 2D. We solve the physics of this mode exactly, including the computation of OTOC. We also study its semiclassical limit and find how the shockwave S-matrix describing near-horizon scattering emerges.

We propose and study a natural extension of the SYK model to two dimensions that presents holographic behavior described by gravity in three dimensions. We also study a natural two-dimensional generalization of the Schwarzian mode, which controls the chaos exponent of the system.

Finally, we study a generalization of the shockwave geometry to include quantum interference effects. This can be used to obtain interesting bounds for general CFTs in higher dimensions.

Acknowledgements

First of all, I thank my advisor Herman Verlinde for his patience and generosity with his time. I would like to thank him for helping me discover my way of doing research. He always had a very inspiring way to approach physics and I enjoyed my experience working with him. I also appreciate countless discussions with Juan Maldacena and I am thankful to him for helpful advice and sharing his insights.

During my grad school years I worked with people from which I learned a lot. Among them, I thank postdocs and other graduate students: Ho Tat Lam, Bruno Le Floch, Aitor Lewkowycz, Aaron Levy, Thomas Mertens, Alexander Zhiboedov, and especially Clay Cordova. Besides doing research, during the first years of my studies I've taken classes from great professors that I'd like to acknowledge: Igor Klebanov, Paul Langacker and Bob Austin.

Before coming to Princeton I've learned a lot from professors at the University of Buenos Aires during my undergraduate studies: Esteban Calzetta, Fernando Lombardo, Diego Mazzitelli, Juan Pablo Paz. Special thanks to my friends from Argentina: Pablo Alcain, Belen Farias, Federico Lago, Rodrigo Lugones, Quimey Pears Stefano that made me feel at home every time I went back.

I thank also all the amazing friends I've met in Princeton that have made my experience here so exciting and unique: Debayan Mitra, Mykola Dedushenko, Aitor Lewkowycz and Fela Bagur, Will Coulton, Zach Sethna, Farzan Beroz, Nele Callebaut, Shai Chester, Kenan Diab, Josh Hardenbrook, Luca Iliesiu, Christian Jepsen, Vladimir Kirilin, Pablo Mosteiro, Vadim Munirov, Seth Olsen, Grisha Tarnopolsky and Jose Zamalloa.

I am lucky to have a very supportive family who was always there when I needed them. My mom Susana taught me how to be the best version of myself, always understood me and without her I wouldn't be able to approach my goals. Gracias, mama. My older sister Romina was a good example while growing up, she was kind

to me and she is the best sister I would ever wish to have. Gracias, Romina. Olya is not only my wife but also my best friend, I feel infinitely happier since she became a part of my life. Thank you, Olya. Our family friend Nancy who always encouraged me to be better. Gracias, Nancy.

To my mother Susana and the memory

of my grandfather Mercurio Fiasche.

Contents

List of Tables

List of Figures

Chapter 1

Introduction

Most of modern theoretical physics is built on two frameworks. One is quantum mechanics (QM). Its relativistic version, quantum field theory (QFT) describes physics from the elementary particles appearing in the Standard Model to condensed matter systems. Even though it has not been tested, it is believed that the principles of quantum mechanics are valid throughout *all* scales. The second theory is General Relativity (GR). This describes gravitational interactions which become relevant at the largest scales, from planetary to cosmological.

Both theories have been extremely successful within their range of applicability, but they have resisted a unification of their principles. From a theoretical front, naive attempts to combine the two theories have failed (we will give a concrete example below). Evidently, finding the principles from which gravity and QM emerge requires new ideas. One of the most widespread advances lately has been the idea of viewing quantum mechanics and gravity not as independent phenomena but as different equivalent descriptions of the same physics. This is one of the main lessons that String Theory has taught us through dualities.

Even though these discussions are in theory well motivated one could ask why should we even care about finding such a theory of quantum gravity, if in the end we

cannot see these regimes together in a lab. Consider for example the Large Hadron Collider (LHC). Processes involving elementary particles where QFT is relevant are being measured at energies of the order of 10^4 GeV. To observe quantum gravitational effects we would need to go to 10^{19} GeV which seems ridiculous considering the status of current technology. Nevertheless nature has given us such a high energy accelerator for free: the Big Bang. If we trace back the cosmological evolution, due to its expansion, early enough in time relevant energies would be so high that combined effects of quantum mechanics and gravity become unavoidable. This is a very interesting problem since it would give an understanding of the origin of the universe. Presumably this might also shed some light on other issues like the nature of dark matter or dark energy.

This is a very complicated problem to solve. We will focus instead on another important problem where strong gravitational effects are relevant: black holes. These are objects so massive and dense that nothing, not even light, can escape them (classically) beyond their event horizon. This is a fruitful example where one can apply a naive combination of classical GR and QM concepts that lead to a contradiction. This was done by mainly Bekenstein and Hawking. According to Bekenstein [1] black holes should be thought of as carrying an entropy proportional to the area of its event horizon

$$S_{\rm BH} = \frac{A}{4L_P^2}, \tag{1.0.1}$$

where $L_P = \sqrt{G_N\hbar/c^3} \approx 10^{-35}$m stands for the Planck length. This is a huge degeneracy for objects which classically have 'no hair'. To give some rough estimates, a black hole of the mass of the sun ($\approx 10^{30}$kg) would have to be compressed to a radius of 3km to become a black hole. In this case its Bekenstein entropy would be around $S \sim 10^{77}$. (This is 20 orders of magnitude larger that the sun's actual internal entropy!)

The nature of this entropy was clarified (to some extent) when Hawking discovered that black holes emit thermal radiation [2] with a temperature dependent on the black hole total mass M given by

$$T_H = T_{\rm Pl}\frac{M_{\rm Pl}}{8\pi M}, \tag{1.0.2}$$

where $M_{\rm Pl} = \sqrt{\hbar c/G_N} \sim 10^{-8}$kg and $T_{\rm Pl} = \sqrt{\hbar c^5/(k_B^2 G_N)} \sim 10^{32}$K are the Planck mass and temperature respectively. For the case of the sun mass black hole $M/M_{\rm Pl} \sim 10^{38}$ this is extremely small $10^{-8}K$. This is not necessarily an issue, the universe is full of black holes and it might be possible to find them small enough to give an appreciable effect. Hawking derived this effect from studying quantum field in the black hole background. Therefore when QM and GR are put together, even black holes evaporate.

Black holes should be thought as a statistical system with a really large number of microstates and a temperature of evaporation. A serious issue was realized later by Hawking [3]. Quantum evolution is unitary, meaning information cannot be destroyed. Black hole evaporation is in a clear conflict with unitarity since the post-evaporation thermal radiation carries no information about the initial matter that created the black hole. This is called the information paradox [3]. It is believed that an answer to this question will require an understanding of the basic principles of quantum gravity. For example, one of the successes of String Theory was a microscopic understanding of the black hole entropy [4], which eventually led to a proposal for a non-perturbative definition of quantum gravity on spaces with negative cosmological constant, by means of gauge/gravity dualities [5].

In this thesis we will study several aspects of black hole physics focusing on the region near their event horizon. This was studied early on by Dray and 't Hooft [6, 7] and recently led to a connection between black holes and quantum chaos by studying near-horizon scattering in the context of gauge/gravity dualities. If one takes a generic CFT a natural question to ask is whether its gravitational dual supports black holes

or not. This is an important question which is not easy to answer, since simple theories that are solvable do not support black holes, while theories that do are very complicated (we will see later a quantum mechanical toy model that is an exception of this rule). As we will review below, quantum chaos is believed to give an answer to this question. By studying the growth of commutators one can diagnose whether the bulk contains an event horizon or not. The punch line is that the Lyapunov exponent is dual to the surface gravity at the horizon. In the rest of this chapter we will explain these ideas in more detail.

1.1 The S-matrix Ansatz

An important ingredient to study physics near the event horizon of a black hole is the shockwave solution studied by 't Hooft [6, 7]. This metric includes the backreaction produced by a high-energy relativistic particle. The idea of 't Hooft S-matrix ansatz is roughly the following. Particles moving close to the horizon get blue-shifted and generate a large backreaction that affects the Hawking quanta being detected at late times. Therefore it was believed that this would be an important aspect of black hole physics since (a very coarse-grained version of) the information of the infalling matter can be recovered from the Hawking radiation. In the next section we will analyze these ideas in the context of AdS/CFT, where this found a very precise interpretation as quantum chaos of the boundary CFT.

1.1.1 Shockwaves in Flat Space

Before moving on to black holes, let us begin with empty D-dimensional Minkowski space parametrized as $x = (t, y^1, \ldots, y^{D-2}, x^{D-1})$ with metric

$$ds^2_{\text{flat}} = 2dx^+dx^- + dy^2, \tag{1.1.1}$$

where $x^{\pm} = x^{D-1} \pm t$ are null coordinates, and we use the index $i = 1, \ldots, D-2$ to parametrize the coordinates y of transverse space. To simplify expressions we chose units for which $c = G_N = k_B = \hbar = 1$.

One can think about the shockwaves in the following way. We know the exact geometry of a particle of point-mass M at rest, the Schwarzschild black hole. A Lorentz transformation allows us to write a solution for a moving massive particle. Then we can take the limit of a large boost to obtain the shockwave geometry due to a high-energy relativistic particle propagating in flat space. This exact solution of Einsteins equations was discovered in 1971 by Aichelburg and Sexl [8]. The derivation outlined in this paragraph can be found in [6].

Another approach which is computationally simpler is to model the high-energy particle by a stress tensor localized in the worldline of the particle. For concreteness take

$$T_{++}^{\text{part.}} = 4P^{-}\delta^{D-2}(y)\delta(x^{+}). \tag{1.1.2}$$

This models a relativistic particle moving along $x^+ = 0$ with momentum P^- and localized in transverse space $y = 0$. One can then plug in this stress tensor in Einstein's equations derived from the action $S = \int \sqrt{g}R$, where R is the Ricci tensor. The metric is

$$ds^2 = ds^2_{\text{flat}} - 2f(y)\delta(x^+)(dx^+)^2, \tag{1.1.3}$$

where the function that appears on the last term is

$$f(y) = -P^{-}\frac{\kappa}{|y|^{D-4}}, \tag{1.1.4}$$

where κ is a (D-dependent) numerical constant which is not too important for our purposes. For the case $D = 4$ the power law decay becomes a logarithm. The important feature is the fact that this is proportional to the momentum of the particle. On these backgrounds Einstein's equations become linear in $f(y)$ and it is possible to

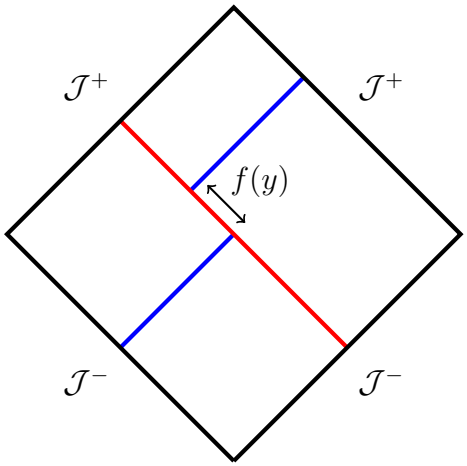

Figure 1.1: Penrose diagram of flat space. Null past and future infinity is denoted $\mathcal{J}^{\pm}$. A shockwave generated by a high energy particle (red line). The trajectory of a probe particle is shown in blue.

find *exact* solutions for an arbitrary mass distribution in transverse space. Moreover, this geometry is an exact solution even if higher derivative terms are added to the Einstein-Hilbert action [9].

To understand the Aichelburg-Sexl metric it is useful to analyze the equations of motion of probe particles moving in it. For either $x^+ < 0$ or $x^+ > 0$ the geometry is flat space and its geodesics are straight. Therefore the geometry is specified by what happens to a particle when it crosses the $x^+ = 0$ line. To answer this question we need to write down the equation of motion of a particle and analyze what happens near $x^+ = 0$. The effect is a shift, a time delay, along the x^- direction given by

$$\Delta x^- = f(y). \tag{1.1.5}$$

We show this in Figure 1.1. The red line denotes the high-energy particle backreacting on the geometry while the blue line denotes a low energy probe. Moreover the particle also gets refracted in the transverse direction as $\Delta \frac{dy^i}{dx^+}\big|_{x^+=0} = \partial^i f(y)$. This effect will not be too important in what follows but in general should be taken into account.

1.1.2 The black hole S-matrix

First we will generalize the shockwave metric to a black hole background. We will focus on the case of asymptotically flat space, leaving the case of negative cosmological constant (relevant for holography) for the next section.

We will focus in this section on the four-dimensional case. The metric of a static black hole found by Schwarzschild [10] is given by

$$ds^2_{\rm BH} = -\left(1-\frac{2M}{r}\right)dt^2 + \frac{dr^2}{1-\frac{2M}{r}} + r^2 d\Omega^2, \tag{1.1.6}$$

where Ω denotes the angular coordinates. This choice of coordinates describes observers outside of the black hole. Far away $r \gg M$ the metric becomes flat. We will refer to t and the energy associated to this choice of time as Schwarzchild time and energy. In terms of Kruskal coordinates $X^{\pm} \sim e^{r^\star \pm t}$, the metric becomes [1]

$$ds^2_{\rm BH} = \frac{32M^3 e^{-r/2M}}{r} dX^+ dX^- + r^2 d\Omega_2^2. \tag{1.1.7}$$

These coordinates are well defined across the horizon (at $X^{\pm}=0$) and can be extended to the extended wormhole geometry shown in Figure 1.2.

Now focus on an outgoing particle that exits the past horizon and moves very close to the future black hole horizon. Due to horizon blue-shift ($g_{tt} \to 0$ at the horizon) this particle will be highly boosted (with respect to an asymptotic observer) even if its energy is not too high when it reaches the boundary (an important example is a Hawking quanta for which $E \sim 1/M$). Following the discussion in the previous section we could imagine modeling this particle by a localized stress energy tensor

$$T^{\rm part.}_{--} = 4P^+ \delta^2(\Omega - \Omega')\delta(X^-), \tag{1.1.8}$$

[1] The radial coordinate used here is $r^\star = r + 2M\log|r-2M|$.

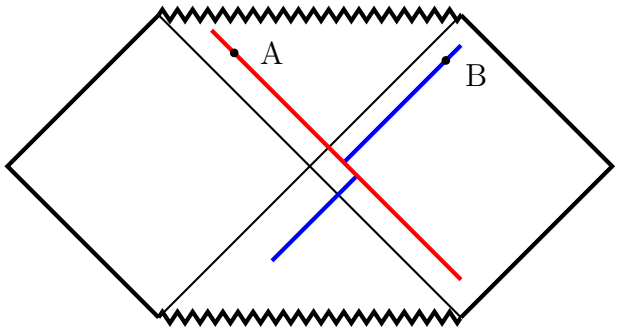

Figure 1.2: Penrose diagram of the extended Schwarzchild black hole. A shockwave generated by a high energy particle is shown by a red line (could correspond to infalling matter). The trajectory of a probe particle is shown in blue (describing a Hawking quanta for example).

where $\Omega \in S^2$ parametrizes transverse space, Ω' denotes the position of the particle, and P^+ denotes the Kruskal momentum of the particle. The geometry that this particle produces is very similar to the flat space case, namely

$$ds^2 = ds^2_{\rm BH} - \frac{32M^3 e^{-r/2M}}{r} f(\Omega)\delta(X^+)(dX^+)^2. \tag{1.1.9}$$

Similarly to the flat space case, this extra term generates a time delay on particles that cross $X^+ = 0$. The shift is still given by $\Delta X^- = f(\Omega)$. Nevertheless, the equation of motion for $f(\Omega)$ is modified from the flat space case due to the curvature of spacetime. Nevertheless the solution has the same features $f(\Omega) \sim P^- g(\Omega, \Omega')$, with g a universal function that depends on space-time dimension (for a spherical matter distribution it becomes a constant and eliminate refraction effects on transverse space).

This exact solution of Einstein's equations was found in 1984 by Dray and 't Hooft [6] (see also [11] and [12] for more details). We show a diagram of this geometry in Figure 1.2. Here we have considered a particle moving very close to the horizon. Dray and 't Hooft also found similar solutions with high energy particles moving far from the horizon, which involves gluing black hole geometries with different masses.

We are now in a position to describe 't Hooft's S-matrix Ansatz. Suppose we have a black hole which already formed and is slowly evaporating such that we can approximate the geometry by the Schwarzchild solution. At some time we throw matter to the black hole. How does this information escape?

In [6, 13] the authors gave an answer and proposed an S-matrix that describes how part of this information might come out. Consider a particle falling into a black hole at early times. Consider also a Hawking quanta that *if the matter particle had not been thrown* would be detected at a certain late time. As shown in Figure 1.2 these particles interact close to the black hole horizon if the time difference between throwing the particle and measuring the Hawking quanta Δt is large. This interaction occurs at very high energy. We can approximate the backreaction of these particles by shockwaves near the horizon (any other interaction will be presumably subleading). The interaction produces a time delay to the Hawking quanta

$$\Delta X^- \approx f(\Omega, \Omega') P^{\text{in}}(\Omega'). \tag{1.1.10}$$

For an arbitrary matter distribution one integrates over Ω'. By looking at the transformation between Kruskal and Schwarzchild frame, it is important to notice that this delay grows exponentially with the time difference between emission and detection Δt, namely

$$\Delta X \sim e^{2\pi T_H \Delta t}, \tag{1.1.11}$$

where T_H corresponds to the Hawking temperature. Since the time delay of the Hawking quanta is generated by its conjugated momentum we can write a proposal for this S-matrix as

$$\mathcal{S} = \exp\left(i \int d\Omega d\Omega' P^{\text{in}}(\Omega) f(\Omega, \Omega') P^{\text{out}}(\Omega') \right), \tag{1.1.12}$$

where P^{in} denotes the energy distribution of the infalling matter, while P^{out} corresponds to the observed particle leaving the black hole. For the particular case that the momentum of the incoming and outgoing particles are localized in the transverse space S^2 this can be simplified as $\mathcal{S} = e^{iP^+P^-}$ where $P^{+/-} = P^{\text{out/in}}$. We will refer to this result as the Dray-'t Hooft S-matrix.

This proposal gives a nice idea of how the information of matter thrown to the black hole can be eventually imprinted on the Hawking radiation. A drawback of this proposal is the insensitivity of the S-matrix to other quantum numbers other than energy. Another issue is that, if the boost of the particles near the horizon is large enough, the time-delay of the Hawking quanta might be large enough to send the quanta back inside of the black hole. Another issue of this interpretation is the fact that even though an asymptotic observer detects Hawking modes, an infalling observer will see the vacuum, and no particle to scatter with. For the purpose of this introduction, we simply take this idea as a motivation for the content of next section.

Finally, even if this S-matrix would reproduce all the information of the matter particle going in, this would contradict the no-cloning principle of quantum mechanics [14]. One could argue that contrary to usual QFT expectations, a measurement at point A in Figure 1.2 does not commute with a measurement at B. The source of this commutator is the shockwave geometry and generates a $[\mathcal{O}_A, \mathcal{O}_B]$ that increases exponentially with time. A detailed analysis of this effect was studied by Kiem, Verlinde and Verlinde [15]. The authors propose the principle of complementarity as a resolution: two modes that when propagated backwards generate such a large backreaction should be thought of as complementary descriptions of the same operator in the Hilbert space.

Another interesting feature is the possibility of time folds. To recover the information about the infalling particle one could evolve the black hole forward in time and detect the state of the Hawking quanta. Then one should evolve it back, throw

the infalling particle, evolve forward again and compare the final state of the Hawking particle. This is an out-of-time ordered process. In the next section we will see how the ideas in these final paragraphs fit in the context of gauge/gravity dualities. Growth of commutators and out-of-time-ordered processes are key in studying quantum chaos, which in turn is dual to high energy scattering near the event horizon.

1.2 Holography and Quantum Chaos

The holographic principle for quantum gravity was enunciated by 't Hooft in 1993 [16] (see also [17]). This idea is best understood in the context of AdS/CFT, with the first concrete example found by Maldacena in 1997 [5], see also [18, 19]. This consisted of a duality between type IIB string theory in an $\mathrm{AdS}_5 \times \mathrm{S}^5$ background with a gauge theory, $SU(N)$ $\mathcal{N} = 4$ supersymmetric Yang-Mills, living in the four dimensional boundary of AdS (without gravity).

Since 1997 several other examples were discovered that allowed to generalize this conjecture and claim that any CFT in d-dimensions (the boundary) is dual to a quantum gravitational theory in $\mathrm{AdS}_{D=d+1}$ (the bulk). Most examples for the bulk theory involve string theory with a low energy description by Einstein gravity (possibly plus some matter). Other examples involve Vasiliev gravity [20] which has a dynamical metric but the physics is highly non-local as opposed to Einstein gravity.

If a black hole exists in the bulk, it is dual to a thermal state in the boundary. The boundary temperature and entropy are equal to the Hawking temperature and Bekenstein entropy of the black hole in the bulk. The extended geometry of a black hole in AdS is believed to be dual to the thermo-field doubled state that purifies the thermal state of the boundary [21] (see equation (1.2.6) below). Particles moving outside the black hole are dual to (single-trace) operator insertions in the boundary CFT.

In the context of AdS/CFT one can give a very precise interpretation of the near-horizon scattering studied by Dray and 't Hooft. Basically, the Dray-'t Hooft S-matrix is dual to the statement that the boundary conformal field theory (CFT) presents maximal quantum chaos.

1.2.1 Quantum Chaos

Classical chaos gives a measure of how sensitive is a dynamical system to initial conditions [22]. Take a system with a large number N degrees of freedom such that its phase space is parametrized as $X = (q_i, p_i)$ with $i = 1, \ldots, N$. Take trajectories $X(t)$ which is fixed by initial conditions $X(0)$. The derivative of $X(t)$ with respect to $X(0)$ gives a measure of sensitivity to initial conditions. In a chaotic system this quantity grows exponentially with time with a rate defined as the Lyapunov exponent λ. This can be written in terms of Poisson brackets as $\{X_i(t), X_j(0)\} \sim e^{\lambda t}$. For arbitrary observables $V(X(t))$ and $W(X(t))$ made up of phase space variables, this implies that for a chaotic system

$$\{V(t), W(0)\} \sim e^{\lambda t}. \tag{1.2.1}$$

In general this rate might depend on the choice of operators. In the context of thermodynamics classical chaos is fundamental for systems to be able to thermalize.

This analysis can be extended to quantum mechanics. First one replaces phase space with Hilbert space and Poisson brackets with commutators. The analog of the observables V and W are operators acting on the Hilbert space. To avoid phase cancellations consider the commutator square [2]. Then for a state ρ quantum chaos is

[2]Imagine taking the expectation value of the commutator. This is related by the Kubo formula to the linear response change in $\delta\langle V\rangle$ when one adds a perturbation $\delta H = W$ to the Hamiltonian. This quantity decays too fast, corresponds to quasi-normal modes of the black hole and not near horizon scattering.

diagnosed by

$$\langle |[V(t), W(0)]|^2 \rangle \sim \frac{1}{N^2} e^{\lambda t}, \tag{1.2.2}$$

where $\langle \mathcal{O} \rangle = \mathrm{Tr}[\rho \mathcal{O}]$ and N^2 roughly corresponds to the number of degrees of freedom (e.g. the central charge for a CFT). For a thermal system at temperature $T = 1/\beta$ we take large times to be $t \gg t_d$ with dissipation time $t_d \approx \beta$. This commutator cannot increase indefinitely and saturates at the scrambling time $t_s \sim \beta \log N$. Therefore we will consider systems with large N where there is a clear distinction between dissipation and scrambling scale $t_d \ll t \ll t_s$.

This signature of quantum chaos was introduced in 1969 by Larkin and Ovchinnikov [23]. Experimental methods to measure similar observables was developed, for example, by Jalabert and Pastawski [24] using the Loschmidt echo.

By expanding (1.2.2) most terms are either time or anti-time ordered. For a thermal state and times $t \gg 1/\beta$ these correlators thermalize. Nevertheless other terms give out-of-time ordered correlators (OTOC). The OTOC are the ones responsible for the exponential growth in (1.2.2) for chaotic systems. It is therefore useful to directly study instead

$$F(t) = \frac{\langle V^\dagger(t) W^\dagger(0) V(t) W(0) \rangle}{\langle V(t) V(0) \rangle \langle W(t) W(0) \rangle}. \tag{1.2.3}$$

Then the statement of a large N system displaying quantum chaos is the statement that

$$F(t) \approx f_0 - \frac{f_1}{N^2} e^{\lambda_L t} + \ldots, \tag{1.2.4}$$

where $f_{0/1}$ are order 1 (positive) constants. Before moving on to the bulk interpretation we will mention a bound obtained by Maldacena, Shenker and Stanford [25] which under reasonable assumptions is valid for any quantum system

$$\lambda_L \leq \frac{2\pi}{\beta} = \frac{2\pi k_B T}{\hbar}, \tag{1.2.5}$$

where in the right hand side we rewrote the expression in arbitrary units to clarify its classical limit $\hbar \to 0$. In the next section we will explain how black holes saturate this bound on chaos. To give some order of magnitude understanding of this bound, the maximal Lyapunov exponent of a quantum system dual to a solar mass black hole is given by $1/\lambda_L^{\text{sun}} = 10^{-5}$ s. On the other extreme, the maximal Lyapunov exponent of a system at room temperature is $1/\lambda_L^{\text{roomT}} = 10^{-14}$ s.

1.2.2 Bulk Perspective

The bulk interpretation of the growth of commutators involved in the definition of quantum chaos was realized by Shenker and Stanford in [26]. The first step is to identify the bulk process that computes an OTOC. The idea of Shenker and Stanford is depicted in Figure 1.3. We will discuss the case of an eternal black hole in AdS. The bulk geometry is believed to be dual to the thermo-field doubled state between CFT_R and CFT_L as

$$|\text{TFD}\rangle = \sum_E e^{-\beta E_n/2} |n\rangle_L \otimes |n\rangle_R. \tag{1.2.6}$$

Then the geometry of Figure 1.3 is computing the overlap between two states living in the Hilbert space $\mathcal{H} = \mathcal{H}_R \otimes \mathcal{H}_L$. These states are given by

$$|\Psi_f\rangle = W^\dagger(t)V^\dagger(-t)|\text{TFD}\rangle, \quad \text{and} \quad |\Psi_i\rangle = V(-t)W(t)|\text{TFD}\rangle. \tag{1.2.7}$$

It is then straight forward to see that the overlap $\langle\Psi_f|\Psi_i\rangle = \langle V^\dagger(-t)W^\dagger(t)V(-t)W(t)\rangle$ is equivalent to the OTOC between V and W and therefore controls the value of commutators between operators at separate times. In this expression V and W are operators acting on the CFT_R. This is a one sided OTOC. We will discuss the two-sided version in chapter 3.

How is this related to the shockwaves of previous sections? From the figure we can see that if the time difference between the insertion of V and W is large, the world-

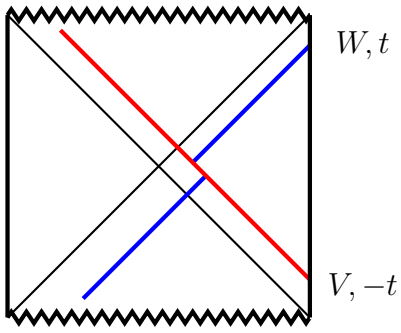

Figure 1.3: Penrose diagram of flat space. A shockwave generated by a high energy particle (red line). The trajectory of a probe particle is shown in blue.

line of the particles in the bulk propagate freely until they meet and interact very close to the horizon. Due to the blue shift the interaction is dominated by the Dray-'t Hooft shockwave S-matrix. One can rewrite the OTOC from the bulk perspective as

$$\langle V_1 W_3 V_2 W_4 \rangle = \int \Psi_1 \Psi_2 \mathcal{S}_{\rm DT} \Psi_3 \Psi_4, \tag{1.2.8}$$

where $\Psi_i(P_i, x_i)$ correspond to wave-functions (form-factors) that propagate the particles freely from the boundary of AdS (at a point x_i) to their meeting point at the horizon (with a Kruskal momentum P_i). The integrals are not explicitly written correspond to the momenta of the particles (and smearing of operators). Then at that point we can approximate the geometry by flat space and their S-matrix by the Dray-'t Hooft Ansatz. Details of this calculation can be found in [27]. For times between dissipation and scrambling times the OTOC normalized by the two-point function becomes

$$F(t) = 1 - \kappa G_N e^{\frac{2\pi}{\beta} t} + \dots, \tag{1.2.9}$$

where κ is some order one positive constant. Since the holographic dictionary tells us that $G_N \sim 1/N^2$, this has the form of (1.2.4). There is a nice interpretation of this formula. The contribution to the scattering amplitude due to the exchange of a spin J particle is given by $\mathcal{A} \sim s^{J-1}$ (an eikonal exponentiation of this amplitude gives the spin-J version of the Dray-'t Hooft S-matrix). The Lyapunov behavior comes from

the fact that, if we throw in a particle with a boundary energy E then the invariant energy of the collision near the horizon is given by $s \sim e^{\frac{2\pi}{\beta}t}$.

Some features (1) the shockwave calculation corresponds to a graviton exchange with $J = 2$. (2) The maximal Lyapunov exponent $\lambda_L = 2\pi/\beta$ corresponds to a gravitational blue-shift at the horizon (equal to the surface gravity), and due to the equivalence principle is universal (cannot depend on the operator), independent on which particle (i.e. single trace operator V) we throw. (3) The bound on chaos show that interactions bounded in spin are not consistent. If the spectrum of spins is unbounded then an infinite sum can resum into an effective Regge trajectory with $J_{\text{eff}} < 2$. This happens for string theory $J_{\text{eff}} \lesssim 2$ and Vasiliev gravity $J_{\text{eff}} \sim 0$.

One can take this and formulate the following conjecture. Say we are given a CFT whose dual we do not know and we want to figure out if the gravity theory supports black holes. In order to *find* the event horizon we need to compute OTOC and verify that for every operator (equivalence principle) the growth of commutators happens at a rate $\lambda_L = 2\pi/\beta$ (surface gravity in general, maybe with subleading stringy corrections). Thanks to AdS/CFT we can conjecture a positive answer to this question for $\mathcal{N} = 4$ SYM, ABJM, etc.

For which kind of theories the answer is negative? For example, it is believed that $U(N)$ Chern-Simons at level k coupled to fundamental matter in 3d is dual to Vasiliev gravity in AdS_4 [28]. Using 3d dualities between CFT one can also find a holographic description of the critical $O(N)$ model and Gross-Neveu model. Can we use these theories to study black hole physics? Given what we have learned we can compute OTOC for the boundary CFT (see for example [29]). This shows that in general $\lambda_L \approx 0$, showing that they do not support black holes.

1.3 Two-Dimensional Holography

An important development in the past years has been the realization by Kitaev [30,31] that certain quantum mechanical models (solvable but chaotic) present holographic behavior, the Sachdev-Ye-Kitaev (SYK) model[3]. Since a large part of this thesis consists in studying this model in some detail we will give a short summary in the following section. Even though the precise bulk theory dual to this model is not known to this date (August 2018) in the low energy regime one can identify a degree of freedom that captures the gravitational dynamics of dilaton-gravity in AdS_2 (which in turn arises from dimensional reduction of near extremal black holes in 4D).

1.3.1 Sachdev-Ye-Kitaev Model

The SYK model consists of a large number N of Majorana fermions ψ_i where $i = 1, \ldots, N$, such that $\{\psi_i, \psi_j\} = \delta_{ij}$. These fermions interact in an all-to-all way through the following Hamiltonian

$$\mathrm{H} = \frac{i^{q/2}}{q!} \sum_{i_1,\ldots,i_q} J_{i_1 i_2 \ldots i_q} \psi_{i_1} \psi_{i_2} \ldots \psi_{i_q}, \tag{1.3.1}$$

where $q > 2$ is an even integer. The original SYK model also displays disorder, meaning that the couplings are taken from a random distribution. We take a Gaussian distribution such that $\overline{J^2_{i_1 \ldots i_q}} = (q-1)! J^2 / N^{q-1}$. The factors of N are chosen such that for large N the free energy is extensive. This is a modification made by Kitaev on models originally studied in a different context by Sachdev and Ye [37, 38].

To solve this theory one can go to a mean field description in terms of bilocal fields

$$G(\tau, \tau') = \frac{1}{N} \sum_i \psi^i(\tau) \psi^i(\tau'), \tag{1.3.2}$$

[3]This QM is supposed to give an exact description of a gravitational 2D system. This is not the same as acoustic black holes that only model QFT on curved fixed backgrounds [32–36].

together with a self energy field denoted by $\Sigma(\tau,\tau')$. The path integral over the fermions and disorder average can be rewritten as

$$Z=\int[dG][d\Sigma]\ e^{N\left(\log \mathrm{Pf}(\partial_\tau-\Sigma)-\frac{1}{2}\int d\tau' d\tau\left[G(\tau,\tau')\Sigma(\tau,\tau')-\frac{J^2}{q}G(\tau,\tau')^q\right]\right)}. \tag{1.3.3}$$

From now on we can use this action to compute correlators of the bilocal field $G(\tau,\tau')$. For the derivation of this result one assumes that we work at temperatures high enough that no ordered-phase takes place (above spin-glass transition).

To reveal the holographic behavior we will focus on low energies (the IR) such that $1\ll\beta J\ll N$. The equation of motions for correlators of the bi-local field in this limit have an emergent conformal symmetry (this was understood by Georges and Parcollet in [39, 40]). From the UV free fermion correlator $G_{\mathrm{UV}}(\tau,0)=\frac{1}{2}\,\mathrm{sgn}\tau$ in the IR the two-point function becomes

$$G_{\mathrm{IR}}(\tau,\tau')=b_\Delta\frac{1}{|\tau-\tau'|^{2\Delta}}\mathrm{sgn}(\tau-\tau'), \tag{1.3.4}$$

where the scaling dimension is $\Delta=1/q$ and b_Δ is a function that can be found explicitly although the expression will not be very important. The conformal transformation acts as

$$G(\tau,\tau')\to[f'(\tau)f'(\tau')]^{2\Delta}G(f(\tau),f(\tau')), \tag{1.3.5}$$

and we can use this to write a solution of the Schwinger-Dyson equation at finite temperature by performing the reparametrization $\tau\to\tan\frac{\pi\tau}{\beta}$. The answer is then

$$G=\left(\frac{\pi}{\beta\sin\frac{\pi}{\beta}\tau}\right)^{2\Delta}\mathrm{sgn}\tau. \tag{1.3.6}$$

We will show immediately how the pattern of breaking of this symmetry is responsible for the IR dynamics and the emergence of a gravitational mode.

From the bi-local action (1.3.3) we can write the connected part of the four-point function by expanding $G \to G_{\text{s.p.}} + \delta G$, integrating over Σ, and finding the quadratic term in δG. The inverse of the kernel appearing in the quadratic term on δG, gives precisely the connected order $1/N$ four point function. The result is given, very schematically, by

$$\begin{aligned} \mathcal{F}(\tau_i) &\equiv \frac{1}{N^2}\sum_{i,j}\langle\psi^i(\tau_1)\psi^i(\tau_2)\psi^j(\tau_3)\psi^j(\tau_4)\rangle_{\text{conn.}}, \\ &= \langle G(\tau_1,\tau_2)G(\tau_3,\tau_4)\rangle_{\text{conn.}} \sim \frac{1}{N}\frac{K}{1-K}, \end{aligned} \tag{1.3.7}$$

where following [30,31,41,42] we define the kernel (derived from the mean field action) as

$$K(\tau_1,\tau_2;\tau_3,\tau_4) = -J^2(q-1)G(\tau_1,\tau_3)G(\tau_2,\tau_4)G(\tau_3,\tau_4)^{q-2}. \tag{1.3.8}$$

This should be thought of as a matrix with continuous indeces that acts on the second pair of times (then finding $K(1-K)^{-1}$ becomes a complicated problem).This kernel is SL(2,R) invariant (under $\tau \to \frac{a\tau+b}{c\tau+d}$ with $a,b,c,d \in \mathbf{R}$) and can be expanded in conformal blocks. Of course we are considering the low energy regime $\beta J \gg 1$ (since otherwise conformal symmetry is broken). Each term in the sum over conformal blocks corresponds to operators of the form

$$\mathcal{O}_n = \frac{1}{N}\sum_i : \psi^i \ \partial_t^n \psi^i :, \quad \Delta_n = 2\Delta + 1 + 2n + \mathcal{O}(1). \tag{1.3.9}$$

One can also think of these operators as different fluctuation modes of the bilocal field $G(\tau,\tau')$. Nevertheless, if one takes a careful look at the four point function an interesting issue appears, related to the patter of symmetry breaking. There is a mode with $\Delta = 2$, which is associated to fluctuations of the bilocal field that are equivalent to reparametrizations by some $f(\tau)$. This mode, when plugged into the

expression for the four-point function diverges. This is because the moduli space of fluctuations of $f(\tau)$ is non-compact and massless (to leading order in $1/\beta J$).

This might be an inconsistency of the large βJ approximation, but this is not true. The effect of this mode can be accounted in the following way, while keeping the contribution from other modes unchanged. The idea is to integrate over all reparametrization $f(\tau)$ associated to these "zero"-modes of δG. For $\beta J = \infty$ their action is zero. By computing the leading $1/\beta J$ correction one can find an action for this mode that makes the theory finite. This is the Schwarzian action

$$S = C \int d\tau \{f(\tau), \tau\}, \tag{1.3.10}$$

where $C = \alpha_S N/J$ and α_S is an order one number which can be computed numerically. To leading order in $\beta J/N$ one can then expand the four-point function schematically as

$$\mathcal{F} = \mathcal{F}_{\text{disc.}} + \frac{\beta J}{N}\mathcal{F}_{\text{Schw.}} + \frac{1}{N}\mathcal{F}_{\text{conf.}}, \tag{1.3.11}$$

where the first term is the disconnected piece, the last term is the $1/N$ correction from conformal modes (and subleading corrections to reparametrization mode action) and the middle term is this Schwarzian mode corresponding to the breaking of the conformal symmetry. As we indicated (at least for small $\beta J/N$) this latter contribution is enhanced with respect to the conformal part.

This Schwarzian mode, coming from the pattern of breaking of the conformal symmetry, dominates the IR limit of the SYK model. It controls the entropy, free energy and the chaos exponent in this model. This mode presents maximal chaos $\lambda_L = 2\pi/\beta$. We will explain in the next section how this mode emerges from dilaton-gravity in AdS_2.

1.3.2 Jackiw-Teitelboim Model

The gravitational mode giving origin to the Schwarzian action can be obtained from Jackiw-Teitelboim (JT) gravity [43,44] in two dimensions with a negative cosmological constant [45–48]. The action of this theory is

$$S = \frac{1}{16\pi G_N}\left[\int \Phi(R+2) + \int_{\text{bdy.}} \Phi_b K\right] + S_{\text{matter}}. \tag{1.3.12}$$

The near-horizon geometry of a near-extremal black hole in 4D is $\text{AdS}_2 \times S^2$. After reducing on the S^2 one obtains this action with Φ corresponding to the size of S^2. We will analyze this system classically first. The solution to the dilaton equation of motion sets the geometry to AdS_2, with metric

$$ds^2 = \frac{dt^2 + dz^2}{z^2}, \tag{1.3.13}$$

with a group of isometries SL(2,R). One could consider a constant dilaton solution preserving this group of isometries. This situation does not allow finite energy excitations without a catastrophic backreaction [49]. Therefore one needs a dilaton that breaks this conformal symmetry. One can already find a similarity with the pattern of symmetry breaking in the IR limit of the SYK model.

The solution for a non-constant dilaton can be written as

$$\Phi = \Phi_0 + \delta\Phi, \tag{1.3.14}$$

where the precise spacetime dependence of $\delta\Phi$ is not too important. We will only mention that it blows up at the boundary of AdS_2. This forces us to put a cut-off on the AdS geometry where the boundary theory lives, since eventually the approximations would break down if $\delta\Phi$ becomes bigger than Φ_0.

Take as the boundary a trajectory $(t, z) \to (f(t), z(t))$. Fixing a metric boundary condition $g|_{\text{bdy}} = \epsilon^{-2}$, with ϵ small gives $z(t) = \epsilon f'(t)$ so that the cut-off surface is completely fixed by $t \to f(t)$. For the dilaton, a natural boundary condition to consider is $\delta\Phi_b = \Phi_r/\epsilon$ (take Φ_r constant for simplicity). After plugging this in the action one gets

$$S = -\frac{\Phi_r}{8\pi G_N} \int dt \ \{f(t), t\}. \tag{1.3.15}$$

In a quantum version of this theory, the right prescription is to integrate of $f \in \text{Diff}(S^1)$ modulo SL(2,R) transformations $f(t) \to \frac{af(t)+b}{cf(t)+d}$ (but note that SL(2,R) transformations acting on t are broken to only translations). This is the only mode that survives in the JT model and it is equivalent to the IR mode of the SYK model. Matching both theories would give $C = \alpha_S N/J \sim \frac{\Phi_r}{8\pi G_N}$. The value of the dilaton Φ_0 fixes the extremal values. Since we are taking the cut-off surface at $\epsilon \to 0$ and $\delta\Phi \to \infty$, which should be smaller than Φ_0, the Schwarzian theory is valid in the limit $S_{\text{extremal}} \sim \Phi_0 \to \infty$.

The procedure to find observables like correlators of the matter fields is the following. First write their expectation value in rigid AdS_2 forgetting about gravity. For example for a field $\chi(x)$ the boundary four point function is

$$\langle \chi(t_1)\chi(t_2)\chi(t_3)\chi(t_4)\rangle = F_{\text{disc}}(t_i) + \frac{1}{N} F_{\text{conn}}(t_i), \tag{1.3.16}$$

where $F_{\text{disc}}(t_i)$ is the free bulk field answer while $F_{\text{conn}}(t_i)$ corresponds to bulk interactions. To add gravitational interactions perform a reparametrization $t \to f(t)$ and integrate over $f \in \text{Diff}(S^1)/SL(2, R)$ weighted by the Schwarzian action. This generates three types of contributions just like in equation (1.3.11). The term $\mathcal{F}_{\text{Schw.}}$ corresponds to the "gravitational dressing" of the disconnected (non-interacting) piece

of the four-point function. The $1/N$ piece corresponds to interactions of matter fields in the bulk[4].

To summarize, even though the bulk dual of SYK is not the JT model, they belong in the IR to the same "universality class". Gravitational interactions of the dual of SYK are described by the dilaton-gravity part of the JT model. Bulk matter interactions are not universal and a matching has not been found yet (see for example [50]).

1.4 Overview of the Thesis

In chapter 2 we will solve the Schwarzian theory and find its exact correlators, both time ordered and out-of-time-ordered. This will be done by realizing the Schwarzian theory as a certain limit of 2d Liouville theory. This chapter is based on a paper with T. Mertens and H. Verlinde [51].

In chapter 3 we will study the semiclassical limit of the expressions found in chapter 2 and provide more details. We will see the Dray-'t Hooft shockwaves emerge and propose a quantum generalization of the shockwave S-matrix. This is based also on [51] and a paper with H. Lam, T. Mertens and H. Verlinde [52].

In chapter 4 we will move on to $\mathrm{AdS}_3/\mathrm{CFT}_2$. We will propose a SYK-like model in two dimensions which we argue also shows maximal chaos and is related to gravity in AdS_3. This is based on a paper with H. Verlinde [53].

In chapter 5 we will generalize the idea that maximal chaos is determined by the breaking of conformal symmetry from the 1D Schwarzian case to 2D. In 2D CFT conformal symmetry is always broken by an anomaly. Under the assumption that this dominates the dynamics we will show that commutators increase exponentially with maximal Lyapunov exponent. The 2D version of the Schwarzian is proposed to

[4]We could also add gravitational dressing to these interactions but we will mostly neglect them since they are subleading in N.

be the action on coadjoint orbits of the Virasoro group. Finally, we will also propose a discrete lattice model in 2D with maximal chaos and also relate it to quasinormal modes in the two-point function. This is based on a paper with H. Verlinde [54].

In chapter 6 we will consider as an application a generalization of the usual shockwave geometry. We will consider higher derivative terms in the bulk such as $S = \int_{\mathrm{AdS}_D} \phi W^2$, where ϕ is a scalar matter field and W is the trace of the Weyl tensor. This theory supports shockwave geometries which are similar to the ones described in section 1.1.1 (and also exact solutions of equations of motion [55]). The main difference is that besides a time delay, this background might also change the nature of the probe particle (for example, a Higgs particle that hits the shockwave has a non-zero probability of also turning into a graviton). We will find a nice application of this in higher dimensional CFTs. This chapter is based on a paper with C. Cordova and J. Maldacena [56].

Other co-authored articles are [29, 57–61].

Chapter 2

Solving the Schwarzian Theory: Part I

We have reviewed in the Introduction the connection between near horizon physics of black holes and quantum chaos for holographic CFTs dual to those geometries [25,26, 30,31,46,62]. We have also reviewed a recently proposed solvable quantum mechanical model, the SYK model, which exhibits maximal chaos and other characteristics that indicate it has a holographic dual given by a 2D gravity theory on AdS_2 [31, 38, 41, 42, 63–65].

The Schwarzian theory describes the quantum dynamics of a single 1D degree of freedom $f(\tau)$ and forms the theoretical gateway between the microscopic SYK model and the dual 2D dilaton gravity theory [43, 45, 47, 48, 66]. In this chapter and the next we will derive and study the exact correlators of the Schwarzian theory. All the results then can be translated to a 2D dilaton gravity calculation as explained in the Introduction.

We will obtain the exact solution of the Schwarzian theory by relating it to a limit of Liouville theory. This is explained in sections 2.4 and 2.5. In this chapter we will mainly describe this set-up but also give a summary of the results for the correlators

in section 2.2. We will also extend this to the supersymmetric cases in a final section 2.6. In the next chapter we will give more details on how to derive it and some further applications and lessons.

2.1 The Schwarzian Action

To fix notation, at finite temperature the action we will study is given by

$$S[f] = -C\int_0^\beta d\tau \left(\{ f, \tau \} + \frac{2\pi^2}{\beta^2} f'^2 \right) \tag{2.1.1}$$

$$= -C\int_0^\beta d\tau \{ F, \tau \}, \qquad F \equiv \tan\left(\frac{\pi f(\tau)}{\beta} \right), \tag{2.1.2}$$

where C is the coupling constant of the zero-temperature theory. Here $f(\tau+\beta) = f(\tau)+\beta$ runs over the space Diff(S^1) of diffeomorphisms on the thermal circle, and

$$\{ f, \tau \} = \frac{f'''}{f'} - \frac{3}{2}\left(\frac{f''}{f'} \right)^2 \tag{2.1.3}$$

denotes the Schwarzian derivative (As a $0+1$ field theory, the variable F is more natural as a scalar field at finite temperature since $F(0) = F(\beta)$). Since C has dimensions of inverse energy we would like to find a proper dimensionless parameter that tunes the coupling of the theory.

A convenient choice of variables is obtained by taking $\tau \to \frac{\beta}{2\pi}\tau$, and correspondingly $f \to \frac{\beta}{2\pi} f$, such that now the size of the thermal circle becomes 2π. With this choice of scale the action prefactor becomes $C \to 2\pi C/\beta$. From this expression becomes clear that the dimensionless coupling constant of the theory is given by the combination $\kappa \equiv 2\pi C/\beta$. The theory becomes perturbative for $\kappa \to \infty$ and strongly coupled for $\kappa \to 0$. The weak coupling regime can happen if either C is large or the temperature is high. Correspondingly the strong coupling regime can happen if C is small or the temperature is too low.

In the context of SYK $C \sim N/J$ and the coupling constant becomes $\kappa \sim N/\beta J$. In the context of the JT dilaton gravity $C \sim \Phi_r/G_N$, the renormalized dilaton at the cut-off surface. Since the Schwarzian is obtained when the cut-off surface is pushed to the boundary, the Schwarzian describes the near horizon limit of a 4D near extremal black hole with a very large extremal entropy.

We will turn to the symmetries of the theory now. The action $S[f]$ is invariant under $SL(2,\mathbb{R})$ Möbius transformations that act on F via

$$F \to \frac{aF+b}{cF+d}. \tag{2.1.4}$$

The model possesses a corresponding set of conserved charges ℓ_a that generate the $\mathfrak{sl}(2,\mathbb{R})$ algebra $[\ell_a, \ell_b] = i\epsilon_{abc}\ell_c$ and commute with the Hamiltonian H. In fact, as reviewed in section 2.3, the Hamiltonian H is found to be equal to the $SL(2,\mathbb{R})$ Casimir, $H = \frac{1}{2}\ell_a\ell_a$. The energy spectrum and dynamics are thus uniquely determined by the $SL(2,\mathbb{R})$ symmetry. Regarding local symmetries acting on τ, only a $U(1)$ remains, associated to translations.

The Schwarzian theory is integrable and expected to be exactly soluble at any value of the inverse temperature β. In the following, we will label the energy eigenvalues E in terms of the $SL(2,\mathbb{R})$ spin $j = -\frac{1}{2} + ik$ via

$$E(k) = -j(j+1) \;=\; \frac{1}{4} + k^2. \tag{2.1.5}$$

The constant $\frac{1}{4}$ can be removed by choosing appropriate normal ordering in the quantum theory, and we will drop it throughout most of this work. If we mod out by the overall $SL(2,\mathbb{R})$ symmetry, the partition sum

$$Z(\beta) = \int_{\mathcal{M}} \mathcal{D}f\, e^{-S[f]} \tag{2.1.6}$$

reduces to an integral over the infinite dimensional quotient space

$$\mathcal{M} = \text{Diff}(S^1)/SL(2,\mathbb{R}). \tag{2.1.7}$$

This space $\mathcal{M}$ equals the coadjoint orbit of the identity element $\mathbf{1} \in \text{Diff}(S^1)$, which is known to be a symplectic manifold that upon quantization gives rise to the identity representation of the Virasoro group $\text{Diff}(S^1)$, i.e. the identity module of the Virasoro algebra [67–69]. We choose the functional measure $d\mu(f)$ to be the one derived from the symplectic form on $\mathcal{M}$, which as shown in [70–73] takes the form $\mathcal{D}f = \prod_\tau df/f'$.

The fact that the space $\mathcal{M}$ is a symplectic manifold was exploited in [73] to show that the partition function Z is one-loop exact and given by

$$Z(\beta) = e^{S_0+\beta E_0}\Big(\frac{2\pi C}{\beta}\Big)^{3/2} e^{2\pi^2 C/\beta} \;=\; e^{S_0+\beta E_0}\int_0^\infty d\mu(k)\, e^{-\beta E(k)} \tag{2.1.8}$$

with $E(k) = k^2/2C$ and where the integration measure is given in terms of k by $d\mu(k) = dk^2 \sinh(2\pi k)$, and $dk^2 = 2kdk$. We have separated a divergent zero-temperature, or extremal, entropy S_0 and energy E_0. This encompass all the divergencies of the Schwarzian theory, a possible UV completion being the SYK-model. In this chapter we will focus on the near-extremal dynamics. The exact result for the spectral density near extremality

$$\rho(E) = \sinh\big(2\pi\sqrt{2CE}\big) \tag{2.1.9}$$

is further indication that the Schwarzian theory is completely soluble and we will show that this is indeed the case.

We will make use of the more detailed property that the space $\mathcal{M}$ in (2.1.7) forms the quantizable coadjoint orbit space that gives rise to the identity module of the Virasoro algebra. This observation implies that the correlation functions of the

Schwarzian theory

$$\left\langle \mathcal{O}_1 \dots \mathcal{O}_n \right\rangle = \frac{1}{Z}\int_{\mathcal{M}} \mathcal{D}f\, e^{-S[f]}\, \mathcal{O}_1 \dots \mathcal{O}_n = \frac{1}{Z}\mathrm{Tr}\big(e^{-\beta H}\, \mathcal{O}_1 \dots \mathcal{O}_n\big) \tag{2.1.10}$$

can be obtained by taking a large central charge c limit of correlation functions of a soluble 2D CFT with Virasoro symmetry. We will explain and use this relation to explicitly compute the correlation functions of a natural class of $SL(2,\mathbb{R})$ invariant observables $\mathcal{O}_i$. (Different observables were studied in Appendix D of [51]). We will now begin by summarizing our main results.

2.2 Overview of results

We will study the correlation functions of the following bi-local operators

$$\mathcal{O}_\ell(\tau_1,\tau_2) \equiv \left(\frac{\sqrt{f'(\tau_1)f'(\tau_2)}}{\frac{\beta}{\pi}\sin\frac{\pi}{\beta}[f(\tau_1)-f(\tau_2)]}\right)^{2\ell}. \tag{2.2.1}$$

We can think of this expression as the two-point function $\mathcal{O}_\ell(\tau_1,\tau_2) = \langle \mathcal{O}(\tau_1)\mathcal{O}(\tau_2)\rangle_{\mathrm{CFT}}$ of some 1D 'matter CFT' at finite temperature coupled to the Schwarzian theory, or equivalently, as the boundary-to-boundary propagator of a bulk matter field coupled to the 2D dilaton-gravity theory in a classical black hole background.

The bi-local operator (2.2.1) is invariant under the $SL(2,\mathbb{R})$ transformations (2.1.4). This in particular implies that $\mathcal{O}_\ell$ commutes with the Hamiltonian H of the Schwarzian theory. Therefore the bi-local operators are diagonal between energy eigenstates. We will see that the time-ordered correlation functions of $\mathcal{O}_\ell(\tau_1,\tau_2)$ indeed only depend on the time-difference $\tau_2-\tau_1$.

We will give the explicit formulas for the correlation function with one and two insertions of the bi-local operator $\mathcal{O}_\ell$ [1]. We will call these the two-point and four-

[1] Even though we will focus on two- and four-point functions we can compute any $2n$-point correlator. We will comment on this in the next chapter.

point functions, since they depend on two and four different times τ_i, respectively. In the holographic dual theory they correspond to the AdS_2 gravity amplitude with one and two boundary-to-boundary propagators. We will compute the out-of-time ordered (OTO) four point function, which exhibits maximal Lyapunov behavior and contains the gravitational scattering amplitudes of the bulk theory as an identifiable subfactor.

Two-point function

The two-point function at finite temperature is defined by the functional integral with a single insertion of the bi-local operator

$$\left\langle \mathcal{O}_\ell(\tau_1,\tau_2)\right\rangle = \frac{1}{Z}\int \mathcal{D}f\, e^{-S[f]}\,\mathcal{O}_\ell(\tau_1,\tau_2) \;=\; \tau_2 \;\overset{\ell}{\frown}\; \tau_1 \tag{2.2.2}$$

Here we introduced a diagrammatic notation that will be useful below.

The two-point function of the Schwarzian theory at zero temperature was obtained in [71, 72]. As we will show in section 2.5, the generalization of their result to finite temperature is given by a double integral over intermediate $SL(2,\mathbb{R})$ representation labels k_1 and k_2

$$\left\langle \mathcal{O}_\ell(\tau_1,\tau_2)\right\rangle = \int \prod_{i=1}^{2} d\mu(k_i)\; \mathcal{A}_2(k_i,\ell,\tau_i). \tag{2.2.3}$$

We will call the integrand the 'momentum space amplitude'. In section 2.5 we will obtain the following explicit formula for $\mathcal{A}_2(k_i,\ell,\tau_i)$

$$\mathcal{A}_2(k_i,\ell,\tau_i) = e^{-(\tau_2-\tau_1)\frac{k_1^2}{2C}-(\beta-\tau_2+\tau_1)\frac{k_2^2}{2C}}\;\; \frac{\Gamma(\ell\pm ik_1\pm ik_2)}{\Gamma(2\ell)}, \tag{2.2.4}$$

where $\Gamma(x\pm y\pm z)$ is short-hand for the product of four gamma functions with all four choices of signs. In the following sections, we will derive the above result from the

relation between the Schwarzian theory and 2D Virasoro CFT, by taking a suitable large c limit of known results in the latter.

We will also perform a number of non-trivial checks on the result. In particular, it reduces to the zero-temperature result of [71, 72] in the limit $\beta \to \infty$. We also check that it reduces to the saddle point calculation of the Schwarzian action when $C \to \infty$.

Propagators and vertices

From the above expression for the two-point function, we can extract the following combinatoric algorithm, analogous to the Feynman rules, for computing time-ordered correlation functions of bi-local operators in the Schwarzian theory. We remark that these rules still generate a non-perturbative answer for the Schwarzian theory and merely represent a convenient packaging of the exact amplitudes.

We represent the momentum space amplitude $\mathcal{A}_2(k_i, \ell, \tau_i)$ diagrammatically as

$$\mathcal{A}_2(k_i, \ell, \tau_i) \;=\;$$

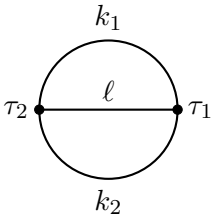

(2.2.5)

The thermal circle factorizes into two propagators, one with 'momentum' k_1 and one with 'momentum' k_2. The Feynman rule for the propagator and vertices read

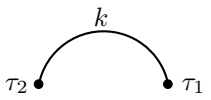

$$= \; e^{-\frac{k^2}{2C}(\tau_2 - \tau_1)} \,, \qquad$$

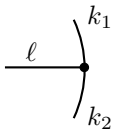

$$= \; \gamma_\ell(k_1, k_2). \tag{2.2.6}$$

The propagator with momentum k represents the phase factor between τ_1 and τ_2 of an energy eigenstate with energy $E = k^2/2C$.

Each vertex corresponds to a factor

$$\gamma_\ell(k_1,k_2) \;=\; \sqrt{\frac{\Gamma(\ell \pm ik_1 \pm ik_2)}{\Gamma(2\ell)}}. \tag{2.2.7}$$

This vertex factor represents the matrix element of each endpoint of the bi-local operator between the corresponding two energy eigenstates labeled by k_1 and k_2. This can be obtained by comparing this expansion with the one obtained from $\mathrm{Tr}[e^{-\beta H}O_1O_2]$ assuming a continuous spectrum with density of states $\mu(k)$.

Time ordered 4-point function

The time-ordered 4-point function comes in different types, depending on the ordering of the four different times. The simplest ordering is

$$\big\langle \mathcal{O}_{\ell_1}(\tau_1,\tau_2)\,\mathcal{O}_{\ell_2}(\tau_3,\tau_4)\big\rangle \;=\; \tag{2.2.8}$$

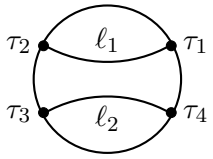

where we assume that the four times are cyclically ordered via $\tau_1 < \tau_2 < \tau_3 < \tau_4$. This ordering ensures that the legs of the two bi-local operators do not cross each other. This time-ordered 4-point function is given by a triple integral over intermediate momenta

$$\big\langle \mathcal{O}_{\ell_1}(\tau_1,\tau_2)\,\mathcal{O}_{\ell_2}(\tau_3,\tau_4)\big\rangle = \int \prod_{i=1}^{3} d\mu(k_i)\;\mathcal{A}_4\big(k_i,\ell_i,\tau_i\big). \tag{2.2.9}$$

The momentum amplitude is represented by the diagram

$$\mathcal{A}_4\big(k_i,\ell_i,\tau_i\big) \;=\; \tag{2.2.10}$$

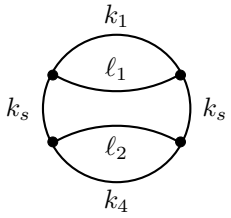

Here we took into account the aforementioned result that the bi-local operators commute with the Hamiltonian, so that the same energy eigenstate (labeled by the momentum variable k_s) appears on both sides of each bi-local operator.

Applying the Feynman rules formulated above, we find that the momentum amplitude of the time-ordered four point function reads

$$\mathcal{A}_4\big(k_i,\ell_i,\tau_i\big) = e^{-\frac{k_1^2}{2C}(\tau_2-\tau_1)-\frac{k_4^2}{2C}(\tau_4-\tau_3)-\frac{k_s^2}{2C}(\beta-\tau_2+\tau_3-\tau_4+\tau_1)}\,\gamma_{\ell_1}(k_1,k_s)^2\gamma_{\ell_2}(k_s,k_4)^2. \quad (2.2.11)$$

In section 2.5, we will explicitly compute the four-point function from the relationship between the Schwarzian and 2D CFT and confirm that this is indeed the correct result.[2]

OTO 4-point function

Finally we will turn to our main interest, the out-of-time-ordered 4-point function [30, 31]. We will diagrammatically represent the OTO 4-point function as

$$\big\langle\, \mathcal{O}_{\ell_1}(\tau_1,\tau_2)\, \mathcal{O}_{\ell_2}(\tau_3,\tau_4)\,\big\rangle_{\rm OTO} = \quad (2.2.13)$$

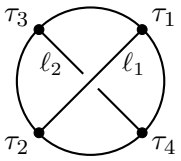

where in spite of their new geometric ordering along the circle, we in fact assume that the four time instances continue to be ordered according to $\tau_1 < \tau_2 < \tau_3 < \tau_4$. Operationally, we define the OTO correlation function via analytic continuation starting from the time ordered correlation function with the ordering $\tau_1 < \tau_3 < \tau_2 < \tau_4$ as indicated by the above diagram. Since for this configuration, the legs of the bi-local

[2]Note that the amplitude (2.2.11) factorizes into a product of two 2-point amplitudes

$$\mathcal{A}_4\big(k_i,\ell_i,\tau_i\big) = e^{\beta\frac{k_s^2}{2C}}\,\mathcal{A}_2\big(k_1,k_s,\ell_1,\tau_{21}\big)\,\mathcal{A}_2\big(k_4,k_s,\ell_2,\tau_{43}\big) \quad (2.2.12)$$

and thus indeed only depends on the two time differences $\tau_{21} = \tau_2 - \tau_1$ and $\tau_{43} = \tau_4 - \tau_3$.

operators do in fact cross, the resulting time ordered 4-point function differs from the analytic continuation of the uncrossed 4-point function (2.2.11).

In section 3.2, we will show that the OTO correlation function can be expressed as an integral over four momentum variables

$$\big\langle \mathcal{O}_{\ell_1}(\tau_1,\tau_2)\,\mathcal{O}_{\ell_2}(\tau_3,\tau_4)\big\rangle_{\rm OTO} = \int\prod_{i=1}^{4} d\mu(k_i)\;\mathcal{A}_4^{\rm OTO}\big(k_i,\ell_i,\tau_i\big), \tag{2.2.14}$$

where the momentum space amplitude is represented by the following diagram (to avoid clutter, we again suppressed the times τ_i labeling the end points of the bi-local operators)

$\mathcal{A}_4^{\rm OTO}\big(k_i,\ell_i,\tau_i\big)\;=$ 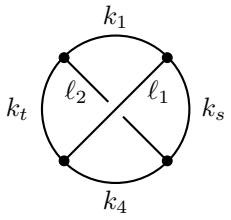

(2.2.15)

Note that we now have four different momentum variables k_i. The correlation function will indeed depend on all four time differences $\tau_{i+1}-\tau_i$.

The final answer for the momentum amplitude of the OTO 4-point function reads

$$\begin{aligned}\mathcal{A}_4^{\rm OTO}\big(k_i,\ell_i,\tau_i\big) \;&=\; e^{-\frac{k_1^2}{2C}(\tau_3-\tau_1)-\frac{k_t^2}{2C}(\tau_3-\tau_2)-\frac{k_4^2}{2C}(\tau_4-\tau_2)-\frac{k_s^2}{2C}(\beta-\tau_4+\tau_1)} \\ &\times \gamma_{\ell_1}(k_1,k_s)\gamma_{\ell_2}(k_s,k_4)\gamma_{\ell_1}(k_4,k_t)\gamma_{\ell_2}(k_t,k_1)\times R_{k_sk_t}\left[\begin{smallmatrix} k_4 & \ell_2 \\ k_1 & \ell_1\end{smallmatrix}\right].\end{aligned} \tag{2.2.16}$$

Comparing with the diagram (2.2.15), we recognize the same propagators and vertex factors as before. However, the momentum amplitude now also contains an additional factor $R_{k_sk_t}\left[\begin{smallmatrix} k_4 & \ell_2 \\ k_1 & \ell_1\end{smallmatrix}\right]$, which takes into account the effect of the two crossing legs in the diagram (2.2.15). From the holographic dual perspective, it represents the scattering amplitude of particles in the AdS_2 black hole background [26, 74]. Computing

this crossing kernel is one of the main goals of this chapter. We will describe this computation in section 3.2.

The crossing kernel

The role of the crossing kernel is to relate OTO with TO operators

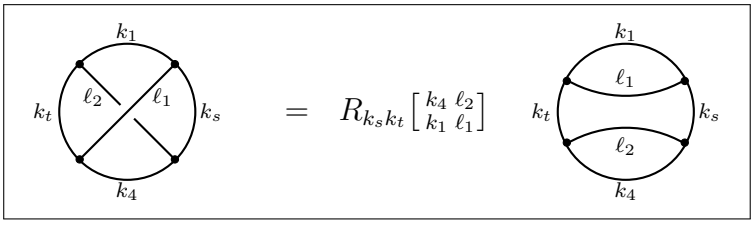

(2.2.17)

An alternative name for the crossing kernel is the R-matrix. The matrix $R_{k_s k_t}$ in fact depends on six numbers, $k_1, k_4, k_s, k_t, \ell_1$ and ℓ_2, that all label the spin of a corresponding sextuplet of representations of $SL(2,\mathbb{R})$. It satisfies the unitarity property

$$\int d\mu(k)\; R_{k_s k} R^{\dagger}_{k k_t} = \frac{1}{\rho(k_s)}\,\delta(k_s - k_t), \qquad\qquad \rho(k) = 2k\sinh(2\pi k). \tag{2.2.18}$$

The explicit form of the R-matrix can be found in several different ways. The most convenient method uses the relation between the Schwarzian QM and 2D CFT. In section 3.2 we will compute$R_{k_s k_t}\left[\begin{smallmatrix} k_4 & \ell_2 \\ k_1 & \ell_1 \end{smallmatrix}\right]$ by taking a large c limit of the CFT R-matrix that expresses the monodromy of 2D conformal blocks under analytic continuation over the lightcone. This 2D crossing kernel is explicitly known, thanks to the work of Ponsot and Teschner [75], see also [76, 77]. As shown in [75], the 2D kernel can be expressed as a quantum 6j-symbol of the non-compact quantum group $U_q(\mathfrak{sl}(2,\mathbb{R}))$. Taking the large c limit of their formulas, we obtain that

$$R_{k_s k_t}\left[\begin{smallmatrix} k_4 & \ell_2 \\ k_1 & \ell_1 \end{smallmatrix}\right] \;=\; \mathbb{W}(k_s, k_t; \ell_1 + ik_4, \ell_1 - ik_4, \ell_2 - ik_1, \ell_2 + ik_1) \tag{2.2.19}$$

$$\times\, \gamma_{\ell_1}(k_1, k_s)\gamma_{\ell_2}(k_s, k_4)\gamma_{\ell_1}(k_4, k_t)\gamma_{\ell_2}(k_t, k_1)$$

where $\mathbb{W}(a,b,c,d,e,f)$ denotes the Wilson function, defined as a particular linear combination of two generalized hypergeometric functions ${}_4F_3$. The Wilson function was introduced in [78, 79], where it was shown that the above expression in fact coincides with the classical 6j-symbol of the Lie group $SU(1,1) \sim SL(2,\mathbb{R})$.

The appearance of the 6j-symbols in OTO correlation functions should not come as a surprise. States and operators in the Schwarzian theory are specified by a representation label of $SL(2,\mathbb{R})$. The crossing kernel relates the OTO 4-point function with the corresponding time-ordered amplitude. It thus applies an isomorphism between two different orderings of taking a triple tensor product. The 6j-symbols satisfy some remarkable identities known as the pentagon and hexagon identities. From the point of view of the Schwarzian theory, these identities are consistency requirements that follow from locality, analyticity and associativity of the operator algebra.

2.3 Schrödinger formulation

In this section, we outline the Hamiltonian formulation of the Schwarzian theory, and how it is related to other 1D systems with $SL(2,\mathbb{R})$ symmetry. We temporarily set $\beta = 2\pi$. The reader familiar with the basic properties of Schwarzian QM can choose to skip this section.

2.3.1 Zero temperature

We first consider the Schwarzian theory at zero temperature. In this limit, the $\dot{f}^2$-term is dropped in the action (2.1.1), reducing it to the pure Schwarzian action $S = \int d\tau \, \{f,\tau\}$.[3] To transit to a Hamiltonian description, it is useful to recast the Lagrangian into a first order form as

$$L = \pi_\phi \dot{\phi} + \pi_f \dot{f} - (\pi_\phi^2 + \pi_f e^\phi). \tag{2.3.1}$$

[3]Here, in this section only, we will write $\dot{f}(\tau)$ instead of $f'(\tau)$.

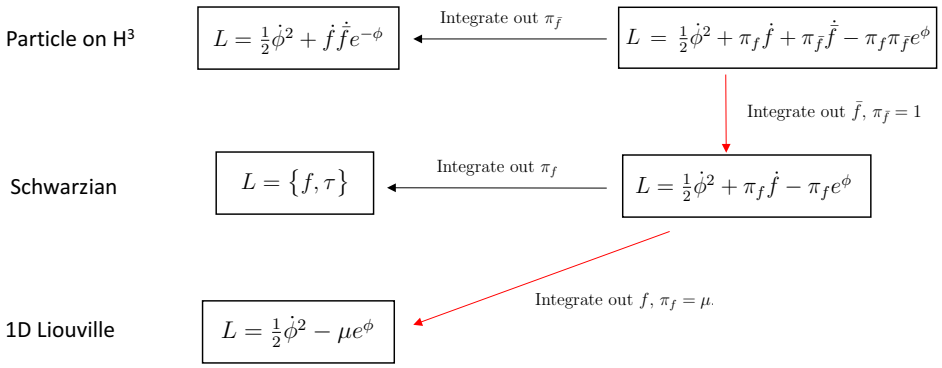

Figure 2.1: Overview of different models with underlying $SL(2,\mathbb{R})$ symmetry. Red lines indicate one-way lines: they are projections that reduce the dimension of the phase space.

This first-order form makes clear that the Schwarzian theory has a four dimensional phase space, labeled by two pairs of canonical variables (ϕ, π_ϕ) and (f, π_f). Alternatively, we may view the quantity π_f as a Lagrange multiplier, enforcing the constraint $\dot{f} = e^{\phi}$. Setting $\phi = \log \dot{f}$ and integrating out π_ϕ, it is readily seen that the above first-order Lagrangian indeed reduces to the Schwarzian theory. Upon quantization, the variables satisfy canonical commutation relations $[f, \pi_f] = i$ and $[\phi, \pi_\phi] = i$.

The invariance of the Schwarzian action under Möbius transformations

$$f \to \frac{af + b}{cf + d} \tag{2.3.2}$$

implies the presence of a set of conserved charges

$$\ell_{-1} = \pi_f, \qquad \ell_0 = f\pi_f + \pi_\phi, \qquad \ell_1 = f^2\pi_f + 2f\pi_\phi + e^{\phi},$$

that satisfy an $\mathfrak{sl}(2,\mathbb{R})$ algebra. The Hamiltonian H is equal to the quadratic Casimir

$$H = \pi_\phi^2 + \pi_f e^{\phi} = \ell_0^2 - \tfrac{1}{2}\{\ell_{-1}, \ell_1\} \tag{2.3.3}$$

and thus manifestly commutes with the $SL(2,\mathbb{R})$ symmetry generators. In particular, we can define a mutual eigenbasis of H and $\pi_f = \ell_{-1}$

$$\pi_f \big|\lambda, k\big\rangle = \lambda \big|\lambda, k\big\rangle, \qquad H\big|\lambda, k\big\rangle = E(k)\big|\lambda, k\big\rangle, \qquad E(k) \equiv \tfrac{1}{4} + k^2, \tag{2.3.4}$$

which spans the complete Hilbert space of the theory.

The 1D Schwarzian theory is closely related to the free particle on the 3D Euclidean AdS space H_3^+ with coordinates $(\phi, f, \bar{f})$ and metric $ds^2 = d\phi^2 + 2e^{-\phi} df d\bar{f}$, and to 1D Liouville theory. The different 1D models and their connections are summarized in Figure 2.1. The H_+^3 model has $SL(2,\mathbb{R}) \times SL(2,\mathbb{R})$ symmetry, which is broken to $SL(2,\mathbb{R})$ by setting the momentum variable $\bar{\pi}_f$ equal to a constant. Similarly, the reduction to the 1D Liouville theory proceeds by setting $\pi_f = \mu$, which breaks all symmetry.

2.3.2 Finite temperature

Putting the theory at finite temperature (we continue to set $\beta = 2\pi$ for convenience) reintroduces the extra $\dot{f}^2$-term in the action (2.1.1). The effect of this term in the first order formulation is taken into account by changing the Hamiltonian to

$$H = \pi_\phi^2 + \pi_f e^{\phi} + e^{2\phi}. \tag{2.3.5}$$

Upon solving the constraint $\dot{f} = e^{\phi}$, the added term reduces to $e^{2\phi} = \dot{f}^2$. This Hamiltonian still has $SL(2,\mathbb{R})$ symmetry generated by the charges

$$\begin{aligned} \ell_{-1} &= \cos^2(f)\,\pi_f - \sin(2f)\pi_\phi + \cos(2f)e^{\phi}, \\ \ell_0 &= \tfrac{1}{2}\sin(2f)\,\pi_f + \cos(2f)\pi_\phi + \sin(2f)e^{\phi}, \\ \ell_1 &= \sin^2(f)\,\pi_f + \sin(2f)\pi_\phi - \cos(2f)e^{\phi}. \end{aligned} \tag{2.3.6}$$

These charges satisfy $[\ell_0, \ell_{\pm 1}] = \mp \ell_{\pm 1}$ and $[\ell_1, \ell_{-1}] = 2\ell_0$ and all commute with the Hamiltonian, which can again be identified with the quadratic Casimir operator $H = \ell_0^2 - \frac{1}{2}\{\ell_1, \ell_{-1}\}$. The $SL(2,\mathbb{R})$ symmetry generated by these charges acts via broken linear transformations on the uniformizing variable F

$$F \to \frac{aF+b}{cF+d}, \qquad F = \tan(f/2), \qquad ad - bc = 1. \tag{2.3.7}$$

Since $\pi_f = \ell_1 + \ell_{-1}$ commutes with H, we can again define a mutual eigenbasis (2.3.4) that span the full Hilbert space of the model. The Schrödinger wavefunctions of the eigenstates take the form $\Psi_{\lambda,k}(f,\phi) = e^{i\lambda f}\psi_{\lambda,k}(\phi)$ where $\psi_{\lambda,k}(\phi)$ solves the Schrödinger equation

$$\left(-\partial_\phi^2 + \lambda e^{\phi} + e^{2\phi}\right)\psi_{\lambda,k}(\phi) = k^2 \psi_{\lambda,k}(\phi), \tag{2.3.8}$$

given by a 1D particle in a Morse potential $V(\phi) = \lambda e^{\phi} + e^{2\phi}$. The solutions are given in terms of Whittaker W-functions. The full eigenmode functions normalized in the flat measure $df\, d\phi$ are given by

$$\Psi_{\lambda,k}(f,\phi) = \sqrt{\frac{k\sinh(2\pi k)}{4\pi^3}}\left|\Gamma\big(ik + \lambda/2 + 1/2\big)\right| e^{i\lambda f} e^{-\phi/2}\, W_{-\lambda/2,ik}\left(2e^{\phi}\right). \tag{2.3.9}$$

2.3.3 Particle in a magnetic field

There exists an interesting and useful connection between the Schwarzian model and a particle on the hyperbolic plane H_2^+ in a constant magnetic field [80]. The Landau problem on H_2^+ was first analyzed by A. Comtet and P. J. Houston in [81]. A main result of [81], which also turns out to be useful for our problem, is an explicit formula for the spectral density of states.

Writing the H^2_+ metric as $ds^2 = d\phi^2 + e^{-2\phi}df^2$, the Lagrangian of the particle is given by

$$S = \int dt \left(\frac{1}{4}\dot{\phi}^2 + \frac{1}{4}e^{-2\phi}\,\dot{f}^2 + B\dot{f}e^{-\phi}\right), \tag{2.3.10}$$

which identifies the magnetic vector potential as $qA_f = Be^{-\phi}$ with q the charge of the particle. The Hamiltonian of this system, for fixed constant B, is

$$H_B = p_\phi^2 + \left(p_f e^{\phi} - B\right)^2, \tag{2.3.11}$$

where we denoted the canonical conjugate variables by p_ϕ and p_f. The model is again invariant under Möbius transformations (2.3.2) and possesses a corresponding set of $SL(2,\mathbb{R})$ symmetry generators

$$\ell_{-1}=p_f \quad , \quad \ell_0 = fp_f + p_\phi \quad , \quad \ell_1 = f^2p_f + 2fp_\phi - p_f e^{2\phi} + 2Be^{\phi}. \tag{2.3.12}$$

Once again, the Hamiltonian is equal to the quadratic Casimir. The normalized simultaneous eigenmodes of p_f (with eigenvalue ν) and H_B (with eigenvalue $E(k) = \frac{1}{4} + k^2 + B^2$) take the form [81]

$$\Psi_{\nu,k}(f,\phi) = \sqrt{\frac{k\sinh(2\pi k)}{4\pi^3|\nu|}}\,\left|\Gamma\big(ik - B + 1/2\big)\right| e^{i\nu f}\, e^{-\phi/2}\, W_{B,ik}\left(2|\nu|e^{\phi}\right). \tag{2.3.13}$$

This should be compared with formula (2.3.9) for the eigenmodes of the Schwarzian model.

Using the above formula for the eigenmodes, it is straightforward to compute the density of states for the Landau problem on H^2_+. The result for spectral measure reads

$$d\mu_B(k) = \rho_B(k)dk = dk^2 \frac{\sinh(2\pi k)}{\cosh(2\pi k) + \cos(2\pi B)}. \tag{2.3.14}$$

We can use this result to compute the spectral measure of the Schwarzian theory via the following observation [80]. Upon shifting $\phi \to \phi - \log(-2B)$ with $B \to i\infty$, the Hamiltonian H_B reduces to

$$H_B = p_\phi^2 + p_f e^\phi + B^2, \tag{2.3.15}$$

which, up to the irrelevant constant B^2-contribution, coincides with the Hamiltonian (2.3.3) for the Schwarzian model at zero temperature. We can use this correspondence to derive the exact formula for the spectral measure (2.1.9) of the Schwarzian theory quoted in the introduction. Starting from Comtet's result (2.3.14) and using that $\cos(2\pi B)$ diverges as $B \to i\infty$, we deduce that (up to an irrelevant overall normalization) $d\mu(k) = dk^2 \sinh(2\pi k)$.

2.4 Partition function: a 2D Perspective

In this section we will study the path integral formulation of the Schwarzian theory at finite temperature. In particular, we will use its relationship to the group $\mathrm{Diff}(S^1)$ to reformulate 1D Schwarzian QM as a suitable large c limit of 2D Virasoro CFT.[4]

The partition function of the Schwarzian theory (2.1.1) is defined as the integral

$$Z(\beta) = \int \frac{\mathcal{D}f}{SL(2,\mathbb{R})}\, e^{-S[f]} \tag{2.4.1}$$

over invertible functions f, satisfying the periodicity and monotonicity constraints $f(\tau+\beta) = f(\tau)+\beta$ and $f'(\tau) > 0$. The space of functions with these properties specifies the group $\mathrm{Diff}(S^1)$ of diffeomorphisms of the circle, also known as the Virasoro group.

[4]Related ideas are formulated in [82].

The $SL(2,\mathbb{R})$ quotient in (2.4.1) indicates that the functional integral runs over the infinite dimensional quotient space

$$\mathcal{M} \;=\; \mathrm{Diff}(S^1)/SL(2,\mathbb{R}) \tag{2.4.2}$$

of diffeomorphisms modulo the group of Möbius transformations (2.3.7) acting on $F = \tan(\frac{\pi f}{\beta})$. This space $\mathcal{M}$ is called the coadjoint orbit of the identity element $\mathbf{1} \in \mathrm{Diff}(S^1)$, which is known to be a symplectic manifold [67, 68]. Its symplectic form takes the following form

$$\omega \;=\; \int_0^{2\pi} dx \,\left[\frac{df' \wedge df''}{f'^2} - df \wedge df'\right]. \tag{2.4.3}$$

This observation was used by Stanford and Witten [73] to evaluate the functional integral with the help of the Duistermaat-Heckman (DH) formula [83].

The DH formula applies to any integral over a symplectic manifold of the schematic form

$$I = \int \mathrm{dpdq}\, e^{-\,\mathrm{H(p,q)}} \tag{2.4.4}$$

where H(p,q) generates, via the Poisson bracket $\{q,p\} = 1$, a U(1) symmetry of the manifold. In this chapter we will apply a somewhat different argument: instead of the DH theorem, we will use the general fact that the phase space integral of the form (2.4.4) is equal to the $\hbar \to 0$ limit of the trace of the quantum operator $e^{-\mathrm{H(p,q)}}$ over the Hilbert space obtained by quantizing the phase space:

$$I = \lim_{\hbar\to 0}\; \mathrm{Tr}\big(e^{-\,\mathrm{H(p,q)}}\big). \tag{2.4.5}$$

The physical intuition that underlies this equality is that for small $\hbar$, the Hilbert space admits an orthogonal basis of states each localized within a Planck cell in phase space.

The trace then takes the form of a sum over all Planck cells, which in the $\hbar \to 0$ limit reduces to the phase space integral defined via the symplectic measure.

The strategy that we plan to follow is to exploit the fact that, if there exists a precise way to quantize the phase space $\mathcal{M}$ and construct the corresponding Hilbert space, then the formula (2.4.5) provides an exact and efficient way of computing the integral I.

2.4.1 Spectral density from modular bootstrap

In our problem, the phase space $(\mathcal{M}, \omega)$ specified by equations (2.4.2) and (2.4.3) can be quantized through the standard methods of co-adjoint orbit quantization. The details of this quantization step are explained in detail in [67–70]. It is customary to label the quantization parameter $\hbar$ via

$$\hbar = \frac{24\pi}{c} \tag{2.4.6}$$

and introduce the following basis of $SL(2,\mathbb{R})$ invariant functions on $\mathcal{M}$

$$L_n = \frac{\beta c}{48\pi^2} \int_0^\beta d\tau \, e^{2\pi i n \tau/\beta} \, \big\{F, \tau\big\}. \tag{2.4.7}$$

The main statement that we will need for our purpose is that in the quantum theory, these functions L_n become identified with the generators of the Virasoro algebra

$$[L_n, L_m] = (n-m)L_{n+m} + \frac{c}{12}(n^3 - n)\delta_{n+m} \tag{2.4.8}$$

at central charge c. The classical limit $\hbar \to 0$ corresponds to the large central charge limit $c \to \infty$. The Hilbert space of the quantum theory is given by the identity module of the Virasoro algebra, i.e the linear space spanned by all states obtained by acting with L_{-n}'s with $n > 2$ on the $SL(2,\mathbb{R})$ invariant vacuum state $|0\rangle\!\rangle$.

The Schwarzian action (in this section we take $C = 1/2$ for simplicity)

$$S[f] = -\frac{1}{2}\int_0^\beta d\tau \, \{F, \tau\} \; = \; -\frac{24\pi^2}{\beta c} \, L_0 \tag{2.4.9}$$

is the generator of a $U(1)$ symmetry $f(\tau) \to f(\tau + \delta)$. This fact was used in [73] to invoke the DH formula and conclude that the partition function $Z(\beta)$ is one-loop exact.

For our purpose, the relevant observation is that the exponential of the Schwarzian action can be expressed as an evolution operator

$$e^{-S[f]} = q^{L_0}, \qquad\qquad q \equiv e^{-\frac{24\pi^2}{\beta c}} \tag{2.4.10}$$

in the quantum theory. We are now ready to apply the above argument, that relates the phase space integral (2.4.4) and the $\hbar \to 0$ limit of the trace (2.4.5), to the Schwarzian partition function (2.4.1). We obtain the following identity

$$Z(\beta) = \lim_{\substack{c\to\infty \\ q\to 1}} \mathrm{Tr}\big(q^{L_0}\big), \qquad\qquad q^{\frac{c}{24}} = e^{-\frac{\pi^2}{\beta}} = \text{fixed}. \tag{2.4.11}$$

where the trace is over the identity module of the Virasoro algebra. The quantity $\chi_0(q) = \mathrm{Tr}(q^{L_0})$ is the identity character of the Virasoro algebra. Geometrically, it represents the torus partition function of a chiral identity sector of a 2D CFT. Taking the limit $q \to 1$ amounts to sending the modular parameter $\tau \to 0$. In this limit, the torus degenerates into an infinitesimally thin circular tube. The long direction of the circular tube is the original thermal circle of the Schwarzian theory. The short direction is a fiducial circle that we added in order to write the integral over $\mathcal{M}$ as a trace.

The identity character of a $c > 1$ CFT takes the form

$$\mathrm{Tr}\big(q^{L_0}\big) \equiv \chi_0(q) = \frac{q^{\frac{1-c}{24}}(1-q)}{\eta(\tau)}, \tag{2.4.12}$$

where $\eta(\tau)$ denotes the Dedekind eta function $\eta(\tau) = q^{\frac{1}{24}}\prod_{n=1}^{\infty}(1-q^n)$ with $q = e^{2\pi i\tau}$.[5] The factor $(1-q)$ in the above formula for the identity character accounts for the presence of the null state $L_{-1}|0\rangle = 0$.

It is now straightforward to combine equations (2.4.11)-(2.4.12) and extract an exact expression for the Schwarzian partition function. This can be done in two ways. First, from the identity $\eta(-\frac{1}{\tau}) = \sqrt{\tau_2}\eta(\tau)$ we derive that for $q \sim 1$, we can replace $\eta(\tau) \sim (\tau_2)^{-1/2}e^{-i\pi/(12\tau)}$. Using this result, we can directly take the large c limit of equation (2.4.11) and deduce that $Z(\beta)$ takes the following form

$$Z(\beta) = e^{S_0+\beta E_0}\left(\frac{\pi}{\beta}\right)^{3/2}\exp\left(\frac{\pi^2}{\beta}\right). \tag{2.4.14}$$

Here we absorbed a (divergent) zero-point entropy S_0 and a zero-point energy E_0 contribution in the prefactor. This formula matches with the exact result found in [73, 84].

Alternatively, we can apply the modular transformation $\tau \to -1/\tau$ directly to the identity character $\chi_0(q)$ as a whole, and use the known formula for the modular S-matrix for $c > 1$ Virasoro CFT to decompose the result in terms of Virasoro characters in the dual channel. For this it is convenient to parametrize the highest weights Δ of

[5] We apologize to the reader for temporarily also using the symbol τ for the modular parameter $q = e^{2\pi i\tau}$ of the torus. Using equation (2.4.11), we can express the modular parameter τ in terms of the temperature β of the Schwarzian and the central charge c of the auxiliary 2D CFT via

$$\tau = \frac{12\pi i}{\beta c}. \tag{2.4.13}$$

the Virasoro representations and the central charge c as follows[6]

$$\Delta(P) = \frac{Q^2}{4} + P^2, \qquad\qquad c \,=\, 1 + 6Q^2 \,=\, 1 + 6\big(b + b^{-1}\big)^2. \tag{2.4.15}$$

The modular transformation rule of the Virasoro characters then reads

$$\chi_0\,(q) = \int_0^\infty dP\ S_0^P\ \chi_P(\tilde{q}), \qquad \tilde{q} \,=\, e^{-\frac{\beta c}{6}}, \qquad \chi_P(\tilde{q}) \,=\, \frac{\tilde{q}^{P^2}}{\eta(\tilde{\tau})}, \tag{2.4.16}$$

where the modular S-matrix is given by

$$S_0^P = 4\sqrt{2}\sinh\big(2\pi b P\big)\sinh\Big(\frac{2\pi P}{b}\Big). \tag{2.4.17}$$

We now set $k = \frac{P}{b}$, $E = b^{-2}(\Delta - \frac{c-1}{24}) = k^2$ and take the limit $b \to 0$ (which sends $c \to \infty$) while keeping k, E fixed. In this limit

$$S_0^P \,\sim\, 2k\sinh(2\pi k), \qquad\qquad \chi_P(\tilde{q}) \,\sim\, e^{-\beta k^2}. \tag{2.4.18}$$

The second formula has a clear physical significance. The large c limit sends $\tilde{q} \to 0$, which turns the operator $\tilde{q}^{L_0}$ into a projection operator on the lowest energy state in the given channel. Combining (2.4.11), (2.4.16) and (2.4.18) we obtain that

$$Z(\beta) = \int_0^\infty d\mu(k)\, e^{-\beta E(k)}, \qquad\qquad d\mu(k) = d(k^2)\sinh(2\pi k), \tag{2.4.19}$$

reproducing the result obtained in [73]. The answer for arbitrary C can be found by dimensional analysis or simply replacing $E(k) = k^2 \to k^2/2C$.

While the explicit formula (2.4.19) for the spectral density is not a new result, our derivation provides a new and useful perspective on the Schwarzian theory. Specifi-

[6]This parametrization is familiar from Liouville CFT. We emphasize, however, that in this section we are using completely general properties of genus one Virasoro characters.

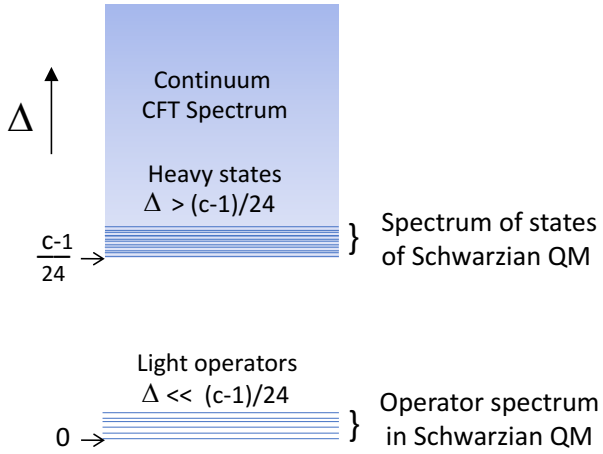

Figure 2.2: The spectrum of states in the Schwarzian theory arise from the CFT spectrum of states with conformal dimension $\Delta = \frac{c-1}{24} + b^2 E$, in the limit $b \to 0$. The operators in the Schwarzian are all light CFT operators with conformal dimension $\Delta = \ell$.

cally, it indicates that the 1D model arises as a special $c \to \infty$ limit of 2D Virasoro CFT, in which we only keep the states with conformal dimensions Δ close to the threshold $\Delta_c = \frac{c}{24}$ (Figure 2.2).

The above modular bootstrap argument identifies a natural spectral density on the space of Virasoro representations, given by the modular S-matrix element S_0^P [85]. This spectral density is not a specific property of a particular 2D CFT, but a universal measure analogous to the Plancherel measure on the space of continuous series representations of $SL(2,\mathbb{R})$. This measure is defined for any value of the central charge c. We have shown that, after taking the large c limit while zooming in close to $\Delta_c = \frac{c-1}{24}$, it coincides with the exact spectral density of the Schwarzian theory. In the following sections we will generalize this observation with the aim of studying correlation functions.

2.4.2 Spectral density from ZZ branes

As further preparation for the study correlation functions, it is useful to derive the formula for the spectral density from yet another slightly different perspective. As

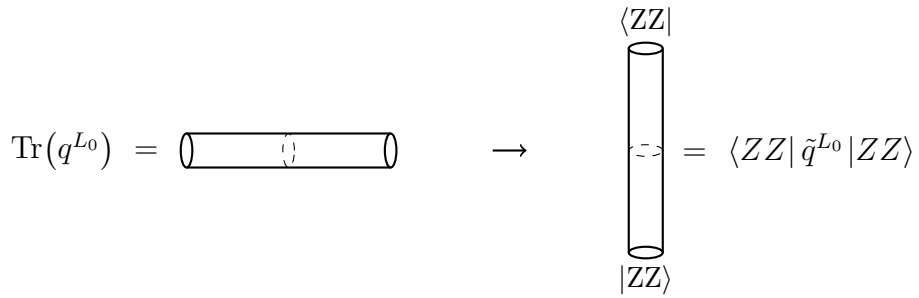

Figure 2.3: The identity character can be represented as the annulus partition sum of the Virasoro CFT, or by using channel duality, as the transition amplitude between two ZZ boundary states.

mentioned above, the identity character $\chi_0(q)$ represents the chiral genus one partition function of the identity sector of the Virasoro CFT. Alternatively, we can identify $\chi_0(q)$ with the partition function of the Virasoro CFT on the annulus. This annulus partition function is equal a trace over an open string sector of the Virasoro CFT, or by using channel duality, as the transition amplitude between two ZZ boundary states [86–88].

$$\chi_0(q) = \langle ZZ|\tilde{q}^{L_0}|ZZ\rangle. \tag{2.4.20}$$

The Schwarzian theory arises in the limit $q \to 1$, which in the dual closed string channel corresponds to the limit $\tilde{q} \to 0$, as shown in Figure 2.3. Note that the insertion of the ZZ branes cuts the thermal circle of the Schwarzian theory into two halves.[7]

The ZZ boundary state is given as an integral over Ishibashi boundary states [87, 88][8]

$$|ZZ\rangle = \int_0^\infty dP\, \Psi_{\mathrm{ZZ}}(P)\, \|P\rangle\!\rangle, \qquad \Psi_{\mathrm{ZZ}}(P) = \frac{2\pi i P}{\Gamma(1-2ibP)\Gamma(1+\frac{2iP}{b})}. \tag{2.4.21}$$

[7] This approach to the geometric quantization of the Virasoro group seems related to the one put forward in [89] for compact groups, but using a topological theory instead of a CFT.

[8] Here and in the following, we drop irrelevant overall constant factors.

In the limit we are considering the boundary states are associated to a circle with a radius that goes to zero (if we map the cylinder to the complex plane) and this allows us to approximate $\|P\rangle\!\rangle \to |P\rangle$. This is the main feature that will allow us later to compute correlation functions since it can be used to turn a correlation function between ZZ-branes into an integral of a correlation function on the sphere. Using this and taking $\tilde{q} = e^{-\beta/b^2}$, where β is the temperature of the Schwarzian theory, the partition function becomes

$$Z = \int_0^\infty dP \; |\Psi_{\rm ZZ}(P)|^2 \; e^{-\beta \frac{P^2}{b^2}}, \qquad |\Psi_{\rm ZZ}(P)|^2 = \sinh\big(2\pi b P\big) \sinh\Big(\frac{2\pi P}{b}\Big). \tag{2.4.22}$$

For small b this integral is dominated by states with P of order b. Therefore we define $P = kb$ and take the $b \to 0$ limit; we recover the result (2.4.19).

2.5 Schwarzian correlators from ZZ branes

In this section we will exploit the relationship between the Schwarzian theory and Virasoro CFT to compute finite temperature correlation functions of $SL(2,\mathbb{R})$ invariant operators in the Schwarzian theory. Here we will explain mainly how these correlators are related to Liouville theory. In the next chapter we will give the details about how to go from the concepts of this section to the concrete results summarized in 2.2.

The simplest such operator is the Schwarzian itself. Its correlation functions are completely fixed by symmetries and are described in Appendix A of [51].

A more interesting class of correlation functions are those involving the bi-local operators

$$\mathcal{O}_\ell(\tau_1, \tau_2) \equiv \left(\frac{\sqrt{f'(\tau_1) f'(\tau_2)}}{\frac{\beta}{\pi} \sin \frac{\pi}{\beta} [f(\tau_1) - f(\tau_2)]} \right)^{2\ell}. \tag{2.5.1}$$

These operators naturally live on the 2D space $\mathcal{K}$ parametrized by pairs of points (τ_1, τ_2) on the thermal circle. We will call $\mathcal{K}$ kinematic space, since it plays an

analogous geometrical role as the kinematic space associated with 2D holographic CFTs [90, 91].

To exhibit the geometry of kinematic space $\mathcal{K}$, let us – motivated by the form (2.5.1) of the bi-local operators – associate to any point $(u, v) \in \mathcal{K}$ a classical field $\phi_{cl}(u, v)$ via

$$e^{\phi_{cl}(u,v)} = \frac{\sqrt{f'(u)f'(v)}}{\frac{\beta}{\pi}\sin\frac{\pi}{\beta}[f(u) - f(v)]}. \tag{2.5.2}$$

This field satisfies the Liouville equation

$$\partial_u \partial_v \phi_{cl}(u, v) = e^{2\phi_{cl}(u,v)}. \tag{2.5.3}$$

Hence kinematic space $\mathcal{K}$ naturally comes with a constant curvature metric $ds^2 = e^{2\phi(u,v)}dudv$, and looks like a hyperbolic cylinder with an asymptotic boundary located at $u = v$. Note, however, that the metric on kinematic space is now a dynamical quantity that depends on the dynamical diffeomorphism $f(\tau)$.

From the saddle-point solution (2.5.2) for the field ϕ we see that the Liouville vertex operators $e^{2\ell\phi(u,v)}$ and the bi-local operators $\mathcal{O}_\ell(\tau_1, \tau_2)$ placed between two ZZ branes become identical, if we identify $u = \tau_1$ and $v = \tau_2$. Motivated by this, we will propose the following identification between the correlation functions of both theories

Insertion of $\mathcal{O}_\ell(\tau_1, \tau_2)$ in Schwarzian $\quad\leftrightarrow\quad$ Insertion of $V_\ell = e^{2\ell\phi(\tau_1,\tau_2)}$ in Liouville

In the next chapter we will present detailed evidence in support of this proposal by deriving the results in section 2.2.

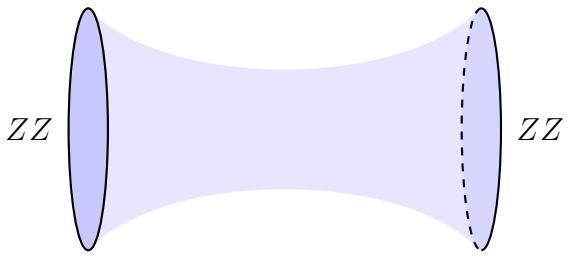

Figure 2.4: Geometry of the classical Liouville background between two ZZ branes.

2.5.1 ZZ branes and kinematic space

Given the similarity between the two geometric structures, it is tempting to look for a direct identification between the kinematic space $\mathcal{K}$ and the geometry of Liouville CFT bounded by two ZZ-branes. To make this idea more explicit, let us consider Liouville CFT with ZZ branes placed at the spatial positions $\sigma = 0$ and $\sigma = \pi$. The time direction is parametrized by τ. The action describing this system is

$$S = \frac{c}{192\pi} \int d\tau \int_0^\pi d\sigma \, \left[(\partial\phi)^2 + 4\mu e^{2\phi} \right] \tag{2.5.4}$$

For our application, the only role of the Liouville CFT is to provide a convenient geometrical description of the Virasoro partition function and conformal blocks. Indeed, Liouville theory is known to be equivalent to the geometric Lagrangian associated with the symplectic form ω on Diff(S^1) quoted in the previous section.[9]

We introduce the light-cone coordinates $u = \tau + \sigma$ and $v = \tau - \sigma$. We are interested in the limit $c \to \infty$. In this limit, the functional integral localizes on the space of classical solutions to the Liouville equation of motion. The boundary conditions of ϕ are that the regions near $\sigma = 0$ and $\sigma = \pi$ corresponds to the asymptotic regions of a hyperbolic cylinder. It is shown in [92] that the lowest energy solution

[9]The parameters $Q = b + b^{-1}$ and P used in the expressions (2.4.15) of the central charge c and the conformal dimension Δ are naturally identified with the background charge of the Liouville CFT and the 'Liouville momenta' of the vertex operators V_P with conformal dimension Δ.

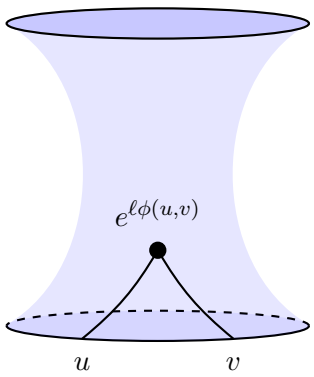

Figure 2.5: The kinematic space of the Schwarzian theory. The bi-local operator (2.5.1) in the 1D QM is represented by a local Liouville CFT vertex operator in the 2D bulk. The boundary of the kinematic space corresponds to the limit where the two end-points of the bi-local operator coincide.

is $4\mu^4 e^{2\phi} = \sin^{-2}\sigma$. Written in the form $ds^2 = e^{2\phi}dudv$ this describes a hyperbolic geometry of the form shown in Figure 2.4.

As explained e.g. in [93], the most general classical solution of Liouville theory can be obtained by starting with a representative $\phi(u, v)$ for a given conformal class and then apply a general conformal transformation $e^{2\phi(u,v)} \to f'(u)f'(v)e^{2\phi(f(u),f(v))}$. The most general solution thus takes the form given in equation (2.5.2), after performing a rescaling that maps the distance between the ZZ-branes from π to $\beta/2$. These solutions are all isomorphic to the geometry shown in Figure 2.5. We can interpret this 2d space as a kinematic space of the Schwarzian theory. Note, however, that in our case, the kinematic space is in fact dynamical.

Finally, we remark that the equivalence between the Schwarzian and the large c limit of Liouville CFT is of course not surprising. It is well-known that the Liouville stress tensor $T = \frac{1}{2}(\phi')^2 + \phi''$ reduces to the Schwarzian derivative when evaluated on a general classical solution of the form (2.5.2). This observation can be used to show that the Liouville lagrangian in a combined large c and DLCQ limit reduces to the Schwarzian action.

2.6 Supersymmetric Schwarzian

In the previous sections we presented a picture where the Schwarzian theory is completely solved in terms of known objects of 2D Liouville theory. In this section we will generalize these arguments to the supersymmetric cases. These theories can likewise be realized as the low energy effective theory of certain supersymmetrized SYK models [94]. For the $\mathcal{N}=1$ Schwarzian theory it is also known how it arises from a Jackiw-Teitelboim supergravity approach [95].

2.6.1 $\mathcal{N}=1$ Schwarzian theory

The super-Schwarzian is defined in $\mathcal{N}=1$ (τ,θ) superspace by:

$$\mathrm{Sch}(\tau) \equiv \mathrm{Sch}_f(\tau) + \theta \mathrm{Sch}_b(\tau) = \frac{D^4\theta'}{D\theta} - 2\frac{D^3\theta' D^2\theta'}{(D\theta')^2}, \tag{2.6.1}$$

with $D = \partial_\theta + \theta\partial_\tau$ the superderivative and $\theta' = \sqrt{\partial_\tau f}\left(\theta + \eta + \frac{1}{2}\theta\eta\partial_\tau\eta\right)$ as defined in [96,97] for the reparametrization f and its superpartner η. Via the same arguments as for the bosonic theory, we can view the super-Schwarzian theory as the $c\to\infty$ limit of $\mathcal{N}=1$ super-Liouville theory between a pair of ZZ-branes. As usual, one has different sectors depending on the fermionic boundary conditions both between the ZZ-branes (open channel) and along the small circle (closed channel). This gives four possibilities NS, R, $\widetilde{NS}$ or $\widetilde{R}$, where the tilde means that we insert a $(-1)^F$ in the partition function for the corresponding sector.

From the 2D Liouville perspective, different choices of brane configurations and different sectors correspond to the quantization of different coadjoint orbits. The one relevant for the application of the $\mathcal{N}=1$ Schwarzian as a low energy theory is

$$\mathrm{Diff}\left(S^{1|1}\right)/\mathrm{OSp}(1|2). \tag{2.6.2}$$

The path integral over this space was formulated and studied in [94] and [73]. This space is parametrized by a bosonic mode $f(\tau)$ associated to reparametrizations and a fermionic mode $\eta(\tau)$. From the 2D perspective it will turn out the relevant sector is $\widetilde{NS}$. Following the same procedure as in the construction of bosonic branes in Liouville one can solve the modular bootstrap to find the exact partition function associated to ZZ-branes in this section [98, 99]. For the $\mathcal{N}=1$ case it is still given by the identity character

$$Z_{\mathcal{N}=1} = \chi_0^{\widetilde{NS}}(q) = \mathrm{Tr}_{\mathrm{NS}}(-1)^F q^{L_0-\frac{c}{24}} = q^{-\frac{c-1}{24}}\ (1+q)\sqrt{\frac{\theta_4(\tau)}{\eta(\tau)^3}}. \tag{2.6.3}$$

Taking a parametrization similar to the bosonic case $q = e^{-\frac{48\pi^2}{\beta c}}$ and the limit $c \to \infty$ we obtain

$$Z_{\mathcal{N}=1} = e^{S_0^{\mathcal{N}=1}}\ \left(\frac{\pi}{\beta}\right)^{1/2} \exp\Big(\frac{\pi^2}{\beta}\Big), \tag{2.6.4}$$

where $S_0^{\mathcal{N}=1}$ denotes the zero-point entropy of the system. It is possible to see explicitly from (2.6.3) that because of supersymmetry, we obtain a vanishing zero-point energy $E_0^{\mathcal{N}=1} = 0$, although the zero-point entropy is still divergent $S_0^{\mathcal{N}=1} \sim \log b$. The modular transformation of this character automatically gives the exact density of states of the theory

$$\chi_0^{\widetilde{\mathrm{NS}}}(q) = \int_0^\infty dP\ S_0^P\ \chi_P^{\mathrm{R}}(\tilde{q}), \qquad \tilde{q} = e^{-\frac{\beta c}{12}}, \qquad \chi_P(\tilde{q}) = \sqrt{\frac{\theta_4(\tilde{\tau})}{\eta(\tilde{\tau})}}\frac{\tilde{q}^{P^2}}{\eta(\tilde{\tau})}, \tag{2.6.5}$$

where the modular S-matrix corresponding to the $\mathcal{N}=1$ extension of the Virasoro algebra is given by

$$S_0^P = 4\cosh\big(2\pi b P\big)\cosh\Big(\frac{2\pi P}{b}\Big). \tag{2.6.6}$$

Notice that the modular transformation turns the $\widetilde{NS}$ sector into the R-sector. Taking the appropriate limit to recover the Schwarzian theory gives a density of states

$$Z_{\mathcal{N}=1}(\beta) = \int_0^\infty d\mu(k)\, e^{-\beta E(k)}, \qquad d\mu(k) = dk\cosh(2\pi k), \tag{2.6.7}$$

which matches the result found in [73].

The modular bootstrap of $\mathcal{N}=1$ super-Liouville also provides an expression for the ZZ-brane wavefunction. Moreover, a generalization of the DOZZ formula which gives the OPE coefficients of local operators is also known. Combining these two pieces of information, in the same way as was done for the bosonic case, we can obtain correlation functions of local operators between the branes [10]. The details and outcomes of these calculations can be found in Appendix C of [51].

The main observable is a $\mathcal{N}=1$ generalization of the one studied in the bosonic case, which we denote by

$$\mathcal{O}_\ell(\tau_1,\tau_2) \equiv \left(\frac{\sqrt{f'(\tau_1)f'(\tau_2)}}{\frac{\beta}{\pi}\sin\frac{\pi}{\beta}[f(\tau_1)-f(\tau_2)]}\right)^{2\ell} + \text{(fermion bilinears)}. \tag{2.6.8}$$

The explicit form of the extra fermionic terms is given in Appendix C of [51]. The exact expectation value of this operator $G_\ell^\beta(\tau_1,\tau_2) = \langle \mathcal{O}_\ell^{\mathcal{N}=1}(\tau_1,\tau_2)\rangle$ is given by

$$\begin{aligned} G_\ell^\beta(\tau_1,\tau_2) \;=\; & \frac{2e^{-\frac{\pi^2}{\beta}}}{\pi^{5/2}\beta^{-1/2}}\int dk_1 dk_2\,\cosh(2\pi k_1)\cosh(2\pi k_2)\, e^{-\tau k_1^2-(\beta-\tau)k_2^2} \\ & \times\left(\frac{\Gamma\big(\frac{1}{2}+\ell\pm i(k_1-k_2)\big)\Gamma\big(\ell\pm i(k_1+k_2)\big)}{\Gamma(2\ell)} + (k_2\to -k_2)\right) \end{aligned} \tag{2.6.9}$$

where $\tau=\tau_{12}$. The two-point function of its superpartner can also be computed, and we refer to Appendix C of [51] for the result.

[10] The only interesting correlator is when a NS vertex operator is inserted, as inserting one R vertex operator yields zero, by (spacetime) fermion number conservation.

Stress tensor insertions in Liouville theory lead to (the bosonic piece of) super-Schwarzian insertions that are dealt with completely analogously as in the bosonic case, and leads to the constant energy $\langle \mathrm{Sch}_b(\tau)\rangle = \frac{1}{\beta} + \frac{2\pi^2}{\beta^2}$. The fermionic piece $\mathrm{Sch}_f(\tau)$ analogously arises from the Liouville supercurrent T_F (with R- boundary conditions along the circle) and has a zero one-point function due to worldsheet fermion conservation. Its two-point function does not vanish, and is just as the bosonic stress tensor two-point function constant up to contact terms. The constant piece is readily seen to be the square root of the corresponding bosonic piece, due to $G_0^2 = L_0$ in the parent 2d theory. Importantly, it requires the same $1/b^2$ rescaling to define a finite quantity: $T_F(w) \to \frac{1}{2b^2}\mathrm{Sch}_f(\tau)$, consistent with 1d supersymmetry: $T_F(w) + \theta T(w) \to \mathrm{Sch}_f(\tau) + \theta \mathrm{Sch}_b(\tau)$.

Going beyond the two-point function, one finds again a Feynman diagram decomposition which is structurally identical to the bosonic case. The spectral measure now takes the form

$$d\mu(k) = dk \cosh(2\pi k), \tag{2.6.10}$$

while the vertices for bosonic and superpartner insertions are respectively given by

$$\gamma_\ell(k_1,k_2)^2 = \frac{\Gamma\big(\frac{1}{2}+\ell \pm i(k_1-k_2)\big)\Gamma\big(\ell \pm i(k_1+k_2)\big) + (k_2 \to -k_2)}{2\Gamma(2\ell)}, \tag{2.6.11}$$

$$\gamma^\Psi_\ell(k_1,k_2)^2 = \frac{(k_1+k_2)^2\Gamma\big(\frac{1}{2}+\ell \pm i(k_1-k_2)\big)\Gamma\big(\ell \pm i(k_1+k_2)\big) + (k_2 \to -k_2)}{2\Gamma(2\ell)}. \tag{2.6.12}$$

The R-matrix should be computed by taking the Schwarzian limit of the $U_q(\mathfrak{osp}(1|2))$ quantum group 6j-symbols for four Ramond continuous near-parabolic insertions and two light NS insertions. While several results are known on this object, the fusion matrix with this specific configuration is not yet available [100, 101].

Finally, we briefly comment on the possibility of considering other fermionic boundary conditions. Using either the characters or the known wavefunctions, one

Sector	$2d$	$1d$
NS	$\mathrm{Tr}_{NS} q^{L_0 - c/24}$	bosonic
$\widetilde{NS}$	$\mathrm{Tr}_{NS}(-)^F q^{L_0 - c/24}$	Z
R	$\mathrm{Tr}_{R} q^{L_0 - c/24}$	bosonic
$\widetilde{R}$	$\mathrm{Tr}_{R}(-)^F q^{L_0 - c/24}$ = Witten index = 0	Witten index = 0

Table 2.1: Table of 2D boundary conditions for supersymmetric Liouville versus the 1D theory that remains in the Schwarzian limit.

immediately deduces that the spectral density for both the R- and the NS-sector is given by

$$\rho(E) = \sinh(2\pi\sqrt{E}). \tag{2.6.13}$$

The characters and their 1d Schwarzian limit are summarized in table 2.1. Only one interesting supersymmetric sector remains in the 1D limit, and that is the one of the $\mathcal{N} = 1$ Schwarzian theory introduced above. For NS- and R-sectors, no fermionic zero-mode along the circle survives and these sectors then give non-supersymmetric 1D thermal models, identical to the bosonic theory. The partition function of the $\widetilde{R}$-sector contains periodic zero-modes along the circle and periodic fermionic boundary conditions along the Schwarzian thermal circle, identifying it as the Witten index both in 2D and in 1D.

2.6.2 $\mathcal{N} = 2$ Schwarzian theory

In this section we want to identify which sector of $\mathcal{N} = 2$ super-Liouville generates the path integral over the orbit

$$\mathrm{Diff}\big(S^{1|2}\big)/\mathrm{OSp}(2|2), \tag{2.6.14}$$

relevant for the $\mathcal{N} = 2$ super-Schwarzian theory [94, 97].

The character of the identity representation is given by

$$\mathrm{ch}_{\widetilde{NS}}(q,y) = \mathrm{Tr}_{\mathrm{NS}}(-1)^F q^{L_0-\frac{c}{24}} y^{\ell_0} = \frac{e^{\pi i \hat{c}\frac{z^2}{\tau}}\, q^{-\frac{1}{4b^2}}(1-q)}{(1-yq^{\frac{1}{2}})(1-y^{-1}q^{\frac{1}{2}})}\frac{\theta_3(q,-y)}{\eta(\tau)^3}, \tag{2.6.15}$$

where $\hat{c} = \frac{c}{3} = 1 + \frac{2}{b^2}$. A special feature of the $\mathcal{N}=2$ case is that this is not equal to the partition function of a pair of ZZ-branes anymore. In [102] T. Eguchi and Y. Sugawara solved the modular bootstrap for $\mathcal{N}=2$ super-Liouville, see also [103]. They found that, in order to do this, one is forced to take a sum over spectral flow. Moreover, the construction only works for rational central charge $\hat{c} = 1 + \frac{2K}{N}$ for any $K, N \in \mathbb{Z}$. The partition function of the pair of ZZ-brane is equal to the extended character which is defined as

$$Z_{\mathcal{N}=2} = \chi_0^{\widetilde{NS}}(q,y) = \sum_{n\in N\mathbf{Z}} q^{\frac{\hat{c}}{2}n^2} y^{\hat{c}n} \mathrm{ch}_{\widetilde{NS}}(q,y). \tag{2.6.16}$$

We will take N to be finite and $K \to \infty$ to take the $c \to \infty$ limit. Taking the limit $\tau \to \frac{2\pi}{\beta}b^2$ and $z = \alpha\tau$ with α fixed, equation (2.6.16) becomes

$$Z_{\mathcal{N}=2} = \frac{4}{\pi}\sum_{n\in N\mathbf{Z}} \frac{\cos\pi(\alpha+n)}{1-4(\alpha+n)^2}\, e^{\frac{\pi^2}{\beta}\left(1-4(\alpha+n)^2\right)}. \tag{2.6.17}$$

This expression coincides with the exact partition function found in [73] if we identify α to be proportional to the chemical potential. The parameter N corresponds to the size of the compact boson present in the $\mathcal{N}=2$ multiplet. From a path integral point of view (as opposed to invoking the modular bootstrap) the same happens in $\mathcal{N}=2$ super-Liouville, since besides the field ϕ we have another boson which is compact, usually denoted Y, with a coupling similar to bosonic sine-Liouville theory. Finally, this parameter also corresponds to the R-charge of the fermions in the SYK model.

As anticipated, we find that all divergences in this limit disappear. We find $E_0^{\mathcal{N}=2} = 0$ due to supersymmetry as in the $\mathcal{N}=1$ case, but we also find a finite

zero-point entropy $S_0^{\mathcal{N}=2} = \log \frac{4}{\pi}$. This seems to indicate that even though bosonic and $\mathcal{N} = 1$ Schwarzian theory should be interpreted as a low energy effective theory of a QM system, the $\mathcal{N} = 2$ super-Schwarzian might be a well-defined theory by itself.

Following the procedure applied to the bosonic case, we can read off the density of states of the theory from the modular properties of the identity character. The modular transformation of the identity character in the $\widetilde{NS}$ sector is given by

$$\begin{aligned} \mathrm{ch}_{\widetilde{NS}}\Big(\frac{-1}{\tau}, \frac{z}{\tau}\Big) \;=\; & \int_{-\infty}^{\infty} d\omega \int_0^{\infty} dp \frac{\sinh(\pi \mathcal{Q} p)\sinh(2\pi \frac{p}{\mathcal{Q}})}{\mathcal{Q}\big|\sinh \pi\left(\frac{p}{\mathcal{Q}} + i\frac{\omega}{\mathcal{Q}^2}\right)\big|^2} \mathrm{ch}^{\mathrm{R}}_{\mathrm{cont}}(p, \omega; \tau, z) \\ & + 2\sum_{n\in\mathbf{Z}} \int_{-\frac{1}{2}}^{\frac{1}{2}} d\omega \;\; \cos \pi\omega \;\; \mathrm{ch}^{\mathrm{R}}_{\mathrm{BPS}}(\omega, n; \tau, z), \end{aligned} \tag{2.6.18}$$

where $\mathcal{Q}^2 = 2K/N$. The integral is over the continuous representation with Liouville momenta p and R-charge ω in the R-sector. The second line corresponds to a sum over BPS states in the R-sector. These can have arbitrary charge ω but the $\mathcal{N} = 2$ super-Virasoro algebra implies that they have a fixed dimension $\Delta^{\mathrm{R}}_{\mathrm{BPS}} = \frac{c}{24}$ independent of the charge. We give some more details of these representations and their characters in Appendix C of [51]. A similar formula also exists for the modular transformation of the extended characters

$$\begin{aligned} \chi_{\widetilde{NS}}\Big(\frac{-1}{\tau}, \frac{z}{\tau}\Big) \;=\; & \frac{1}{N} \sum_{m\in\mathbf{Z}_{2NK}} \int_0^{\infty} dp \frac{\sinh(\pi \mathcal{Q} p)\sinh(2\pi \frac{p}{\mathcal{Q}})}{\mathcal{Q}\big|\sinh \pi\left(\frac{p}{\mathcal{Q}} + i\frac{\omega}{\mathcal{Q}^2}\right)\big|^2} \; \chi^{\mathrm{R}}_{\mathrm{cont}}\Big(p, \frac{m}{N}; \tau, z\Big) \\ & + \frac{2}{N} \sum_{n\in\mathbf{Z}} \sum_{m=1}^{N-1} \;\; \sin \pi\frac{m}{N} \;\; \chi^{\mathrm{R}}_{\mathrm{BPS}}\Big(\frac{m}{N} - \frac{1}{2}, n; \tau, z\Big). \end{aligned} \tag{2.6.19}$$

At finite N the expressions look similar but now instead of having an integral over charges we have a sum over discrete charges. This was one of the original motivation to take spectral flow into account, since having a continuum of charges does not seem physical.

Before writing down the density of states as a function of energy and charge we will restrict to the case $\alpha = 0$ to match (2.6.19) with the expression found in [73]. If we take (2.6.19) in the appropriate limit, and perform the integrals over ω, using some results left for the appendix, we directly obtain

$$\rho_{\alpha=0}(E) = \sum_{n\in\mathbf{Z}} \frac{2\cos\pi n}{1-4n^2}\left(\frac{\sqrt{1-4n^2}I_1\big(2\pi\sqrt{(1-4n^2)E}\big)}{\sqrt{E}} + \delta(E)\right), \tag{2.6.20}$$

where the integral over the Bessel function comes from the integral over non-BPS states and the delta function comes from the BPS states. While this is obtained in [73] by performing an inverse Laplace transform, in our approach both terms have a physical origin. For arbitrary α, (2.6.19) gives the following density of states as a function of both energy and charge

$$\begin{aligned} Z(\beta,\alpha) \;=\; & \frac{1}{N}\sum_{m\in\mathbf{Z}}\int_{\frac{m^2}{4N^2}}^{\infty}\frac{dE}{8E}\sinh\Big(2\pi\sqrt{E-\tfrac{m^2}{4N^2}}\Big)\,e^{-\beta E}\,\big(y^{\frac{m}{N}+\frac{1}{2}}+y^{\frac{m}{N}-\frac{1}{2}}\big) \\ & + \frac{2}{N}\sum_{m=1}^{N-1}\;\int_0^{\infty}dE\;\sin\pi\frac{m}{N}\;\delta(E)\;e^{-\beta E}\;y^{\frac{m}{N}-\frac{1}{2}}. \end{aligned} \tag{2.6.21}$$

From this expression we can obtain the density of states $\rho(E,Q)$. If we redefine the chemical potential such that charge is either integer or half-integer $y \to y^N$ and shift m in order to get a dependence y^Q then we obtain

$$\rho_{\rm cont}(E,Q) \;=\; \frac{1}{8N}\frac{\sinh(2\pi\sqrt{E-E_0^+(Q)})}{E}\;\Theta(E-E_0^+(Q)) \;+\; \big(+\leftrightarrow-\big), \tag{2.6.22}$$

$$\rho_{\rm disc}(E,Q) \;=\; \delta(E)\;\frac{2}{N}\cos\pi\frac{Q}{N}\;\;\Theta(2|Q|-N), \tag{2.6.23}$$

where $\Theta(x)$ corresponds to the Heaviside step function and we defined the two charge-dependent threshold energies as following $E_0^{\pm}(Q) \equiv \big(\frac{Q}{2N}\pm\frac{1}{4}\big)^2$.

The modular transformation gives us explicit expressions for these densities which would be hard to find otherwise, agreeing with the DH calculation [73]. The zero

energy contribution from BPS states appears only for a finite charge range $2|Q| < \frac{N}{2}$. The continuous part of the spectrum consists of two terms that start contributing at different energies. The lowest one gives the minimum energy possible for the continuous spectrum with a fixed charge, which is

$$E_{\min}(Q) = \left(\frac{|Q|}{2N} - \frac{1}{4}\right)^2 . \tag{2.6.24}$$

Finally, depending on whether N is even or odd, the sum over charges is either over integer Q or half-integer Q respectively.

Having understood the relation between Liouville theory and the Schwarzian, we will derive correlators in the next chapter.

Chapter 3

Solving the Schwarzian Theory: Part II

In the previous chapter we describe the construction derived in [51] to relate the Schwarzian correlators to a limit of 2D Liouville CFT, and summarize the main results.

In this chapter we will present the details regarding the derivation of the correlators. We will begin by deriving time ordered two- and four-point functions in section 3.1.1.

Then, using known properties of Virasoro blocks we will derive the OTOC of the Schwarzian theory in section 3.2. This is important in its own right since it will allow us to understand gravitational bulk scattering for the Jackiw-Teitelboim dilaton-gravity theory in nearly AdS_2. In particular, we will propose a non-perturbative generalization of the 2D version of the Dray-'t Hooft S-matrix by identifying it with $SL(2,R)$ exchange algebra (through its $6j$-symbols) in section 3.3. We check this correspondence by comparing the large C semiclassical limit with the shockwave S-matrix.

We consider a final application of the exact correlators derived in this chapter by studying the large C and large ℓ limit of time-ordered correlators. In section 3.4 we give a simple picture of the bulk geometric backreaction due to such heavy operators.

3.1 Schwarzian Correlators

3.1.1 Two-point function

First we will focus on the expectation value of a single bi-local operator $G_\ell(\tau_1, \tau_2) = \langle \mathcal{O}_\ell(\tau_1, \tau_2) \rangle$, which is a natural observable as explained in the previous chapters. This corresponds to the gravitational dressing of a two-point function of local operators. Based on the proposal of [51] explained above

$$\text{Insertion of } \mathcal{O}_\ell(\tau_1, \tau_2) \text{ in Schwarzian } \leftrightarrow \text{ Insertion of } V_\ell = e^{2\ell\phi(\tau_1,\tau_2)} \text{ in Liouville}$$

we will compute the one-point function of the operator $V_\ell = e^{2\ell\phi(\tau_1,\tau_2)}$ between ZZ-branes. Via the method of images, we can map this one-point function to the chiral two-point function on a torus. There is no known closed expression for this two-point function for finite c. Nevertheless we will be able to compute it in the limit relevant for the comparison with the Schwarzian theory.

Using the known wavefunction (2.4.21) of the ZZ-branes and approximating the Ishibashi states by primary states we can write (dropping overall constant prefactors)

$$\langle ZZ|V_\ell(z,\bar{z})|ZZ\rangle = \int dP dQ \ \Psi^\dagger_{\text{ZZ}}(P)\Psi_{\text{ZZ}}(Q)\langle P|V_\ell(z = e^{\frac{\tau_1}{b^2}}, \bar{z} = e^{-\frac{\tau_2}{b^2}})|Q\rangle. \quad (3.1.1)$$

We are taking the limit $b \to 0$ in which the spatial circle in the closed string channel is going to zero. This enables us to use the minisuperspace approximation for the Liouville CFT wavefunctions, which in effect amounts to a truncation of the full CFT

to the zero-mode. Thus we can compute the correlation function in the following way

$$\langle ZZ|V_\ell|ZZ\rangle = \int dPdQ\ \Psi^\dagger_{ZZ}(P)\Psi_{ZZ}(Q)\langle P|e^{-(\beta-\tau)H}e^{2\ell\phi}e^{-\tau H}|Q\rangle, \tag{3.1.2}$$

where the external states are associated to a wavefunction of the Liouville zero mode

$$\Psi_P(\phi) = \langle\phi|P\rangle = \frac{2}{\Gamma\left(-\frac{2iP}{b}\right)}\ K_{2iP/b}\left(e^\phi\right). \tag{3.1.3}$$

This state has energy $E = P^2/b^2$. If we call $P = bk_2$ and $Q = bk_1$, the integral that gives the amplitude between states $|P\rangle$ and $|Q\rangle$ matches exactly with the $b \to 0$ limit of the DOZZ formula [104, 105]

$$\langle P = bk_2|e^{2\ell\phi}|Q = bk_1\rangle = \int d\phi\ \Psi^\dagger_P(\phi)\Psi_Q(\phi)e^{2\ell\phi} = \frac{\Gamma(\ell \pm i(k_1 \pm k_2))}{\Gamma(2ik_2)\Gamma(2ik_1)\Gamma(2\ell)}. \tag{3.1.4}$$

Combining this result with the known exact form (2.4.21) of the wavefunction of the ZZ-branes and dividing by the partition function, we obtain the following formula for the Euclidean two-point function of the Schwarzian theory

$$G^\beta_\ell(\tau_1,\tau_2) = \frac{\left(\frac{\beta}{2\pi^2 C}\right)^{3/2}}{2\sqrt{\pi}e^{\frac{2\pi^2 C}{\beta}}}\int d\mu(k_1)d\mu(k_2)\,e^{-|\tau|\frac{k_1^2}{2C}-(\beta-|\tau|)\frac{k_2^2}{2C}}\ \frac{\Gamma\left(\ell \pm i(k_1 \pm k_2)\right)}{(2C)^{2\ell}\Gamma(2\ell)} \tag{3.1.5}$$

where $\tau = \tau_{12}$, $d\mu(k) = dk^2\sinh(2\pi k)$ and the $\pm$ signs mean that one multiplies the Γ-functions with all combinations of signs.[1] In this final answer we reinserted the C dependence but in the rest of this chapter we will go back to units in which $C = 1/2$. This expression is valid for $-\beta < \tau < \beta$ and needs to be periodically continued beyond this interval. This was done for Euclidean time, to obtain the Lorenzian two-point function we need to Wick rotate τ to imaginary values which will be discussed shortly. If the Schwarzian is thought of as a low energy limit of the SYK model then

[1] $\Gamma\left(\ell \pm i(k_1 \pm k_2)\right) = \Gamma\left(\ell + i(k_1+k_2)\right)\Gamma\left(\ell + i(k_1-k_2)\right)\Gamma\left(\ell - i(k_1+k_2)\right)\Gamma\left(\ell - i(k_1-k_2)\right)$.

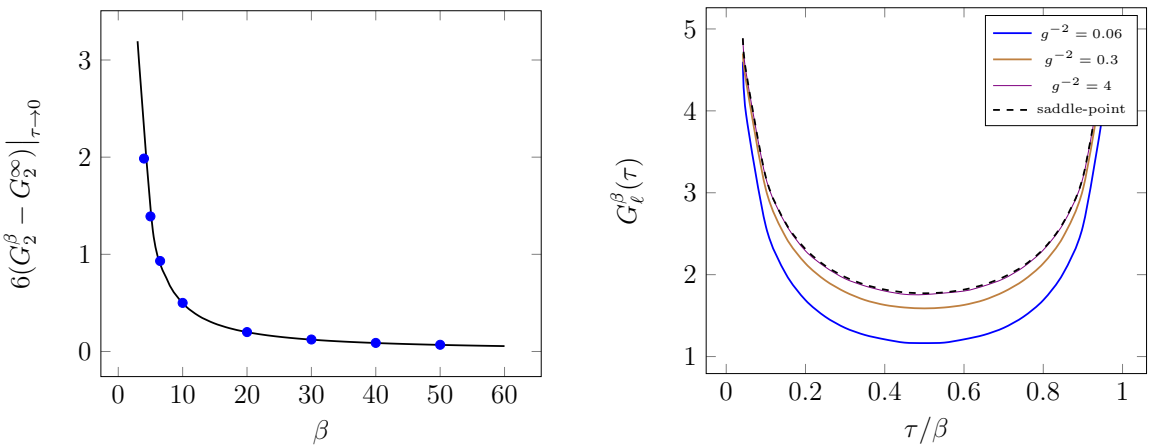

Figure 3.1: Left: Numerical evaluation of the $\tau \to 0$ limit of $6(G^\beta(\tau) - G^\infty(\tau))$ (blue dots), which coincides with $\langle\{\tan \frac{\pi f(\tau)}{\beta}, \tau\}\rangle$ (full black line). Right: Exact two-point function for $\ell = 1/4$, and different values of β. We indicate the parameter $g^{-2} = \frac{2\pi}{\beta}$.

$\ell = 1/q$ is the conformal dimension of the fermions in the theory, if the interaction involves q fermions.

In the remainder of this subsection we will check this result in special limiting regimes. First we can check that (3.1.5) behaves for $\tau_{12} \to 0$ as $G_\ell^\beta(\tau_1, \tau_2) = \tau_{12}^{-2\ell} + ...$ This is the expected behavior. We can also take the zero-temperature limit $\beta \to \infty$. In this limit, our two-point function reduces to

$$G_\ell^\infty(\tau_1, \tau_2) = \int dk^2 \sinh(2\pi k)\, e^{-|\tau| k^2} \frac{\Gamma^2(\ell + ik)\Gamma^2(\ell - ik)}{2\pi^2\, \Gamma(2\ell)}, \tag{3.1.6}$$

which coincides with the result found in [71, 72]. In particular this implies that in the zero-temperature limit the two-point function at large times $\tau \to \infty$ behaves as a power-law independently of ℓ as

$$G_\ell^\infty(\tau_1, \tau_2) = \frac{\Gamma(\ell)^4}{2^{2\ell}\Gamma(2\ell)} \frac{1}{\tau_{12}^{3/2}} + \dots\,, \quad \tau \to \infty. \tag{3.1.7}$$

This behavior matches with the numerical computation done in [71,72] using the SYK model.

For the case $\ell = 1$ we can go further, since we know that the next-to-leading order term for $\tau_{12} \to 0$ is given by the Schwarzian itself:

$$\left(\frac{\pi \sqrt{f'(\tau_1) f'(\tau_2)}}{\beta \sin \frac{\pi}{\beta}[f(\tau_1) - f(\tau_2)]} \right)^2 = \frac{1}{\tau_{12}^2} + \frac{1}{6} \left\{ \tan \frac{\pi f(\tau)}{\beta}, \tau \right\} + \dots \tag{3.1.8}$$

This will give us a non-trivial check on the temperature dependence of the exact two-point function. We can obtain the expectation value of the Schwarzian by taking derivatives of the partition function

$$\left\langle \left\{ \tan \frac{\pi f(\tau)}{\beta}, \tau \right\} \right\rangle = \frac{2\pi^2}{\beta^2} + \frac{3}{\beta} + \text{const.} \tag{3.1.9}$$

The constant factor depends in part on the zero-point energy. We can eliminate this factor by substracting the zero-temperature limit of the correlation function

$$\left. \frac{G_1^\beta(\tau) - G_1^\infty(\tau)}{1/6} \right|_{\tau \to 0} = \frac{2\pi^2}{\beta^2} + \frac{3}{\beta}. \tag{3.1.10}$$

We checked numerically that our formula matches this expectation, as shown in Figure 3.1.

We can also take the weakly coupled (large C) limit. In our conventions, since we are keeping C fixed, this limit is equivalent to taking $\beta \to 0$ with τ/β fixed. In this regime, quantum corrections are suppressed and correlation functions should be well-approximated by replacing the saddle-point solution

$$\mathcal{O}_\ell^{\text{cl}}(\tau_1, \tau_2) = \left(\frac{\pi}{\beta \sin \frac{\pi}{\beta} \tau} \right)^{2\ell}. \tag{3.1.11}$$

We have checked that our exact result (3.1.5) indeed has this property, see Figure 3.1. In the next chapter we will focus on the semiclassical limit of the results found in this section and we will present details of how to derive (3.1.11).

Real-time two-point function and the thermofield double

To conclude this section, we will make some remarks on the real-time continuation and physical application of these results.

The two-point function (3.1.5) has a branch point at $\tau = 0$ and two branch cuts running on both sides along the real axis. This is because no spacelike separated points exist in 0+1D. This can then be periodically continued along the entire τ-axis (Figure 3.2), with periodic branch cuts.

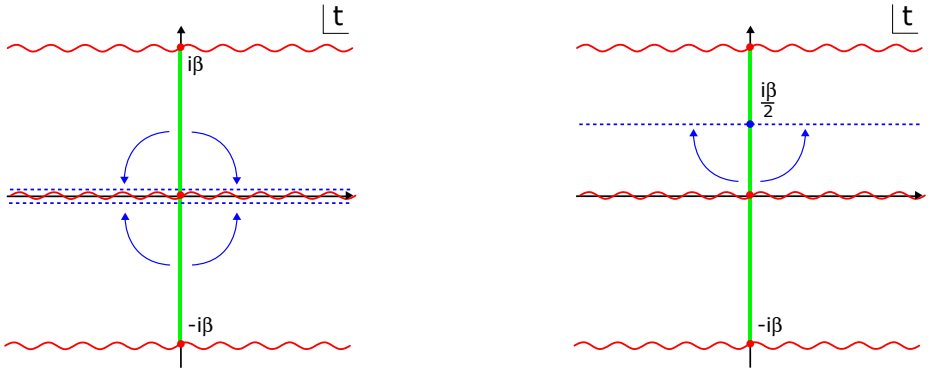

Figure 3.2: Left: Analytic structure of the two-point function. The green line represents the Euclidean regime. Time-ordered and anti-time-ordered Lorentzian two-point functions can be found by analytically continuing these expressions to respectively $t \pm i\epsilon$ (blue lines). Right: Relevant analytic continuation for the thermofield double two-point function.

In real time, two possible continuations exist by setting $i\tau \to t \pm i\epsilon$, where the $+$ sign is for $\tau > 0$ and the $-$ sign for $\tau < 0$. These correspond to Lorentzian time-ordered $G^+_\ell(t_1, t_2)$ and anti-time-ordered two-point functions $G^-_\ell(t_1, t_2)$ respectively, for $t_1 > t_2$ given as expectation values of the following bilocal operators:

$$\begin{aligned} \mathcal{O}^+_\ell(t_1, t_2) &= \langle \mathcal{O}_\ell(t_1)\mathcal{O}_\ell(t_2)\rangle_{\text{CFT}}\,, \\ \mathcal{O}^-_\ell(t_1, t_2) &= \langle \mathcal{O}_\ell(t_2)\mathcal{O}_\ell(t_1)\rangle_{\text{CFT}}\,, \end{aligned} \tag{3.1.12}$$

where $\mathcal{O}_\ell^\pm(t_1,t_2) \equiv \left(\frac{\sqrt{f'(t_1)\,f'(t_2)}}{\frac{\beta}{\pi}\sinh\frac{\pi}{\beta}[f(t_1)-f(t_2)]\pm i\epsilon}\right)^{2\ell}$. The explicit expression for $G_\ell^\pm(t)$ reads (ignoring the constant prefactor, and with $\gamma_\ell(k_1,k_2)$ as given in equation (2.2.7))

$$G_\ell^\pm(t) \;=\; \int d\mu(k_1)d\mu(k_2)\, e^{\pm itk_1^2-(\beta\pm it)k_2^2} e^{-\epsilon k_1^2-\epsilon k_2^2}\,\gamma_\ell(k_1,k_2)^2 \tag{3.1.13}$$

with Gaussian damping introduced by ϵ. The $\epsilon \to 0^+$ limit is well-defined for both cases, but in general different. This means the commutator of time-separated operators:

$$\mathcal{O}_\ell^+(t_1,t_2) - \mathcal{O}_\ell^-(t_1,t_2) = \langle[\mathcal{O}_\ell(t_1),\mathcal{O}_\ell(t_2)]\rangle_{\rm CFT}\,, \tag{3.1.14}$$

does not vanish in expectation values:

$$G_\ell^+(t_{12}) - G_\ell^-(t_{12}) = \left\langle \mathcal{O}_\ell^+(t_1,t_2) - \mathcal{O}_\ell^-(t_1,t_2)\right\rangle \neq 0. \tag{3.1.15}$$

This is as expected since all points are timelike separated on the 1D line. Likewise, one can consider other real-time two-point functions of interest, such as the retarded correlator: $G_\ell^{\rm ret}(t_1,t_2) = \left(G_\ell^+(t_1,t_2) + G_\ell^-(t_1,t_2)\right)\theta(t_{12})$.

The long-time behavior of these correlators is easy to determine due to destructive oscillations of the k_i-integrals, and gives (ignoring irrelevant prefactors)

$$G_\ell^\pm(t) \to \frac{1}{t^{3/2}}\frac{1}{(\beta\pm it)^{3/2}}\beta^{3/2}. \tag{3.1.16}$$

At intermediate times (or zero temperature) for which $1 \ll t \ll \beta$, $G_\ell^\pm(t) \sim 1/t^{3/2}$ and at long times $t \gg \beta$, $G_\ell^\pm(t) \sim 1/t^3$. In either case, the correlator decreases monotonically to zero. Hence no Poincaré recurrences occur at very long times. The Schwarzian theory is rather peculiar from this perspective, as it has a continuum of states, thereby foiling the standard argument for recurrences, but its density of states or entropy do not exhibit a volume-divergence. Instead the divergence in the entropy

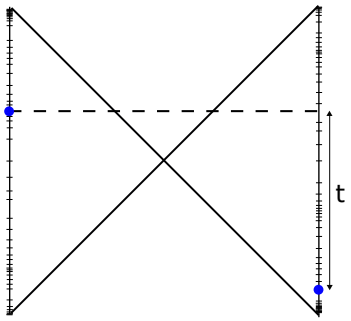

Figure 3.3: Two-point left-right correlator in a thermodouble system. The Schwarzian path integral contains time reparametrizations of the boundary lines that are constrained to start and end at the same points as the eternal black hole time coordinate. A sample clock-ticking configuration is drawn.

arises due to an infinite S_0 (which was irrelevant for our entire discussion), signaling that one needs to go back to its UV completion (e.g. SYK) to understand the very long time behavior of the theory.

Replacing $\tau \to \tau + \frac{\beta}{2}$ has the effect of moving one operator insertion to the thermal copy of the thermofield double, which in the small coupling (small C) limit is just the eternal AdS_2 black hole (Figure 3.3) [21]. We note that our discussion here does not assume a holographic bulk; in a sense we will see what can be deduced of the alleged bulk dual purely from the Schwarzian system. In real time

$$\langle \text{TFD}| \, \mathcal{O}_\ell^L \, (t_1) \, \mathcal{O}_\ell^R (t_2) \, |\text{TFD}\rangle = \left\langle \mathcal{O}_\ell \left(\tfrac{i\beta}{2} - t_1\right) \mathcal{O}_\ell (t_2) \right\rangle_{\text{CFT}} = \mathcal{O}_\ell \left(\tfrac{i\beta}{2} - t_1, t_2\right) \quad (3.1.17)$$

(the minus sign in front of t_1 on the right hand side corresponds to time running oppositely in the double, but can be ignored in this discussion) where the thermofield double state is

$$|\text{TFD}\rangle = \frac{1}{\sqrt{Z}} \sum_i e^{-\frac{\beta E_i}{2}} \, |*i\rangle_L \otimes |i\rangle_R \, . \quad (3.1.18)$$

When performing the Lorentzian real-time continuation, no branch cuts are encountered and G^+ and G^- coincide (see Figure 3.2). In particular the commutator vanishes, confirming that all points on opposite sides of the thermofield double are

spacelike separated. This indicates that the bulk spacetime has a horizon, and that looks identical to the eternal black hole space-time [21]. It is interesting that the causal structure of the dual bulk can be decoded from these correlation functions. Quantum fluctuations of the time reparametrization $f(\tau)$ in themselves are not sufficient to allow communication between both sides. This is of course expected, as to make the wormhole traversable, one would need to add an explicit interaction connecting the two copies of the thermofield double [106] [107]. Ignoring the prefactors, the real-time thermodouble correlator can immediately be written down:

$$G_\ell^{LR}(t) \;=\; \int d\mu(k_1) d\mu(k_2)\; e^{-\left(\frac{\beta}{2}+it\right)k_1^2-\left(\frac{\beta}{2}-it\right)k_2^2}\,\frac{\Gamma\big(\ell \pm i(k_1 \pm k_2)\big)}{\Gamma(2\ell)}. \tag{3.1.19}$$

Taking the small temperature limit, one obtains

$$G_\ell^{LR}(t) \;\to\; \frac{\beta^{3/2}}{\left(\frac{\beta}{2}-it\right)^{3/2}\left(\frac{\beta}{2}+it\right)^{3/2}} \;\to\; 0. \tag{3.1.20}$$

This behavior corresponds to the disappearance of left-right correlation in the extremal black hole limit, generalizing this statement from just the classical saddle point to the full quantum gravity regime.

3.1.2 Four-point function

Next we consider the time-ordered four point function, given by the two-point function of two bi-local operators.

$$G_{\ell_1\ell_2}(\tau_1,\tau_2,\tau_3,\tau_4) \;=\; \big\langle \mathcal{O}_{\ell_1}(\tau_1,\tau_2)\mathcal{O}_{\ell_2}(\tau_3,\tau_4)\big\rangle. \tag{3.1.21}$$

There are different choices for how to order the four different times. Here we will assume that the time instances are cyclically ordered via $\tau_1 < \tau_2 < \tau_3 < \tau_4$. In the

diagrammatic representation of the amplitudes, this ordering ensures that the legs of the two bi-local operators do not cross each other, as indicated in the left-hand side diagram of Figure 3.5.

We will compute this four-point function by applying the dictionary between the Schwarzian and 2D Liouville CFT. This leads us to consider the following two-point function of primary operators between two ZZ-branes

$$G_{\ell_1\ell_2} \;=\; \langle ZZ|V_{\ell_1}(z_1,\bar{z}_1)V_{\ell_2}(z_2,\bar{z}_2)|ZZ\rangle. \tag{3.1.22}$$

As explained above, this can be interpreted as a four point function (3.1.21) in the Schwarzian theory if we identify $z_1 \to \tau_2$, $\bar{z}_1 \to \tau_1$, $z_2 \to \tau_3$ and $\bar{z}_2 \to \tau_4$. For the time-ordered operator, the locations $(z_1, \bar{z}_1)$ and $(z_2, \bar{z}_2)$ are chosen to be timelike separated, as indicated on the left-hand side in Figure 3.4, so that their past lightcones do not intersect.

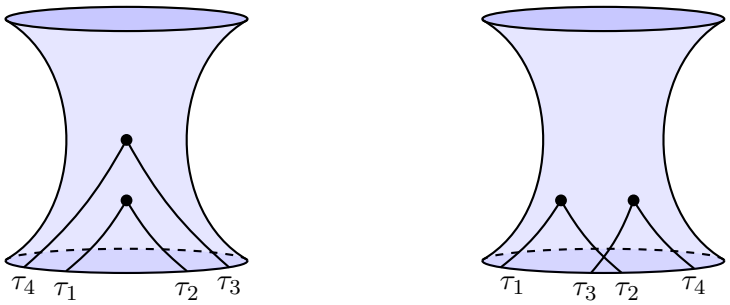

Figure 3.4: The four-point function in the Schwarzian theory corresponds to a two-point function of two bulk Liouville vertex operators. If the two bulk operators are timelike separated (left), the correlation function and the end-points of the two bi-local operators are time ordered. If the two bulk operators are spacelike separated (right), the legs of the bi-local operators cross each other. Both are thus related by the CFT monodromy matrix that relates the timelike separated and spacelike separated two-point functions.

As before, we can go to the closed string channel and write the four point function as

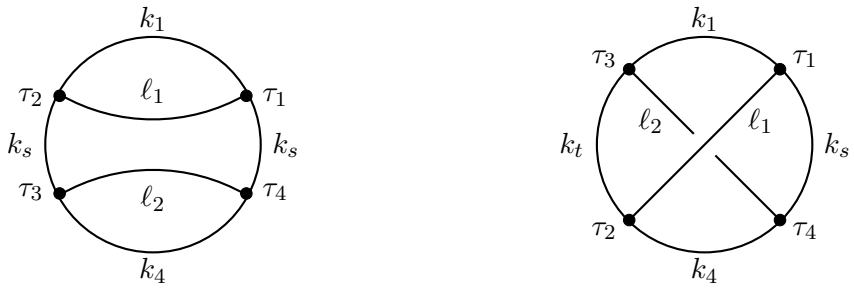

Figure 3.5: The diagrammatic representation of the two types of four-point functions. The left diagram depicts the time-ordered four-point function (3.1.21) with $\tau_1 < \tau_2 < \tau_3 < \tau_4$. The diagram on the right represents the out-of-time ordered four point function: in contrast with the geometric ordering, we assume that the four time instances are still ordered as $\tau_1 < \tau_2 < \tau_3 < \tau_4$.

$$G_{\ell_1\ell_2} = \int dP dQ\ \Psi^{\dagger}_{\rm ZZ}(P)\Psi_{\rm ZZ}(Q)\ \langle P|V_{\ell_1}(z_1,\bar{z}_1)V_{\ell_2}(z_2,\bar{z}_2)|Q\rangle. \tag{3.1.23}$$

In the Schwarzian limit we are allowed to replace the Ishibashi states $\|P\rangle\rangle$ by the corresponding primary states $|P\rangle$. The correlation function on the right-hand side is computed on the sphere and can be expanded in conformal blocks in the $V_{\ell_2}V_Q \to V_{\ell_1}V_P$ channel.

We thus arrive at the following representation for the time-ordered four point function in terms of 2D CFT data

$$\langle P|V_{\ell_1}(z_1,\bar{z}_1)V_{\ell_2}(z_2,\bar{z}_2)|Q\rangle\ = \tag{3.1.24}$$
$$\int dP_s\ C(-P,\ell_1,P_s)\,C(-P_s,\ell_2,Q)\ \mathcal{F}_{P_s}\left[\begin{smallmatrix}\ell_1 & \ell_2\\ P & Q\end{smallmatrix}\right](z_1,z_2)\ \mathcal{F}_{P_s}\left[\begin{smallmatrix}\ell_1 & \ell_2\\ P & Q\end{smallmatrix}\right](\bar{z}_1,\bar{z}_2)$$

where $C(1,2,3)$ is the DOZZ OPE coefficient. The cross-ratios in these formulae are given by $z = z_1/z_2$ and $\bar{z} = \bar{z}_1/\bar{z}_2$. The conformal blocks are defined by the following normalization

$$\mathcal{F}_{P_s}\left[\begin{smallmatrix}\ell_1 & \ell_2\\ P & Q\end{smallmatrix}\right](z_1,z_2) = z_1^{\Delta_P-\Delta_s}z_2^{\Delta_s-\Delta_Q}\left(1+\ldots\right) \tag{3.1.25}$$

where the $\ldots$ denote higher order terms in z and $\bar{z}$. To take the Schwarzian limit, we set $P = bk_1$, $Q = bk_4$ and send $b \to 0$, while simultaneously sending $z \to 0$. In

this limit the conformal block becomes trivial (As we will see in the next section, the 2D conformal blocks exhibit non-trivial monodromy properties under analytic continuation. These will turn out to be an essential ingredient in the computation of out-of-time-ordered correlation functions). Using the same notation as in the previous section, we obtain[2]

$$G^{\beta}_{\ell_1\ell_2} = \int dk_1^2 dk_4^2 dk_s^2 \, \sinh 2\pi k_1 \sinh 2\pi k_4 \sinh 2\pi k_s \tag{3.1.26}$$
$$\times \, e^{-k_1^2(\tau_2-\tau_1)-k_4^2(\tau_4-\tau_3)-k_s^2(\beta-\tau_2+\tau_3-\tau_4+\tau_1)} \, \frac{\Gamma(\ell_2 \pm ik_4 \pm ik_s)\,\Gamma(\ell_1 \pm ik_1 \pm ik_s)}{\Gamma(2\ell_1)\,\Gamma(2\ell_2)}.$$

This integral expression is only valid in the regime $\tau_4 > \tau_3 > \tau_2 > \tau_1$.

The formula (3.1.26) is identical to the result (2.2.11) quoted in the Introduction. Again, it is possible to disentangle the full expression (3.1.26) into propagators and vertices. Or conversely, applying the Feynman rules outlined in section 2.2 to the diagram on the left in Figure 3.5, we directly obtained the full result (3.1.26) for the time-ordered four-point function.

For later reference, we summarize the above calculation of the four point function by means of the following diagram:

$$G_{\ell_1\ell_2} = \int dP\, dQ\, dP_s \; \Psi^{\dagger}_{\rm ZZ}(P)\Psi_{\rm ZZ}(Q) \;\times$$

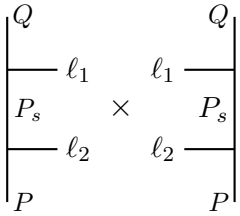

As indicated, the insertion of the ZZ states splits the thermal circle into two halves, each given by a chiral conformal block of the 2D Virasoro CFT. Each half has the

[2]The zero-temperature limit factorizes as $G^{\infty}_{\ell_1\ell_2} = G^{\infty}_{\ell_1} G^{\infty}_{\ell_2}$. This zero-temperature result is in agreement with [71, 72]. This factorization would not have happened had we computed the time-ordered correlator $\langle \mathcal{O}_{\ell_1}(\tau_1,\tau_4)\mathcal{O}_{\ell_2}(\tau_2,\tau_3)\rangle$.

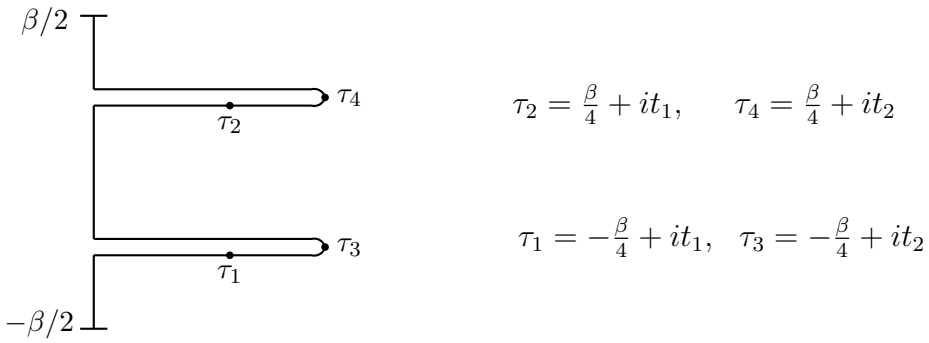

Figure 3.6: Time ordering prescription for the out-of-time ordered four point function at finite inverse temperature β. Note that the time operator insertion at τ_3 acts before the operator insertion at τ_2, even though in real time $t_1 = \mathrm{Im}(\tau_2)$ is earlier than $t_2 = \mathrm{Im}(\tau_3)$.

same intermediate momentum P_s, and all momenta are integrated over. In the figure, we have absorbed the OPE coefficients into the definition of the conformal blocks.

3.2 OTO four point function

In this section we consider the out-of time ordered four-point function

$$G^{\mathrm{OTO}}_{\ell_1\ell_2}(\tau_1, \tau_2, \tau_3, \tau_4) = \left\langle \mathcal{O}_{\ell_1}(\tau_1, \tau_2)\mathcal{O}_{\ell_2}(\tau_3, \tau_4)\right\rangle_{\mathrm{OTO}} \tag{3.2.1}$$

The OTO prescription can be implemented in different ways. One convenient choice is to complexify the time coordinates, and choose the real and imaginary parts as follows

$$\tau_1 = -\frac{\beta}{4} + it_1, \qquad \tau_2 = \frac{\beta}{4} + it_1, \qquad \tau_3 = -\frac{\beta}{4} + it_2 \qquad \tau_4 = \frac{\beta}{4} + it_2, \tag{3.2.2}$$

and consider a time contour prescription as indicated in Figure 3.6.

To compute the OTO correlation functions, one could try to explicitly perform the three integrals in equation (3.1.26) for the time-ordered correlation function, write $G_{\ell_1\ell_2}$ as an analytic function of the four times τ_i and then perform the appropriate

analytic continuation. However, at present we do not know how to perform the integrals explicitly, so this direct approach is not practical. Luckily, the 2d perspective of the Schwarzian theory as a limit of 2D Virasoro CFT theory gives another way to solve the problem. In this section we will combine the calculation presented above with the ideas of [74] to compute the exact OTO four-point function. Technical details are delegated to Appendix 3.6.

Most recent studies of OTO correlation functions in (putative) chaotic systems have focused on the time-dependence. However, as originally pointed out in [74], to exhibit the dynamical mechanism that underlies the Lyapunov behavior, it is equally informative to study the four-point function in Fourier space, in which one fixes the energies of the intermediate states. The latter approach is also more naturally incorporated into our construction of the Schwarzian amplitudes in terms of the momentum space amplitudes.

Before we turn to the derivation, let us first write out the explicit form for the OTO four point function, as follows from the application of the Feynman rules presented in section 2.2 to the diagram on the right-hand side of Figure 3.5:

$$\begin{aligned} G^{\rm OTO}_{\ell_1\ell_2} &= \int dk_1^2 dk_4^2 dk_s^2 dk_t^2 \, \sinh 2\pi k_1 \sinh 2\pi k_4 \sinh 2\pi k_s \sinh 2\pi k_t \\ &\times \frac{\left|\Gamma(\ell_2 + ik_4 \pm ik_s)\Gamma(\ell_1 + ik_1 \pm ik_s)\Gamma(\ell_2 + ik_1 \pm ik_t)\Gamma(\ell_1 + ik_4 \pm ik_t)\right|}{\Gamma(2\ell_1)\,\Gamma(2\ell_2)} \\ &\times R_{k_s k_t}\left[\begin{smallmatrix} k_4 & \ell_2 \\ k_1 & \ell_1 \end{smallmatrix}\right] \times e^{-k_1^2(\tau_3-\tau_1)-k_t^2(\tau_3-\tau_2)-k_4^2(\tau_4-\tau_2)-k_s^2(\beta-\tau_4+\tau_1)}. \end{aligned} \tag{3.2.3}$$

The essential new ingredient in this expression is the R-matrix $R_{k_s k_t}\left[\begin{smallmatrix} k_4 & \ell_2 \\ k_1 & \ell_1 \end{smallmatrix}\right]$. Its explicit form is given in Appendix 3.6. By gauge/gravity duality this quantity describes the S-matrix corresponding to scattering of particles close to the horizon of a black hole. In other words, the integrand is already capturing the information we need to relate the out-of-time-ordered correlation function to gravitational properties of the

event horizon. In the remainder of this section, we will explain how the above result arises from the correspondence with 2D CFT, how to extract the time dependence and Lyapunov behavior, and how it matches with $2 \to 2$ scattering via gravitational shockwaves.

3.3 The R-matrix

The OTO four-point function in the Schwarzian theory corresponds to a two-point function of two bulk Liouville vertex operators that are spacelike separated, so that the past lightcones of the two operators cross each other as indicated on the right in Figure 3.4. From the point of view of the 2D CFT, this means that one of the chiral conformal blocks has been analytically continued to an OTO conformal block

$$\begin{aligned} G^{\text{OTO}}_{\ell_1\ell_2} &= \langle ZZ|V_{\ell_1}(z_1,\bar{z}_1)V_{\ell_2}(z_2,\bar{z}_2)|ZZ\rangle_{\text{OTO}}, \\ &= \int dPdQ\ \Psi^{\dagger}_{\text{ZZ}}(P)\Psi_{\text{ZZ}}(Q)\ \langle P|V_{\ell_1}(z_1,\bar{z}_1)V_{\ell_2}(z_2,\bar{z}_2)|Q\rangle_{\text{OTO}}. \end{aligned} \tag{3.3.1}$$

where the integrand factorizes in terms of CFT kinematic data as

$$\begin{aligned} &\langle P|V_{\ell_1}(z_1,\bar{z}_1)V_{\ell_2}(z_2,\bar{z}_2)|Q\rangle_{\text{OTO}} = \\ &\int dP_s\ C(-P,\ell_1,P_s)\,C(-P_s,\ell_2,Q)\ \mathcal{F}^{\text{OTO}}_{P_s}\left[\begin{smallmatrix}\ell_1 & \ell_2\\ P & Q\end{smallmatrix}\right](z_1,z_2)\ \mathcal{F}_{P_s}\left[\begin{smallmatrix}\ell_1 & \ell_2\\ P & Q\end{smallmatrix}\right](\bar{z}_1,\bar{z}_2) \end{aligned} \tag{3.3.2}$$

Here the OTO label indicates that we have applied a specific monodromy transformation to the 2D conformal block. The effect of this monodromy transformation in the Schwarzian limit can be found in the following way.

The argument of the s-channel conformal block is $z = z_1/z_2$, which goes to zero in the time-ordered case. Inserting the two operators in opposite order gives $z' = 1/z = z_2/z_1 \to \infty$. The 2D conformal block behaves non-trivially in the limit where

the cross ratio becomes infinite. Even though we do not know the explicit expression for the full conformal block, we can use the R-matrix transformation of Ponsot and Teschner [75]

$$\mathcal{F}_{P_s}\left[\begin{smallmatrix}2 & 3\\ 1 & 4\end{smallmatrix}\right](z') = \int dP_t\ R_{P_sP_t}\left[\begin{smallmatrix}2 & 3\\ 1 & 4\end{smallmatrix}\right]\ \mathcal{F}_{P_t}\left[\begin{smallmatrix}3 & 2\\ 1 & 4\end{smallmatrix}\right](1/z') \tag{3.3.3}$$

to extract its exact behavior in the large cross-ratio regime $z' \to \infty$ by using the fact that the conformal block inside the integral in (3.3.3) becomes trivial for $z = 1/z' \to 0$. Inserting the transformed conformal block into (3.3.1) and (3.3.2), we obtain the momentum integral representation of the out-of-time-ordered four-point function. The total calculation procedure can be graphically represented as

$$G^{\text{OTO}}_{\ell_1\ell_2} = \int dPdQ\ \Psi^{\dagger}_{\text{ZZ}}(P)\Psi_{\text{ZZ}}(Q)\ \times \int dP_s$$

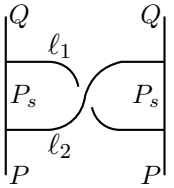

$$= \int dPdQ\ \Psi^{\dagger}_{\text{ZZ}}(P)\Psi_{\text{ZZ}}(Q)\ \times \int dP_s dP_t\ \ R_{P_sP_t}$$

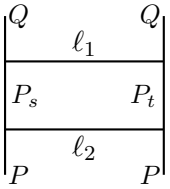

Our remaining task is to compute the appropriate large c limit of the crossing kernel of 2D CFT conformal blocks. This calculation is performed in Appendix 3.6. The 2d crossing kernels, i.e. the F-matrix and R-matrix, are explicitly known and expressed in terms of $U_q(\mathfrak{sl}(2,\mathbb{R}))$ $6j$-symbols [75]. Perhaps unsurprisingly, we will find that in the Schwarzian limit the Ponsot-Teschner result for the quantum 6j-symbols reduces to known expressions for the classical 6j-symbols of $SU(1,1)$.

The R-matrix and fusion matrix of 2D Virasoro conformal blocks are related via

$$R_{\alpha_s\alpha_t}\left[\begin{smallmatrix}\alpha_3 & \alpha_2\\ \alpha_4 & \alpha_1\end{smallmatrix}\right] = e^{2\pi i(\Delta_2+\Delta_4-\Delta_s-\Delta_t)} F_{\alpha_s\alpha_t}\left[\begin{smallmatrix}\alpha_3 & \alpha_2\\ \alpha_4 & \alpha_1\end{smallmatrix}\right]. \tag{3.3.5}$$

The F-matrix, in turn, is expressed in terms of the quantum $6j$-symbol via [77]

$$F_{\alpha_s\alpha_t}\left[\begin{smallmatrix}\alpha_3 & \alpha_2\\ \alpha_4 & \alpha_1\end{smallmatrix}\right] = |S_b(2\alpha_t)S_b(2\alpha_s)|\sqrt{\frac{C(\alpha_4,\alpha_t,\alpha_1)C(\bar{\alpha}_t,\alpha_3,\alpha_2)}{C(\alpha_4,\alpha_3,\alpha_s)C(\bar{\alpha}_s,\alpha_2,\alpha_1)}}\left\{\begin{smallmatrix}\alpha_1 & \alpha_2 & \alpha_s\\ \alpha_3 & \alpha_4 & \alpha_t\end{smallmatrix}\right\}_b, \quad (3.3.6)$$

where $S_b(x)$ denotes the double Sine function and $C(\alpha_3,\alpha_2,\alpha_1)$ is the DOZZ three point function [104, 105]. In the 1D limit, we need to take two α's to be real and proportional to $\alpha_i = b\ell_i$ with ℓ_i finite and the other four of the form $\alpha_j = \frac{Q}{2} + ibk_j$ with k_j finite. Specifically, we will choose

$$\begin{aligned}
&\alpha_1 = \ell_1 b, && \alpha_2 = \frac{Q}{2} + ibk_2, && \alpha_s = \frac{Q}{2} + ibk_s,\\
&\alpha_3 = \ell_3 b, && \alpha_4 = \frac{Q}{2} + ibk_4, && \alpha_t = \frac{Q}{2} + ibk_t.
\end{aligned}$$

For the application to the Schwarzian theory, we must further take the classical limit of the quantum 6j-symbols

$$\left\{\begin{smallmatrix}\ell_1 & k_2 & k_s\\ \ell_3 & k_4 & k_t\end{smallmatrix}\right\} \equiv \lim_{b\to 0}\ 2\pi b^3\left\{\begin{smallmatrix}\alpha_1 & \alpha_2 & \alpha_s\\ \alpha_3 & \alpha_4 & \alpha_t\end{smallmatrix}\right\}_b. \quad (3.3.7)$$

Returning to equation (3.3.3) and using the above formulas, we are now obtain an explicit expression for the large z limit of . The conformal block in the right hand side again becomes trivial since $z' = 1/z \to 0$. The answer can be written as (see Appendix 3.6)

$$\begin{aligned}
\mathcal{F}_{P_s}^{\mathrm{OTO}}\left[\begin{smallmatrix}2 & 3\\ 1 & 4\end{smallmatrix}\right](\tau) \;&=\; \int dP_t\ e^{-\tau P_t^2/b^2}\ R_{P_sP_t}\left[\begin{smallmatrix}2 & 3\\ 1 & 4\end{smallmatrix}\right] \\
&= \int dk_t^2 \sinh 2\pi k_t\, e^{-k_t^2\tau}\ \left|\frac{\Gamma(\ell_1 + ik_4 \pm ik_t)\Gamma(\ell_3 + ik_2 \pm ik_t)}{\Gamma(\ell_1 + ik_2 \pm ik_s)\Gamma(\ell_3 + ik_4 \pm ik_s)}\right|\ \left\{\begin{smallmatrix}\ell_1 & k_2 & k_s\\ \ell_3 & k_4 & k_t\end{smallmatrix}\right\}
\end{aligned} \quad (3.3.8)$$

with the 6j-symbol as defined via (3.3.7). Note that in the 1D limit the dimensions of the operators that appear in the phase factor in equation (3.3.5) are all equal to $\frac{c}{24} + \mathcal{O}(1/c)$. The phase factor thus becomes trivial.

To obtain the out-of-time-ordered four point function we make the above substitution inside of the integral expression (3.3.2). This leads to the final expression given in equation (3.2.3), where we define the Schwarzian R-matrix via

$$R_{k_s k_t}\left[\begin{smallmatrix} k_4 & \ell_2 \\ k_1 & \ell_1 \end{smallmatrix}\right] = \left\{\begin{smallmatrix} \ell_1 & k_1 & k_s \\ \ell_2 & k_4 & k_t \end{smallmatrix}\right\}. \tag{3.3.9}$$

With this definition, the R-matrix is naturally a unitary operator relative to the spectral measure $d\mu(k)$.

3.3.1 Schwarzian $6j$-symbols

In this section we present the explicit expression for the Schwarzian limit of the $6j$-symbols of the Virasoro CFT. A general expression for this quantity at finite c, and its relation with the monodromy of the 2D conformal blocks, was found by B. Ponsot and J. Teschner in [75]. For our purpose, we need to take the large c limit outlined above. Details of the calculation are given in Appendix 3.6. After some straightforward algebra, one arrives at the somewhat daunting looking integral expression (3.6.17). The integral can be done by the method of residues. The final result can be organized in the following symmetric expression

$$\begin{aligned}\left\{\begin{smallmatrix} \ell_1 & k_2 & k_s \\ \ell_3 & k_4 & k_t \end{smallmatrix}\right\} \;=\; & \sqrt{\Gamma(\ell_1 \pm ik_2 \pm ik_s)\Gamma(\ell_3 \pm ik_2 \pm ik_t)\Gamma(\ell_1 \pm ik_4 \pm ik_t)\Gamma(\ell_3 \pm ik_4 \pm ik_s)} \\ & \times \mathbb{W}(k_s, k_t; \ell_1 + ik_4, \ell_1 - ik_4, \ell_3 - ik_2, \ell_3 + ik_2),\end{aligned} \tag{3.3.10}$$

where we define $\Gamma(x \pm y \pm z)$ as a shorthand for the product of the gamma function with four combinations of signs. The function that appears in the right hand side is a rescaled version of the Wilson function introduced by W. Groenevelt [78,79]. The original function introduced in [78,79] is denoted by $\mathbb{W}(\alpha, \beta; a, b, c, d) = \phi_\alpha(\beta; a, b, c, 1-d)$ and it is proportional to a generalized hypergeometric function ${}_7F_6$ evaluated at $z = 1$ whose coefficients depend on α, β, a, b, c and d.

Given that the above expression was obtained as a limit of the quantum 6j-symbol, it is natural to suspect that the result can be interpreted as a classical $6j$-symbol. The above indeed matches with the $6j$-symbol associated to the Lie algebra $\mathfrak{su}(1,1)$ found by W. Groenevelt [78, 79]. The heavy operators with label k_i correspond to the principal unitary series representations of $\mathfrak{su}(1,1)$, while the light operators ℓ_i correspond to the discrete series.[3] The expression (3.3.9) enjoys tetrahedral symmetry that acts by permutations on the six spin labels.[4] In addition, the 6j-symbols satisfy the unitarity condition

$$\int dk_s\, \rho(k_s) \begin{Bmatrix} \ell_1 & k_2 & k_s \\ \ell_3 & k_4 & k_t \end{Bmatrix}^\dagger \begin{Bmatrix} \ell_1 & k_2 & k_s \\ \ell_3 & k_4 & k_{t'} \end{Bmatrix} = \frac{1}{\rho(k_t)}\, \delta(k_t - k_{t'}), \tag{3.3.11}$$

with $\rho(k) = 2k \sinh(2\pi k)$, which underscores the proposed holographic interpretation of the R-matrix (3.3.9) as describing a gravitational scattering amplitude in the bulk. This unitarity condition is also responsible for the crossing symmetry of the 2D Liouville four point function [75].

Wilson functions also appeared recently as a fusion matrix of conformal blocks in a toy-model CFT with $SL(2,\mathbb{R})$ symmetry [108] [109]. It would be interesting to understand how these two approaches are related.

[3] Note that even though $SU(1,1)$ and $SL(2,\mathbb{R})$ are isomorphic, their tensor categories are different and they have different $6j$-symbols.

[4] The classical 6j-symbol of any Lie group can indeed be written as the expectation value of six Wilson lines, glued together into a tetrahedron, of the corresponding 2D BF-gauge theory.

3.3.2 Gravitational Scattering and Chaos

In this section we will present evidence that our following proposal of the full gravitational S-matrix in the Jackiw-Teitelboim model

$$\mathrm{R-Matrix} \quad \leftrightarrow \quad \mathrm{Gravitational\ \ S-matrix} \tag{3.3.12}$$

is correct. This is done in detail in [52]. In [52] we show how time ordered correlators coincide with free propagation in the bulk when one takes the semiclassical limit of ℓ fixed and C large.

In particular the Fourier-space amplitudes of time-ordered correlators correspond to bulk-to-boundary propagators of free fields in AdS_2. This is true for an arbitrary correlator as long as it is time-ordered. Changes in $E(k)$ are related to energies as measured by an asymptotic observer. This is true in the Jackiw-Teitelboim approximation of dilaton-gravity. Fields only interact through the Schwarzian gravitational dressing which is suppressed for large C.

For example take the two-point function. The exact answer was given in equation (3.1.13). After labeling the integration variables as $k_2^2 = E$ and $k_1^2 = E + \omega$ the real-time two-point function can be written in the form

$$G_\ell^{\pm}(t) \sim \int dE\, \rho(E)\, e^{-\beta E} \int d\omega\, e^{i\omega t}\, |\mathcal{A}_E(\omega, \ell)|^2, \tag{3.3.13}$$

where we include in the amplitude $\mathcal{A}_E$ the density of states $\rho(E+\omega)$ and the gamma functions coming from the OPE coefficients in equation (3.1.5). If we take $\omega \ll E$ then $|\mathcal{A}_E(\omega, \ell)|^2 \sim \Gamma\big(\ell \pm i\frac{\omega}{2\sqrt{E}}\big)$. This amplitude $\mathcal{A}_E(\omega, \ell)$ is the Fourier transform of a bulk-to-boundary propagator.

As we reviewed in the introduction, OTOC are highly sensitive to gravitational interactions through shockwaves. Therefore we expect to see the semiclassical S-

matrix emerge for these quantities. We will focus on this quantity in the following sections.

We have shown that the characteristic behavior of the OTO correlation function is governed by an R-matrix in the form of a 6j-symbol. This R-matrix is a unitary matrix, that incorporates the gravitational bulk scattering amplitude in momentum space. In this section we summarize how one can extract the characteristic Lyapunov exponent from the R-matrix. Our discussion here closely follows the derivation given in section 1 of [74] for case of $\mathrm{AdS}_3/\mathrm{CFT}_2$.

The R-matrix depends on six parameters, $\ell_1, \ell_3, k_2, k_4, k_s$ and k_t. Following [74], let us label the four momenta as follows

$$\begin{aligned} k_2 &= \mathrm{M}, & k_s &= \mathrm{M}+\alpha, \\ k_4 &= \mathrm{M}+\omega, & k_t &= \mathrm{M}+\beta. \end{aligned} \tag{3.3.14}$$

We will assume that we are in the regime $\mathrm{M} \gg \alpha, \beta, \omega \gg \ell_1, \ell_3$. So to isolate the leading order behavior, we will set $\ell_1 = \ell_3 = 0$. In this notation, the explicit integral formula for the R-matrix takes the form

$$\begin{aligned} R_{\alpha\beta} = & \int_{\mathcal{C}} \frac{du}{2\pi} \frac{\Gamma(u)\Gamma(i\alpha-u)\Gamma(i(\alpha-\omega)-u)\Gamma(u-i(\alpha+\beta-\omega))}{\Gamma(u-i\alpha)\Gamma(u-i\alpha+i\omega)} \Gamma(u-2i\mathrm{M}_{2\alpha})\Gamma(u+2i\mathrm{M}_{\beta+\omega-\alpha}) \\ & \times \sqrt{\frac{\Gamma(-i\alpha)\Gamma(i\beta)\Gamma(i(\omega-\alpha))\Gamma(-i(\omega-\beta))}{\Gamma(i\alpha)\Gamma(-i\beta)\Gamma(-i(\omega-\alpha))\Gamma(i(\omega-\beta))}} \sqrt{\frac{\Gamma(2i\mathrm{M}_\alpha)\Gamma(-2i\mathrm{M}_\beta)\Gamma(2i\mathrm{M}_{\alpha+\omega})\Gamma(-2i\mathrm{M}_{\beta+\omega})}{\Gamma(-2i\mathrm{M}_\alpha)\Gamma(2i\mathrm{M}_\beta)\Gamma(-2i\mathrm{M}_{\alpha+\omega})\Gamma(2i\mathrm{M}_{\beta+\omega})}} \end{aligned} \tag{3.3.15}$$

where $2i\mathrm{M}_\alpha = 2i\mathrm{M} + i\alpha$, etc.

How do we extract physical information from this expression for $R_{\alpha\beta}$? Since in the Schwarzian QM, it represents an exchange property of the momentum space amplitude, it is useful to label the operators by means of their momentum, or rather, by means of the amount they shift the momentum of the state on which they act.

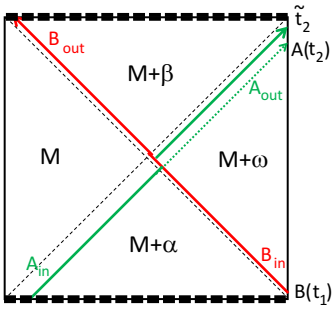

Figure 3.7: The R-matrix describes the gravitational shockwave interaction between an infalling and outgoing matter perturbation near a black hole horizon. The particle trajectories divide the space-time into four regions.

Concretely, we can define the action of a momentum space operator A_ω via the algebraic rule

$$A_\omega \, |\mathrm{M}\rangle = \gamma_A(\omega) \, \big|\mathrm{M}+\omega\big\rangle, \tag{3.3.16}$$

where $|\mathrm{M}\rangle$ denotes an energy eigenstate with $SL(2,\mathbb{R})$ spin $j = -\frac{1}{2}+i\mathrm{M}$, with $\gamma_A(\omega) = \gamma_{\ell_A}(\mathrm{M}, \mathrm{M}+\omega)$ the vertex function. This algebraic rule allows us to multiply operators and keep track of the time dependence through the usual Schrödinger evolution. This prescription works as long as the operators are time-ordered.

The R-matrix (3.3.15) prescribes what happens if we exchange two operators and place them in out-of-time order. Schematically,

$$B_{\omega-\alpha} \, A_\alpha \, |\mathrm{M}\rangle = \sum_\beta R_{\alpha\beta} \; A_{\omega-\beta} \, B_\beta \, |\mathrm{M}\rangle. \tag{3.3.17}$$

Here $\sum_\beta$ is short-hand for $\int d\beta \rho(\mathrm{M}+\beta)$ with $\rho(\mathrm{M}+\beta) = (\mathrm{M}+\beta)\sinh(2\pi(\mathrm{M}+\beta))$ the spectral density of the intermediate state $|\mathrm{M}+\beta\rangle$.

From the bulk perspective, this exchange algebra expresses the physical effect of an ingoing perturbation created by $B_{\omega-\alpha}$ (the 'butterfly') on an outgoing signal A, as indicated in Figure 3.7. To see the associated Lyapunov behavior, we need to translate the scattering phase to the time domain. This is done via the standard rules of geometric optics, which is justified since in the regime of interest, the phase

of the R-matrix is rapidly changing with frequency. Focusing on this phase factor, we write

$$R_{\alpha\beta} = e^{iI_{\alpha\beta}}. \tag{3.3.18}$$

Next, we localize the operators A and B in time by considering them as wave-packets with a given approximate frequency. In the leading order stationary phase approximation the exchange relation then takes the form

$$B_{\omega-\alpha}(t_1)\, A_\alpha(t_2) = e^{iI_{\alpha\beta}}\, A_{\omega-\beta}(\tilde{t}_2)\, B_\beta(\tilde{t}_1), \tag{3.3.19}$$

where the value of β, $\tilde{t_2}$ and $\tilde{t_1}$ on the right-hand side are fixed by the stationary phase criterion. Let us introduce the time differences

$$t_\alpha = t_2 - t_1, \qquad\qquad t_\beta = \tilde{t}_2 - \tilde{t}_1. \tag{3.3.20}$$

These time differences are linked through the frequency dependence of the scattering phase $R_{\alpha\beta} = e^{iI_{\alpha\beta}}$ via the Hamilton-Jacobi (geometric optics) equations

$$t_\alpha = -\frac{\partial I_{\alpha\beta}}{\partial E_\alpha} = -\frac{1}{2\mathrm{M}}\frac{\partial I_{\alpha\beta}}{\partial \alpha}, \qquad\qquad t_\beta = \frac{\partial I_{\alpha\beta}}{\partial E_\beta} = \frac{1}{2\mathrm{M}}\frac{\partial I_{\alpha\beta}}{\partial \beta}, \tag{3.3.21}$$

which follow from the fact that both sides of the exchange relation (3.3.19) have the same dependence on α and β.[5]

The prediction from bulk gravity is that the time delay $\tilde{t}_2 - t_2$ of the outgoing signal A due to the perturbation B grows exponentially with the time separation $t_2 - t_1$

$$\tilde{t}_2 - t_2 \sim e^{\lambda_{\mathrm{M}}(t_2 - t_1)}, \qquad\qquad \lambda_{\mathrm{M}} = \frac{2\pi}{\beta_{\mathrm{M}}}, \tag{3.3.22}$$

[5]The phase $I_{\alpha\beta}$ is the generating function of the canonical transformation between the initial and final canonical variables (E_α, t_α) and (E_β, t_β).

with $\beta_{\rm M}$ the temperature of the black hole dual to the state $|{\rm M}\rangle$. We have

$$S({\rm M}) = 2\pi {\rm M}, \qquad E({\rm M}) = {\rm M}^2, \qquad \beta_{\rm M} = \frac{\pi}{\rm M}, \qquad \lambda_{\rm M} = \frac{2\pi}{\beta_{\rm M}} = 2{\rm M}\,. \tag{3.3.23}$$

Can we extract this from the exact expression (3.3.15) for the R-matrix?

We have thus far not been able to find a precise enough way to evaluate the integral 3.3.15. So we will proceed by making a plausible assumption, in the form of the following

Ansatz: in the semiclassical regime, (3.3.15) *is dominated by the residue at* $u = 0$.

The pole at $u = 0$ appears due to the $\Gamma(u)$ factor in the integrand. The above hypothesis is supported by several pieces of evidence. First, a naive application of Stirling and the stationary phase approximation indeed points to the existence of a saddle point near $u = 0$. Secondly, as we will see shortly, via this Ansatz we can make contact with the semi-classical analysis of [74], which applies in the regime of large c and large conformal dimensions $\Delta - \frac{c-1}{24}$ of order c. We leave the further justification of the above simplifying Ansatz for future study.

Evaluating the residue and approximating $\log\big(\frac{\Gamma(i(2{\rm M}+\alpha))}{\Gamma(-i(2{\rm M}+\alpha))}\big) \sim 2i\alpha\log(2{\rm M})$, we find that

$$R^{(u=0)}_{\alpha\beta} = e^{-i(\alpha+\beta-\omega)t_{\rm M}}\ \Gamma(i(\omega-\alpha-\beta))\ \sqrt{\frac{\Gamma(i\alpha)\Gamma(i\beta)\Gamma(-i(\omega-\alpha))\Gamma(-i(\omega-\beta))}{\Gamma(-i\alpha)\Gamma(-i\beta)\Gamma(i(\omega-\alpha))\Gamma(i(\omega-\beta))}}$$

with $t_{\rm M} \simeq \log(2{\rm M})$. Now using Stirling gives

$$\begin{aligned} I_{\alpha\beta} \ \simeq\ & \alpha\log\alpha + \beta\log\beta - (\omega-\alpha)\log(\omega-\alpha) - (\omega-\beta)\log(\omega-\beta) \\ & - (\alpha+\beta-\omega)\log\big(\alpha+\beta-\omega\big) - (\alpha+\beta-\omega)t_R, \end{aligned} \tag{3.3.24}$$

which is identical to the formula for $I_{\alpha\beta}$ derived in [74] from both 2+1D gravity and from 2D Virasoro CFT. Using this expression for $I_{\alpha\beta}$ and the geometric optics

relations (3.3.21) we can now compute the time difference t_β as functions of α, ω, and the time difference t_α

$$t_\alpha - t_R = \frac{1}{\lambda_{\rm M}} \log\Big(\frac{\alpha+\beta-\omega}{2\alpha(\omega-\alpha)}\Big), \quad t_\beta - t_R = \frac{1}{\lambda_{\rm M}} \log\Big(\frac{\alpha+\beta-\omega}{2\beta(\omega-\beta)}\Big), \tag{3.3.25}$$

or equivalently [74]

$$\beta \;=\; \omega - \alpha + 2\alpha(\omega-\alpha)e^{\lambda_{\rm M}(t_\alpha - t_R)}, \tag{3.3.26}$$

$$\alpha \;=\; \omega - \beta + 2\beta(\omega-\beta)e^{\lambda_{\rm M}(t_\beta - t_R)}. \tag{3.3.27}$$

These two relations are identical to the ones derived for the shockwave scattering process near a black hole in 2+1D AdS space-time [26], and also match with the expected behavior in the AdS_2 Jackiw-Teitelboim model. Equation (3.3.26) determines β and t_β as a function of α and the time difference $t_\alpha = t_2 - t_1$. One finds

$$\tilde{t_2} - t_2 = -\frac{1}{\lambda_{\rm M}} \log\Big(\frac{\omega-\alpha}{\beta}\Big) \;\simeq\; \frac{2\alpha}{\lambda_{\rm M}}\, e^{\lambda_{\rm M}(t_2 - t_1 - t_R)}, \tag{3.3.28}$$

which exhibits the expected maximal Lyapunov growth.

3.3.3 Semiclassical Limit of OTOC

In this section we will repeat the previous analysis at the level of the time dependence of correlators. The OTO four-point function can be expressed in terms of this bulk $\mathcal{S}$-matrix and the asymptotic wave functions as reviewed in [52] and explained in [47]. The integrals can be computed explicitly, with the result [47] [6]

$$\frac{\langle V_1 W_3 V_2 W_4\rangle}{\langle V_1 V_2\rangle\langle W_3 W_4\rangle} = z^{-2\ell_1} U(2\ell_1, 1+2\ell_1-2\ell_2, 1/z), \tag{3.3.29}$$

[6] Even though it is not obvious from this expression one can verify using the properties of the hypergeometric function $U(a,b,z)$ that the right hand side is invariant under $\ell_1 \leftrightarrow \ell_2$.

where we define the cross-ratio

$$z = \frac{i\beta}{16\pi C} \frac{e^{\pi(t_3+t_4-t_1-t_2)/\beta}}{\sinh \frac{\pi t_{12}}{\beta} \sinh \frac{\pi t_{34}}{\beta}}. \tag{3.3.30}$$

If we make the choice of the insertions times similar to [47], explicitly $t_1 = -i\frac{\beta}{2}$, $t_2 = 0$, $t_3 = t - i\frac{\beta}{4}$ and $t_4 = t + i\frac{\beta}{4}$, then the cross-ratio becomes $z = \frac{\beta}{16\pi C} e^{\frac{2\pi}{\beta}t}$. The shockwave calculation is valid for $t > 0$ large with this combination z held fixed. The result 3.3.29 captures all the physics contained in the shockwave S-matrix. The Lyapunov behavior is a small part of it (only its small z limit). Unfortunately due to technical reasons a result analogous to 3.3.29 cannot be obtained in higher dimensions.

In this section we will derive the semiclassical limit of the OTOC reproducing (3.3.29) directly from the 2d picture. We will consider units in which $C = 1/2$. Since the dimensionless coupling is $2\pi C/\beta$ the semiclassical limit is equivalent to taking $\beta \to 0$ in these units. This match implies that the semiclassical limit of the R-matrix coincides with the Dray-'t Hooft S-matrix. Schematically we deduced

$$R(C \to \infty) \approx \mathcal{S}_{\text{Dray}-\text{'tHooft}} \tag{3.3.31}$$

since they generate the same OTOC. The left hand side is written in terms of k_i's which match with the Dray-'t Hooft S-matrix written in terms of energies measured by asymptotic observers. A detailed version of this relation was derived in [52].

In the 2d picture, the inverse temperature β of the Schwarzian gives the distance between the ZZ branes. Taking $\beta \to 0$ in the Schwarzian means sending the distance between the ZZ-branes to zero faster than the size of the circle in the extra dimension. Namely, β goes to 0 faster than $q \to 1$, where $q = e^{2\pi i\tau}$ denoted the q-modulus of the 2d annulus. In this limit the Schwarzian becomes equivalent to Liouville between two infinite ZZ-branes, namely on a strip of width β instead of an annulus.

The upshot of the previous argument is that we can reproduce the semiclassical Schwarzian correlators from local operators between two infinite ZZ-branes. The Liouville one-point function, which corresponds to the Schwarzian two-point function, is easy to compute exactly from the 2d CFT perspective, since the system can be mapped to the upper-half-plane by a conformal transformation. The answer immediately has the required form

$$\langle V \rangle_{\text{strip}} = \left(\frac{\pi}{\beta \sin \frac{\pi \tau}{\beta}} \right)^{2\ell}, \tag{3.3.32}$$

where ℓ corresponds to the conformal dimension of the Liouville operator. This can be related to the real time answer by analytic continuation.

Now we compute the Liouville 2pt function/Schwarzian 4pt function using this approach. Again, we can map the infinite strip to the upper-half plane, and we take the positions of the two local vertex operator insertions to be z_1 and z_3, while the images of these operators will be denoted by z_2 and z_4 (even though they should strictly be given by z_1^* and z_3^* we will allow them to be generic). The two-point function can be written in two equivalent ways. First, we can take the OPE between the two insertions and between the two images, obtaining

$$\frac{\langle V_1 V_2 W_3 W_4 \rangle}{\langle V_1 V_2 \rangle \langle W_3 W_4 \rangle} = \int dP \, \Psi_{\text{ZZ}}(P) \, C_{VWP} \, \mathcal{F}\left(\begin{smallmatrix} V & V \\ W & W \end{smallmatrix}, P, \eta \right), \tag{3.3.33}$$

where $\eta = \frac{z_{13} z_{24}}{z_{14} z_{23}}$ is the cross-ratio, Ψ_{ZZ} is the ZZ-brane wavefunction, C_{VWP} represents the Liouville OPE coefficient between the operators V, W and an intermediate channel operator with Liouville momentum P. $\mathcal{F}(P, \eta)$ denotes the conformal block in this channel. Another representation of this correlation function can be obtained by performing the OPE between an operator and its image. In this case it was shown that only the vacuum block appears (see section 6 of [88] and also [61] for a different perspective on this result). Defining the new cross ratio via $x = 1 - \eta$ and using the

exponential map $z_i = e^{\frac{2\pi}{\beta}\tau_i}$, the ZZ identity gives

$$\frac{\langle V_1 V_2 W_3 W_4\rangle}{\langle V_1 V_2\rangle\langle W_3 W_4\rangle} = x^{2\Delta_V}\mathcal{F}\left(\begin{smallmatrix} V & W \\ V & W \end{smallmatrix}, \text{vac}, x\right), \qquad x = -\frac{\sinh\frac{\pi t_{12}}{\beta}\ \sinh\frac{\pi t_{34}}{\beta}}{\sinh\frac{\pi t_{32}}{\beta}\ \sinh\frac{\pi t_{41}}{\beta}}. \tag{3.3.34}$$

For fixed $t_1, \ldots, t_4 \sim \mathcal{O}(1)$ and $c \to \infty$, the cross-ratio is finite and the vacuum block becomes trivial, implying that $\langle V_1 V_2 W_3 W_4\rangle \sim \langle V_1 V_2\rangle\langle W_3 W_4\rangle$. For the time-ordered four-point function this is the final answer.

The out-of-time ordered four-point function is equal to the vacuum block evaluated on the second sheet. It turns out this indeed exactly reproduces the shockwave calculation. The vacuum block on the second sheet is found by performing a monodromy operation on the block. As observed in [110], this monodromy remains non-trivial in the combined $x \to 0$ and $c \to \infty$ limit, with the product cx is held fixed and finite. The exact formula for the identity block in this limit was found to be [110]

$$\begin{aligned} \frac{\langle V_1 W_3 V_2 W_4\rangle}{\langle V_1 V_2\rangle\langle W_3 W_4\rangle} &= \lim_{c\to\infty, cx \text{ fixed}} x^{2\Delta_V}\mathcal{F}_{2^{nd}\text{sheet}}\left(\begin{smallmatrix} V & W \\ V & W \end{smallmatrix}, \text{vac}, x\right) \\ &= z^{-2\ell_1} U(2\ell_1, 1 + 2\ell_1 - 2\ell_2, 1/z), \end{aligned} \tag{3.3.35}$$

where the right hand side involves the cross ratio z defined in equation (3.3.30). Here we used the precise relation between the Virasoro central charge c and the Schwarzian coupling $2\pi C/\beta$. This matches exactly with the shockwave calculation in equation (3.3.29).

3.4 Geometric Interpretation

In this section we will review and summarize the semiclassical computation of correlators, its geometric interpretation and connection to backreaction in AdS_2. We consider large C and large ℓ in order to understand backreaction. One approach is to go back to the Jackiw-Teitelboim model [45, 47, 48] and rephrase the path integral

as describing a particle in a magnetic field [80] (see also [107] and [111]). Instead we will start from the exact correlators of [51], take their semiclassical limit and explain how to interpret them as backreaction on the geometry.

For simplicity we focus on the two-point function for operators of dimension ℓ. By semiclassical limit we mean both large C and large ℓ with ℓ/C fixed. The exact two-point function from [51] can be written in two equivalent ways

$$\begin{aligned}\langle \mathcal{O}(\tau)\mathcal{O}(0)\rangle &= \int \prod_{i=1,2} dk_i \rho(k_i)\, e^{-\frac{k_1^2}{2C}\tau - \frac{k_2^2}{2C}(\beta-\tau)} \frac{\Gamma(\ell \pm ik_1 \pm ik_2)}{\Gamma(2\ell)}, \qquad (3.4.1)\\ &= \int \prod_{i=1,2} dk_i d\theta_i\, e^{-I(k_i,\theta_i,\tau,\ell)}, \qquad (3.4.2)\end{aligned}$$

where the action is given by

$$I(k_i,\theta_i,\tau,\ell) = \sum_{i=1,2}\left(\frac{k_i^2}{2C}\tau_i + \theta_i k_i - \log\rho(k_i)\right) + \ell \log\left(\cos\frac{\theta_1}{2} + \cos\frac{\theta_2}{2}\right)^2 + I_0(\ell), \qquad (3.4.3)$$

and we defined $\tau_1 = \tau$ and $\tau_2 = \beta - \tau$ and the density of states $\rho(k) = 2k\sinh 2\pi k$. This second way of expressing the two-point function will be very useful below. We will refer to $I(k_i,\theta_i)$ as the action associated to the two-point function with values k_i and θ_i. At this point this gives an exact expression computing the two-point function, up to an unimportant normalization factor I_0 which appears as a constant term in the action.

What happens in the semiclassical limit for large C? In this case the integrals over k_i and θ_i become dominated by a saddle-point approximation. This happens for $k_i/C \sim \mathcal{O}(1)$ and $\theta_i \sim \mathcal{O}(1)$ since the action becomes $I \sim \mathcal{O}(C)$. This allows one to use saddle-point in this limit. Due to this scaling we define the semiclassical action $I_{\text{s.c.}}$ as

$$I(k_i,\theta_i) = C I_{\text{s.c.}}(k_i,\theta_i). \qquad (3.4.4)$$

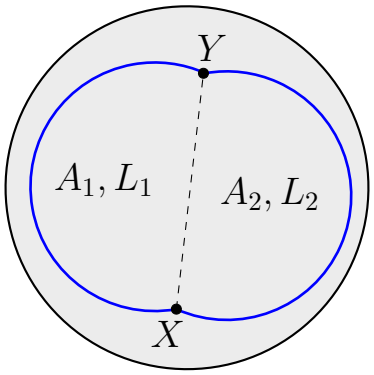

Figure 3.8: Geometric minimization problem. The gray circle is euclidean AdS_2. The blue line is the cut-off boundary of AdS. X and Y correspond to the insertions of the two-point function. We separate the boundary in two arcs of length L_1, L_2 and enclosing area A_1,A_2.

In this limit the action simplifies to

$$CI_{\text{s.c.}}(k_i, \theta_i, \tau, \ell) = \sum_{i=1,2} \left(\frac{k_i^2}{2C}\tau_i + (\theta_i - 2\pi)k_i \right) + \ell \log \left(\cos\frac{\theta_1}{2} + \cos\frac{\theta_2}{2} \right)^2 + I_0. \quad (3.4.5)$$

we see from this expression that we also need to require $\ell \sim \mathcal{O}(C)$ in order to get a non-trivial answer. The saddle-point equations given by $\partial_{k_i} I_{\text{s.c.}} = \partial_{\theta_i} I_{\text{s.c.}} = 0$ simplify for $i = 1, 2$ to

$$\frac{k_i}{C}\tau_i = 2\pi - \theta_i, \quad (3.4.6)$$

$$\frac{k_i}{\sin\frac{\theta_i}{2}} = \frac{\ell}{\cos\frac{\theta_1}{2} + \cos\frac{\theta_2}{2}}. \quad (3.4.7)$$

Following [111] this can be given a geometric meaning. In this work the authors show that the calculation of the two-point function is equivalent to the geometric problem of minimizing an action proportional to the sum of the area enclosed by the boundary curve and an extra term

$$\ell \log\cosh D, \quad (3.4.8)$$

where D is the geodesic distance between the insertions of the two-point function.

The minimization can be done in steps. First one can minimize both halves of the boundary curve independently and get two arcs of a circle. We show this configuration in Figure 3.8. Then the minimization is done with respect to the opening angle and its area. This is manifest in our formula (3.4.5). The variables θ_1 and θ_2 correspond to the opening angle of both circles while k_1 and k_2 are proportional to the radius of curvature of each arc. Moreover the first four terms in (3.4.5) are proportional to the total area inside the boundary curve while the term proportional to ℓ corresponds to the geodesic length between the boundary insertions. It would be interesting to derive this result from a purely geometric perspective.

For concreteness one can check this with an example. If ℓ/C is fixed but much smaller than one then the solutions is $k_1 \sim k_2 = 2\pi C/\beta$ and $\theta_1 = 2\pi\frac{\tau}{\beta}$, $\theta_2 = 2\pi\frac{\beta-\tau}{\beta}$. This is consistent with the two-point function not affecting the geometry and computing simply the renormalized geodesic distance between the points in AdS. On the other hand for ℓ/C fixed and large $k_1 \sim 2\pi C/\tau$, $k_2 \sim 2\pi C/(\beta-\tau)$ and $2\pi - \theta_i \approx 2\pi$. In this limit the points X and Y become close and the boundary turns into two full circles touching at a point, as in Figure 7 of [112]. A similar geometrical analysis can be done for an arbitrary time-ordered correlator and the generalization is straightforward.

3.5 Concluding Remarks

In section 3.1.1 we described how to perform an analytic continuation that takes our finite temperature two-point function to the thermofield double state. Moreover, as explained in section 3.2, the OTO correlators are built up from insertions of the R-matrix, which have a holographic interpretation in terms of gravitational scattering. In section 3.3.2 we give some evidence of the Lyapunov behavior of the OTO correlator when $t \gtrsim \beta$. For even larger times $t \gg C$, starting from equation (3.2.3) we can deduce a power-law decay as $\sim t^{-6}$ consistent with the results of [71, 72].

In [51] we have also constructed a new type of observables that respect the $SL(2,\mathbb{R})$ symmetry. Their correlators can be found exactly through a Knizhnik-Zamolodchikov equation approach. Since they do not seem to play a role in SYK we will not review this here but refer the reader to Appendix D of [51].

To conclude, we mention some other possible generalizations of the formalism presented in this chapter. It would be interesting to extend our analysis of correlation functions to the supersymmetric cases beyond $\mathcal{N} = 1$. The $\mathcal{N} = 2$ theory has an abelian R-symmetry making it a non-trivial extension. $\mathcal{N} = 2$ Liouville theory is also related to 2D black holes through an FZZ-like duality. The $\mathcal{N} = 4$ case would also be instructive, as it would correspond to an SYK-like model with non-abelian symmetry. Another natural generalization is to study the generalized Schwarzian theory that arises by taking the 1D limit of 2D Toda theory (see for example [113]), which has an extended symmetry algebra, and to construct the corresponding generalized SYK model and Jackiw-Teitelboim theory that would have this extended Schwarzian model as its low energy description. Likewise, it would be interesting to understand whether the methods of this chapter can be applied to the 2D Schwarzian theory proposed in [53].

3.6 Appendix: 2d CFT Fusion Matrix

First we will present some definitions and properties of special functions appearing recurrently in Liouville theory, both in the DOZZ formula for the OPE coefficients and in the fusion matrix.

All special function are built upon a deformed version of the Gamma function

$$\Gamma_b(x) \equiv \frac{\Gamma_2(x|b,b^{-1})}{\Gamma_2(Q/2|b,b^{-1})}, \tag{3.6.1}$$

where $\Gamma_2(z|\epsilon_1,\epsilon_2)$ is the Barnes double gamma function. This function is uniquely defined by the properties under a shift in b or b^{-1} of its argument. We are interested in the $b \to 0$ limit. In this regime one can approximate this function by

$$\begin{aligned} \Gamma_b(bx) &\to (2\pi b^3)^{\frac{1}{2}(x-\frac{1}{2})}\Gamma(x), && (3.6.2)\\ \Gamma_b(Q-bx) &\to (2\pi b)^{-\frac{1}{2}(x-\frac{1}{2})}. && (3.6.3) \end{aligned}$$

These approximations can be used to obtain the Schwarzian limit of the DOZZ formula, reproducing the results in the main text.

Finally, in the integral formula for the fusion matrix the relevant combination of Γ_b is called the double-sine function and defined by $S_b(x) \equiv \frac{\Gamma_b(x)}{\Gamma_b(Q-x)}$. The following limit will be useful below. If we keep x fixed and take $b \to 0$ the following limit

$$S_b(bx) \approx (2\pi b^2)^{x-\frac{1}{2}}\Gamma(x). \tag{3.6.4}$$

These and more results can be found in [114]. In the next section of this appendix we will use these approximate expressions to obtain the Schwarzian limit of the fusion matrix.

Now we will compute the fusion matrix. A formula for the $6j$-symbols of $U_q(\mathfrak{sl}(2,\mathbb{R}))$, derived in [77], is given by

$$\begin{aligned} \left\{ \begin{array}{ccc} \alpha_1 & \alpha_2 & \alpha_s \\ \alpha_3 & \alpha_4 & \alpha_t \end{array} \right\}_b &= \Delta(\alpha_s,\alpha_2,\alpha_1)\Delta(\alpha_4,\alpha_3,\alpha_s)\Delta(\alpha_t,\alpha_3,\alpha_2)\Delta(\alpha_4,\alpha_t,\alpha_1) \\ &\quad \times \int_{\mathcal{C}} du S_b(u-\alpha_{12s})S_b(u-\alpha_{s34})S_b(u-\alpha_{23t}) \qquad (3.6.5)\\ &\quad S_b(u-\alpha_{1t4})S_b(\alpha_{1234}-u)S_b(\alpha_{st13}-u)S_b(\alpha_{st24}-u)S_b(2Q-u) \end{aligned}$$

where, following the notations of [77] we defined the following normalization factors

$$\Delta(\alpha_3,\alpha_2,\alpha_1) \equiv \left(\frac{S_b(\alpha_1+\alpha_2+\alpha_3-Q)}{S_b(\alpha_1+\alpha_2-\alpha_s)S_b(\alpha_1+\alpha_s-\alpha_2)S_b(\alpha_2+\alpha_s-\alpha_1)} \right)^{1/2}. \tag{3.6.6}$$

The integral is defined for the cases in which all $\alpha_k \in \frac{Q}{2} + i\mathbb{R}$. The contour $\mathcal{C}$ approaches $2Q + i\mathbb{R}$ at infinity and passes the real axis in the interval $(3Q/2, 2Q)$. In order to take the Schwarzian limit we need an analytic continuation of this formula. Unfortunately, although this representation makes the symmetries of the $6j$-symbol manifest, it does not allow for a natural evaluation in the Schwarzian limit. Instead we will start a representation that does not have the symmetry manifest but makes the analytic continuation straightforward

$$\left\{ \begin{matrix} \alpha_1 & \alpha_2 & \alpha_s \\ \alpha_3 & \alpha_4 & \alpha_t \end{matrix} \right\}_b = \frac{M(\alpha_s, \alpha_2, \alpha_1) M(\bar{\alpha}_4, \alpha_3, \alpha_s)}{M(\alpha_t, \alpha_3, \alpha_2) M(\bar{\alpha}_4, \alpha_t, \alpha_1)} \left\{ \begin{matrix} \alpha_1 & \alpha_2 & \alpha_s \\ \alpha_3 & \bar{\alpha}_4 & \alpha_t \end{matrix} \right\}_b^{\text{an}} \tag{3.6.7}$$

with $\bar{\alpha}_4 \equiv Q - \alpha_4$. The prefactors are defined as

$$M(\alpha_3, \alpha_2, \alpha_1) = \left(\frac{S_b(\alpha_1 + \alpha_2 - \alpha_3) S_b(\alpha_1 + \alpha_2 + \alpha_3 - Q)}{S_b(\alpha_1 + \alpha_3 - \alpha_2) S_b(\alpha_2 + \alpha_3 - \alpha_1)} \right)^{1/2}, \tag{3.6.8}$$

and following [76] we use the following integral representation of the asymmetric $6j$-symbol

$$\left\{ \begin{matrix} \alpha_1 & \alpha_2 & \alpha_s \\ \alpha_3 & \bar{\alpha}_4 & \alpha_t \end{matrix} \right\}_b^{\text{an}} \equiv \frac{S_b(\alpha_2 + \alpha_s - \alpha_1) S_b(\alpha_t + \alpha_1 - \alpha_4)}{S_b(\alpha_2 + \alpha_t - \alpha_3) S_b(\alpha_s + \alpha_3 - \alpha_4)} \int_{-i\infty}^{i\infty} ds \prod_{i=1}^{4} \frac{S_b(U_i + s)}{S_b(V_i + s)} \tag{3.6.9}$$

where the U_i and V_i factors are defined as

$$\begin{aligned} U_1 &= \alpha_s + \alpha_1 - \alpha_2 & V_1 &= 2Q + \alpha_s - \alpha_t - \alpha_2 - \alpha_4 \\ U_2 &= Q + \alpha_s - \alpha_1 - \alpha_2 & V_2 &= Q + \alpha_s + \alpha_t - \alpha_2 - \alpha_4 \\ U_3 &= \alpha_s + \alpha_3 - \alpha_4 & V_3 &= 2\alpha_s \\ U_4 &= Q + \alpha_s - \alpha_3 - \alpha_4 & V_4 &= Q. \end{aligned} \tag{3.6.10}$$

In the limit we are interested in, which we refer to as the Schwarzian limit, we choose the following set of parameters

$$\alpha_1 = \ell_1 b, \qquad \alpha_2 = \frac{Q}{2} + ibk_2, \qquad \alpha_s = \frac{Q}{2} + ibk_s$$
$$\alpha_3 = \ell_3 b, \qquad \alpha_4 = \frac{Q}{2} + ibk_4, \qquad \alpha_t = \frac{Q}{2} + ibk_t$$

It is important to make this identification in this order since otherwise the $b \to 0$ limit will be ill-defined. One can check that all the pre-factors have a well-defined $b \to 0$ limit, by using the identities of the previous appendix involving double sine functions. Having done this, the only non-trivial aspect of the calculation is the integral appearing in the definition, which we denote by

$$I(j_1, k_2, j_3, k_4; k_2, k_t) \equiv \int_{-i\infty}^{i\infty} \frac{ds}{2\pi i}\ 4\pi^2 b^3\ \prod_{i=1}^{4} \frac{S_b(U_i + s)}{S_b(V_i + s)}. \tag{3.6.11}$$

In the Schwarzian limit the integrand becomes

$$4\pi^2 b^4\ \prod_{i=1}^{4} \frac{S_b(U_i + s)}{S_b(V_i + s)} \quad = \quad \frac{\Gamma(s + i[k_t - k_s + k_2 + k_4])\Gamma(s - i[k_s + k_t - k_2 - k_4])}{\Gamma(s + j_1 - i(k_s - k_2))\Gamma(s + j_3 - i(k_s - k_4))}$$
$$\Gamma(s - 2ik_s)\Gamma(s)\Gamma(j_1 + i(k_s - k_2) - s)\Gamma(j_3 + i(k_s - k_4) - s)$$

Before writing down the answer for this integral, let's consider the most general case and solve the following problem

$$I = \int_{-i\infty}^{+i\infty} \frac{ds}{2\pi i}\ \frac{\Gamma(a_1 + s)\Gamma(a_2 + s)\Gamma(a_3 + s)\Gamma(a_4 + s)}{\Gamma(b_1 + s)\Gamma(b_2 + s)}\ \Gamma(A - s)\Gamma(B - s). \tag{3.6.12}$$

This can be computed by the method of residues. The integral is done over the imaginary axis, and we take a contour that leaves the poles of $\Gamma(A - s)$ and $\Gamma(B - s)$ to the right, and all the other poles to the left. For the integral relevant for the computation of the $6j$-symbols this is the proper contour to take. If we close the contour to the right and pick up only the poles of $\Gamma(A - s)$ and $\Gamma(B - s)$, this integral

is given by

$$I = \frac{\Gamma(B-A)\prod_{i=1}^{4}\Gamma(A+a_i)}{\Gamma(A+b_1)\Gamma(A+b_2)}\ {}_4F_3\Big[\begin{matrix} A+a_1 & A+a_2 & A+a_3 & A+a_4 \\ A+b_1 & A+b_2 & 1+A-B & \end{matrix};1\Big] + (A \leftrightarrow B). \tag{3.6.13}$$

For the particular choice of parameters that appear in the $6j$-symbol integral it is instructive to recognize this sum of hypergeometric functions as a Wilson function. This function was introduced in [78, 79] and is defined as

$$\mathbb{W}(\alpha,\beta;a,b,c,d) \equiv \frac{\Gamma(d-a)\ {}_4F_3\Big[\begin{matrix} a+i\beta & a-i\beta & \tilde{a}+i\alpha & \tilde{a}-i\alpha \\ a+b & a+c & 1+a-d & \end{matrix};1\Big]}{\Gamma(a+b)\Gamma(a+c)\Gamma(d\pm i\beta)\Gamma(\tilde{d}\pm i\alpha)} + (a \leftrightarrow d), \tag{3.6.14}$$

where $\tilde{d} = (b+c+d-a)/2$ and $\tilde{a} = (a+b+c-d)/2$. As seen from the definition, this is not the most general sum of hypergeometric functions and it requires a specific relation between its parameters. It is explained in [78, 79] that the Wilson function can also be written as a single ${}_7F_6$ hypergeometric function evaluated at $z = 1$, which makes some non-trivial symmetries of its parameters more transparent.

If we use the general integral result given in equation (3.6.13), and evaluate for the particular parameters of equation (3.6.12), to apply it to the Schwarzian limit of the $6j$-symbol, then we obtain the final answer for the integral as

$$I = \Gamma(d\pm i\beta)\Gamma(\tilde{d}\pm i\alpha)\Gamma(a\pm i\beta)\Gamma(\tilde{a}\pm i\alpha)\ \mathbb{W}(\alpha,\beta;a,b,c,d), \tag{3.6.15}$$

with the identification of $\alpha \to k_s$, $\beta \to k_t$ and

$$\begin{aligned} a &= j_1 + ik_4, & b &= j_1 - ik_4, & c &= j_3 - ik_2, \\ d &= j_3 + ik_2, & \tilde{a} &= j_1 - ik_2, & \tilde{d} &= j_3 - ik_4. \end{aligned} \tag{3.6.16}$$

After including the prefactors we can use this formula for the integral to derive the final expression of the $6j$-symbols of Liouville theory in the Schwarzian limit, equation (3.3.10). This says that the $6j$-symbol is proportional to the Wilson function. Using (3.3.10), let's see how the symmetries of the $6j$-symbols are recovered.

- The Wilson function is symmetric in all the last four arguments. This means there is a symmetry $k_4 \to -k_4$ and $k_2 \to -k_2$. This symmetry is preserved by the prefactor.

- Exchange $j_1 \leftrightarrow j_3$ together with $k_2 \leftrightarrow k_4$, which is also preserved by the prefactor. This is equivalent to the relation $\left\{ \begin{array}{ccc} \alpha_1 & \alpha_2 & \alpha_s \\ \alpha_3 & \alpha_4 & \alpha_t \end{array} \right\} = \left\{ \begin{array}{ccc} \alpha_3 & \alpha_4 & \alpha_s \\ \alpha_1 & \alpha_2 & \alpha_t \end{array} \right\}$.

- In [78, 79] another relation is proven, referred to as duality of the Wilson function,

  $$\mathbb{W}(k_s, k_t; j_1{+}ik_4, j_1{-}ik_4, j_3{-}ik_2, j_3{+}ik_2) = \mathbb{W}(k_2, k_4; j_1{+}ik_t, j_1{-}ik_t, j_3{-}ik_s, j_3{+}ik_s).$$

  This is also preserved by the prefactor and implies $\left\{ \begin{array}{ccc} \alpha_1 & \alpha_2 & \alpha_s \\ \alpha_3 & \alpha_4 & \alpha_t \end{array} \right\} = \left\{ \begin{array}{ccc} \alpha_1 & \alpha_s & \alpha_2 \\ \alpha_3 & \alpha_t & \alpha_4 \end{array} \right\}$.

- Finally, one can also exchange in both the Wilson function and the prefactor $k_s \leftrightarrow k_t$ together with $k_2 \leftrightarrow k_4$, namely

  $$\mathbb{W}(k_s, k_t; j_1{+}ik_4, j_1{-}ik_4, j_3{-}ik_2, j_3{+}ik_2) = \mathbb{W}(k_t, k_s; j_1{+}ik_2, j_1{-}ik_2, j_3{-}ik_4, j_3{+}ik_4),$$

  which implies $\left\{ \begin{array}{ccc} \alpha_1 & \alpha_2 & \alpha_s \\ \alpha_3 & \alpha_4 & \alpha_t \end{array} \right\} = \left\{ \begin{array}{ccc} \alpha_1 & \alpha_4 & \alpha_t \\ \alpha_3 & \alpha_2 & \alpha_s \end{array} \right\}$.

At the level of the Wilson function, the unitarity of the $6j$-symbols has already been proven by Groenevelt. After including the right prefactors, the $6j$-symbol generates an integral transformation equivalent to what he denotes as a Wilson transform of type 1.

To conclude this appendix, we give an integral expression of the $6j$-symbol which will be useful in the main text (here $k_{a\pm b} = k_a \pm k_b$, etc)

$$\left\{ \begin{matrix} \ell_1 & k_2 & k_s \\ \ell_3 & k_4 & k_t \end{matrix} \right\} = \sqrt{\frac{\Gamma(\ell_1 + ik_2 \pm ik_s)\Gamma(\ell_3 - ik_2 \pm ik_t)\Gamma(\ell_1 - ik_4 \pm ik_t)\Gamma(\ell_3 + ik_4 \pm ik_s)}{\Gamma(\ell_1 - ik_2 \pm ik_s)\Gamma(\ell_3 + ik_2 \pm ik_t)\Gamma(\ell_1 + ik_4 \pm ik_t)\Gamma(\ell_3 - ik_4 \pm ik_s)}}$$

$$\times \int_{-i\infty}^{i\infty} \frac{du}{2\pi i} \frac{\Gamma(u)\Gamma(u-2ik_s)\Gamma(u+ik_{2+4-s+t})\Gamma(u-ik_{s+t-2-4})\Gamma(\ell_1+ik_{s-2}-u)\Gamma(\ell_3+ik_{s-4}-u)}{\Gamma(u+\ell_1-ik_{s-2})\Gamma(u+\ell_3-ik_{s-4})}. \tag{3.6.17}$$

Chapter 4

Generalizations of the SYK Model

In previous chapters we have analyzed in a lot of detail the IR dynamics of the SYK quantum mechanical model. In this chapter and the next we will study to what extent we can generalize the lessons from the previous chapters to two dimensional field theories.

We will present a solvable field theory in two dimensions which has an IR description based on the breaking of conformal symmetry, just as the SYK model. We will also analyze to what extent the dynamics of the IR mode is related to gravity in 3D and controls the quantum chaos of the theory. In order to do this we will need to start from UV fermions with an unusual action. This can be thought of as a topological version of the Ising model, as explained in the main text.

In the rest of this section we will give an overview of the results presented in this chapter. In sections 4.1 and 4.2 we will define the model and find a close resemblance of its spectrum with SYK. In section 4.3 we will analyze the IR mode of this theory and how it emerges from gravity in AdS_3.

To begin, we will analyze the pattern of scale invariance in the SYK model and the interplay between the UV and the IR. The SYK model of ϕ_i with $\{\psi_i, \psi_j\} = \delta_{ij}$

with $i = 1, \ldots, N$ is specified by the 1D action

$$S_{\rm SYK} \;=\; \int dt \left(\sum_i \tfrac{\rm i}{2} \psi_i \partial_t \psi_i \;-\; {\rm i}^{\frac{q}{2}} \sum_{i_1,..,i_q} J_{i_1 \ldots i_q} \psi_{i_1} \ldots \psi_{i_q} \right) \tag{4.0.1}$$

Here $J_{i_1 \ldots j_q}$ denotes a set of gaussian random couplings. We can split (4.0.1) as $S = S_{\rm UV} + S_{\rm IR}$. Note that both terms exhibit reparametrization invariance, but that ψ transforms as a scalar in the UV, but has scale dimension $\Delta = 1/q$ in the IR. The SYK model exhibits approximate conformal symmetry in the IR, and has been proposed to give a holographic description of a 2D black hole space-time. The link with the gravity dual finds support in the fact that both sides give rise to an effective 1D Goldstone mode whose action is described by the Schwarzian derivative [31, 42, 46–48, 63, 64, 66].

In this chapter we propose a 2D QFT generalization[1] of the SYK model (4.0.1), which we argue preserves most of the desired features. In particular, via the same reasoning that applies to 1D case, we will argue that the 2D model appears to exhibit conformal symmetry in the IR and gives rise to an emergent Goldstone mode associated with broken 2D reparametrization invariance. We find that the same effective action of the Goldstone mode can also be derived from the 3D AdS gravity action, viewed as a functional of the boundary metric. These results indicate that our 2D model flows in the IR to a holographic 2D CFT, and may thus provide new insight into the dynamical mechanism that underlies $\mathrm{AdS}_3/\mathrm{CFT}_2$ duality.

4.1 The 2D model

In this section, we will give two characterizations of our 2D model. First we introduce the model via its Lagrangian, and then we present a Hamiltonian formulation. We give some special attention to the UV limit of our model.

[1] Proposals for 2D generalizations of SYK with a discretized spatial dimension are given in [115–117].

4.1.1 Lagrangian formulation

A naïve attempt to generalize the SYK model to 2D is to promote the ψ variables to 2D Majorana fermions with a standard kinetic term $\frac{\mathrm{i}}{2}\psi\partial\!\!\!/\psi$. This choice assigns canonical scale dimension $[\psi] = 1/2$. The interaction term then has dimension $q/2$, which is at best marginal. In the 1D action (4.0.1), on the other hand, the UV term assigns ψ scale dimension $[\psi] = 0$, so the interaction term is relevant and the model is strongly coupled in the IR.

To write the 2D generalization of (4.0.1) we introduce fermionic variables ψ_+^i and ψ_-^i with $i = 1, ..., N$. One can think of ψ_+ and ψ_- as the two chiral components of a 2D Majorana fermion. However, to preserve the essential features of the SYK dynamics, we replace the usual fermion kinetic term by the UV term in the following 2D action

$$
\begin{aligned}
S \;&=\; S_{\rm UV} \,+\, S_{\rm IR} \\
S_{\rm UV} \;&=\; \sum_i \int d^2{\rm x}\, \epsilon^{\mu\nu}\, \psi_+^i \partial_\mu \psi_+^i \; \psi_-^i \partial_\nu \psi_-^i \\
S_{\rm IR} \;&=\; \sum_{i_1,\ldots,j_q} \int d^2{\rm x}\; J_{i_1\ldots j_q}\; \psi_-^{i_1} \,\ldots\, \psi_-^{i_q}\; \psi_+^{j_1} \,\ldots\, \psi_+^{j_q}
\end{aligned}
\tag{4.1.1}
$$

where $J_{i_1\ldots j_q}$ denote a set of gaussian random couplings with

$$
\left\langle (J_{i_1\ldots j_q})^2 \right\rangle \;=\; \frac{J^2\,(q-1)!\,q!}{N^{2q-1}} \qquad \text{(no sum)}\ . \tag{4.1.2}
$$

The unconventional kinetic term[2] in $S_{\rm UV}$ is chosen such that ψ has canonical scale dimension $[\psi]_{\rm UV} = 0$. The couplings in $S_{\rm IR}$ thus have dimension $[J] = 2$. The interaction term is therefore relevant and dominates the IR dynamics.

The total action defines a proper relativistic QFT, but does not come with a fixed light cone. Both terms in (4.1.1) do not depend on a choice of metric: the UV term is

[2]The quartic kinetic term in (4.1.1) can be viewed as a fermionic cousin of the Nambu-Goto action. It is also similar to the fermionic Wess-Zumino term that appears in the Green-Schwarz superstring action [118].

topological, whereas the IR term only requires a choice of integration measure. $S_{\rm UV}$ is reparametrization invariant if $\psi_\pm$ transform as scalars, while $S_{\rm IR}$ has reparametrization symmetry provided the fermions transform as $\psi_a^i(\mathrm{x}) \to \left|\det \frac{\partial \tilde{\mathrm{x}}^\mu}{\partial \mathrm{x}^\nu}\right|^{1/2q} \psi_a'^i(\tilde{\mathrm{x}}(\mathrm{x}))$. The fact that the UV and IR transformation laws are different is a first hint that the model may give rise to an effective Goldstone mode associated with broken reparametrization symmetry. The UV and IR action still share area preserving diffeomorphisms as a common symmetry group.

Note that the quartic kinetic term involves a diagonal pairing between the chiral partners ψ_+^i and ψ_-^i, but the IR interaction term does not. The action (4.1.1) is invariant under local Lorentz transformations $\psi_\pm^i \to \lambda^{\pm 1}\psi_\pm^i$. For the UV action, these can act independently on each sector. We will treat the overall local Lorentz invariance as a gauge symmetry.

The quartic kinetic term is a central new ingredient of our proposal. So it is important to understand its physical role and consequences. We have seen some of its desirable properties. Some apparent drawbacks are that it obscures the form of the anti-commutation relations and does not produce a standard fermion propagator. To gain some further insight, let us take a closer look at the theory defined by $S_{\rm UV}$ just by itself.

4.1.2 UV limit: Topological Ising CFT

The UV theory splits up into N decoupled topological theories with a single pair of chiral Majorana fermions each. Let us focus on one of these UV sectors. A nonlinear fermionic action similar to $S_{\rm UV}$ with $N = 1$ was recently considered in [119] in the context of a proposed topological theory of Majorana edge modes of a $p_x + ip_y$ superconductor.[3]

[3] A similar topological fermionic model has also been considered by D. Haldane (private communication).

By introducing Hubbard-Stratonovich variables $e_\mu^\pm$ we can rewrite the UV action as

$$S = \frac{1}{2}\int d^2\mathrm{x}\,\epsilon^{\mu\nu}\big(e_\mu^a\,\psi_a\,\partial_\nu\psi_a\,-\,\epsilon_{ab}\,e_\mu^a\,e_\nu^b\,\big). \tag{4.1.3}$$

with $a = \pm$. This action is manifestly reparametrization and local Lorentz invariant. We can think of the e_μ^a variable as a Cartan zweibein, that parametrizes a dynamical 2D metric and local Lorentz frame. For fixed e_μ^a, the action (4.1.3) has a conventional fermion kinetic term. Integrating out e_μ^a gives back the quartic action.

Let us take a brief look at the classical theory. The equations of motion of (4.1.3) imply

$$\begin{aligned} \epsilon^{\mu\nu}e_\mu^+\psi_+\partial_\nu\psi_+ \,&=\, 0, \qquad & e_\mu^+ \,&=\, \psi_-\partial_\mu\psi_-, \\ \epsilon^{\mu\nu}e_\mu^-\psi_-\partial_\nu\psi_- \,&=\, 0, \qquad & e_\mu^- \,&=\, \psi_+\partial_\mu\psi_+. \end{aligned} \tag{4.1.4}$$

Locally we can introduce two scalar fields $X^\pm$ such that

$$e_\mu^+ = e^{\varphi_+}\partial_\mu X^+, \qquad e_\mu^- \,=\, e^{\varphi_-}\partial_\mu X^-. \tag{4.1.5}$$

We can then solve the equation of motion (4.1.4) by setting $\psi_-(X^-)$ and $\psi_+(X^+)$. So for a moment it looks like ψ_- and ψ_+ behave like a pair of chiral fermions that propagate along two independent light-cone directions specified by X^- and X^+. However, from (4.1.4) and (4.1.5) we also deduce that

$$\epsilon^{\mu\nu}\partial_\mu X^+\partial_\nu X^- \,=\, 0 \tag{4.1.6}$$

which can only be solved if the two light-cone directions in fact coincide. So the UV model (4.1.3) does not have true propagating modes. As we will argue below, it describes a topological field theory.

Introducing a dynamical 2D metric via $g_{\mu\nu} = \eta_{ab} e^a_\mu e^b_\nu$, assembling ψ_+ and ψ_- into a two component fermion, and performing a simple field rescaling $\tilde{\psi} = g^{1/8}\psi$, we may further rewrite (4.1.3) as a standard action of a 2D Majorana fermion coupled to 2D gravity

$$S = \int \sqrt{g}\big(\tfrac{\mathrm{i}}{2}\tilde{\psi}\not{\nabla}\tilde{\psi} - 1\big). \tag{4.1.7}$$

This rewriting of S_{UV} is closely analogous to the procedure that recasts the Nambu-Goto action into that of a free boson coupled to 2D gravity. Minimal models coupled to 2D gravity have been studied extensively, starting with KPZ [120]. Our treatment will need to be somewhat different. In the end, we want to be able to add the IR action in (4.1.1) as an interaction term. Since the interaction term is invariant only under area preserving diffeomorphisms, we are not allowed to treat the full diffeomorphism group as a gauge symmetry of the UV theory. So instead of viewing the model as a gravitational theory, we will treat it as a topological CFT with local gauge invariant observables [121–124].

Equations (4.1.3) and (4.1.7) describe a 2D Ising CFT with gauged Virasoro symmetry. The gauging projects out all Virasoro descendent and leaves only three local observables given by the dressed primary operators: the unit operator $\mathbf{1}$, the spin field σ and

$$\epsilon(\mathrm{x}) = \psi_+(\mathrm{x})\psi_-(\mathrm{x}). \tag{4.1.8}$$

We will call this theory the topological Ising CFT. It is the simplest example of a topological RCFT. Some relevant properties of topological RCFTs are summarized in the appendix. For the purpose of our main discussion here, it is sufficient to note that:

• In Euclidean signature, the correlation functions of local observables are independent of positions of the operators. They equal an integer, given by the number of independent chiral conformal blocks associated with the corresponding CFT corre-

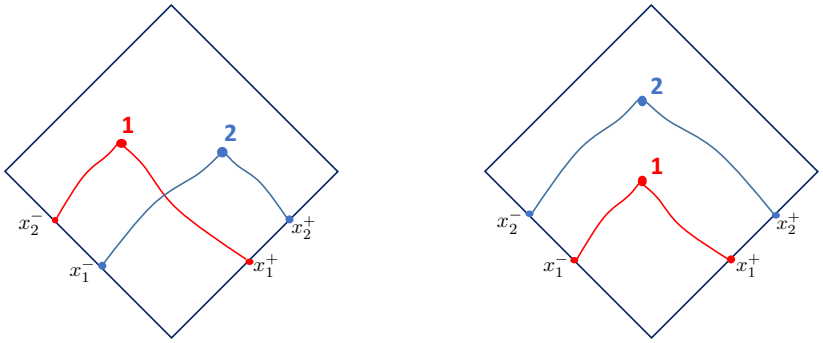

Figure 4.1: In a topological CFT, local operators are attached to two Wilson lines that connect to past null infinity. Whether two operators are space-like or time-like separated is a topological distinction, encoded via the relative ordering of the asymptotic end-points $x_1^\pm$ and $x_2^\pm$ of the respective Wilson lines. The bulk has no fixed metric.

lation function [124].

• The three gauge invariant local observables ϵ, σ and $\mathbf{1}$ all have scale dimension zero. The operator algebra forms a commutative, associative ring isomorphic to the Ising fusion rules

$$\mathbf{1}\times\mathbf{1}=\mathbf{1},\quad \mathbf{1}\times\sigma=\sigma,\quad \mathbf{1}\times\epsilon=\epsilon,\quad \epsilon\times\epsilon=\mathbf{1},\quad \epsilon\times\sigma=\sigma,\quad \sigma\times\sigma=\mathbf{1}+\epsilon.$$

• In Minkowski space, TCFT correlation functions acquire non-trivial position dependence due to operator ordering. This dependence reflects the monodromy of the chiral conformal blocks, or equivalently, the topological braid properties of the chiral CFT operators.

Let us elaborate this last point. Just like in an ordinary RCFT, local observables in a topological RCFT can be factorized into a sum of chiral components. The properties of these chiral components are made most manifest by formulating the TCFT as a gauged WZW model [124]. In this formulation, the chiral operators are attached to a Wilson line of a flat gauge field that stretches out to the corresponding (past or future) null infinity. The Wilson lines encode the topological braid properties of the chiral operators of the CFT.

Hence local operators in a TCFT look as indicated in Figure 4.1. The space-time position of a local operator is labeled by the locations x_i^+ and x_i^- where the Wilson lines attach to past null infinity. Since null infinity of 2D Minkowski space-time is one-dimensional, time ordering again becomes topological. The 2D light-cone thus also becomes a topological notion, that divides 2D space-time into four regions. Correspondingly, for each pair of operators we can distinguish four types of relative separations: past, future, left and right. Thanks to the presence of the Wilson lines, these four are all topologically distinct.

Specializing to the simplest example: for the 2-point function of two ϵ operators in the topological Ising model, the prescription outlined above and in the appendix reduces to

$$\left\langle \mathbb{T}\,\epsilon(1)\epsilon(2)\,\right\rangle_{\text{TCFT}} = \begin{cases} \langle\psi_+(1)\psi_+(2)\rangle\langle\psi_-(1)\psi_-(2)\rangle \;=\; 1 & \text{F} \\ \langle\psi_+(2)\psi_+(1)\rangle\langle\psi_-(1)\psi_-(2)\rangle \;=-1 & \text{R} \\ \langle\psi_+(1)\psi_+(2)\rangle\langle\psi_-(2)\psi_-(1)\rangle \;=-1 & \text{L} \\ \langle\psi_+(2)\psi_+(1)\rangle\langle\psi_-(2)\psi_-(1)\rangle \;=\; 1 & \text{P} \end{cases}$$

The four outcomes correspond to four different operator orderings. Here we introduced the double time ordering symbol $\mathbb{T} = \mathrm{P}_+\mathrm{P}_-$, where $\mathrm{P}_\pm$ denotes the time ordering symbol that orders the operators according to increasing light-cone time $\pm x^\pm$. We can abbreviate the above table as

$$\left\langle \mathbb{T}\epsilon(\mathrm{x}_1)\epsilon(\mathrm{x}_2)\right\rangle_{\text{TCFT}} = \mathrm{sgn}(x_{12}^+)\,\mathrm{sgn}(x_{12}^-) \tag{4.1.9}$$

Here the 2D location $\mathrm{x} = (x^+, x^-)$ of each operator is defined via the position of the end-points of the Wilson lines, as indicated in Figure 4.1. The formula (4.1.9) should be compared with the formula $\langle \mathrm{T}\,\psi(\tau_1)\psi(\tau_2)\rangle = \mathrm{sgn}(\tau_{12})$ for the 2-point function of

a single free Majorana fermion.[4] It forms the basis for the rest of our story. In Appendix 4.6 we sketch how the above result (4.1.9) for the two-point function can be derived from the UV Lagrangian via a functional integral.

More generally, applying the TCFT rules to the n-point function gives that

$$\big\langle\, \mathbb{T}\epsilon(1)\epsilon(2)...\,\epsilon(n)\big\rangle_{\text{TCFT}} = \begin{cases} (-1)^{\#(1,2,...,n)} & n \text{ even} \\ 0 & n \text{ odd} \end{cases} \tag{4.1.10}$$

where $\#(1,2,...,n)$ counts the number of times a pair of operators needs to cross each other's light cone in order to rearrange all operators to be space-like separated. Note that, since ϵ and $\mathbf{1}$ have a unique OPE channel, at most one single chiral conformal block contributes for each n-point function. So the value of the Euclidean n point function is simply equal to 1.

The expression (4.1.10) can be rewritten in somewhat more familiar form as follows

$$\big\langle\, \mathbb{T}\epsilon(\mathrm{x}_1)...\,\epsilon(\mathrm{x}_n)\big\rangle_{\text{TCFT}} = \text{Pf}\big(\text{sgn}(x_{ij}^{+})\big)\,\text{Pf}\big(\text{sgn}(x_{ij}^{-})\big). \tag{4.1.11}$$

A proof of the equality between (4.1.10) and (4.1.11) is given in Appendix A. We see that the non-chiral n-point functions factorize into a product of two chiral factors. This factorization property allows us to define the n-point functions of the chiral Majorana fermions as

$$\big\langle\, \mathbb{T}\,\psi_{\pm}(\mathrm{x}_1)...\,\psi_{\pm}(\mathrm{x}_n)\big\rangle_{\text{TCFT}} = \text{Pf}\big(\text{sgn}(x_{ij}^{\pm})\big) \tag{4.1.12}$$

It is natural to refer to the chiral fields $\psi_+(x^+)$ and $\psi_-(x^-)$ as 'topological 2D Majorana-Weyl fermions'. They arise from the topological Ising model after performing a chiral projection.

[4]The vacuum two-point function of free 1D Majorana fermions remains unchanged at finite temperature [31,42]. The same property holds true for the vacuum two-point function in our topological UV theory. This statement would not be true for 2D Majorana fermions with the usual kinetic term.

Our 2D model (4.1.1) in fact makes essential use of a chiral projection of this kind. Each term in the interaction Lagrangian in (4.1.1) contains an equal number of left- and right chiral fermions, but the pairing can be off diagonal. In other words, the interaction term is built up from general fermion bi-linears $\psi_+^i \psi_-^j$. To allow for such operators with $i \neq j$, while preserving locality, we need to perform an analog of the GSO projection familiar from superstring theory. The complete UV theory is defined by taking a tensor product of N topological Ising models, and then performing a chiral projection that allows us to act with general fermion bi-linears $\psi_+^i \psi_-^j$. Similar to the GSO projection, this eliminates the non-chiral spin operators σ_i of each individual topological Ising model from the UV spectrum. The resulting theory then remains local.

4.1.3 Hamiltonian formulation

We would like to verify that the 2D action (4.1.1) defines a unitary QFT. The Hamiltonian formulation is usually most well adapted for this purpose. So let us write $\mathrm{x} = (x, t)$ and identify the Hilbert space $\mathcal{H}$ of states defined on a constant time-slice. We should then check that there are no negative norm states and that the Hamiltonian generates a unitary time evolution. The formalism of matrix product states [125, 126] will turn out to be helpful.

In many interesting quantum many body systems, the wave function $|\Psi\rangle$ depends in a non-trivial way on the spatial ordering of the quasi-particles. A matrix product state (MPS) representation of a quantum state encodes this spatial dependence by means of an auxiliary quantum system [125, 126]. To define this auxiliary quantum system for our setting, we introduce two collections of N Majorana fermions with anti-commutation relations

$$\{\psi_\pm^i(x), \psi_\pm^j(y)\} = \delta^{ij}, \qquad \{\psi_+^i(x), \psi_-^j(y)\} = 0, \tag{4.1.13}$$

with $i, j = 1, .., N$. Note that the anti-commutator does not depend on the locations x and y. So we can simply set $\psi^i_\pm(x) = \psi^i_\pm$ with $\{\psi^i_\pm, \psi^j_\pm\} = \delta^{ij}$ acting on a $2 \times 2^{N/2}$ dimensional auxiliary Hilbert space. The role of the position x is to keep track of spatial operator ordering within the matrix product state, in the same way that time t can be used to keep track of time ordering for a free 1D Majorana fermion.

States in the Hilbert space $\mathcal{H} = \mathcal{H}_+ \otimes \mathcal{H}_-$ are given by a sum of factorized states $|\Psi^I_+\rangle|\Psi^J_-\rangle$ where I and J represent a multi-index, e.g. $I = \{i_1, ..., i_p\}$ labeling the internal quantum numbers of the chiral Majorana particles. Each factor $|\Psi^I_\pm\rangle$ is represented by a many body wave function in the form of a matrix product state

$$\Psi^{i_1 \dots i_p}_\pm(x^\pm_{i_1}, ..., x^\pm_{i_p}) \;=\; \big\langle n_\pm \big| \, \mathrm{P}_\pm \; \psi^{i_p}_\pm(x^\pm_{i_p}) \dots \; \psi^{i_1}_\pm(x^\pm_{i_1}) \big| 0 \big\rangle \tag{4.1.14}$$

where $|n_\pm\rangle$ is short-hand for the unique fermion number eigen state that gives a non-zero overlap. Here $\mathrm{P}_\pm$ denotes the path ordering symbol that places the operators in spatial order with position $x^\pm_k$ increasing from left to right for Ψ_- and from right to left for Ψ_+. Alternatively, we can write the MPS wave function as a 1D path integral

$$\Psi^{i_1 \dots i_p}_\pm(x^\pm_{i_1}, ..., x^\pm_{i_p}) \;=\; \int [d\psi^i_\pm] \, e^{\pm \sum_i \int dx^\pm \frac{\mathrm{i}}{2} \psi^i_\pm \partial_\pm \psi^i_\pm} \; \psi^{i_p}_\pm(x^\pm_{i_p}) \dots \; \psi^{i_1}_\pm(x^\pm_{i_1})$$

Note that this functional integral is reparametrization invariant in $x^\pm$, and that $\Psi^I_\pm$ is a piece-wise constant function of the positions $x^\pm_{i_k}$. In the case that all ψ^i's have the same index, it reduces to the Pfaffian expression (4.1.12).

This MPS representation provide a natural basis for the energy eigen states of the UV theory described by the quartic Lagrangian (4.1.1) or its HS representation (4.1.3). Due to the reparametrization symmetry, the states only depend on the spatial ordering of the fermionic fields. Moreover, since the Hamiltonian of the UV theory identically vanishes, all MPS states automatically have zero energy.

The Hamiltonian of the full interacting model is defined as a linear mapping on the MPS wave functions. It is given by a pure interaction term $H = \hat{H}_{\rm int}(t) = -\int dx\, \hat{\mathcal{L}}_{int}(x,t)$ with

$$\hat{\mathcal{L}}_{\rm int}(x,t) \;=\; \sum_{i_1,..,j_q} J_{i_1\ldots j_q}\; \hat{\psi}^{i_1}_{+}(x,t)\;\ldots\;\hat{\psi}^{j_q}_{-}(x,t) \tag{4.1.15}$$

the same interaction term as in (4.1.1), and where $\hat{\psi}^{i}_{\pm}(x^{\pm})$ with $x^{\pm} = x \pm t$ now denote operators that insert $\psi^{i}_{\pm}(x^{\pm})$ into the corresponding chiral MPS wave function. Here we reintroduced the time dependence as prescribed by the interaction picture. Note, however, that the free Hamiltonian H identically vanishes. The t dependence is therefore spurious, except for its effect on operator ordering. The dependence on the two light cone coordinates $x^{\pm}$ arises due to the intrinsic path-ordering of the matrix product states.

Integrating the Schrödinger equation produces a double lightcone-time ordering prescription

$$\mathrm{T}\exp\Big(-\mathrm{i}\int dt\, \hat{H}_{\rm int}(t)\Big) \;=\; \mathbb{T}\,\exp\left(\mathrm{i}\int dx^{+}\int dx^{-}\hat{\mathcal{L}}_{\rm int}(x^{+},x^{-})\right) \tag{4.1.16}$$

where $\mathbb{T} \equiv \mathrm{P}_{+}\mathrm{P}_{-}$ puts all operators in order of increasing light cone time, both along the x^{+} and $-x^{-}$ direction. In this way, through the use of the matrix product state formalism, we have made contact with the TCFT prescription outlined in the previous subsection.

The last remaining task is to provide an inner product on $\mathcal{H}$. It seems reasonable to assume that it can be defined such that the states $|\Psi^{I}_{\pm}\rangle$ form an orthonormal basis of the respective chiral Hilbert spaces $\mathcal{H}_{\pm}$. In principle one should be able to derive this inner product from the path-integral formulation, starting from the action (4.1.1), or vice versa, derive the path-integral and the action (4.1.1) from the Hamiltonian formalism outlined here. We leave this problem for future study.

4.2 Schwinger-Dyson equations

Now that we have introduced the 2D model, we would like to analyze its large N dynamics. The factors of N in (4.1.2) are chosen so that the model admits a regular large N limit. We would like to analyze the low point correlation functions of the 2D model, working to leading order in $1/N$. Throughout, we will assume that the standard SYK analysis applies to our 2D model. In particular, we assume that we can use the replica method to take the disorder average, and that the model does not undergo a spin glass transition.

4.2.1 SD equations at large N

The simplest non-trivial correlation function with a regular large N limit is

$$\mathcal{F}(\mathrm{x}_1, \mathrm{x}_2) = \frac{1}{N^2} \sum_{i,j} \left\langle \psi_+^i(x_1)\psi_-^j(x_1)\psi_+^i(x_2)\psi_-^j(x_2) \right\rangle$$

At leading order in $1/N$, it factorizes as

$$\mathcal{F}(\mathrm{x}_1, \mathrm{x}_2) = G_+(\mathrm{x}_1, \mathrm{x}_2) G_-(\mathrm{x}_1, \mathrm{x}_2) \tag{4.2.1}$$

We can identify $G_\pm(\mathrm{x}_1, \mathrm{x}_2)$ with the dressed fermionic two point functions

$$G_\pm(\mathrm{x}_1, \mathrm{x}_2) = \frac{1}{N} \sum_i \left\langle \psi_\pm^i(\mathrm{x}_1)\psi_\pm^i(\mathrm{x}_2) \right\rangle, \tag{4.2.2}$$

with the understanding that each should always appear in the local combination (5.3.10).

To compute the two point functions, we can try to follow the standard SYK procedure and sum all relevant leading order diagrams. We start by writing the UV action in the Hubbard-Stratonovich form (4.1.3) by introducing a total of N Cartan

frames $e_i^\pm$, one for each of the N sectors. It is not difficult to see, however, that by restricting ourselves to observables of the type (4.2.1) and (4.2.2), defined as equal weighted sums over all N sectors, that only the collective field

$$e^\pm \;=\; \frac{1}{N}\,\sum_i\, e_i^\pm \tag{4.2.3}$$

participates in the large N dynamics. More precisely, if we split each frame variable as $e_i^\pm = e^\pm + \tilde{e}_i^\pm$, the deviation $\tilde{e}^\pm$ will decouple in correlation functions of averaged observables. This property follows from the fact that the interaction term between frame variables and $\psi_\pm^i$ is linear in $e_i^\pm$, and that the fermion propagator lines involve a uniform sum over i. So the frame variables always couple via

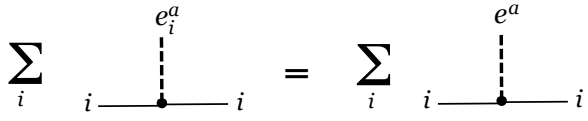

For the computation of large N correlation functions, we can thus replace the frame variables by their large N average (4.2.3) and use the following effective form of the UV action

$$S_{\rm UV} = \frac{1}{2}\int d^2x\,\epsilon^{\mu\nu}\Big(\sum_{i,a} e_\mu^a\,\psi_a^i\partial_\nu\psi_a^i - N e_\mu^+ e_\nu^-\Big). \tag{4.2.4}$$

Notice that there is now an explicit factor of N in front of the last term.

We now proceed to apply the same large N logic as in 1D. We write the perturbation series for fixed e as a sum of 'iterated melon' diagrams [31, 41, 42]. The fermions then have a standard kinetic term and propagator. At the end, we integrate out e, which diagrammatically amounts to connecting all ψ_+ and ψ_- lines by an e propagator

$$\big\langle e_\mu^+(\mathrm{x}_1)\,e_\nu^-(\mathrm{x}_2)\big\rangle = \frac{1}{N}\,\epsilon_{\mu\nu}\delta(x_{12}). \tag{4.2.5}$$

Note that each Wick contraction $\overbrace{e^+\,e^-}$ produces a factor of $1/N$.

A slight problem with the procedure just outlined, however, is that the ψ propagators are singular at $e = 0$, which is the point around which we wish to define the perturbation series. So whenever the e-line connects to a ψ propagator, the ψ propagator in fact collapses to a point. This is not surprising, since we are in fact trying to write a perturbative expansion for an action (4.1.1) without any quadratic term.

A more practical approach is to recast the model in terms of bosonic bi-local dynamical mean fields, given by the two-point function $G_{\pm}(\mathrm{x}_1, \mathrm{x}_2)$ and self-energies $\Sigma^{\pm}(\mathrm{x}_1, \mathrm{x}_2)$.[5] After performing the disorder average and integrating out the fermions, one obtains the following effective action

$$\begin{aligned} S/N \;=\; & -\sum_{a=\pm} \log \mathrm{Pf}(\epsilon^{\mu\nu} e^a_\mu \partial_\nu - \Sigma^a) - \int \epsilon^{\mu\nu} e^+_\mu e^-_\nu \\ & + \frac{1}{2} \iint \big(\Sigma^a G_a - \frac{J^2}{q} (G_+)^q (G_-)^q \big) \end{aligned} \tag{4.2.6}$$

This effective action looks quite similar to the dynamical mean field action of the 1D SYK model [31, 42, 127]. The key new features are the doubling of the number of fields and the presence of the frame variable e^a.

Since the action has an overall factor of N, the Schwinger-Dyson equations for $G_{\pm}$ and $\Sigma^{\pm}$ reduce in the large N limit to the following saddle point equations

$$\Sigma^{\pm}(\mathrm{x}_{12}) \;=\; J^2 G_{\pm}(\mathrm{x}_{12})^{q-1} G_{\mp}(\mathrm{x}_{12})^q, \tag{4.2.7}$$

$$\big(\epsilon^{\mu\nu} e^{\pm}_\mu \partial_\nu G_{\pm} - \; \Sigma^{\pm} * G_{\pm}\big)(\mathrm{x}_{12}) \;=\; \delta^2(\mathrm{x}_{12}), \tag{4.2.8}$$

$$e^{\pm}_\mu(\mathrm{x}_1) \;=\; \frac{\partial G_{\mp}(\mathrm{x}_{12})}{\partial \mathrm{x}_2^\mu}\Big|_{\mathrm{x}_2 \to \mathrm{x}_1}. \tag{4.2.9}$$

[5] Here and in the following we use the same symbols for the dynamical fields as for the on-shell solutions.

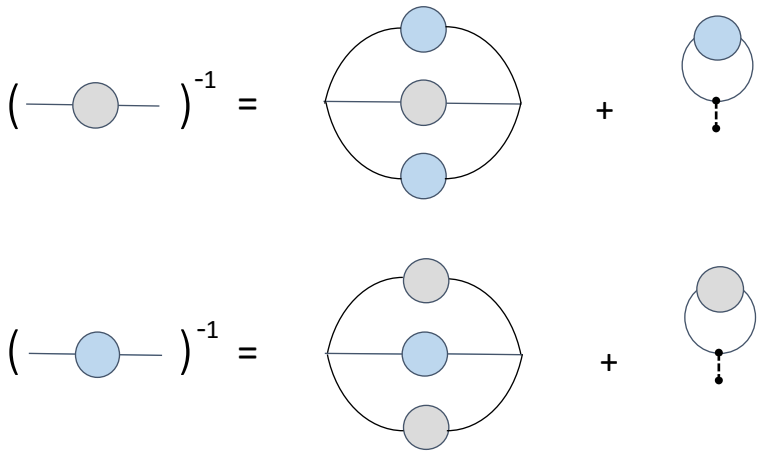

Figure 4.2: Diagrammatic representation of the SD equations (4.2.7), (4.2.8) and (4.2.9) for $q = 2$.

The $*$ in equation (4.2.8) denotes the convolution product. Assuming translation symmetry, equation (4.2.9) yields a constant value for e^a_μ, which on dimensional grounds, is proportional to the temperature β^{-1} times $(\beta^2 J)^{-1/q}$.

We can represent the SD equations in diagrammatic notation as follows. Let us denote the chiral factorization equation (5.3.10) as

$$\mathcal{F}(\mathrm{x}_1, \mathrm{x}_2) \;=\; \tag{4.2.10}$$

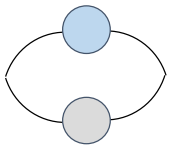

where each line with a blob represents a dressed propagator $G_\pm(\mathrm{x}_{12})$ of the chiral Majorana fermion. The color of the blob represents whether it is a ψ_+ (blue) or a ψ_- (grey).

The SD equations for $q = 2$ are then depicted as in Figure 4.2. The left-hand side denotes each inverse propagator, while the first term on the right-hand side denotes the self-energy. The second term is the contribution from the dynamical kinetic term, which takes the form of a tadpole diagram attached via an e propagator.

4.2.2 Conformal limit

Continuing the standard SYK logic, we first focus on the IR limit. The interaction term then dominates and, working to leading order in $\beta^2 J$, we can drop the UV term. The SD equation (4.2.8) then truncates to

$$\big(G_\pm * \Sigma^\pm\big)(\mathrm{x}_{12}) = -\delta(\mathrm{x}_{12}). \tag{4.2.11}$$

In momentum space (and assuming translation invariance) this further simplifies to

$$G_\pm(\mathrm{k})\Sigma^\pm(\mathrm{k}) = -1. \tag{4.2.12}$$

We will solve equations (4.2.7) and (4.2.11) via a scaling Ansatz momentarily.

Equations (4.2.7)-(4.2.11) are diffeomorphism invariant, and as in the 1D model, this points to a zero mode of the linearized SD equations. In the following subsection, we will exhibit this zero mode by studying the four point function. As a quick preparation, consider a change in $G_\pm$ that corresponds to a reparametrization $(x^+, x^-) \to (x^+ + \epsilon^+, x^- + \epsilon^-)$. In the IR limit this is still a solution of SD equations if we take the Green function and self energy to transform accordingly. The variation of equation (4.2.11) gives the conditions

$$\delta G_\pm * \Sigma^\pm + G_\pm * \delta\Sigma^\pm \;=\; 0. \tag{4.2.13}$$

We can take the product on the right by $(\Sigma^\pm)^{-1} = G_\pm$ to isolate $\delta G_\pm$ and use the expression for $\Sigma^\pm$ in terms of $G_\pm$ in the second term to eliminate the self energy from the equation. The above equation then takes the form, *c.f.* [31] [42]

$$(\delta_{ab} - K_{ab}) * \delta_\epsilon G_b = 0. \tag{4.2.14}$$

where K_{ab} is the integration kernel

$$K_{ab}(x_1...x_4) = -J^2(q-\delta_{ab})G_a(x_{13})G_a(x_{24})L_{ab}(x_{34})$$
$$L_{ab}(x) = \frac{G_+(x)^q G_-(x)^q}{G_a(x)G_b(x)} \tag{4.2.15}$$

This shows that the eigenvalues of the kernel are 1 when evaluated at reparametrizations of the conformal answer. Below we will make this formal conclusion explicit.

Two-point function

We will now study the SD equations, following the approach of [39, 40]. In the IR regime, we adopt the following scaling Ansatz for the dressed propagators and self energies

$$G_\pm(\mathrm{x}) = b\,\frac{\mathrm{sgn}(x^\pm)}{|x^+|^{\Delta\pm s}|x^-|^{\Delta\mp s}}$$
$$\Sigma_\pm(\mathrm{x}) = J^2\,b^{2q-1}\,\frac{\mathrm{sgn}(x^\pm)}{|x^+|^{2-\Delta\mp s}|x^-|^{2-\Delta\pm s}} \tag{4.2.16}$$

with b some constant. Here Δ and s denote the sum and difference of the left- and right scale dimensions. In the following, we will sometimes use the notation $\Delta_\pm = \Delta \pm s$. The sign functions in (4.2.16) implement Fermi statistics, and match with 2-point function of the UV theory. The IR Ansatz breaks the diffeomorphism invariance of the IR theory. A new feature of the 2D model, relative to the 1D case, is that the sign and scaling functions specify a choice of light-cone direction and a signal propagation speed.

The Ansatz (4.2.16) solves the SD equations (4.2.7) and (4.2.11) provided that $\Delta = 1/q$ and

$$J^2b^{2q} = \frac{((1-\Delta)^2-s^2)}{4\pi^2\cot\left(\frac{\pi}{2}(\Delta+s)\right)\tan\left(\frac{\pi}{2}(\Delta-s)\right)} \equiv \alpha_{sq}^2. \tag{4.2.17}$$

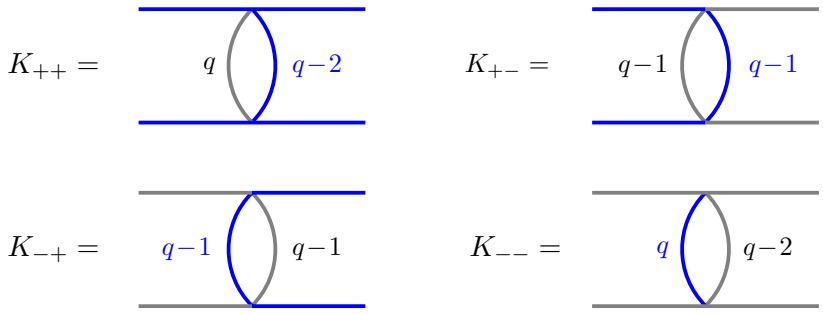

Figure 4.3: Diagrammatic definition of the kernel that gives the four-fermion correlation function. Here each line represents multiple dressed propagators, with multiplicity as indicated.

The value of the spin s is not determined by the SD equations.[6] For generality, we will treat s as a free parameter. The most reasonable and consistent choice is to set $s = \Delta$. We will call this the chiral limit, as it preserves the property that ψ_+ and ψ_- depend only on one light cone coordinate. Note, however, that the $s \to \Delta$ limit has to be taken together with a $J \to \infty$ limit, while keeping b fixed.

Four-point function

Next we study the following four types of four-point functions

$$\mathcal{F}_{ab}(x_1 \dots x_4) \;=\; \frac{1}{N^2}\sum_{i,j}\langle \psi_a^i(x_1)\psi_a^i(x_2)\psi_b^j(x_3)\psi_b^j(x_4)\rangle$$

with $a, b = \pm$. Like the two-point functions, these have to be thought of a part of a locally left-right symmetric correlation function. The $1/N$ corrections to these four point functions can be computed with the help of the kernel K_{ab} introduced in (4.2.15).

To leading order in $1/N$, we have

$$\mathcal{F}_{ab}^{(0)} = \big(-G_a(x_{13})G_a(x_{24}) + G_a(x_{14})G_a(x_{23})\big)\delta_{ab}. \tag{4.2.18}$$

[6] A similar issue appears in [94] for the supersymmetric SYK model.

As explained in [31, 41, 42], the $1/N$ corrections to $\mathcal{F}_{ab}$ are found by summing up the n-th order contributions $\mathcal{F}_{ab}^{(n)}$ defined via the recursive formula

$$\mathcal{F}_{ab}^{(n+1)} \;=\; \sum_{c} K_{ac} * \mathcal{F}_{cb}^{(n)} \tag{4.2.19}$$

where K_{ab} denotes the kernel (4.2.15) and $*$ denotes the double convolution product defined by identifying and integrating over the last two coordinates of K_{ab} and the first two coordinates in $\mathcal{F}_{cb}^{(n)}$. The diagrammatic form of the matrix elements of the kernel is depicted in Figure 5.1.

The iterative procedure gives the following expression

$$\mathcal{F} \;=\; \frac{1}{1-K*}\,\mathcal{F}^{(0)}. \tag{4.2.20}$$

where we have absorbed the matrix product into the definition of $*$. Inserting the conformal Ansatz (4.2.16) into (4.2.15) gives the factorized expression

$$K_{ab} \;=\; -\frac{1}{\alpha_{ab}} K_{ab}^{+}(x_i^{+})\, K_{ab}^{-}(x_i^{-}) \tag{4.2.21}$$

$$\frac{1}{\alpha_{ab}} \;=\; (q-\delta_{ab})\,\alpha_{sq}^{2} \tag{4.2.22}$$

with α_{sq} defined in equation (4.2.17).

Two representative examples of the chiral kernels are

$$K_{++}^{-} \;=\; \frac{1}{|x_{13}^{-}|^{\Delta_-}|x_{24}^{-}|^{\Delta_-}|x_{34}^{-}|^{2-2\Delta_-}} \tag{4.2.23}$$

$$K_{++}^{+} \;=\; \frac{\operatorname{sgn}(x_{13}^{+})\operatorname{sgn}(x_{24}^{+})}{|x_{13}^{+}|^{\Delta_+}|x_{24}^{+}|^{\Delta_+}|x_{34}^{+}|^{2-2\Delta_+}} \tag{4.2.24}$$

with $\Delta_{\pm} = \Delta \pm s$. The action of $K_{ab}^{\pm}$ on the four point functions can be computed with the standard SYK technique, by decomposing each $\mathcal{F}_{ab}$ in terms of eigenfunctions

of the conformal Casimir [30, 31, 41, 42]. These eigenfunctions are given by the three point functions of the fermion with an operator of some given left and right conformal dimension $(h, \bar{h})$. A novel feature of our model is that the eigenvalues of the kernels are given by two different types of integrals. One type of integral looks SYK-like $\int dx_1\, dx_2\, K^{+}_{++}(0, 1, x_1, x_2)\mathrm{sgn}(x_{12})|x_{12}|^{h-\Delta_+}$. We denote the corresponding eigenvalue by $k_{\Delta_+}(h)$. The other type of integral looks like $\int dx_1 dx_2\, K^{-}_{++}(0, 1, x_1, x_2)|x_{12}|^{h-\Delta_-}$. We denote the corresponding eigenvalue by $\tilde{k}_{\Delta_-}(h)$. When acting on an eigenstate the kernel then takes the form

$$K_{ab} \;=\; \frac{1}{\alpha_{ab}} \begin{pmatrix} k_{\Delta_+}(h)\tilde{k}_{\Delta_-}(\bar{h}) & \frac{q}{q-1}\tilde{k}_{\Delta_-}(h)\, k_{\Delta_+}(\bar{h}) \\ \\ \frac{q}{q-1}\tilde{k}_{\Delta_-}(h)\, k_{\Delta_+}(\bar{h}) & \tilde{k}_{\Delta_-}(h)\, k_{\Delta_+}(\bar{h}) \end{pmatrix} \tag{4.2.25}$$

The kernel K_{ab} gives useful information about the spectrum. As a first consistency check, let us act with K on an eigenmode with conformal dimension $(h, \bar{h}) = (2, 0)$. This mode corresponds to the stress tensor, and is expected to describe the effective Goldstone mode associated with broken reparametrization invariance. We find that

$$K_{ab}\Big|_{\substack{h=2 \\ \bar{h}=0}} \;=\; \begin{pmatrix} \frac{(-1+\Delta)(\Delta+s)}{\Delta(2-\Delta-s)} & \frac{-\Delta-s}{\Delta(2-\Delta-s)} \\ \\ \frac{-\Delta+s}{\Delta(2-\Delta+s)} & \frac{(-1+\Delta)(\Delta-s)}{\Delta(2-\Delta+s)} \end{pmatrix} \tag{4.2.26}$$

which manifestly satisfies $\det(\mathbf{1} - K) = 0$. Hence the intermediate states with scale dimension $(2, 0)$ and $(0, 2)$ appear as poles in the conformal strong coupling limit of the expression (4.2.20).

In Figure 4.4 we have plotted $\det(\mathbf{1} - K)$ for chiral intermediate states with left scale dimension h with $\bar{h} = 0$. For illustration, we also included the case $s = 1/2$ given by the dashed magenta graph. The blue graph corresponds to $s = \Delta = 1/q$, which is the chiral limit with $\Delta_- = 0$. In both cases we have set $q = 4$. We see the expected symmetry between h and $1 - h$. For $s = 1/2$, there are additional zeroes

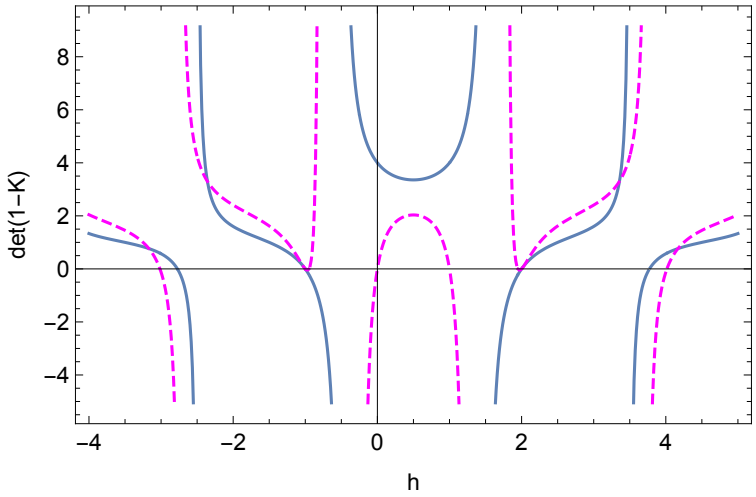

Figure 4.4: Plot of $\det(\mathbf{1}-K)$ as a function of the left scale dimension h with $\bar{h}=0$. The dashed magenta plot corresponds to $\Delta=1/4$ and $s=1/2$, and the blue plot to $\Delta=s=1/4$.

at $h=0$ and 1, which indicates the possible presence of a spin one current, c.f. [94]. The spectrum of zeroes of the $s=\Delta=1/4$ case, on the other hand, looks identical to that of the SYK model. This theory is a plausible candidate for a 2D QFT with maximal chaos. The explicit formula for $\det(\mathbf{1}-K)$ for $\bar{h}=0$, $s=\Delta=1/q$ is

$$\det(\mathbf{1}-K) \;=\; 1 \;+\; \frac{\pi^2(q-2)(q-1)\csc(\frac{2\pi}{q})}{q\Gamma(\frac{2}{q})^2\big(\sin(\pi h)+\sin(\frac{2\pi}{q})\big)\Gamma(2-\frac{2}{q}-h)\Gamma(1-\frac{2}{q}+h)}$$

which coincides with the expression for $1-K$ in the SYK model [31,41,42]. We leave a detailed calculation of the four-point function and the spectrum of states for future work.

4.3 Effective action of the Goldstone mode

We would like to exhibit the effective action of the reparametrization mode. In principle, we could try to follow the procedure used in [30,31,42], compute the correction to the kernel K_{ab} that follows from including the UV term of the action (4.1.1), and use this to find the linearized action of the zero modes. We reserve this calculation for a future project. Here we will instead make a short-cut, which appears justified

in the case that q is small enough so that an expansion in $\epsilon = 1 - 2/q$ is valid [64]. Note that in our model, the $q = 2$ system is still an interacting QFT.

4.3.1 Double Schwarzian action

We start from the dynamical mean field action (4.2.6), and perform the redefinition $\Sigma^{\pm}_{new} = \Sigma^{\pm}_{\text{old}} - \epsilon^{\mu\nu} e^{\pm}_{\mu} \partial_{\nu}$. This redefinition moves all the $e^{\pm}$ dependence into a separate UV term

$$S/N \;=\; S_{\text{UV}} + S_{\text{IR}}$$

$$S_{\text{IR}} \;=\; -\sum_{a=\pm} \log \text{Pf}(\Sigma^a) \;+\; \tfrac{1}{2} \int\!\!\int \Big(\Sigma^a G_a - \tfrac{1}{q} J^2 \, (G_+)^q (G_-)^q \Big) \tag{4.3.1}$$

$$S_{\text{UV}} \;=\; \frac{1}{2} \int d^2\text{x} \, \epsilon^{\mu\nu} \epsilon_{ab} \left(e^a_{\mu} G^b_{\nu} - e^a_{\mu} e^b_{\nu} \right) \tag{4.3.2}$$

Here we defined

$$G^a_{\mu}(\text{x}_1) = \epsilon^{ab} \, \frac{\partial G_b(\text{x}_{12})}{\partial \text{x}_2^{\mu}} \Big|_{\text{x}_2 \to \text{x}_1} \tag{4.3.3}$$

The IR term is the same as before, and leads to the conformal and reparametrization invariant equations of motion (4.2.7) and (4.2.11). However, because Σ^a is the shifted variable, equation (4.2.11) is now exact, and equation (4.2.7) receives a subleading correction due to the presence of the UV term (4.3.2). An exact treatment of the consequences of this correction term could be accessible in the large q limit [42]. We will instead look at the regime $q = 2/(1-\epsilon)$ with ϵ small, and restrict our attention to the chiral limit $s = 1/q$.

The total bosonic action (4.3.1) has the same invariances as the original fermionic action (4.1.1), namely (i) area preserving diffeomorphisms, and (ii) local Lorentz transformations. These symmetries are shared by the UV and IR terms in the action and we will treat both as gauge symmetries. The IR action is also invariant under

local conformal transformations[7]

$$(u, v) \to (x_+(u), x_-(v)). \tag{4.3.4}$$

This conformal symmetry is broken in two separate ways. Picking a particular conformal IR solution of the SD equations spontaneously breaks the local conformal invariance to the global conformal group. This leads to the presence of a Goldstone mode, parametrized by the conformal transformation $(x_+(u), x_-(v))$. Moreover, the UV action is not invariant under the same local conformal transformation rule as the IR action. So it induces a non-trivial effective action for the Goldstone mode.

To get the leading order form of the effective action of the Goldstone mode, we perform a local conformal transformation on the IR propagator. It transforms as

$$G_\pm(u, v, \tilde{u}, \tilde{v}) = [x'_+ x'_+]^{\Delta_+} [x'_- \tilde{x}'_-]^{\Delta_-} \; G_\pm\big(x_\pm, \tilde{x}_\pm\big) \tag{4.3.5}$$

with $(x_\pm, \tilde{x}_\pm) = \big(x_+(u), x_-(v), x_+(\tilde{u}), x_-(\tilde{v})\big)$ and $x'_+ = \partial_u x_+(u)$, etc. In the chiral limit $\Delta_- \to 0$ and $\Delta_+ = \Delta = 1/q = \frac{1}{2}(1-\epsilon)$, the dressed propagator behaves in the conformal regime as $G_\pm(x, \tilde{x}) = \frac{b^{1-\epsilon}}{|x_\pm - \tilde{x}_\pm|^{1-\epsilon}}$. We can now use this expression, transform it via (4.3.5), plug it into the UV action (4.3.2), and extract the dependence on $x_+(u)$ and $x_-(v)$.

The conformal propagator diverges in the coincident limit. This divergence is expected to be removed by the UV modification. A more practical method is to take the coincident limit while subtracting the singular contribution in the (u, v) coordinates. Working to leading order in ϵ and using that

$$\partial_u \left(\frac{\sqrt{x'(u) x'(\tilde{u})}}{|x(u) - x(\tilde{u})|} - \frac{1}{|u - \tilde{u}|} \right) \Bigg|_{\tilde{u} = u} = \frac{1}{12} \big\{ x, u \big\} \tag{4.3.6}$$

[7]In the rest of this subsection, we temporarily move the upper $\pm$ index on $x^\pm$ to a lower index.

with $\{x,u\} = \frac{x'''}{x'} - \frac{3}{2}\left(\frac{x''}{x'}\right)^2$ the Schwarzian derivative, we find that the effective action of the reparametrization modes takes the form

$$\frac{S_{\rm UV}}{N} \;=\; \frac{b}{12}\int du\,dv\,\left(e_v^+\{x_+,u\} + e_u^-\{x_-,v\}\right) - \int \epsilon^{\mu\nu} e_\mu^+ e_\nu^- \tag{4.3.7}$$

After integrating out $e^\pm$, we obtain

$$\frac{S_{\rm UV}}{N} \;=\; \frac{\alpha_S}{J}\int du\,dv\,\{x_+,u\}\{x_-,v\}. \tag{4.3.8}$$

Applying the ϵ expansion method of [64] gives that

$$\alpha_S = \frac{\alpha_{sq}}{144}\left(1-2\epsilon^2\right) + O(\epsilon^4) \tag{4.3.9}$$

with α_{sq} defined in (4.2.17). The effective action (4.3.8) is a functional on the group of the 2D conformal transformations. It generalizes the Schwarzian action for the reparametrization mode of the SYK model. We expect that, by generalizing the analytic and numerical analysis of [42] to the 2D model, it should be possible to compute the pre-coefficient α_S for general values of q.

4.3.2 Free energy and spectral density

By considering the transformation of the Schwarzian derivative under conformal mappings, we can extract useful information about the behavior of the theory on a circle and at finite temperature. At finite temperature, the effective action (4.3.8) receives additional terms

$$\frac{\alpha_S}{J}\int du\,dv\,\left(T_{--}\{x^+,u\} + T_{++}\{x^-,v\} + T_{++}T_{--}\right)$$
$$T_{++} = \frac{\pi^2}{\beta_+^2}(x'_+)^2, \qquad T_{--} = \frac{\pi^2}{\beta_-^2}(x'_-)^2, \tag{4.3.10}$$

with $\beta_\pm$ the left- and right-moving inverse temperature. This term is subdominant at low temperature, but becomes important at distance scales of order the thermal wave length. If we take, say, the left moving high temperature limit, we obtain a single Schwarzian action for the right-movers. This suggests that the 2D model reduces to the 1D SYK model by performing a DLCQ limit.

Equation (4.3.8) captures the explicit breaking of conformal invariance of the IR theory due to UV term in (4.1.1). Its form as a product of two chiral Schwarzian derivatives, as well as the finite temperature correction term (4.3.10), indicates that the leading order correction to the IR conformal field theory takes the form of an irrelevant $T\bar{T}$ deformation, given by the product of the left- and right-moving stress tensors [128–131].

To test this interpretation, let us consider the model on a cylinder with circumference $L = 2\pi$.[8] The conformal mapping from the plane to the cylinder induces a negative Casimir energy, which can be taken into account by setting $\{x_+, u\} = \{x_-, v\} = -1/2$ in equations (4.3.8)-(4.3.10). Now consider the contribution of the effective action of the Goldstone mode to the free energy at finite temperature. Setting $\beta_\pm = \beta$, we find that

$$\begin{aligned} -\beta F &\supset -\frac{N\alpha_S}{J}\int_0^{2\pi} dx \int_0^{\beta} dt \left(-\frac{1}{2} + \frac{\pi^2}{\beta^2}\right)^2 \\ &= \frac{2\pi N\alpha_S}{4J}\left(-\beta + \frac{4\pi^2}{\beta} - \frac{4\pi^4}{\beta^3}\right). \end{aligned} \tag{4.3.11}$$

We wish to compare this result with the free energy of a CFT of central charge c with a $T\bar{T}$ deformation. The energy spectrum and thermodynamics of this class of theories was studied in detail in [128–130], and a holographic interpretation[9] has

[8] So all dimensionful quantities are measured in units of the cylinder radius.

[9] The holographic dual of the $T\bar{T}$ deformation proposed in [131] is closely similar to the candidate AdS_2 dual interpretation of the 1D SYK model developed in [46–48], built on the earlier work [45]. In both cases, the boundary of the AdS space-time is moved into the bulk. On the CFT side, this represents an explicit breaking on conformal invariance and gives rise to an associated dynamical

recently been proposed in [131]. Using the results of [128] [131], one finds that the free energy of a deformed CFT with action $S_{\rm CFT} + \int \mu T\bar{T}$ has the following small temperature expansion

$$-\beta F_{\rm CFT+\mu T\bar{T}} \;=\; -\frac{c\beta}{12} + \frac{\pi^2 c}{3\beta} - \frac{\pi^3 \mu c^2}{72\beta^3} + \ldots \tag{4.3.12}$$

The first two terms are the standard CFT expression for the Casimir energy and specific heat. Comparing the expressions (4.3.11) and (4.3.12) suggests that the IR limit of our model is a 2D CFT with central charge c, and that the leading deviation on conformal invariance is given by a $T\bar{T}$ interaction with coupling μ, with c and μ given by

$$\frac{c}{24\pi} = \frac{N\alpha_S}{4J}, \qquad \mu = \frac{24\pi}{c} = \frac{4J}{N\alpha_S}. \tag{4.3.13}$$

This reciprocal relation between c and μ precisely agrees with the relationship derived from the holographic dictionary proposed in [131].

By performing an inverse Laplace transform of the partition function $Z(\beta) = e^{-\beta F}$ with respect to β, we can extract the spectral density as a function of the energy E:

$$\rho(E) \;\propto\; \exp\left(2\pi\sqrt{\frac{cE}{3}}\left(1 - \frac{3E}{2c} + \ldots\right)\right) \tag{4.3.14}$$

The leading term is the Cardy formula[10] and the subleading term reflects the explicit breaking of conformal symmetry. This formula precisely matches with the low energy expansion of the exact equation of state $EL - \frac{\mu}{4}E^2 = \frac{3}{2\pi c}S^2$ relating the energy and the entropy $S = \log\rho(E)$ of the $T\bar{T}$ deformed CFT [131], provided we set $L = 2\pi$ and μ as in (4.3.13).

pseudo-Goldstone mode. We will make the AdS_3 interpretation of the action (4.3.8) more explicit in the next subsection.

[10]Here E is defined such that the CFT ground state has negative Casimir energy $E/L = -c/12$.

4.3.3 Relation with AdS_3 gravity

The double Schwarzian action (4.3.8) can be related to the 3D AdS gravity action as follows.

In the above derivation we identified the effective Goldstone degree of freedom with the group of 'passive' conformal reparametrizations (4.3.4). To match with the gravity side, it is convenient to represent the Goldstone mode as an 'active' 2D conformal transformation

$$(x^+, x^-) \to \big(U(x^+), V(x^-)\big) \tag{4.3.15}$$

defined as the inverse mapping of (4.3.4). In terms of (U, V), the effective action (4.3.8) reads

$$\frac{S[U,V]}{\alpha_S N/J} = \int d^2\mathrm{x}\, \mathcal{S}_+(U)\mathcal{S}_-(V), \tag{4.3.16}$$

where $\mathcal{S}_+(U)$ and $\mathcal{S}_-(V)$ are defined via

$$\mathcal{S}_+(U)\,\partial_+ U = \{U, x^+\}, \qquad \mathcal{S}_-(V)\,\partial_- V \,=\, \{V, x^-\}. \tag{4.3.17}$$

We will now show that the effective action (4.3.16) is equal to the 3D gravity action

$$S[U,V] = \, S_{\mathrm{grav}}[U,V] \tag{4.3.18}$$

evaluated on a suitable classical solution of 3D gravity defined on a AdS_3 space-time with finite radial cut-off, specified as follows. Let B denote the boundary of the cut-off AdS_3 space-time. We define the Einstein action via

$$S_{\mathrm{grav}} \,=\, \frac{1}{16\pi G_N}\int\sqrt{g}\big(R - 2\Lambda\big) + \frac{1}{8\pi G_N}\int_B (K+1)$$

where, besides the usual extrinsic curvature term K, we included a boundary cosmological constant identical to the standard counter term used in holographic renormalization. The classical solution associated with (U, V) is defined via the boundary condition that the pull back of the 3D bulk metric to B is a flat 2D metric given by

$$ds^2|_B = dUdV \; = \; U'(x^+)V'(x^-)dx^+dx^-. \tag{4.3.19}$$

The holographic identification (4.3.18) holds if we identify the bulk Newton constant as

$$\frac{1}{16\pi G_N} = \frac{N\alpha_S}{4J}. \tag{4.3.20}$$

Equation (4.3.18) looks a little surprising at first. One might think that, since the gravity action is reparametrization invariant, it should be independent of $U(x^+)$ and $V(x^-)$. Recall, however, that the Lagrangian changes by a total derivative under an active diffeomorphism, and that 2D conformal transformations necessarily extend all the way to null infinity. A helpful way to visualize the asymptotic region is by mapping the 2D space-time onto a Penrose diagram. The conformal transformations are then analogous to the BMS group. Once we choose a preferred reference coordinate system, the dependence of the action on $U(x^+)$ and $V(x^-)$ becomes finite and computable.

The holographic identification (4.3.18) can be derived in various ways. One is direct computation. Another route is to show that the action (4.3.16) satisfies the Hamilton-Jacobi equation that governs the radial evolution of a classical action in 3D gravity. An instructive derivation goes via the following three basic steps.

First we reintroduce the frame variables $e^\pm$ and rewrite (4.3.16) as the minimum over $e^\pm$ of

$$\int d^2x \left(e^-_- \mathcal{S}_+(U) + e^+_+ \mathcal{S}_-(V) - \epsilon^{\mu\nu} e^+_\mu e^-_\nu \right) \tag{4.3.21}$$

Next we introduce the background zweibein

$$E^+_\mu dx^\mu = dU, \qquad E^-_\mu dx^\mu = dV \tag{4.3.22}$$

and make use of the relationship between the Polyakov-Liouville action (viewed as a functional of the zweibein)

$$S_{\rm L}[E] = \frac{1}{8\pi}\int R\,\Box^{-1}R, \qquad\qquad g_{\mu\nu} = \eta_{ab}\,E^a_\mu E^b_\nu \tag{4.3.23}$$

and the Schwarzian derivative to write

$$\frac{S[U,V]}{\alpha_S N/J} = \min_e \Big(S_{\rm L}\big(E+e\big) \,-\, \int \epsilon^{\mu\nu} e^+_\mu e^-_\nu \Big). \tag{4.3.24}$$

Here we used that, in the linearized approximation, $S_{\rm L}[E+e] = \int (e^-_-\,\mathcal{S}_+(U) + e^+_+\,\mathcal{S}_-(V))$. Note that the Polyakov action vanishes for the flat metric (4.3.22) and that $\{U,x\} = -\frac{1}{2}(\phi')^2 + \phi''$ with $\phi = \log U'$.

Since the Polyakov action arises by integrating out a 2D CFT, the identity (4.3.24) is yet another indication that the IR theory describes a 2D CFT in a fluctuating metric $g_{\mu\nu} = \eta_{ab}(E^a_\mu + e^a_\mu)(E^b_\nu + e^b_\nu)$. Integrating out the metric fluctuations first produces a CFT with a $T\bar{T}$ deformation.

The third and final step in the derivation of (4.3.18) uses an (underappreciated) result of Freidel that establishes a direct transformation between the 3D Einstein action evaluated on a classical background and the Polyakov action evaluated on the boundary metric [132]

$$S_{\rm grav}[E] = \min_e \Big(S_{\rm L}\big(E+e\big) \,-\, \int \epsilon^{\mu\nu} e^+_\mu e^-_\nu \Big) \tag{4.3.25}$$

Here $S_{\text{grav}}(E)$ is the classical bulk gravity action with boundary conditions $g_{\mu\nu} = \eta_{ab} E^a_\mu E^b_\nu$. The formula (4.3.25) forms the basis of the holographic interpretation of the $T\bar{T}$ deformed theory proposed in [131]. In our context, it provides the link between 3D gravity and the choice of kinetic term in our proposed 2D analog of the SYK model. A detailed derivation of the relation (4.3.25) can be found in [132].

4.4 Conclusion

We have proposed a 2D QFT generalization of the SYK model, consisting of N Majorana fermions with a random non-linear interaction. While the quartic kinetic term of our action (4.1.1) looks somewhat unconventional, it can be rewritten as in (4.1.3) as a conventional quadratic kinetic term coupled to a dynamical metric. The total action is invariant under area preserving diffeomorphisms and local Lorentz transformations. We treat both invariances as gauge symmetries.

We have presented evidence that the model exhibits conformal symmetry in the IR, and that the low energy dynamics is dominated by an emergent Goldstone-like mode associated with the breaking of conformal reparametrization symmetry. Just as in SYK, this symmetry breaking is introduced by the fact that UV action assigns a lower scale dimension $[\psi]_{\text{UV}} = 0$ to the Majorana fermions than the relevant interaction term, which prescribes that $[\psi]_{\text{IR}} = 1/q$. Some questions that need further study are: Is there a principle that fixes the IR value of the spin s, or is it an adjustable parameter? What do the Hilbert space, energy spectrum, partition function and correlation functions look like?

The motivation for our study is to find new examples of strongly coupled 2D QFTs with potential gravity duals and to elucidate the role of the reparametrization mode in the holographic dictionary. While our model still needs to be put on firmer footing, there are encouraging signs that it is well defined and exhibits the hallmarks of a holographic dual to AdS_3 gravity. In particular, it seems plausible that the

conformal symmetry is non-linearly realized in terms of the reparametrization mode. In [54] we have shown that this uniquely dictates the commutation relations of the Goldstone modes and implies maximal Lyapunov growth of out-of-time ordered correlation functions. In view of the results of [54] [74] and the discussion in section 4.3.3, we expect that the effective theory of the reparametrization mode should be closely related to Liouville theory. A natural route towards making this relationship concrete is to postpone the integral over Hubbard-Stratonovich variable $e^{\pm}$ and to extract its effective action by making use of equation (4.3.24).

Finally, it is natural to speculate whether a similar approach could lead to proposed generalizations of the SYK model to higher dimensions. The UV action has an obvious reparametrization invariant generalization

$$\epsilon^{ab\ldots f}\epsilon^{\mu\nu\ldots\sigma}\,\psi_a\partial_\mu\psi_a\,\psi_b\partial_\nu\psi_b\ldots\psi_f\partial_\sigma\psi_f.$$

Adding a ψ^{qD} interaction term would again be a relevant deformation, and the two terms combined would be invariant under volume preserving diffeomorphisms. However, it seems premature to pursue this generalization without first obtaining a better understanding of the landscape of lower dimensional examples.

4.5 Appendix: Topological RCFT

What is a topological RCFT? A rational CFT is a CFT with an infinite chiral algebra $\hat{\mathfrak{g}} \supset \text{Vir}$ and a finite set of primary fields $\mathcal{O}_i$. For minimal models, $\hat{\mathfrak{g}}$ equals the Virasoro algebra. A topological RCFT is defined by gauging the chiral algebra $\hat{\mathfrak{g}}$. This projects the operator content to the set of primary fields, and removes all position dependence of the Euclidean correlation functions of local operators. All known RCFT can be represented as coset WZW models, and all known topological RCFTs

can be formulated as fully gauged WZW models. The topological Ising model is a gauged $\mathfrak{su}(2)_k$ coset with $k = 2$.

In Euclidean space, the four-point correlation function of local operators $\mathcal{O}_i = \mathcal{O}_i(\mathrm{x}_i)$ in a TCFT are specified via the following simple rule [122–124]

$$\big\langle \mathcal{O}_1\mathcal{O}_2\mathcal{O}_3\mathcal{O}_4 \big\rangle_{\text{TCFT}} = \dim\big(\mathcal{H}_{1234}\big),$$

where $\mathcal{H}_{1234}$ denotes the linear vector space spanned by the chiral conformal blocks

$\mathcal{F}_{\mathrm{a}}(1234)$ =

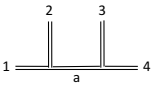

associated with the corresponding CFT correlation function. This rule satisfies all axioms of 2D TQFT [121]. For gauged WZW models, the above prescription naturally follows from the identification of $\mathcal{H}_{1234}$ with the Hilbert space of a 3D Chern-Simons theory in the presence of four Wilson lines. Schematically

$$\mathcal{F}_{\mathrm{a}}(1234) = \mathrm{W}_1(1)\mathrm{W}_2(2)\mathrm{W}_3(3)\mathrm{W}_4(4)|0\rangle_{\mathrm{CS}}. \tag{4.5.1}$$

The CS functional integral on $\mathbb{R}^2 \times S^1$ reduces to the TCFT amplitude on $\mathbb{R}^2$ and takes the form of a sum of inner products between the left and right chiral conformal blocks [122–124]

$$\big\langle \mathcal{O}_1\mathcal{O}_2\mathcal{O}_3\mathcal{O}_4 \big\rangle_{\text{TCFT}} = \sum_{\mathrm{a}} \langle \mathcal{F}_{\mathrm{a}} | \mathcal{F}_{\mathrm{a}} \rangle = \mathrm{tr}_{\mathcal{H}_{1234}}\big(\mathbb{K}\big).$$

Here we used the conventional RCFT normalization of conformal blocks, for which the fusion and braid operations are represented as unitary matrices. In this unitary basis, the OPE coefficients are all given by integer fusion coefficients N_{ijk}. The local

observables thus form a commutative, associative ring isomorphic to the fusion algebra

$$\mathcal{O}_i \times \mathcal{O}_j = \sum_k N_{ijk}\, \mathcal{O}_k. \tag{4.5.2}$$

In Minkowski space-time, operator ordering plays a non-trivial role. Local operators in an RCFT decompose as a sum of factorized terms $\mathcal{O}(x^+, x^-) = \sum_s \mathcal{V}_s^+(x^+)\mathcal{V}_s^-(x^-)$. The $\mathcal{V}_s^\pm$ are known as chiral vertex operators. Chiral vertex operators of the same chirality satisfy non-trivial braiding relations, and can be thought of as end points of light-like Wilson lines. Whenever a $\mathcal{V}_j$ passes through the light-cone of another $\mathcal{V}_k$, the corresponding chiral conformal block undergoes a non-trivial monodromy. E.g.

$$\mathcal{F}_{\rm a}(1234) \;=\; \sum_{\rm b} R^{\epsilon}_{\rm ab}\mathcal{F}_{\rm b}(1324) \qquad \text{or} \qquad$$

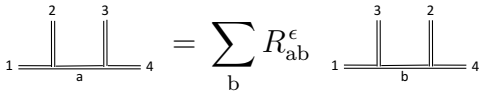

Here R_{ab} is known as the R-matrix and $\epsilon = \pm 1$. This choice of sign indicates that the braiding move depends on orientation. The ordering of chiral vertex operators is encoded via the end-point of the corresponding Wilson lines, as indicated in Figure 4.1.

In non-chiral correlation functions, the above monodromy produces a discontinuity when operators pass through each others light-cone. The monodromy of the left- and right-light cone have opposite orientation, so the total monodromy cancels out when two operators pass through both of each other's light-cones. Hence the Euclidean correlation functions are single valued and the non-chiral CFT thus remains local.

The same chiral decomposition and dependence on operator ordering holds true in a topological RCFT. The TCFT correlation functions thus acquire a non-trivial position dependence

$$\left\langle \mathcal{O}_1\mathcal{O}_2\mathcal{O}_3\mathcal{O}_4 \right\rangle_{\rm TCFT} = \sum_{\rm a,b} \langle \mathcal{F}_{\rm a}|R^{\epsilon}_{\rm ab}|\mathcal{F}_{\rm b}\rangle = \mathrm{tr}_{\mathcal{H}_{1234}}(R)$$

where R^{ϵ}_{ab} is the R-matrix that implements the braiding operation that re-arranges all operators into space-like separated positions. The above discussion easily generalizes to higher n-point functions.

Applying this general prescription to the special case of the n point functions of the operators $\epsilon(\mathrm{x}) = \psi_+(\mathrm{x})\psi_-(\mathrm{x})$ gives the result (4.1.10). The relevant R matrix in this case is simply equal to the (-1) factor that implements Fermi statistics. The equality between (4.1.10) and (4.1.11) then follows directly by applying the definition of the Pfaffian

$$\mathrm{Pf}(M) = \frac{1}{2^n n!}\varepsilon_{i_1 j_1 i_2 j_2 \ldots i_n j_n} M_{i_1 j_1} M_{i_2 j_2} \ldots M_{i_n j_n} \tag{4.5.3}$$

for the case that $M_{ij} = \mathrm{sgn}(x_{ij})$ (with $x = x^{\pm}$). One can make a permutation of the n points such that they are in order of increasing x. This can be recast as a permutation of the indices that gives an overall factor of $(-1)^P$ where P is the parity of the permutation. Then the value is fixed by the Pfaffian when the points are ordered such that $x_1 < x_2 < \ldots < x_n$. This gives a factor of $(-1)^{n/2}$. Since n is even, the total factor is equal to 1 for the product (4.1.11) of the left- and right-Pfaffian.

4.6 Appendix: Two point function from path integral

In this appendix we sketch a formal path integral derivation of the UV correlation function given in equation (4.1.11) starting from the Lagrangian formulation of the theory (4.1.3). In the main text we argued that the natural gauge invariant observables of this theory are products of the form $\epsilon(\mathrm{x}) = \psi_+(\mathrm{x})\psi_-(\mathrm{x})$. For simplicity we will focus on the two-point function $\left\langle \bar{\epsilon}(\mathrm{x})\, \epsilon(0) \right\rangle$ of a slightly modified theory, in which

the fermionic variables $\psi_\pm$ are both replaced by complex fermions

$$\begin{aligned} S &= \frac{1}{2}\int d^2\mathrm{x}\,\epsilon^{\mu\nu}\big(\,e^a_\mu\,\bar\psi_a\,\partial_\nu\psi_a\,-\,\epsilon_{ab}\,e^a_\mu\,e^b_\nu\,\big), \\ &= \frac{1}{2}\int d^2\mathrm{x}\,\big(\,e^+\wedge\bar\psi_+ d\psi_+ + e^-\wedge\bar\psi_- d\psi_- - e^+\wedge e^-\,\big). \end{aligned} \tag{4.6.1}$$

The generalization of the calculation outlined below to general n-point functions of the theory with real fermions is more involved but straightforward.

We will compute the two-point function $\big\langle\bar\epsilon(\mathrm{x})\,\epsilon(0)\big\rangle$ by performing the path integral in steps: we first do the path integral over the fermions with fixed $e^\pm$ and then we integrate over the HS variable $e^\pm$

$$\big\langle\bar\epsilon(\mathrm{x})\,\epsilon(0)\big\rangle = \mathcal{N}^{-1}\int[de^\pm]\;e^{\frac{i}{2}\int e^+\wedge e^-}\big\langle\bar\psi_+(\mathrm{x})\,\psi_+(0)\big\rangle_{e^+}\big\langle\psi_-(\mathrm{x})\,\bar\psi_-(0)\big\rangle_{e^-}. \tag{4.6.2}$$

Here $\mathcal{N}$ is a normalization factor. Next we make use of the reparametrization symmetry of the action (4.6.1) to choose a gauge in which $e^\pm = e^\pm_\pm\,dx^\pm$. We will call this the light-cone gauge, as it fixes the dynamical light-cone to align with the $x^\pm$ coordinate axes. In this gauge, the coordinate system $\mathrm{x} = (x^+, x^-)$ is linked to the frame variable $e^\pm$ and this in particular means that the seemingly local operator $\epsilon(\mathrm{x})$ is in fact non-local when expressed as covariant observable.

The fermion propagator in the light-cone gauge is given by

$$\begin{aligned} \big\langle\bar\psi_+(\mathrm{x})\,\psi_+(0)\big\rangle_{e^+}\big\langle\psi_-(\mathrm{x})\,\bar\psi_-(0)\big\rangle_{e^-} &= \frac{\delta(x^+)}{e^+_+(\mathrm{x})}\,\mathrm{sgn}(x^-)\times\frac{\delta(x^-)}{e^-_-(0)}\,\mathrm{sgn}(x^+) \\ &= \frac{\delta^2(\mathrm{x})}{e^+_+(\mathrm{x})\,e^-_-(0)}\times\mathrm{sgn}(x^+)\,\mathrm{sgn}(x^-). \end{aligned} \tag{4.6.3}$$

This looks like an unpractical observable, since it involves the inverse of the frame fields. We can put it in a more manageable form via a Schwinger parametrization $\frac{1}{e^\pm_+} = \int_0^\infty d\lambda^+ e^{-\lambda^+ e^+_+}$. Inserting this and performing the gaussian path integral over

the HS fields gives

$$\begin{aligned}\mathcal{N}^{-1}\int[de^{\pm}]\; e^{\frac{i}{2}\int e^{+}\wedge e^{-}}\frac{\delta^{2}(\mathrm{x})}{e_{+}^{+}(\mathrm{x})\,e_{-}^{-}(0)} &= \mathcal{N}^{-1}\int_{0}^{\infty}d\lambda^{+}d\lambda^{-}e^{\frac{1}{2}\lambda^{+}\lambda^{-}\delta^{(2)}(\mathrm{x})}\delta^{(2)}(\mathrm{x}),\\ &= \frac{2}{\mathcal{N}}\int_{0}^{\infty}\frac{d\lambda^{+}}{\lambda^{+}}\int_{0}^{\infty}d\lambda^{-}\frac{\partial}{\partial\lambda^{-}}e^{\frac{1}{2}\lambda^{+}\lambda^{-}\delta^{(2)}(\mathrm{x})},\\ &= \frac{2}{\mathcal{N}}\int_{0}^{\infty}\frac{d\lambda^{+}}{\lambda^{+}}\;=\;1. \end{aligned}\tag{4.6.4}$$

In the first line we performed the integral over the HS field, using the fact that the propagator gives a contact term $\langle e_{+}^{+}(\mathrm{x})e_{-}^{-}(0)\rangle = -i\delta^{(2)}(\mathrm{x})$. In the second line we rewrote the delta function as a derivative with respect to λ^{-}, which allows us to integrate by parts and evaluate at $\lambda^{-}=0$. This cancels all spacetime dependence of the correlation function (4.6.4), yielding a divergent constant which we choose to cancel out by the overall normalization constant $\mathcal{N}$. We thus obtain

$$\left\langle\bar{\epsilon}(\mathrm{x})\,\epsilon(0)\right\rangle = \mathrm{sgn}(x^{+})\,\mathrm{sgn}(x^{-}).\tag{4.6.5}$$

This is the TCFT correlator quoted in the main text. It takes the form of the product of two 1D propagators. Note that the cancellation of the delta-function factors is essentially enforced by the fact that $\epsilon(\mathrm{x})$ has canonical scaling dimension equal to zero.

The above derivation of the two point function from the four-fermion UV action (4.1.1) is admittedly somewhat formal and should be supplemented with the right $i\epsilon$'s to make each step well-defined.

The generalization to n-point function requires a bit more effort, but a combination of fermi statistics, Wick's theorem and dimensional analysis essentially prescribes that the final result must take the form (4.1.11).

We leave a more complete and careful path-integral derivation of the result (4.1.11) to future work but we hope this preliminary calculation clarifies the topological nature of the UV theory.

Chapter 5

Conformal Symmetry and Quantum Chaos

In the previous chapter we have proposed a 2D field theoretic version of the SYK model. The IR mode of this model controls the thermodynamics, thermalization, quasi-normal modes and chaos exponent of the theory. In this chapter we will be more general, go beyond SYK-like proposals, and extend these ideas to 2D CFTs.

Since conformal symmetry is always broken by an anomaly (we have in mind large c) we would like to find a universal theory describing this Goldstone-like mode in 2D. This would not mean that any CFT is maximally chaotic but rather that theories with an IR dynamics dominated by this mode saturate the chaos bound. We will study to what extent this theory controls the chaos exponent and saturates the chaos bound. We will also analyze properties of Ruelle resonances (quasi-normal mode frequencies) and relate these time scales to the location of singularities in OPE coefficients. We also define a toy model using discrete Liouville theory that shares both features. In the following section we begin by giving a summary and overview of results.

5.1 Overview

As reviewed in the introduction, characteristics of chaotic systems, such as Lyapunov behavior, scrambling and Ruelle resonances, can be effectively isolated by studying out-of-time ordered correlation functions [30,31,41,62,133–136]. Many body quantum chaos is interesting in its own right, but usually hard to quantify. Identifying simple models or general mechanisms that exhibit aspects of quantum chaos is therefore a worthwhile goal. In this chapter we make three interrelated observations that may help 1) identify a new class of toy models in the form of a simple lattice model built out of parafermionic spin variables 2) clarify the relationship between maximal quantum chaos and the non-linear realization of conformal symmetry at finite temperature, 3) relate the spectrum of Ruelle resonances to analytic properties of OPE coefficients in the CFT. We now briefly describe each of the three components of our story.

1) A discrete model of many body quantum chaos

Useful many body systems that may exhibit chaos are quantum spin chains and matrix models. Another interesting example is the SYK model, which is solvable at strong coupling, maximally chaotic, and exhibits emergent conformal symmetry at low energies [31]. Our model of interest combines ingredients and properties of both examples, with the added feature that its Lyapunov behavior can be exhibited via weakly coupled effective field theory. The model described below is a minor specialization of the class of integrable lattice models introduced by Faddeev, Kashaev and Volkov [137–141].

The model is assembled from a collection of $\mathbb{Z}_N$ parafermionic operators $\mathrm{f_n}$, labeled by an integer $1 \leq n \leq L$ with L some large odd integer. We identify $\mathrm{f_{L+1}} \equiv \mathrm{f_1}$, so the integers n label points on a 1D periodic lattice. The $\mathrm{f_n}$ satisfy the algebra

$$\mathrm{f_{2n\pm1} f_{2n}} = \mathrm{q^2\, f_{2n} f_{2n\pm1}}, \qquad \mathrm{q} = \mathrm{e^{i\pi/N}}, \tag{5.1.1}$$

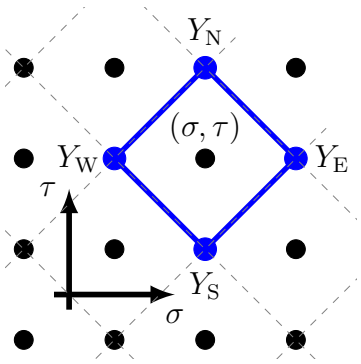

Figure 5.1: The discrete model is defined on a rhombic lattice. We indicated the center (σ, τ) of the diamond $(\sigma \pm 1, \tau \pm 1)$. The equation of motion (5.1.3) expresses the variable at the top of the diamond in terms of the other three.

while $[\mathrm{f_n}, \mathrm{f_m}] = 0$ for $|m-n| \geq 2$. This parafermion algebra can be realized on a finite dimensional Hilbert space $\mathcal{H} = V_1 \otimes V_2 \otimes ... \otimes V_L$ with V_n an N-dimensional vector space attached to the link between site n and $n+1$, on which $\mathrm{f_n}$ and $\mathrm{f_{n+1}}$ act via appropriate clock and shift matrices. In the end, we imagine taking the continuum limit $L \to \infty$. The integer N is assumed to be large but finite. As we will see shortly, N will be proportional to the central charge of the low energy effective CFT.

The time-evolution is discrete and specified as follows [137–139]. We relabel the variables $\mathrm{f_n}$ by means of two integers $\mathrm{f}_{\sigma,\tau}$ with $\sigma + \tau =$ even, via $\mathrm{f}_{2\mathrm{r},0} = \mathrm{f}_{2\mathrm{r}}$ and $\mathrm{f}_{2\mathrm{r}+1,1} = \mathrm{f}_{2\mathrm{r}+1}$. The relabeled variables specify the initial condition of the model. The time evolution will generate a discrete, cylindrical 1+1-D space time formed by a rhombic lattice. The time evolution proceeds via a local propagation rule [137–139]. We can focus on a single diamons shaped lattice cell

$$e_{\rm N} \equiv \mathrm{f}_{\sigma,\tau+1}\,, \qquad \mathrm{e_S} \equiv \mathrm{f}_{\sigma,\tau-1}\,, \qquad \mathrm{e_W} \equiv \mathrm{f}_{\sigma-1,\tau}\,, \qquad \mathrm{e_E} \equiv \mathrm{f}_{\sigma+1,\tau}. \tag{5.1.2}$$

The evolution equation of the model reads

$$e_{\rm N}\, e_{\rm S} \;=\; \frac{e_{\rm W} e_{\rm E}}{(1+e_{\rm W})(1+e_{\rm E})} \tag{5.1.3}$$

Equation (5.1.3) is the simplest example of a Y-system. It specifies the variable $e_{\rm N}$ at the top of the diamond shaped lattice cell in terms of the other three variables $e_{\rm E}, e_{\rm W}$ and $e_{\rm S}$, see Figure (5.1). The Y-system (5.1.3) defines an integrable lattice model, that can be recognized as a discretized version of 2D hyperbolic geometry [137–139]. The exchange relation (5.1.1) amounts to a quantization of this hyperbolic geometry.[1]

The lattice model is a well defined quantum system, albeit one with a discrete time evolution. The model has been constructed [137–139] so that in the large L and IR limit, it describes a 2D continuum CFT with a non-linearly realized conformal symmetry with central charge $c = 1 + 6(b + b^{-1})^2$ with $b^2 = 1/N$. As we will explain, this CFT exhibits maximal Lyapunov behavior, and an infinite set of Ruelle resonances matching the quasi-normal frequencies of the BTZ black hole [142].

It may seem surprising that an integrable model can display properties characteristic of many body quantum chaos. To address this potential worry, one could choose to perturb the system away from integrability. One could add disorder e.g. by using the freedom of normalization of the $\mathrm{f}_{\rm n}$ to set $\mathrm{f}_{\rm n}{}^\dagger \mathrm{f}_{\rm n} = \kappa_{\rm n} \mathbf{1}_{\rm N\times N}$, with $\kappa_{\rm n}$ random real numbers picked from a narrow probability distribution centered around $\overline{\kappa_{\rm n}} = \kappa$. Alternatively, one could add frustration e.g. by including a next-to-neighbor interaction in the time step rule (5.1.2) and (5.1.3) via

$$\mathrm{f}_{\sigma,\tau+1}\,\mathrm{f}_{\sigma,\tau-1} \;=\; (1+\epsilon \mathrm{f}^{-1}_{\sigma+3,\tau})(1+\epsilon \mathrm{f}^{-1}_{\sigma-3,\tau})/(1+\mathrm{f}^{-1}_{\sigma+1,\tau})(1+\mathrm{f}^{-1}_{\sigma-1,\tau}). \tag{5.1.4}$$

Since the features of quantum chaos will already become apparent in the unperturbed model, we will instead focus on this idealized case, while ignoring the role of exact integrability. Indeed, we can note that there are other systems, such as $\mathcal{N} = 4$ SYM theory at large N, that are believed to be both integrable and chaotic. We will return to this point in the concluding section.

[1] In some way, one may view the model as a many body analogue of a hyperbolic billiard.

2) Lyapunov from Goldstone

A central part of our reasoning consists of a new physical derivation of the Lyapunov behavior of an irrational CFT at finite temperature. The idea is as follows. 1+1-D CFTs are characterized by an infinite conformal symmetry group, given by reparametrizations of the lightcone coordinates u and v

$$(u, v) \ \rightarrow \ (\xi(u), \eta(v)) \tag{5.1.5}$$

This conformal symmetry is broken by the conformal anomaly and by the presence of a finite energy density at finite temperature (and by the UV-cut-off). For a CFT with a dense asymptotic energy spectrum, it is then natural to expect that the conformal symmetry is non-linearly realized in terms of a light Goldstone mode.

This motivates us to consider the effective field theory of the relevant Goldstone excitation, described by the chiral field $\xi(u)$ in (5.1.5) that parameterizes the conformal group. The effective Lagrangian is uniquely fixed by symmetries, and given by the geometric action of the Virasoro group [70]. In section 5.2, we will use this insight to derive the commutation relations of the Goldstone fields $\xi(u)$ and $\eta(v)$. We will find that the thermal expectation value of the commutators squared

$$\left\langle \, [\xi(u), \xi(0)]^2 \, \right\rangle \sim e^{\lambda u}, \qquad\qquad \left\langle \, [\eta(v), \eta(0)]^2 \, \right\rangle \sim e^{\lambda v}, \tag{5.1.6}$$

initially grow exponentially with the time separation, with a temperature dependent Lyapunov exponent $\lambda = 2\pi/\beta$. In fact, we will derive the somewhat more precise result that, inside a thermal expectation value, the commutator between two generic

local operators takes the form[2]

$$\big[W(t_1), V(t_2)\big] \simeq \epsilon e^{\lambda t_{12}} \partial_{t_1} W(t_1)\, \partial_{t_2} V(t_2) \tag{5.1.7}$$

with ϵ some constant proportional to $1/c$. This result, which holds for time-like separations in the intermediate range $c \gg \lambda t_{12} \gg 1$, matches with the bulk interpretation of the commutator as resulting from a near horizon gravitational shockwave interaction [15, 26].

The role of the modes $u \to \xi(u)$ and $v \to \eta(v)$ play the same role as the pseudo-Goldstone mode $t \to f(t)$ appearing in the IR effective description of quantum mechanical models like SYK. In this case the conformal symmetry is both spontaneously and explicitly broken.

3) Ruelle resonances as poles in OPE coefficients

A main characteristic of a chaotic system is that it thermalizes: out of time ordered correlation functions decay to zero at late times. The approach toward equilibrium is governed by Ruelle resonances [143]. They appear as poles in the Fourier transform of the thermal two-point function, or in systems that obey the eigenstate thermalization hypothesis (ETH) [144–148], the matrix element between two excited states with total energy M

$$G(\omega) = \int dt\, \langle M|\mathcal{O}(t)\mathcal{O}(0)|M\rangle\, e^{i\omega t} \tag{5.1.8}$$

The Ruelle resonances of holographic 2D CFTs are well studied [142, 149]. As argued in [150], the matrix element reduces (for small t) to the thermal 2-point function. Its Fourier transform $G(\omega)$ has poles at resonant frequencies

$$\omega = -\frac{4\pi i}{\beta}(n + h), \tag{5.1.9}$$

[2]Here for simplicity we only consider the time dependence of the correlator. In general, the left- and right-moving sectors each may have their own temperature and Lyapunov exponents $\lambda_{\text{L,R}} = 2\pi/\beta_{\text{L,R}}$.

that coincide with the quasi-normal modes of the BTZ black hole [142]. By factorizing the matrix element (5.1.8) in the intermediate channel, we can write

$$G(\omega) = \sum_{|i\rangle \in \mathcal{H}_{CFT}} \delta(M+\omega-E_i) \left|\langle M|\mathcal{O}|i\rangle\right|^2 \tag{5.1.10}$$

$$= \rho(M+\omega) \left|\langle M|\mathcal{O}\,|M+\omega\rangle\right|^2 \tag{5.1.11}$$

where we used that in the Cardy regime, we can replace the spectral density $\rho(E) = \sum_{|i\rangle} \delta(E-E_i)$ by a continuous distribution, and label the CFT states by their energy. We learn that the Ruelle resonances dictate the analytic structure of the matrix element of a light operator $\mathcal{O}$ between two highly excited states. This indicates that the resonances must show up as poles in the OPE coefficient of a light operator and two heavy operators. Or in AdS-dual terms, the quasi-normal modes should show up as poles in the absorption and emission amplitudes of wave perturbations by a BTZ black hole.

In section 5.4 we will show that the analytic continuation of the OPE coefficients of the continuum limit of our model indeed has poles located at the expected frequencies (5.1.9). This supports the statement that the continuum limit of the model is ergodic.

5.2 Lyapunov from Goldstone

Consider an irrational 2D CFT with central charge $c \gg 1$ with an asymptotic density of states given by the Cardy formula, and with a sparse low energy spectrum. We place the CFT on a circle, parameterized by a periodic coordinate x with period 2π. We introduce light-cone coordinates $(u, v) = (t-x, t+x)$.

Consider a finite energy state with a constant expectation value for, say, the left-moving energy momentum tensor

$$\big\langle T(u)\big\rangle = L_0 \gg \frac{c}{12} \tag{5.2.1}$$

In this regime, we can associate to the state a finite inverse temperature $\frac{\beta}{2\pi} = \sqrt{\frac{c}{24L_0}}$.

Let us perform a general conformal transformation (5.1.5). We require that

$$\xi(u+2\pi) = \xi(u) + 2\pi \tag{5.2.2}$$

The expectation value of the energy momentum tensor transforms non-trivially

$$\big\langle T(u)\big\rangle = L_0\,\xi'^2(u) + \frac{c}{12}\,S_\xi(u) \tag{5.2.3}$$

with S_ξ the Schwarzian derivative

$$S_\xi(u) = \frac{1}{2}\Big(\frac{\xi''(u)}{\xi'(u)}\Big)^2 - \Big(\frac{\xi''(u)}{\xi'(u)}\Big)' \tag{5.2.4}$$

The spontaneous breaking of conformal symmetry is displayed via the ξ-dependence of this expectation value. Indeed, we can compare the relation (5.2.3) with the expression for the energy-momentum tensor of a fluid. The first term is analogous to the usual kinetic energy $\frac{1}{2}\rho v^2$, whereas the second term in (5.2.3) is the familiar vacuum contribution due to the conformal anomaly. It has a well-known physical explanation in terms of the Hawking-Unruh effect: the coordinate change from u to $\xi(u)$ reshuffles the positive frequency (annihilation) and negative frequency (creation) modes, and thus alters the notion of the vacuum state.

Our physical assumption is that, for irrational CFTs at large c and in the Cardy regime, it becomes accurate to treat the coordinate transformation $\xi(u)$ as a Gold-

stone field, in terms of which the conformal symmetry is non-linearly realized. Adopting this logic, we thus promote $\xi(u)$ to an operator, that acts within the Hilbert subspace spanned by all states with energy density close to L_0, and their descendants. Within this subspace, we can remove the expectation value in (5.2.3) and elevate the equality in (5.2.3) to an *operator identity*

$$T(u) = L_0 \xi'^2(u) + \frac{c}{12} S_\xi(u). \tag{5.2.5}$$

As we will see shortly, the expression (5.2.5) for the energy-momentum tensor in terms of $\xi(u)$ is familiar from the geometric quantization of Diff(S^1), the group of (chiral) conformal transformations in 2D.

A cautious reader may view equation (5.2.5) simply as a (in)convenient parameterization of the energy momentum tensor $T(u)$. However, another way to state our assumption is that the symmetry parameter $\xi(u)$ acts as a genuine local quantum field that creates and annihilates local physical excitations. Given that $\xi(u)$ is a scalar and $T(u)$ is the generator of conformal transformations, we know that[3]

$$\big[T(u_1), \xi(u_2)\big] \;=\; \hbar\, \xi'(u_2)\delta(u_{12}) \qquad\qquad \hbar \equiv \frac{6}{c} \tag{5.2.6}$$

$$\big[T(u_1), T(u_2)\big] \;=\; -\hbar(T(u_1) + T(u_2))\delta'(u_{12}) + \frac{\hbar}{2}\delta'''(u_{12}). \tag{5.2.7}$$

The emergence of a light Goldstone mode at finite temperature can be explained as a physical consequence of the fact that an irrational CFT in the Cardy regime has an extremely dense energy spectrum.

[3]Here we absorb a factor of $\hbar \equiv 6/c$ in the definition of $T(u)$. This is a customary step, that exhibits the fact that the commutation relations (5.2.6) and (5.2.7) become semi-classical at large c.

Equations (5.2.6) and (5.2.7) become semi-classical in the large c limit. From equation (5.2.1) we see that the field $\xi(u)$ has expectation value

$$\left\langle\, \xi(u) \,\right\rangle \,=\, u \tag{5.2.8}$$

So semi-classically, we can think of the Goldstone field as: $\xi(u) = u +$ small fluctuations.

We are now ready to state the main technical result of this section:

The three relations (5.2.5), (5.2.6) and (5.2.7) uniquely determine the commutation relation of the Goldstone field $\xi(u)$, and are sufficient to derive the Lyapunov growth of commutators.

Working to leading order in $1/c$, one finds that [151] [92, 93]

$$\big[\xi(u_1), \xi(u_2)\big] \,=\, \frac{\epsilon(u_{12})}{L_0} \,+\, \frac{\sinh(\lambda\tau(u_1,u_2))}{L_0 \sinh \pi\lambda} \tag{5.2.9}$$

$$\tau(u_1,u_2) \,=\, \xi(u_1) - \xi(u_2) - \pi\epsilon(u_{12}), \qquad\qquad \lambda = \sqrt{\frac{24L_0}{c}} \tag{5.2.10}$$

with $\epsilon(x)$ the stair step function, defined via $\epsilon'(x) = 2\delta(x)$ with $\delta(x)$ the periodic delta-function: $\epsilon(x) = 2n{+}1$ for $x \in (2\pi n, 2\pi(n{+}1))$. The same argument and derivation goes through for the right-movers. So we also have a right-moving Goldstone mode $\eta(v) = v +$ small fluctuations, that satisfies the analogous commutation relation (5.2.9).[4] The left- and right-moving Goldstone fields commute $[\xi(u), \eta(v)] = 0$.

A detailed derivation of equation (5.2.9) and (5.2.10) can be found in [151] [92,93]. Here we give a short summary. The constituent relation (5.2.5) between the energy-

[4]For simplicity we will assume that the left and right movers have the same temperature.

momentum tensor and the field $\xi(u)$ can be decomposed as

$$T(u) \;=\; \varphi'^2(u) - 2\varphi''(u), \tag{5.2.11}$$

$$\varphi(u) \;=\; \frac{\lambda}{2}\,\xi(u) + \frac{1}{2}\log\bigl(\lambda\xi'(u)\bigr). \tag{5.2.12}$$

The commutation relations (5.2.6) and (5.2.7) then follow from the free field commutator

$$[\varphi(u_1), \varphi(u_2)] = \hbar\,\epsilon(u_{12}), \tag{5.2.13}$$

with $\hbar = 6/c$. So our task has been simplified: all we need to do is use relation (5.2.12) to solve of $\xi(u)$ in terms of $\varphi(u)$, and use the chain rule to deduce the commutator of $\xi(u_1)$ and $\xi(u_2)$ from the free field commutator (5.2.13) of φ.

The free field $\varphi(u)$ is periodic up to a shift

$$\varphi(u + 2\pi) = \varphi(u) + \pi\lambda. \tag{5.2.14}$$

Using this fact, equation (5.2.12) integrates to [92]

$$\xi(u) = \frac{1}{\lambda}\log\left(\int_0^{2\pi} dy\,\frac{e^{2\varphi(u+y)-\lambda\pi}}{\sinh\pi\lambda}\right) \tag{5.2.15}$$

With this relation and equation (5.2.13) in hand, it is now a relatively straightforward calculation to derive the result (5.2.9) and (5.2.10).

Let us turn to the physical consequences of equations (5.2.9) and (5.2.10). We observe that λ is equal to the maximal Lyapunov exponent $\lambda = 2\pi/\beta$. We will assume that $\lambda \gg 1$, i.e. the thermal wave length is very short compared to the size of the spatial circle. The second term in the commutator (5.2.9), and its right-mover counter part, thus grows exponentially with the coordinate differences u_{12} and v_{12} over the

range

$$\beta \ll |u_{12}| < 2\pi, \qquad \beta \ll |v_{12}| < 2\pi. \tag{5.2.16}$$

We will restrict our attention to this coordinate range. In this regime, equation (5.2.9) implies that the commutator between two local functions $\hat{f}(u_2) \equiv f(\xi(u_2))$ and $\hat{g} \equiv g(\xi(u_1))$ of the Goldstone fields satisfy

$$[\hat{f}(u_1), \hat{g}(u_2)] \simeq e^{\lambda(|u_{12}|-2\pi)}\ \hat{f}'(u_1)\hat{g}'(u_2). \tag{5.2.17}$$

Here we used equation (5.2.8) to replace $\xi(u) \to u$ on the r.h.s. We would like to translate equation (5.2.17) into a statement about the commutator between local CFT operators.

Consider some local CFT operator $\mathcal{O}(u, v)$. Under the conformal transformation (5.1.5) it transforms as

$$\mathcal{O}(u, v) \to \xi'(u)^{h_{\text{L}}}\eta'(v)^{h_{\text{R}}}\mathcal{O}\big(\xi(u), \eta(v)\big) \tag{5.2.18}$$

Hence local operators are indeed non-trivial functions of the dynamical Goldstone fields.

It is logical to take this observation one step further, and, similarly as we did for the energy-momentum tensor, assume that local operators $\mathcal{O}(u, v)$ can be represented as c-number valued functions of the operator valued fields $\xi(u)$ and $\eta(v)$ and their derivatives. The collection of these functions is determined by the spectrum and operator algebra of the CFT. Their form is constrained by the locality requirement that space-like separated operators commute. This condition is very restrictive: it

prescribes that primary local operators are all of the form [92, 93, 152–154]

$$\mathcal{O}_h(u,v) \;=\; \big(f(u,v)\big)^h, \tag{5.2.19}$$

$$f(u,v) \;=\; \frac{\lambda^2 \xi'(u)\eta'(v)}{4\sinh^2\big(\frac{\lambda}{2}(\xi(u)-\eta(v))\big)}\,. \tag{5.2.20}$$

Equations (5.2.9) and (5.2.10) can then be used to compute the commutation relations between time-like separated operators, as follows.

The accepted test for Lyapunov growth of the commutator between two local operators W and V is to compute the expectation value

$$\big\langle W_\epsilon(u,v)\big[W(u,v),V(0,0)\big]V_\epsilon(0,0)\big\rangle \tag{5.2.21}$$

where the subscript $_\epsilon$ indicates a small displacement. This expectation value is equal to the difference between a time ordered and an out-of-time-ordered (OTO) correlation function. The OTO correlation function is obtained via analytic continuation of the time ordered correlation functions, where one circles, say, the coordinate u around the origin. This operation amounts to analytic continuation of the left-moving conformal blocks to the second Riemann sheet. Of course, we could also choose to do the analytic continuation using the coordinate v. This would have given the same final result.

The full-circle-monodromy $\mathbf{M}$ of a conformal block is the square $\mathbf{M} = \mathbf{R}^2$ of half-circle-monodromy known as the R-operation. The R-operator, acting on the left conformal blocks, re-orders the left-moving parts of the operators W and V. In the linearized regime, i.e. to leading order in $1/c$, we can write $\mathbf{R} \simeq \mathbf{1} - \mathbf{r}$ with $\mathbf{r}$ the perturbative operation that takes the commutator between the left-moving parts of W and V. The full-circle-monodromy is $\mathbf{M} \simeq \mathbf{R}^2 = \mathbf{1} - 2\mathbf{r}$ and thus the full commutator inside (5.2.21) is equal to acting with $(\mathbf{1} - \mathbf{M}) = 2\mathbf{r}$ on the two operators W and V.

From equation (5.2.17) we then deduce that

$$\big[W(u_1,v_1),V(u_2,v_2)\big] \;\simeq\; 2e^{\lambda(u_{12}-u_0)}\;\partial_{u_1}W(u_1,v_1)\partial_{u_2}V(u_2,v_2) \tag{5.2.22}$$

This result, which holds for time like separation in the regime (5.2.16), displays the maximal Lyapunov behavior and the linearized gravitational effect of an early incoming perturbation (created by V) on the arrival time of the outgoing signal (detected by W).

We end with a brief comment on the extension to higher orders. As indicated by the description of the monodromy moves, one expects that the commutator (5.2.22) exponentiates to a non-perturbative exchange relation. Fourier transforming the left-moving coordinate via $W_\alpha(v) = \int du\, e^{i\alpha u}W(u,v)$, this exchange algebra is expected to take the following form

$$W_\alpha(v_1)V_{\omega-\alpha}(v_2) = \sum_\beta M_\alpha{}^\beta\, V_\beta(v_2)\, W_{\omega-\beta}(v_1). \tag{5.2.23}$$

If we assume that the bulk interaction is dominated by gravity, then AdS/CFT makes a precise prediction for the monodromy matrix $M_\alpha{}^\beta$ [74]. The prediction precisely matches with the monodromy matrix of Liouville CFT [74].

5.3 A Chaotic Lattice Model

In this section, we will connect the FKV lattice model, defined by equations (5.1.1), (5.1.2) and (5.1.3), with the above effective CFT derivation of Lyapunov behavior.

The motivation for studying the lattice model is two-fold. First, the geometric theory of the Goldstone fields $\xi(u)$ and $\eta(v)$ is an effective theory, that only becomes accurate at finite temperature and long distance scales. Like all effective field theories, it does not define a fully consistent CFT by itself, nor does it have a unique UV

completion. There are two ways in which one can try to embed an effective field theory into a self-consistent quantum system: a) look for an explicit UV completion, or b) introduce an explicit UV regulator. Approach b) is more practical.

A second motivation is that one can hope that the lattice model, by virtue of being more well defined, may allow for more explicit dynamical understanding of the underlying mechanism for chaos. Indeed, it turns out that the lattice Liouville model can be formulated in a way that preserves the geometric appeal of the continuum theory [137–139]

The Y-system (5.1.3) and the expression (5.2.19) of local operators in terms of the function (5.2.20) both have a direct connection with hyperbolic geometry. To see this, we first note that the 1+1-D metric defined by

$$ds^2 = f(u,v)dudv = \frac{\lambda^2 d\xi d\eta}{\left(2\sinh(\frac{\lambda}{2}(\xi-\eta))\right)^2} \tag{5.3.1}$$

describes a hyperbolic space-time with constant negative curvature. The authors of [137–139] gave a beautiful discretized description of this 2D hyperbolic metric as follows.

We can write equation (5.3.1) as

$$f(u,v) = \frac{1}{\Delta^2}\frac{\left(e^{\lambda\xi(u+\Delta)} - e^{\lambda\xi(u-\Delta)}\right)\left(e^{\lambda\eta(v+\Delta)} - e^{\lambda\eta(v-\Delta)}\right)}{\left(e^{\lambda\xi(u+\Delta)} - e^{\lambda\eta(v+\Delta)}\right)\left(e^{\lambda\xi(u-\Delta)} - e^{\lambda\eta(v-\Delta)}\right)} \tag{5.3.2}$$

with Δ an infinitesimal coordinate shift. Note that this expression for $f(u,v)$ looks like a cross-ratio. So it is invariant under Möbius transformations. Now consider the values of $f(u,v)$ in four nearby points, separated by null shifts Δ

$$\begin{aligned} \mathrm{f}_{\sigma,\tau-1} &= f(u,v), & \mathrm{f}_{\sigma+1,\tau} &= f(u+\Delta,v), \\ \mathrm{f}_{\sigma-1,\tau} &= f(u,v+\Delta), & \mathrm{f}_{\sigma,\tau+1} &= f(u+\Delta,v+\Delta). \end{aligned} \tag{5.3.3}$$

These four cross-ratios depend on six functions $e^{\lambda\xi(u)}, e^{\lambda\xi(u\pm\Delta)}$, $e^{\lambda\eta(v)}$, and $e^{\lambda\eta(v\pm\Delta)}$, but thanks to the Möbius invariance, only three of the six functions are independent. Therefore, the four cross-rations (5.1.2) satisfy one relation [137–139]. Putting $\Delta = 1$, it reads

$$\mathrm{f}_{\sigma,\tau+1}\,\mathrm{f}_{\sigma,\tau-1} \;=\; \frac{\mathrm{f}_{\sigma+1,\tau}\mathrm{f}_{\sigma-1,\tau}}{(1+\mathrm{f}_{\sigma+1,\tau})(1+\mathrm{f}_{\sigma-1,\tau})}. \tag{5.3.4}$$

This confirms that the equation of motion of the FKV lattice model is a discretization of the hyperbolic metric (5.3.1). The parafermionic algebra

$$\mathrm{f_n f_{n\pm1}} \;=\; \mathrm{q}^2\,\mathrm{f_{n+1} f_n} \tag{5.3.5}$$

defines a quantization of the space of discretized hyperbolic metrics.

Our new observation is that this lattice model can serve as a useful prototype of quantum chaos. The most direct way to substantiate this claim would be compute an out-of-time ordered four-point function of local operators

$$\left\langle\, \mathrm{f}_{\sigma,\tau+\mathrm{t}+1}\left[\mathrm{f}_{\sigma,\tau+\mathrm{t}-1}, \mathrm{f}_{\sigma,\tau+1}\right] \mathrm{f}_{\sigma,\tau-1}\,\right\rangle_{\beta} \tag{5.3.6}$$

at finite temperature, as a function of the time difference t. While this would in principle be doable, we will leave this task to future work. Instead we will cut the computation short, by banking on the results of [137–139, 141] that show that the above lattice model in the large L limit approaches continuum Liouville CFT. Together with the result of the previous section, this is sufficient to demonstrate that the continuum limit of the lattice model displays maximal Lyapunov behavior.

For completeness, let us display a few more elements of the dictionary. Working to leading order at large N

$$\begin{aligned} e^{\varphi^+_{\rm n}}\, e^{\varphi^+_{\rm m}} &= e^{\varphi^+_{\rm m}}\, e^{\varphi^+_{\rm n}}\, q^{2\epsilon_{\rm nm}} & \qquad e^{\varphi(u_2)} e^{\varphi(u_1)} &= e^{\varphi(u_1)} e^{\varphi(u_2)} e^{\hbar\epsilon(u_{12})} \\ e^{\varphi^+_{\rm n+L}} &= e^{2\pi\lambda}\, e^{\varphi^+_{\rm n}} & \qquad e^{\varphi(u+4\pi)} &= e^{2\pi\lambda}\, e^{\varphi(u)} \\ \tfrac{\rm L}{2\pi}\, e^{\varphi^+_{\rm n}} &= e^{\frac{\lambda}{2}\xi_{\rm n}} - e^{\frac{\lambda}{2}\xi_{\rm n-1}} & \qquad e^{\varphi(u)} &= \partial_u\, e^{\frac{\lambda}{2}\xi(u)} \end{aligned} \tag{5.3.7}$$

The right column lists the formulas (5.2.13), (5.2.14) and (5.2.12) that were used to derive the commutation relation (5.2.9) of the left-moving Goldstone variable $\xi(u)$. The left column is the lattice version of the same set of relations, with $\epsilon_{\rm nm}$ the discretized stair-step function. We can write a parallel set of formulas that represent the right-moving modes $\varphi(v)$ and $\eta(v)$ in terms of lattice variables $\varphi^-_{\rm n}$ and $\eta_{\rm n}$.

Lattice variables $\varphi^\pm_{\rm n}$ that satisfy the exchange relation in (5.3.7) are obtained from the local operators ${\rm f}_{\rm n}$ in two steps [137–139] [141]. First we define two mutually commuting sets of chiral operators ${\rm w}^\pm_{\rm n}$ via

$$ {\rm w}^+_{\rm n} \,=\, q\, {\rm f}_{\rm 2n+1} {\rm f}^{-1}_{\rm 2n+2}, \qquad\qquad {\rm w}^-_{\rm n} \,=\, q\, {\rm f}_{\rm 2n+1} {\rm f}^{-1}_{\rm 2n}. \tag{5.3.8}$$

These satisfy the algebra ${\rm w}^\pm_{\rm n} {\rm w}^\pm_{\rm m} = q^{\pm 2\omega_{\rm mn}}\, {\rm w}^\pm_{\rm m} {\rm w}^\pm_{\rm n}$, with $\omega_{\rm mn} = {\rm sgn}(m-n)\delta_{|m-n|,1}$. The chiral variables $\varphi^\pm_{\rm n}$ are then defined as

$$ \varphi^\pm_{\rm n} \,=\, \sum_{\rm m} \epsilon_{\rm nm} \log {\rm w}^\pm_{\rm m}, \qquad \varphi^\pm_{\rm n+L} = \varphi^\pm_{\rm n} + 2\pi\lambda, \qquad 2\pi\lambda = \frac{1}{L} \sum_{\rm n=1}^{\rm L} \log {\rm w}^\pm_{\rm n}. \tag{5.3.9}$$

At the initial time $\tau = 0$, we can recover the single valued local parafermionic operators ${\rm f}_{\rm 2n}$ from the non-local chiral variables via

$$ {\rm f}_{\rm 2n} \,=\, e^{\varphi^-_{\rm n}}\, e^{\varphi^+_{\rm n}} \tag{5.3.10}$$

This is the lattice version of the relation $e^{2\phi(u,v)} = e^{\varphi(u)+\varphi(v)}$ that expresses a non-chiral free field vertex operator into the product of the two chiral vertex operators. We note, however, that the time evolution (5.3.4) does not amount to free field propagation.

Among many other non-trivial results, [137–139] and [141] give an explicit construction of a unitary time evolution operator U that implements the time step (5.3.4)

$$\mathrm{f}_{\sigma,\tau+1} \;=\; \mathrm{U}^{\dagger}\,\mathrm{f}_{\sigma,\tau-1}\,\mathrm{U}. \tag{5.3.11}$$

This time evolution does not preserve the chiral factorization (5.3.10). However, it is shown that there exists a Bäcklund operator B that solves the time evolution via

$$\mathrm{f}_{\sigma,\tau} \;=\; \mathrm{B}^{-1}\, e^{\varphi^{+}_{\frac{1}{2}(\sigma-\tau)}} e^{\varphi^{-}_{\frac{1}{2}(\sigma+\tau)}}\,\mathrm{B} \tag{5.3.12}$$

This Bäcklund operation is causal but highly non-local, and no explicit representation of B is known at present. Indeed, as exemplified by this equation, all non-trivial dynamics of the Liouville lattice model is encoded in the way in which the two chiral sectors get mixed and become entangled under the time evolution step (5.3.4). Our results are evidence that this mixing and entangling is happening in a maximally efficient way.

Our argument that the lattice model exhibits maximal Lyapunov growth is a copy of the effective CFT derivation presented in section 5.2. The three relations in the left column of equation (5.3.7) specify the commutation relations of the ξ_{n} variables, in the same way as the right column fixes the commutator algebra of $\xi(u)$. The commutator algebra is expected to approach the continuum result (5.2.9) in the large L limit. Our working assumption is that the exact solution (5.3.12) of the lattice model leads to an expression of the local operators $\mathrm{f}_{\sigma,\tau}$ in terms of the chiral modes ξ_{n} and η_{n} that mirrors formula (5.3.2). Via the same reasoning as in section 5.2, this

expression can then be used to verify that the lattice model is local and to establish that the OTO four point function (5.3.6) grows exponentially with time.

5.4 Ruelle Resonances

In this section we will expand on the topic of Ruelle resonances, which provide another signature of chaos and ergodicity. We will briefly review these concepts and then use the intuition for large c irrational conformal field theories to translate the knowledge about these resonances into concrete CFT data. We will introduce a notion of OPE coefficients (of light operators between heavy states) as analytic functions of energy. We will see that the presence of Ruelle resonances, in combination with the conformal bootstrap and AdS/CFT, impose stringent constraints on the form of these analytic OPE functions. We will then verify that the known OPE coefficients of the effective CFT of section 5.2 and the continuum limit of the lattice model of section 5.3 satisfy all these physical requirements.

4.1 Ruelle resonances in CFT

Ruelle resonances are poles in the Fourier transform of linear response functions that govern thermalization, the decay process towards thermal equilibrium after a quench. Consider a small perturbation produced by a local operator $\mathcal{O}_{\rm b}(x)$ to the Hamiltonian

$$\delta H = \int J(x)\mathcal{O}_{\rm b}(x). \tag{5.4.1}$$

Here $J(x)$ is an external source. Then one can study how this perturbation influences the time evolution of the expectation value of some other operator $\langle\mathcal{O}_{\rm a}(0)\rangle$, which for convenience we place at $x = 0$. By expanding the evolution operator to linear order

$$\delta\langle\mathcal{O}_{\rm a}(0)\rangle = \int dx'\, G^{\rm ret}_{\rm ab}(x')J(x'), \tag{5.4.2}$$

where $G^{\rm ret}_{\rm ab}(x) = \theta(t)\langle[\mathcal{O}_{\rm a}(x), \mathcal{O}_{\rm b}(0)]\rangle$ (with t = time component of x) is the retarded Green's function. $G^{\rm ret}_{\rm ab}(x)$ may be expressed in terms of two point functions as

$$G^{\rm ret}_{\rm ab}(x) = \theta(t)\big(G^{+}_{\rm ab}(x) - G^{-}_{\rm ab}(x)\big), \tag{5.4.3}$$

with $G^{+}_{\rm ab}(x) = \langle\mathcal{O}_a(x)\mathcal{O}_{\rm b}(0)\rangle$ the time ordered two point function and $G^{-}_{\rm ab}(x) = \langle\mathcal{O}_b(0)\mathcal{O}_{\rm a}(x)\rangle$ the out-of-time-ordered two point function. Equation (5.4.2) is the basis of linear response theory, from which one can deduce transport properties such as the Kubo formula. Response functions are usually analyzed in the frequency domain. The Ruelle resonances appear as poles in the complex frequency plane. The imaginary part of the location of the poles determines the relaxation time. The leading behavior in $\delta\langle\mathcal{O}_{\rm b}\rangle(t)$ is governed the viscous hydrodynamical mode with the smallest imaginary part.

We are interested in studying this response function in a pure state microcanonical ensemble, defined by some highly excited CFT state $|M\rangle$ with a large scale dimension $M \gg \frac{c}{12}$, so deep in the Cardy regime. The two-point functions of interest are given by the matrix elements of the two light operators $\mathcal{O}_{\rm a}$ and $\mathcal{O}_{\rm b}$ between two heavy states

$$\begin{aligned} G^{+}_{\rm ab}(u,v) &= \langle M|\mathcal{O}_{\rm a}(u,v)\mathcal{O}_{\rm b}(0)|M\rangle \\ G^{-}_{\rm ab}(u,v) &= \langle M|\mathcal{O}_{\rm b}(0)\mathcal{O}_{\rm a}(u,v)|M\rangle \end{aligned} \tag{5.4.4}$$

For 2D CFTs at large c, it has been argued in [150] that the matrix elements (5.4.4) are dominated by the identity conformal block (which for $G^{+}(u,v)$ is given by the term with $h = 0$ on the left in Figure 5.2.) For large c, this identity block is well

approximated by the thermal 2-point function on an infinite 1D space

$$G^{\pm}_{\rm ab}(u,v) \;\simeq\; \delta_{\rm ab}\left(\frac{\pi/\beta}{\sinh\left(\frac{\pi}{\beta}(u\pm i\epsilon)\right)}\right)^{2h}\left(\frac{\pi/\beta}{\sinh\left(\frac{\pi}{\beta}(v\pm i\epsilon)\right)}\right)^{2h}. \tag{5.4.5}$$

with $\beta = \pi\sqrt{c/6M}$. This is a useful result, that supports both the ETH and the dual identification of the two point function as the boundary-to-boundary propagator of a bulk field in a BTZ black hole background.

The validity of equations (5.4.5) is somewhat limited, however. It only holds for spatial separations that are small compared to the size of the spatial circle, and for the OTO two-point function, the time difference must be short compared to the scrambling time, since otherwise one enters the Lyapunov regime. On the gravity side, the perturbation $\mathcal{O}_{\rm b}$ creates an incoming wave that may collide with the outgoing wave detected by $\mathcal{O}_{\rm a}$, and thereby substantially affect its future trajectory. This gravitational effect will show up as a modification of the OTO two-point function $G^{-}(u,v)$, and was studied in section 5.2. Here we will focus on the late time behavior of the time ordered 2-point function $G^{+}(u,v)$.

The incoming wave deforms the black hole horizon state. The subsequent ring down of the black hole towards equilibrium is the dual of the thermalization process of the CFT. Both processes are governed by an infinite set of resonances. On the gravity side, these resonances are the quasi-normal modes. These can be analyzed perturbatively, by considering small fluctuations of fields propagating in the neighborhood of the black hole horizon. These resonant quasi-normal frequencies are an infinite series of complex numbers, labeled by a non-negative integer n via [142]

$$\omega = \pm k - i\frac{4\pi}{\beta}(n+h). \tag{5.4.6}$$

with k is the momentum of the infalling mode and h the conformal dimension of the fluctuating field. This result was derived using the Poincaré patch, corresponding

with a CFT on an infinite line, and with vanishing Dirichlet boundary conditions at infinity [142].[5] It is reasonable to assume that the result generalizes to black holes in global AdS, with a periodic spatial boundary, by replacing the momentum k by an integer angular momentum ℓ.

In the CFT, the quasi-normal modes manifest themselves as Ruelle resonances, that appear as poles in the Fourier transform of the retarded thermal Green's function (5.4.3)

$$G^{\rm ret}_{\rm ab}(\omega,\ell) \;=\; \int du \int dv\; e^{i\frac{1}{2}(\omega+\ell)u} e^{i\frac{1}{2}(\omega-\ell)v}\; G^{\rm ret}_{\rm ab}(u,v), \tag{5.4.7}$$

which via equation (5.4.5) yields a spectrum that matches with the gravity prediction (5.4.6). Our goal in this section is to use the presence of these Ruelle poles to extract useful information about the OPE coefficients of the CFT. Earlier papers with results that overlap with this section are [150, 155].

4.2 Resonances and OPE coefficients

As a preparation, let us look at the different conformal block expansions of the matrix elements (5.4.4), as shown schematically in Figure (5.2). We temporarily rotate to euclidean signature and set $(u,v) = (z,\overline{z})$. The first equal sign of these identities represents the crossing symmetry relation

$$G_{\rm ab}(z) = \sum_{\omega} {\rm C}_{\rm aMM+\omega} {\rm C}^{\rm M+\omega}_{\rm Mb} \left|\mathcal{F}_{\rm M+\omega}\left[\begin{smallmatrix}{\rm M}&{\rm M}\\{\rm a}&{\rm b}\end{smallmatrix}\right](z)\right|^2 \;=\; \sum_{\rm h} {\rm C}^{\rm h}_{\rm MM}\, {\rm C}_{\rm ahb} \left|\mathcal{F}_{\rm h}\left[\begin{smallmatrix}{\rm M}&{\rm a}\\{\rm M}&{\rm b}\end{smallmatrix}\right](1-z)\right|^2 \tag{5.4.8}$$

where $\mathcal{F}_h\left[\begin{smallmatrix}{\rm M}&{\rm M}\\{\rm a}&{\rm b}\end{smallmatrix}\right](z)$ represents the Virasoro block shown on the left in Figure (5.2). We see that crossing symmetry relates the 't-channel block' with heavy intermediate

[5] Notice that this Dirichlet boundary condition eliminates all gravitational excitations corresponding to the Virasoro descendants in the CFT. This restriction will become relevant later.

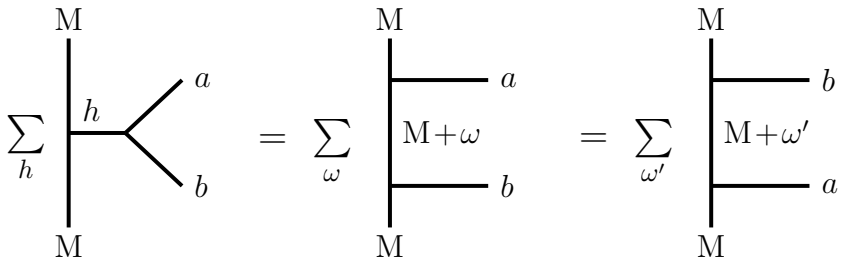

Figure 5.2: Diagrammatical representation of crossing symmetry and the exchange algebra of the CFT correlation function of two heavy operators, labeled by M, and two light ones, labeled by a and b.

channel (labeled by M+ ω) to the 's-channel block' with a light intermediate channel (labeled by h).

The second relation in Figure (5.2) is the exchange algebra relation,

$$\sum_{\omega} \mathrm{C}_{\mathrm{aMM+\omega}}\,\mathrm{C}^{\mathrm{M+\omega}}_{\mathrm{Mb}}\left|\mathcal{F}_{\mathrm{M+\omega}}\left[\begin{smallmatrix}\mathrm{M}&\mathrm{M}\\ \mathrm{a}&\mathrm{b}\end{smallmatrix}\right](z)\right|^2 \;=\; \sum_{\omega'} \mathrm{C}_{\mathrm{bMM+\omega'}}\,\mathrm{C}^{M+\omega'}_{\mathrm{Ma}}\left|\mathcal{F}_{\mathrm{M+\omega'}}\left[\begin{smallmatrix}\mathrm{M}&\mathrm{M}\\ \mathrm{b}&\mathrm{a}\end{smallmatrix}\right](1/z)\right|^2, \quad (5.4.9)$$

that imposes locality in the Euclidean region. In Lorentzian language, it implies that the R-matrix $R_{\omega,\omega'}$ that relates the chiral time-ordered conformal block (labeled by M $+\omega$) to the out-of-time-ordered conformal block (labeled by M$+\omega'$) is an appropriate unitary transformation, so that in the euclidean region, it cancels out between the left- and right-movers of the complete CFT four-point function. After rotating to Lorentz signature, the R-matrix does show up in a non-trivial way, in the relation between the time-ordered Green's function $G^{+}_{\mathrm{ab}}(u,v)$ and the OTO Green's function $G^{-}_{\mathrm{ab}}(u,v)$ [74].

We wish to extract information regarding the Fourier transform of G_{ab} from its expansion (5.4.8) in conformal blocks, in the channel shown in the middle of Figure (5.2). This is not directly possible, since no explicit expression for the Virasoro conformal blocks is known. So let us take a step back and write the crossing symmetry formula as a sum over primary operators and descendants. Let γ^{ω}_{n} denote the n-th coefficient

of the Laurent expansion of the Virasoro conformal block $\mathcal{F}_{\mathrm{M}+\omega}\left[\begin{smallmatrix}\mathrm{M} & \mathrm{M}\\ \mathrm{a} & \mathrm{b}\end{smallmatrix}\right](z)$. From now on we focus on the diagonal part of the two point function $G_{\mathrm{ab}}(u,v) = G(u,v)\,\delta_{\mathrm{ab}}$. It has the following expansion

$$G(u,v) \;=\; \sum_{|i\rangle} G_{\omega_{i,L}}(u)\, G_{\omega_{i,R}}(v) \tag{5.4.10}$$

$$G_{\omega_L}(u) \;=\; \sum_{n_L} \mathrm{C}_{\mathrm{aMM}+\omega_{\mathrm{L}}}\; \gamma_{n_L}^{\omega_L}\; e^{i(\omega_L+n_L)u} \tag{5.4.11}$$

and a similar formula holds for $G_{\omega_R}(v)$. Here $|i\rangle$ runs over all conformal primary states of the CFT in the neighborhood of the high energy state $|M\rangle$. In the sum we allowed all states with different left- and right conformal dimension $(\Delta_{i,L}, \Delta_{i,R}) = (M+\omega_{i,L}, M+\omega_{i,R})$.

We want to take the Fourier transform (5.4.7) with respect to both light-cone coordinates. It is useful to introduce the spectral density of CFT primary states

$$\rho(\omega_L,\omega_R) = \sum_{|i\rangle} \delta(\mathrm{M}+\omega_L-\Delta_{i,L})\delta(\mathrm{M}+\omega_R-\Delta_{i,R}). \tag{5.4.12}$$

We then have

$$G^{\mathrm{ret}}(\omega,\ell) = \int \frac{d\omega'}{2\pi}\, \frac{G(\omega',\ell)}{\omega'-\omega-i\epsilon} \tag{5.4.13}$$

$$G(\omega,\ell) \;=\; \sum_{n_L,n_R} \;\mathrm{C}_{\mathrm{aMM}+\omega_L-n_L}\mathrm{C}_{\mathrm{aMM}+\omega_R-n_R}\; \gamma_{n_L}^{\omega_L}\; \gamma_{n_R}^{\omega_R}\; \rho(\omega_L-n_L,\omega_R-n_R), \tag{5.4.14}$$

with $\omega_L = \frac{1}{2}(\omega+\ell)$ and $\omega_R = \frac{1}{2}(\omega-\ell)$. For a given CFT, $G^{\mathrm{ret}}(\omega,\ell)$ contains exact information about the spectrum of primary fields, in the form of a dense set of poles along the real axis, with residues equal to the corresponding OPE coefficient. The Ruelle resonances appear as a series of poles in $G^{\mathrm{ret}}(\omega,\ell)$ located off the real axis.

Based on equation (5.4.5) and the results of [150] and [142], we expect that their location should match with the quasi-normal frequencies (5.4.6).

The spectrum of an irrational CFT at large c becomes very dense in the Cardy regime. In this type of situation, it is customary to treat the spectrum as a continuum with spectral density given by the Cardy formula, and elevate the OPE coefficients to continuous functions of the conformal weights. The Ruelle resonances are then expected to arise as poles in the analytic continuation of the OPE coefficients.[6]

Let us summarize. The OPE coefficients between light and heavy operators satisfy several non-trivial compatibility conditions: they solve the CFT bootstrap equations (5.4.8) and (5.4.9), and must be compatible with the known location (5.4.6) of the Ruelle resonances. The question is: do these conditions uniquely fix the form of the OPE coefficients, in the universal high energy regime in which the CFT spectrum is governed by the Cardy formula? Do we know of any solutions to these conditions?

4.3 Ruelle from Liouville

The answer to the last question is affirmative: Liouville theory solves both conditions. The bootstrap program of Liouville CFT is by now on firm footing [76]. Our new observation is that the OPE coefficients of Liouville CFT, given by the famous DOZZ formula [104, 105], indeed exhibit a series of poles that precisely match with the quasi-normal frequencies (5.4.6) of the BTZ black hole. This observation gives extra support to the proposal that Liouville theory should be viewed as the effective CFT that captures universal high energy behavior of holographic CFTs. As we will discuss in the concluding section, this result also sheds light on whether the lattice model of section 5.3 has ergodic dynamics or not.

Liouville CFT has a continuous spectrum labeled by the momentum variable α via $\Delta_\alpha = \alpha(Q-\alpha)$ with $c = 1+6Q^2$ and $Q = b+b^{-1}$. In section 5.6 we review the

[6]Evidently, the Ruelle poles do not arise from the density of states. The Laurent coefficients γ_n^ω are fixed by conformal symmetry and they only exhibit poles for frequencies associated to degenerate states. The degenerate states appear at different locations than the quasi-normal modes.

expression for the three point function $C(\alpha_1, \alpha_2, \alpha_3)$ for a light operator, labeled by α_1, and two heavy operators, labeled by α_2 and α_3. Denoting the conformal dimensions as $\Delta_1 = h$, $\Delta_2 = \mathrm{M}$ and $\Delta_3 = \mathrm{M}+\omega$, the corresponding Liouville momenta are

$$\alpha_1 \simeq bh, \qquad \alpha_3 - \alpha_2 \simeq i\frac{\omega}{2\sqrt{\mathrm{M}}} = ib\,\frac{\beta}{4\pi}\,\omega \tag{5.4.15}$$

where $\beta = 2\pi/b\sqrt{\mathrm{M}}$ is the inverse temperature associated with the state M.

The DOZZ three-point function $C(\alpha_1, \alpha_2, \alpha_3)$ has a rich pole structure. As explained in Appendix 5.6, the series of poles that are relevant to our physical situation are located at

$$\alpha_1 + \alpha_3 - \alpha_2 = nb, \qquad n \in \mathbb{Z}, \tag{5.4.16}$$

which via equations (5.4.15) and (5.4.16) tells us that $C_{\mathrm{h\,M\,M+\omega}}$ has poles at

$$\omega = -i\frac{4\pi}{\beta}(n+h). \tag{5.4.17}$$

Plugging this into (5.4.14), and doing the integral (5.4.13), we learn that the retarded Green's function $G^{\mathrm{ret}}(\omega, \ell)$ has poles for

$$\begin{aligned} \omega &= -\ell + 2n_L - i\frac{4\pi}{\beta}(n+h), \\ \omega &= \ell + 2n_R - i\frac{4\pi}{\beta}(n+h). \end{aligned} \qquad n \in \mathbb{N}. \tag{5.4.18}$$

These are the Ruelle resonances that govern the thermalization dynamics of Liouville CFT. Notice that relative to the list (5.4.6) of BTZ quasi-normal modes, the series (5.4.18) reveals additional poles shifted by the excitation numbers n_L and n_R of the left- and right-moving Virasoro descendants. These additional poles arise because in our CFT calculation, we did not exclude the possibility that the incoming wave

created by $\mathcal{O}_{\rm a}$ also excites boundary gravitons. If we ignore the energy stored in the boundary gravitons, we recover the expected BTZ result (5.4.6).

5.5 Conclusions

In this chapter we have made three observations that clarify the geometric origin of chaotic behavior in irrational 2D CFTs. We argued that in holographic CFTs at finite temperature, conformal symmetry is non-linearly realized by means of universal Goldstone-like fields $\xi(u)$ and $\eta(v)$, that describe the near-horizon gravitational dynamics of the dual theory. The effective field theory is weakly coupled and its maximal Lyapunov behavior can be demonstrated at the semi-classical level.

We used this insight to propose a new toy model for quantum chaos in the form of the FKV lattice model, with an integrable equation of motion given by a Y-system. Integrability may seem unhelpful for generating ergodic behavior. Indeed, integrable systems are seen as prototypical counter-examples for the ETH: their single state microcanonical ensemble is understood to be described by the generalized Gibbs ensemble (GGE), which has many chemical potentials, one for each conserved quantity [156]. However, this reasoning assumes that the state that defines the microcanonical ensemble is an (approximate) eigenstate of many or all conserved quantities. Instead, if we choose an energy eigenstate that otherwise is a random linear superposition of eigenstates of all other conserved quantities, then the usual ETH can still apply. The conserved quantities in the FKV lattice model are highly non-local, and with respect to local observables the dynamics still looks random and thermalizing. As discussed in the introduction, this random dynamics can be reinforced by introducing some degree of disorder.

Indeed the discrete model seems particularly useful for studying propagation of entanglement, and even though the continuum limit is expected to be described by a CFT, the entanglement propagation generated by the Y-system rule (5.1.3) is non-

ballistic and mixes left- and right-moving signals. Our conjecture that the lattice dynamics is ergodic is further supported by the fact that the continuum limit of the model is expected to be described by Liouville theory, which via the observation of section 5.4 has Ruelle resonances that prescribe the approach towards thermal equilibrium.

Of course, underlying all three observations in this chapter, is the idea that the bulk gravitational dynamics of holographic 2D CFTs is accurately captured by 2D Liouville CFT [74]. This emergent Liouville field can be viewed as encoding the dynamical interplay between geometric entanglement and energy flow. This interpretation combines the idea of kinematic space [90, 157], that the entanglement entropy $S(u,v)$ of an interval $[u,v]$ between two space-like separated points $x=u$ and $x=v$ describes a metric on a 2D hyperbolic space via

$$ds^2 = \partial_u \partial_v S(u,v)\, du dv, \tag{5.5.1}$$

with the first law of entanglement thermodynamics

$$\delta S(u,v) = \delta K(u,v) = \int_u^v dx\, P_{[u,v]}(x)\, \delta T_{00}(x) \tag{5.5.2}$$

with $P_{[u,v]}(x)$ the conformal Killing vector associated with the Rindler Hamiltonian $K(u,v)$ of the interval $[u,v]$. Equation (5.5.2) can be integrated into an expression for the energy-momentum tensor $T_{\alpha\beta}$ in terms of the entanglement entropy $S(u,v)$, which looks exactly like the Liouville energy momentum tensor, via the identification

$$\phi(u,v) = S(u,v) \tag{5.5.3}$$

of the Liouville field with the entanglement entropy. Note that both quantities define locally constant curvature metrics, and both transform inhomogeneously under

coordinate transformations. Hence the dynamics of kinematic space seems intimately connected with the emergence of an effective Liouville field in holographic 2D CFT.

5.6 Appendix: DOZZ three point function

In this appendix we summarize the DOZZ formula for the OPE coefficients of Liouville theory [104, 105]. A nice review can be found in [158]. After introducing the formula we will study its analytic properties which are relevant for the application we consider in the main text.

The DOZZ formula computes the OPE coefficients between three primary operators of Liouville theory. These operators are labeled by a complex parameter α and can be written in terms of the Liouville field $\varphi(z,\overline{z})$ in the following way

$$V_{\alpha_j}(z,\overline{z}) = e^{2\alpha_j\varphi(z,\overline{z})}, \qquad j=1,2,3. \tag{5.6.1}$$

The dimension of the state in term of its label is $\Delta_\alpha = \overline{\Delta}_\alpha = \alpha(Q-\alpha)$. As usual the central charge is $c = 1+6Q^2$ and $Q = b+\frac{1}{b}$, where b is a positive real parameter. The semiclassical limit $c \gg 1$ corresponds to $b \ll 1$. That is the limit we are interested in, although the result for Liouville theory is supposed to be valid more generally. Now we can state the DOZZ formula which for generic $\alpha_{1,2,3}$ and b is given by

$$C(\alpha_1,\alpha_2,\alpha_3) = \frac{\left[\pi\mu\gamma(b^2)b^{2-2b^2}\right]^{\left(Q-\sum_i\alpha_i\right)/b}\Upsilon_0\Upsilon_b(2\alpha_1)\Upsilon_b(2\alpha_2)\Upsilon_b(2\alpha_3)}{\Upsilon_b(\sum_i\alpha_i - Q)\Upsilon_b(\alpha_1+\alpha_2-\alpha_3)\Upsilon_b(\alpha_1-\alpha_3-\alpha_2)\Upsilon_b(\alpha_2+\alpha_3-\alpha_1)}, \tag{5.6.2}$$

where μ is the cosmological constant, $\gamma(x) \equiv \Gamma(x)/\Gamma(1-x)$ and $\Upsilon_0 = \frac{d\Upsilon_b(x)}{dx}\big|_0$. $\Upsilon_b(x)$ is an entire function. It is usually defined by analytic continuation of an integral representation valid for $0 < \mathrm{Re}(x) < Q$ which can be found in [104, 105]. Here we will not need more information about this function other that its zeros since it gives the position of the poles in the DOZZ formula in terms of the α's. Specifically, they are

located at

$$x = -\frac{m}{b} - bn, \quad x = \frac{m'+1}{b} + b(n'+1), \quad m, m', n, n' \in \mathbb{Z}^+. \tag{5.6.3}$$

Looking at the formula (5.6.2) we see all the poles are located in terms of the labels α at

$$\begin{aligned}
\alpha_1 + \alpha_2 + \alpha_3 - Q &= -\frac{m}{b} - bn, \quad \text{or} \quad \frac{m'+1}{b} + (b+1)n', && (5.6.4)\\
\alpha_1 + \alpha_2 - \alpha_3 &= -\frac{m}{b} - bn, \quad \text{or} \quad \frac{m'+1}{b} + (b+1)n', && (5.6.5)\\
\alpha_1 - \alpha_2 + \alpha_3 &= -\frac{m}{b} - bn, \quad \text{or} \quad \frac{m'+1}{b} + (b+1)n', && (5.6.6)\\
\alpha_2 + \alpha_3 - \alpha_1 &= -\frac{m}{b} - bn, \quad \text{or} \quad \frac{m'+1}{b} + (b+1)n'. && (5.6.7)
\end{aligned}$$

These are all the poles of the OPE coefficients. Now we will use the semiclassical limit to identify the poles that are physically relevant for the discussion in the main text, i.e. the ones that survive the $b \to 0$ limit. The external operators that we are interested in are such that one is light, α_1, two are heavy, α_2 and α_3, and the difference between the two heavy operators is small. This means we fix the scaling with b in the $b \to 0$ limit such that $\alpha_1 \sim b$, $\alpha_2 \sim \alpha_3 \sim b^{-1}$ and $\alpha_3 - \alpha_2 \sim b$. Then it is clear that the relevant poles to retain are the ones in equation (5.6.5) and (5.6.6) for only n non zero. These two sets of poles for $n > 0$ can be combined into a single formula

$$\alpha_1 + \alpha_3 - \alpha_2 = bn, \quad n \in \mathbb{Z}, \tag{5.6.8}$$

where now n runs over all the integers. We see this has the right scaling since both the left and right hand side scale as b in the semiclassical limit. All the rest of the poles disappear in the heavy-heavy-light limit we are interested in here.

Chapter 6

Interference Effects

In the introduction we explained the relation between black holes, quantum chaos and gravitational shockwaves. We have studied these features for quantum mechanics and CFTs in the previous chapters.

In this chapter we will study a different aspect of shockwaves solutions. We will consider bulk theories in AdS_D and study (without black holes) the effect of higher derivative terms in the action. In [159] the authors showed that the constrain of a positive time delay (equivalent to the averaged null energy condition) puts constrains on purely gravitational terms like $S \sim \int R^2$ or $S \sim \int R^3$. In this chapter we will study an interference effect of shockwaves that will allow us to put constrains on non-minimal coupling between matter and gravity such as $S = \alpha \int \phi W^2$. These shockwaves not only produce a time delay but also has a probability of inducing a transition $\phi \to g$, where g indicates the graviton. The nature of this shockwave is explained in section 6.8. The bounds we obtain on this coupling α can be found in section 6.6. For a general theory roughly $\alpha \lesssim R^2_{\text{AdS}}$. If we furthermore assume a local bulk theory one can easily improve this to $\alpha \lesssim \ell^2_{\text{str}}$ [1].

[1] The string length ℓ^2_{str} gives the scale of the lowest mass higher spin field in the bulk. If the bulk theory is local then $\ell_{\text{s}} \ll R_{\text{AdS}}$.

Besides the application for local bulk physics, this can be turn around and obtain general bounds for an arbitrary CFTs. This is done by relating a non-local version of the shockwave with a conformal collider experiment where one measures the integrated energy at infinity [160]. The coupling of $S \sim \int \phi W^2$ is related to $C_{TT\mathcal{O}}$ and we will put bounds on this OPE coefficient in general theories.

To make the presentation as clear as possible we start from this point of view in sections 6.3, 6.4 and 6.5, and later focus on the bulk interpretation described in the previous paragraph. We leave some applications to de-Sitter and inflation to section 6.7.

6.1 Introduction

We consider the conformal collider physics experiment discussed in [160]. In that setup, we produce a localized excitation by acting with a smeared operator near the origin of spacetime. Then we measure the energy flux at infinity per unit angle. Requiring that the energy flux is positive imposes constraints on the three-point function coefficients. This method was used to constrain three-point functions of the stress tensor in [160–162].

In this chapter we use this same method to constrain the three-point functions of two stress tensors and another operator $\langle TT\mathcal{O}\rangle$. The new idea consists of creating the initial state by a linear combination of a stress tensor operator and the operator $\mathcal{O}$. The three-point function $\langle TT\mathcal{O}\rangle$ appears as a kind of interference term in the expression for the energy. Requiring that the total contribution to the energy flux is positive imposes a non-trivial upper bound on the absolute magnitude of this three-point correlator. We apply these ideas to general scalar operators $\mathcal{O}$ as well as conserved currents with spin one, J, where we use it to put bounds on the gravitational anomaly in $d = 4$ CFTs. Because the bound arises from quantum mechanical interference effects, these bounds are stronger than those obtained in states created

by a single primary local operator and its descendants (though the resulting bounds involve more OPE coefficients).

This energy flux at infinity is given by an integral of the stress tensor. On the boundary of Minkowski space this integral is simply the average null energy $\mathcal{E} = \int dx^- T_{--}$. We review this in section 6.2. Physically, we expect that this energy should be positive for all angles. Recently, the average null energy condition was proven using entanglement entropy methods [163] as well as reflection positivity euclidean methods [164]. When we create a localized state using the stress tensor, this energy distribution is completely determined by the three-point function of the stress tensor. Two of the insertions correspond to the insertions creating the state in the bra and the ket. The third corresponds to the one measuring the energy flux at infinity. The resulting bounds could also be obtained by requiring standard reflection positivity of the euclidean theory [165, 166]. However, the conformal collider calculations provide an efficient way to extract the results.

One of our main results is a sum rule constraining the OPE coefficients of scalar primary operators $\mathcal{O}$ with the energy-momentum tensor T. In spacetime dimensions $d \geq 4$ there is a single OPE coefficient controlling the $\langle TT\mathcal{O}\rangle$ three-point function. We find that this data is constrained as

$$\sum_{\text{Scalar Primaries } \mathcal{O}_i} |C_{TT\mathcal{O}_i}|^2 \ f(\Delta_i) \leq N_B \ , \tag{6.1.1}$$

where N_B is one of the three OPE coefficients in $\langle TTT\rangle$ (the one occurring in a theory of free bosons), and the non-negative function $f(\Delta)$ is given explicitly by

$$f(\Delta) = \frac{(d-1)^3 d \pi^{2d} \Gamma\left(\frac{d}{2}\right) \Gamma(d+1) \Gamma(\Delta) \Gamma\left(\Delta - \frac{d-2}{2}\right)}{(d-2)^2 \Gamma\left(\frac{\Delta}{2}+2\right)^4 \Gamma\left(\frac{d+\Delta}{2}\right)^2 \Gamma\left(d-\frac{\Delta}{2}\right)^2} \ . \tag{6.1.2}$$

This function arises by doing the integrals involved in smearing the operator as well as in computing the energy flux. We derive this bound in detail in section 6.3,

and discuss some simple physical consequences such as its interpretation in free field theories, large N holographic systems, and general implications for the asymptotics of OPE coefficients.

In section 6.4 we consider analogous results in spacetime dimension three. This case is special because the three-point functions of interest admit both parity preserving and parity violating structures. The bounds we find generalize those recently obtained in [167]. We apply our results to large N Chern-Simons matter theories, and further use them to obtain predictions on OPE coefficients $C_{TT\mathcal{O}}$ for scalars in the Ising model using the recent results of the conformal bootstrap [168]. For instance, we find that operator ε has an OPE coefficient constrained as

$$|C_{TT\varepsilon}| \leq 1.751 |C_{TT:\phi^2:}| \ , \tag{6.1.3}$$

where the right-hand side is the value in the free scalar theory based on the field ϕ.

In section 6.5 we consider bounds in four-dimensional CFTs with a global symmetry current J. We apply the same techniques to obtain universal constraints on the gravitational anomaly of the current J.

In section 6.6 we show that the $\langle TT\mathcal{O}\rangle$ correlator can be generated from a gravity theory in AdS_{d+1} through a higher derivative term, $\int \phi W^2$, in the bulk effective action. We match the coefficient of this term to the $C_{TT\mathcal{O}}$ coefficient in the boundary theory by performing the same collider experiment in the bulk, where it involves propagation through a shock wave. One interesting feature of this presentation is that the resulting bound is independent of the mass of ϕ. Thus, the Δ dependence of (6.1.1) is purely kinematic and results from translating the boundary three-point function coefficient to a bulk interaction. We use our AdS presentation to show that α' corrections satisfy the bound.

In section 6.7 we extrapolate the bounds we obtained in AdS to "quasi bounds" on the coefficients of the effective action in de Sitter space. We call them "quasi-bounds" because, unfortunately, for de-Sitter we do not know how to prove a sharp bound. We can think of these as a good indication for where the bulk effective theory should break down. We apply these "quasi-bounds" to constrain the amplitude of chiral gravity waves, and to constrain the violations of the inflationary "consistency condition" for the two-point function. Both of these effects arise from higher curvature couplings of the form ϕW^2 or $\phi W W^*$.

6.2 ANEC and the Conformal Collider

6.2.1 The Average Null Energy Condition

The null energy condition is a central assumption in many classical theorems of general relativity. These results allow us to exclude unphysical spacetimes where causality violation, naked singularities, or other physical pathologies occur [169].

If we move beyond classical field theory, these results appear to be in doubt. Quantum effects lead to fluctuations that prohibit any local operator from having a positive expectation value in every state [170]. (We review these ideas in Appendix A of [56].) In particular the local energy density and other components of the energy-momentum tensor have negative expectation value in some states.

Deeper investigation reveals a potential resolution. While components of the energy-momentum tensor are pointwise non-positive, a weaker hypothesis, the so-called average null energy condition, is often sufficient to enforce causal behavior [171]. This condition states that the integral along a complete null geodesic of the null energy density is a positive definite operator

$$\mathcal{E} = \int_{-\infty}^{\infty} dx^- \; T_{--} \geq 0 \; . \tag{6.2.1}$$

Recently there has been significant interest in understanding the average null energy condition (6.2.1) in the context of local quantum field theories. In [164], an argument was given establishing (6.2.1) in conformal field theories by examining the constraints of causality on the light-cone operator product expansion. In [163], an alternative argument was given linking the average null energy operator to entanglement entropy, then establishing positivity using strong subadditivity. These information theoretic methods have also been extended to obtain new inequalities strengthening (6.2.1) [172].

Given that the average null energy in quantum field theory is now a theorem, it is interesting to take it as input and use it to constrain conformal field theory data.

6.2.2 The Conformal Collider

An efficient way to extract consequences of the average null energy condition in CFTs is to use the conformal collider setup of [160]. This technique is closely related to deep inelastic scattering experiments in conformal field theory [160, 173]. As we review, in the context of AdS/CFT these bounds arise from demanding causality of the bulk theory in a shockwave background.

The specific physical problem of interest is to create a disturbance in a conformal field theory and then to measure the correlation of energy deposited at various angles at future null infinity (see Figure 6.1).

The states in which we measure the energy are obtained by acting with local operators $\mathcal{O}(x)$ on the Lorentzian vacuum $|0\rangle$. We further give these states definite timelike momentum q.[2] Thus we examine the state

$$|\mathcal{O}(q,\lambda)\rangle = \mathcal{N}\int d^dx\ e^{-iqt}\ \lambda\cdot\mathcal{O}(x)|0\rangle\ , \tag{6.2.2}$$

[2]For technical reasons it is sometimes useful to create a localized wavepacket instead of an exact momentum eigenstate. This subtlety will not affect our discussion.

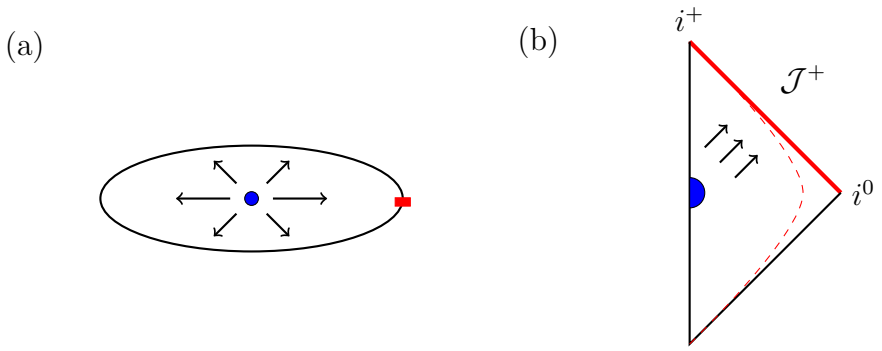

Figure 6.1: In the conformal collider experiment (a), the energy created by a localized excitation (blue) is measured far away by a calorimeter (red). (b) For a CFT, this is equivalent to measuring the energy at null infinity $\mathcal{J}^+$.

where λ is a polarization tensor accounting for the possible spin of $\mathcal{O}$, and $\mathcal{N}$ is a normalization factor defined such that (6.2.2) has unit norm.

We now measure the energy at null infinity in this state. In d dimensions null infinity is a sphere S^{d-2} and we parameterize it by a unit vector n.

$$\langle \mathcal{E}(n) \rangle_{\lambda \cdot \mathcal{O}} = \lim_{r \to \infty} r^{d-2} \int_{-\infty}^{\infty} dx^- \, \langle \mathcal{O}(q,\lambda) | T_{--}(x^-, rn) | \mathcal{O}(q,\lambda) \rangle \ . \tag{6.2.3}$$

The average null energy condition implies that the resulting function is non-negative as a function of the direction n.

Since we are working in a conformal field theory this energy expectation value may be explicitly evaluated. Indeed the object being integrated in (6.2.3) is a three-point function $\langle \mathcal{O}T\mathcal{O} \rangle$ in Lorentzian signature with a prescribed operator ordering. Thus, the result of (6.2.3) is an explicit function of OPE coefficients.

External States Created by T

Let us review the essential details of this calculation in the case where the external state is created by an energy momentum tensor. In general in $d \geq 4$ spacetime dimensions, the three-point function of energy-momentum tensors may be parameterized in

terms of three independent coefficients

$$\langle TTT\rangle = N_B\langle TTT\rangle_B + N_F\langle TTT\rangle_F + N_V\langle TTT\rangle_V \ , \tag{6.2.4}$$

where the various B, F, V structures are those that arise in a theory of respectively free bosons, fermions, or $(d-2)/2$ forms.[3] Our conventions are such that for free fields, N_B counts the number of real scalars, N_F the total number of fermionic degrees of freedom (e.g. it is $2^{\lfloor d/2\rfloor}$ for a Dirac fermion), and N_V counts the number of degrees of freedom in a $(d-2)/2$ form (for a single such field this number is $\Gamma(d-1)/\Gamma(d/2)^2$).

A single linear combination of these coefficients is fixed by the conformal Ward identity, and related to the two-point function coefficient C_T of energy momentum tensors

$$C_T = \frac{1}{\Omega_{d-1}^2}\left(\frac{d}{d-1}N_B + \frac{d}{2}N_F + \frac{d^2}{2}N_V\right) \ . \tag{6.2.5}$$

where Ω_n is the area of a sphere S^n.[4] As another point of reference let us briefly specialize to the case of four-dimensional theories. In that case, the coefficients of the three-point function are related to conformal anomalies a, c that parameterize the trace of the energy-momentum tensor in a general metric background

$$\langle T^\mu_\mu\rangle[g] = \frac{c}{16\pi^2}W^2 - \frac{a}{16\pi^2}E^2 \ , \tag{6.2.6}$$

where W is the Weyl tensor and E is the Euler density. The coefficient c is proportional to C_T, while

$$a = \frac{1}{1440}(4N_B + 11N_F + 124N_V) \ . \tag{6.2.7}$$

Returning to case of general dimensions we now investigate the null energy operator using these three-point functions. It is useful to organize the calculation using

[3] In odd d there is no free field associated to the structure parameterized by N_V, but nevertheless there is still a structure. See [162, 174] for details.

[4] $\Omega_{n-1} = 2\pi^{n/2}/\Gamma(n/2)$.

the relevant symmetries, which are rotations on the null S^{d-2}. In addition, the three-point function of T's is parity invariant.[5] It follows that the most general expression for the null energy is

$$\langle \mathcal{E}(n) \rangle_{\lambda \cdot T} = \frac{q}{\Omega_{d-2}} \left[1 + t_2 \left(\frac{\lambda^*_{ij} \lambda_{ik} n^j n^k}{|\lambda|^2} - \frac{1}{d-1} \right) + t_4 \left(\frac{\lambda^*_{ij} \lambda_{kl} n^i n^j n^k n^l}{|\lambda|^2} - \frac{2}{d^2-1} \right) \right] , \tag{6.2.8}$$

where the constants have been fixed so that the total energy of the state is q, and t_2 and t_4 are computable functions of N_B, N_F, N_V.

A useful way to understand the answer is to view the vector n as fixed and to decompose the states (parameterized by their polarizations) under the remaining symmetry group $SO(d-2)$. For example, the polarization that has spin zero under rotations around the $\vec{n}$ axis is

$$\lambda^0_{ij} \propto \left(n_i n_j - \frac{\delta_{ij}}{(d-1)} \right) \tag{6.2.9}$$

In a similar way we can write polarization tensors that have spin one and spin two under rotation around the $\vec{n}$ axis. The energy flux in the direction n is the same for every state in a fixed $SO(d-2)$ representation, and we denote them by qT_i/Ω_{d-2}. Explicitly carrying out the integrals gives:

$$\begin{aligned} T_0 &= \left(1 - \frac{t_2}{d-1} - \frac{2t_4}{d^2-1} \right) + \frac{d-2}{d-1}(t_2 + t_4) = \rho_0(d) \left(\frac{N_B}{C_T} \right) , \\ T_1 &= \left(1 - \frac{t_2}{d-1} - \frac{2t_4}{d^2-1} \right) + \frac{t_2}{2} = \rho_1(d) \left(\frac{N_F}{C_T} \right) , \\ T_2 &= 1 - \frac{t_2}{d-1} - \frac{2t_4}{d^2-1} = \rho_2(d) \left(\frac{N_V}{C_T} \right) , \end{aligned} \tag{6.2.10}$$

[5] In $d = 3$ the three-point function has a parity odd piece which we discuss in section 6.4.

where the index labels the $SO(d-2)$ charge and in the above $\rho_i(d)$ is a positive function that depends only on the spacetime dimension (and not the OPE coefficients). Their explicit form can be found in Appendix B of [56].

Additional symmetries imply constraints on the parameters above. In any superconformal field theory we have $t_4 = 0$. For holographic CFTs dual to Einstein gravity the parameters are $t_2 = t_4 = 0$, giving angle independent energy one-point functions $T_0 = T_1 = T_2 = 1$.

Returning to the general discussion, we can see from (6.2.10) that the average null energy condition implies the inequalities

$$N_B \geq 0 \ , \qquad N_F \geq 0 \ , \qquad N_V \geq 0 \ . \tag{6.2.11}$$

One significant remark concerning the bounds (6.2.11) is that they may clearly be saturated in free field theories. Conversely, it has been argued [175] that any theory that saturates the conformal collider bounds must be free. The fact that the bounds may be saturated in actual CFTs illustrates that the conformal collider is an efficient way of extracting the implications of the average null energy condition. Namely, we could not possibly get a stronger bound, otherwise we would run into a contradiction with free theories.

6.3 Bounds on $TT\mathcal{O}$ in $d \geq 4$

We now turn to our main generalization of the conformal collider bounds reviewed in section 6.2.2. We explore the consequences of the average null energy condition in more general states than those created by a single primary operator. Specifically in this section we will investigate states which are obtained by a linear combination of primary operators. We will find that the average null energy condition in such states yields new inequalities on OPE coefficients.

In this section, the states we consider will be created by a linear combination of the energy-momentum tensor and a general scalar hermitian operator $\mathcal{O}$. We parameterize such a state in terms of normalized coefficients v_i

$$|\Psi\rangle = v_1|T(q,\lambda)\rangle + v_2|\mathcal{O}(q)\rangle \ . \tag{6.3.1}$$

The energy one-point function in the collider experiment is now a matrix

$$\langle\Psi|\mathcal{E}(n)|\Psi\rangle = v^\dagger \begin{pmatrix} \langle T(q,\lambda)|\mathcal{E}(n)|T(q,\lambda)\rangle & \langle T(q,\lambda)|\mathcal{E}(n)|\mathcal{O}(q)\rangle \\ \langle T(q,\lambda)|\mathcal{E}(n)|\mathcal{O}(q)\rangle^* & \langle\mathcal{O}(q)|\mathcal{E}(n)|\mathcal{O}(q)\rangle \end{pmatrix} v \ . \tag{6.3.2}$$

The average null energy condition implies that this matrix is positive definite. This is a stronger condition than requiring that the diagonal entries are positive and will imply new inequalities on OPE coefficients.

The majority of the entries in this matrix have already been computed. For instance, in section 6.2.2 we reviewed the portion of the matrix involving the energy expectation value in states created by the energy momentum tensor. Even simpler is the entry involving the expectation value in the scalar state which gives rise to a uniform energy distribution

$$\langle\mathcal{O}(q)|\mathcal{E}(n)|\mathcal{O}(q)\rangle = \frac{q}{\Omega_{d-2}} \ . \tag{6.3.3}$$

It remains to determine the off-diagonal entries in the matrix. It is again useful to organize the expected answer using the rotation group on the null sphere. Clearly we have

$$\langle T(q,\lambda)|\mathcal{E}(n)|\mathcal{O}(q)\rangle \sim \lambda_{ij}n^i n^j \ . \tag{6.3.4}$$

Therefore, the only polarization of the energy momentum tensor that participates in the non-trivial interference terms is the scalar T_0 aligned along the axis n (see equation (6.2.9)).

To extract this matrix element we require the three-point function $\langle TT\mathcal{O}\rangle$. In all $d \geq 4$, the conservation constraints on T imply that this correlator is fixed in terms of a single OPE coefficient $C_{TT\mathcal{O}}$. We set conventions for our normalization of this OPE coefficient by examining a simple OPE channel. Specifically we restrict all operators to a two-plane, spanned by complex coordinates $z, \bar{z}$. Then the OPE is

$$T_{zz}(z)T_{\bar{z}\bar{z}}(0) \sim \frac{C_{TT\mathcal{O}}}{|z|^{2d-\Delta}}\mathcal{O}(0) \ . \tag{6.3.5}$$

If we further assume that $\mathcal{O}$ is hermitian then the OPE coefficient $C_{TT\mathcal{O}}$ is real. Additional details of this correlator including the full d-dimensional Lorentz covariant OPE and relation to the spinning correlator formalism of [176] are given in Appendix B of [56].

Based on these remarks, we can in general parameterize the energy flux in the direction n coming from the off-diagonal matrix element (6.3.4) as

$$\langle T(q,\lambda_0)|\mathcal{E}(n)|\mathcal{O}(q)\rangle = \frac{q}{\Omega_{d-2}}\left(\frac{C_{TT\mathcal{O}}}{\sqrt{C_T C_{\mathcal{O}}}}h(\Delta)\right) \ , \tag{6.3.6}$$

where $h(\Delta)$ is some universal function that may be extracted from the conformal collider calculation, and the factors of C_T and $C_{\mathcal{O}}$ arise from normalizing the states. The relevant portion of the energy matrix (6.3.2) is two-by-two and takes the form

$$\frac{q}{\Omega_{d-2}}\begin{pmatrix} T_0 & \frac{C_{TT\mathcal{O}}}{\sqrt{C_T C_{\mathcal{O}}}}h(\Delta) \\ \frac{C^*_{TT\mathcal{O}}}{\sqrt{C_T C_{\mathcal{O}}}}h(\Delta) & 1 \end{pmatrix} \ . \tag{6.3.7}$$

Positivity of this matrix therefore leads to the constraint

$$\frac{|C_{TT\mathcal{O}}|^2}{C_T C_{\mathcal{O}}} |h(\Delta)|^2 \leq T_0 \ . \tag{6.3.8}$$

More generally we may instead consider the collider experiment in a state created by T plus a general linear combination of primary scalar operators. Positivity of the resulting energy matrix is then equivalent to the following sum rule

$$\sum_{\text{Scalar Primaries } \mathcal{O}_i} \frac{|C_{TT\mathcal{O}_i}|^2}{C_T C_{\mathcal{O}}} \ |h(\Delta_i)|^2 \leq T_0 \ . \tag{6.3.9}$$

The explicitly computation of the function $h(\Delta)$ can be found in Appendix B of [56]. By combining the result with the expression (6.2.10), we may reexpress the bound as

$$\sum_{\text{Scalar Primaries } \mathcal{O}_i} \frac{|C_{TT\mathcal{O}_i}|^2}{C_{\mathcal{O}}} \ f(\Delta_i) \leq N_B \ , \tag{6.3.10}$$

where $f(\Delta)$ is given as

$$f(\Delta) = \frac{(d-1)^3 d \pi^{2d} \Gamma\left(\frac{d}{2}\right) \Gamma(d+1) \Gamma(\Delta) \Gamma\left(\Delta - \frac{d-2}{2}\right)}{(d-2)^2 \Gamma\left(\frac{\Delta}{2}+2\right)^4 \Gamma\left(\frac{d+\Delta}{2}\right)^2 \Gamma\left(d-\frac{\Delta}{2}\right)^2} \ . \tag{6.3.11}$$

6.3.1 Analysis of the Bound

We now turn to an analysis of the consequences of the general bound (6.3.10). The function $f(\Delta)$ has a number of significant properties.

- Expanded near the unitarity bound we find a first order pole:

$$f\left(\frac{d-2}{2} + x\right) \sim \frac{1}{x} \ . \tag{6.3.12}$$

Therefore in any family of theories, an operator $\mathcal{O}$ which is parametrically becoming free (i.e. $\Delta = (d-2)/2 + x$ with x tending to zero) must have $|C_{TT\mathcal{O}}|$ vanish at least as fast as $\sqrt{x}$.

- For large Δ we find exponential growth

$$f(\Delta) \sim \frac{4^{\Delta}}{\Delta^{\frac{7d}{2}+4}} \ . \tag{6.3.13}$$

We may use this growth to approximate the sum in the bound for scalar operators of large Δ. Indeed, let $\rho(\Delta)$ denote the asymptotic density of scalar primary operators. From convergence of the sum we then deduce that for large Δ the spectral weighted OPE coefficients must decay exponentially fast

$$\rho(\Delta)\frac{|C_{TT\mathcal{O}}|^2}{C_{\mathcal{O}}} \leq \frac{\Delta^{\frac{7d}{2}+3}}{4^{\Delta}} \ . \tag{6.3.14}$$

These estimates agree with those implied by convergence of the OPE expansion found in [177] for scalar operators.

- If Δ is an even integer greater than or equal to $2d$ we find that $f(\Delta)$ vanishes. We can understand the necessity of this as follows. We can imagine a large N CFT dual to weakly coupled theory of gravity. In such theories we can consider the sequence of operators $\mathcal{O} =: T^{AB}\partial^{2n}T_{AB} :$. At large N the dimensions of these operators are fixed to $\Delta = 2d + 2n$. Moreover, for these operators $\frac{C^2_{TT\mathcal{O}}}{C_{\mathcal{O}}}$ is of order C_T^2. Thus, compatibility with the bound (6.3.10) for large C_T, requires that $f(\Delta)$ vanishes at these locations.

  The above argument does not explain why $f(\Delta)$ has double zeros. But the double zeros imply that the bound may be obeyed at subleading order, where

we include the anomalous dimensions of these operators which scale as $1/C_T$, by truncating the sum on n.[6]

- The function $f(\Delta)$ is non-zero for $\Delta = d$. Therefore the bound (6.3.10) may be applied to marginal operators. In that context, it constrains the change in C_T at leading order in conformal perturbation theory.

6.3.2 Free Field Theories and Destructive Interference

Let us investigate the bound further in free field theories. These examples are interesting because the bound (6.3.10) is saturated.

Consider first a theory of a free real boson ϕ in dimension d. There is a $\mathbb{Z}_2$ global symmetry under which ϕ is odd and the energy-momentum tensor T is even. Therefore we need only consider scalars made from an even number of ϕ's. Since the explicit expression for T is quadratic in the free fields, the only possible scalars that may contribute to the bound are $:\phi^2:$ and $:\phi^4:$.

By a simple inspection of the Wick contractions we deduce that $:\phi^4:$ has vanishing $TT\mathcal{O}$ correlation function[7]. Meanwhile $:\phi^2:$ has

$$\frac{|C_{TT\mathcal{O}}|^2}{C_{\mathcal{O}}} = \frac{(d-2)^4\Gamma(d/2+1)^4}{8\pi^{2d}(d-1)^4} \ . \tag{6.3.15}$$

This exactly saturates the bound (6.3.10).

We can also consider the bound applied to free fields of different spin. In $d = 4$ the theory of free fermions or free gauge bosons have vanishing N_B. Therefore the bound implies that for all scalar operators $\mathcal{O}$ either $C_{TT\mathcal{O}}$ vanishes, or $\mathcal{O}$ has dimension $2d + 2n$ for non-negative integer n.

[6] We thank E. Perlmutter for comments on this point.

[7] The contractions imply that $\langle TT : \phi^4 : \rangle \propto \langle T : \phi^2 : \rangle \langle T : \phi^2 : \rangle$, which is zero since two-point functions of different operators vanish.

It is straightforward to directly verify this prediction. For instance consider the free vector. The gauge invariant field strength gives rise to two local operators $F^+_{\mu\nu}$ and $F^-_{\mu\nu}$, which are respectively self-dual and anti-self-dual two-forms. Note that this free field theory enjoys a continuous electromagnetic duality symmetry under which $F^\pm_{\mu\nu}$ rotate with opposite charge. The energy-momentum tensor $T_{\mu\nu}$ is neutral under this transformation, and hence a scalar operator $\mathcal{O}$ with non-vanishing $C_{TT\mathcal{O}}$ must also be neutral. If we recall that $F^+_{\mu\nu}F^{-\mu\nu}$ vanishes identically, then we see that the lowest dimension neutral scalar operator is $(F^+_{\mu\nu}F^{+\mu\nu})(F^-_{\alpha\beta}F^{-\alpha\beta})$. Since this has dimension eight, the weight function $f(\Delta)$ vanishes. Moreover all other scalar operators that are neutral have larger even integer dimension. Thus, the bound is obeyed.

A more physical way to understand why the bound is saturated in the free scalar theory is to visualize the state created by local operators.

Let us consider the action of an operator with non-zero energy but zero spatial momentum. If the operator is a bilinear in the fields, such as the stress tensor in a free theory, then it will create a pair of particles with back to back spatial momenta. Of course, the operator creates a quantum mechanical superposition of states where these momenta point in various directions. For a scalar bilinear operator we get an s-wave superposition. For the stress tensor we get a superposition determined by the polarization tensor.

As in previous sections, we measure the energy in the angular direction n and hence can focus on the properties of the wavefunction for the pair of particles in that particular direction. As in section 6.2.2 it is convenient to decompose the polarization tensors of the operators according to their angular momentum around the n axis. We can then easily check that a spin zero state T_0 can be produced only in a theory of scalars, a spin one state T_1 can be produced only in a theory of fermions, and T_2 only in a theory of vectors (or $d/2-1$ forms), see Figures 6.2(a,b,c). This explains formula 6.2.10.

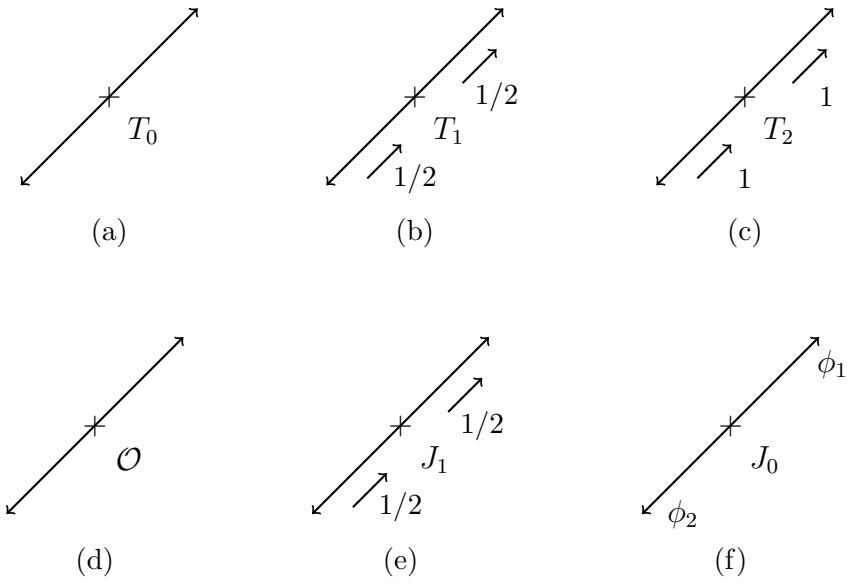

Figure 6.2: We consider operators with zero spatial momentum that create a pair of free particles. In (a,b,c) we consider a stress tensor operator. We decompose the stress tensor according to the spin around that axis. (a) The spin zero state is obtained for scalars, spin one for fermions (b) and spin two for vectors or self-dual forms (c). (d) is the state produced by a scalar operator with can interfere with (a). (e) is produced by a current with spin one along the observation axis and can interfere with (b). (f) is a current with spin zero along the observation axis in a theory of scalars. It cannot interfere with (a).

A scalar operator of the form $\mathcal{O} =: \phi^2 :$, where ϕ is an elementary scalar, can also produce a back to back combination of scalar particles, see Figure 6.2(d). Along the direction of observation this combination has the same form as the one produced by T_0, in Figure 6.2(a). It is clear that we can make a quantum mechanical superposition so that the wavefunction for the pair vanishes along that particular observation direction. This saturates the bound because we get zero energy along that direction. For that superposition of T and $\mathcal{O}$ the energy along other directions is still non-zero.

A similar argument helps us understand why we also saturate the $\langle TTJ \rangle$ correlator bound in the four dimensional theory of a Weyl fermion (see section 6.5). In that case we can make a superposition of the state T_1 in Figure 6.2(b) with the state J_1 in 6.2(e). Notice that we are using that J couples to a chiral fermion. If there

was another fermion with the same helicity but opposite charge, as it would be the case for a vector-like current, then we would have an additional contribution to the state created by the current that will have a relative minus sign compared to the other charged particle pair. On the other hand, for the state created by the stress tensor these two contributions have the same sign, therefore we cannot destructively interfere them.

This highlights that the bound comes from a quantum mechanical interference effect. We saturate the bound through a destructive interference effect that prevents particles from going into a particular direction. It is important to note that this is an interference for the pair of particles. For example, if we consider a theory of scalars with a $U(1)$ symmetry generated by a current J, then in a basis of real scalars the current will create two different scalars, say ϕ^1 and ϕ^2. This cannot interfere with the state created by the stress tensor where we have the same scalar for the two particles indicated in Figure 6.2(a).

6.4 Bounds on $TT\mathcal{O}$ in $d = 3$

In this section we will consider the case of $d = 3$ separately. There are two reasons for doing this. First, the stress-tensor three-point function has two parity even structures, instead of three as in $d \geq 4$, and has a parity odd piece which is special to $d = 3$. Secondly, the correlation function $\langle TT\mathcal{O}\rangle$ also has an extra parity odd structure special to $d = 3$ [178].

First we consider external states created by the stress-tensor. We parametrize the three-point function of energy-momentum tensors as

$$\langle TTT\rangle = N_B\langle TTT\rangle_B + N_F\langle TTT\rangle_F + N_{\text{odd}}\langle TTT\rangle_{\text{odd}} \ , \tag{6.4.1}$$

where N_B and N_F already appeared in the $d \geq 4$ case and $N_{\rm odd}$ parametrizes a new structure. We use the same convention for the explicit expression for $\langle TTT\rangle_{\rm odd}$ as in [167][8]. In $d \geq 4$ the energy one-point function of the collider experiment has a $SO(d-2)$ symmetry for the calorimeter direction n. The linearly independent tensor polarizations are organized as scalar, vectors or tensors with respect to this symmetry. In $d = 3$ the group becomes $SO(1)$ and there are only two types of polarizations, which we take as

$$\lambda_0 = \frac{1}{\sqrt{2}} \begin{pmatrix} 1 & 0 \\ 0 & -1 \end{pmatrix} , \quad \lambda_1 = \frac{1}{\sqrt{2}} \begin{pmatrix} 0 & 1 \\ 1 & 0 \end{pmatrix} . \tag{6.4.2}$$

The collider energy one-point function for an arbitrary polarization has the structure

$$\langle \mathcal{E}(n)\rangle_{\lambda\cdot T} = \frac{q}{2\pi}\left[1+t_4\left(\frac{|\lambda_{ij}n^i n^j|^2}{|\lambda|^2}-\frac{1}{4}\right)+d_4\frac{\varepsilon^{ij}(n_i n^m \lambda_{jm}\lambda^*_{kp}n^k n^p + n_i n^m \lambda^*_{jm}\lambda_{kp}n^k n^p)}{2|\lambda|^2}\right] . \tag{6.4.3}$$

To obtain a bound on these parameters we can consider a state created by $|\Psi\rangle = v_1|T(q,\lambda_0)\rangle + v_2|T(q,\lambda_1)\rangle$. The energy matrix becomes

$$\langle\Psi|\mathcal{E}(n)|\Psi\rangle = \frac{q}{2\pi} v^\dagger \begin{pmatrix} T_0 & T_{\rm odd} \\ T_{\rm odd} & T_1 \end{pmatrix} v , \tag{6.4.4}$$

where $T_1 = 1-t_4/4$, $T_0 = 1+t_4/4$ and $T_{\rm odd} = d_4/4$. These parameters were computed in [167] in terms of the $\langle TTT\rangle$ parameters N_B, N_F and $N_{\rm odd}$ obtaining

$$C_T T_1 = \frac{3}{16\pi^2}N_F , \quad C_T T_0 = \frac{3}{16\pi^2}N_B , \quad C_T T_{\rm odd} = \frac{3}{16\pi^2}N_{\rm odd} . \tag{6.4.5}$$

For supersymmetric CFTs $t_4 = 0$ just as in the case $d \geq 4$. Also, CFTs dual to Einstein gravity have $t_4 = d_4 = 0$.

[8] We identify our $N_{\rm odd}$ with their $\pi^4 p_T/3$.

The average null energy condition implies that the matrix (6.4.4) is positive definite. This implies t_4 and d_4 lie inside a circle $t_4^2 + d_4^2 \leq 4^2$, or equivalently $N_B \geq 0$, $N_F \geq 0$, and $N_{\text{odd}}^2 \leq N_B N_F$.

Now we will generalize this construction along the same lines as presented in section 6.3. We will consider a superposition between stress tensor and a scalar operator states

$$|\Psi\rangle = v_1|T(q,\lambda_0)\rangle + v_2|T(q,\lambda_1)\rangle + v_3|\mathcal{O}(q)\rangle \ . \tag{6.4.6}$$

As anticipated above, for $d = 3$ the correlation function $\langle TT\mathcal{O}\rangle$ is now determined by two parameters

$$\langle TT\mathcal{O}\rangle = C_{TTO}^{\text{even}}\langle TT\mathcal{O}\rangle_{\text{even}} + C_{TTO}^{\text{odd}}\langle TT\mathcal{O}\rangle_{\text{odd}} \ , \tag{6.4.7}$$

where the even part is given by specializing the arbitrary d correlator $d = 3$, and our choice of normalization for the odd part is given explicitly in Appendix B of [56]. We can make our conventions for this latter term as in (6.3.5) in the following way. We can define $C_{TT\mathcal{O}}^{\text{odd}}$ by the following OPE

$$T_{zz}(z,\bar{z},y=0)T_{zy}(0) \sim C_{TT\mathcal{O}}^{\text{odd}}\frac{\bar{z}}{4|z|}\mathcal{O}(0) \ , \tag{6.4.8}$$

where the three spatial coordinates are $(z,\bar{z},y)$.

Using this normalization, the energy one-point function is given in terms of a three-by-three matrix as

$$\langle\Psi|\mathcal{E}(n)|\Psi\rangle = \frac{q}{2\pi}v^\dagger \begin{pmatrix} T_0 & T_{\text{odd}} & \frac{C_{TTO}^{\text{even}}}{\sqrt{C_T C_\mathcal{O}}}h_{3d}^{\text{even}}(\Delta) \\ T_{\text{odd}} & T_1 & \frac{C_{TTO}^{\text{odd}}}{\sqrt{C_T C_\mathcal{O}}}h_{3d}^{\text{odd}}(\Delta) \\ \frac{C_{TTO}^{\text{even}\,*}}{\sqrt{C_T C_\mathcal{O}}}h_{3d}^{\text{even}}(\Delta) & \frac{C_{TTO}^{\text{odd}\,*}}{\sqrt{C_T C_\mathcal{O}}}h_{3d}^{\text{odd}}(\Delta) & 1 \end{pmatrix} v \ , \tag{6.4.9}$$

where the functions $h_{3d}^{\text{even}}(\Delta)$ and $h_{3d}^{\text{odd}}(\Delta)$ can be obtained as

$$h_{3d}^{\text{odd}}(\Delta) = \frac{12\sqrt{6}\pi^2\sqrt{\Gamma(2\Delta-1)}}{\Gamma(\frac{\Delta+1}{2})\Gamma(\Delta+3)}\frac{1}{\Gamma(\frac{7-\Delta}{2})}\ , \tag{6.4.10}$$

$$h_{3d}^{\text{even}}(\Delta) = \frac{12\sqrt{6}\pi^2\sqrt{\Gamma(2\Delta-1)}}{\Gamma(2+\frac{\Delta}{2})\Gamma(\Delta+3)}\frac{1}{\Gamma(3-\frac{\Delta}{2})}\ . \tag{6.4.11}$$

Demanding positive definiteness of the energy matrix gives several types of constraints which involve the scalar OPE coefficients. Two of these bounds are easy to generalize to an arbitrary number of scalar operators

$$\sum_i \frac{|C_{TT\mathcal{O}_i}^{\text{even}}|^2}{C_{\mathcal{O}_i}} f_{\text{even}}(\Delta_i) \leq N_B\ , \qquad \sum_i \frac{|C_{TT\mathcal{O}_i}^{\text{odd}}|^2}{C_{\mathcal{O}_i}} f_{\text{odd}}(\Delta_i) \leq N_F\ , \tag{6.4.12}$$

where we defined $f_{\text{odd/even}} = |h_{3d}^{\text{odd/even}}|^2/3$. We can consider the positivity of the determinant of the 3×3 matrix. This gives an independent bound which together with the bound on $\langle TTT\rangle$ is sufficient for the positivity of the energy one-point function

$$N_B\frac{|C_{TT\mathcal{O}_i}^{\text{even}}|^2 f_{\text{even}}(\Delta_i)}{C_T C_{\mathcal{O}_i}} + N_F\frac{|C_{TT\mathcal{O}_i}^{\text{odd}}|^2 f_{\text{odd}}(\Delta_i)}{C_T C_{\mathcal{O}_i}} - 2N_{\text{odd}}\frac{\text{Re}[C_{TT\mathcal{O}_i}^{\text{even}}\sqrt{f_{\text{even}}(\Delta_i)}C_{TT\mathcal{O}_i}^{\text{odd}}\sqrt{f_{\text{odd}}(\Delta_i)}]}{C_T C_{\mathcal{O}_i}} \leq N_B N_F - N_{\text{odd}}^2\ . \tag{6.4.13}$$

This bound can also be generalized to include an arbitrary number of scalar operators. However, as opposed to the situation in section 6.3, the bounds involving different number of operators are independent. Their expressions in this case become more cumbersome and we will omit them here.

The (6.4.10) (6.4.11) have similar properties as the one appearing for the $d \geq 4$ bound. Namely they diverge at the unitarity bound $\Delta = 1/2$ and have zeros at $6+2n$ (even) and $7+2n$ (odd) for integer n. The zeros in the even case were explained by the existence of operators with two stress tensors in theories that are

dual to weakly coupled gravity, see the last point in section 6.3.1. The odd ones have the same explanation, except that now the scalar operators have the structure $\epsilon^{ABC}T_{AD}\partial^{2n}\partial_C T_{BD}$.

6.4.1 Chern-Simons Matter Theories

In this section we apply the bounds derived to large N Chern Simons theories at level k coupled to fundamental matter. For definiteness we will consider fundamental fermions. We will denote the 't Hooft coupling by $\theta = \pi N/2k$. The elements of the energy matrix involving the stress tensor were computed in [167] using the explicit large N expressions for the stress tensor three-point function [179]. The result is

$$T_1 = 2\cos^2\theta \ , \quad T_0 = 2\sin^2\theta \ , \quad T_{\rm odd} = 2\sin\theta\cos\theta \ . \tag{6.4.14}$$

Using the conventions in, for example, [180] we can compute the off-diagonal elements involving stress-tensor mixed with a scalar operator. In the fermionic theory we consider the scalar denoted by $\mathcal{O} \sim \psi\bar{\psi}$ has dimension $\Delta = 2$. The final result for the energy matrix is

$$\langle\Psi|\mathcal{E}(n)|\Psi\rangle = \frac{q}{2\pi}v^\dagger \begin{pmatrix} 2\cos^2\theta & 2\sin\theta\cos\theta & \sqrt{2}\cos\theta \\ 2\sin\theta\cos\theta & 2\sin^2\theta & \sqrt{2}\sin\theta \\ \sqrt{2}\cos\theta & \sqrt{2}\sin\theta & 1 \end{pmatrix} v \ . \tag{6.4.15}$$

As a function of the 't Hooft coupling, this matrix has the property that all the minors have vanishing determinant. This implies saturation for all types of superposition of states. For the case of the stress tensor this was noted in [167], but we find that this is a more general feature for states where we also act with $\mathcal{O}$.

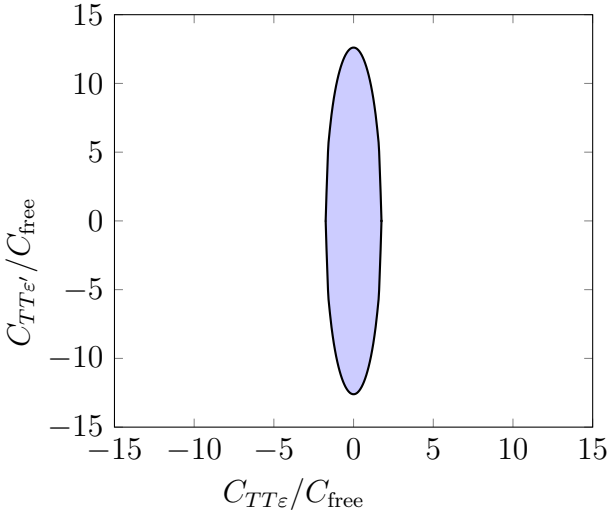

Figure 6.3: 3d Ising model allowed region for $C_{TT\varepsilon}$ and $C_{TT\varepsilon'}$.

Even though we do not have a concrete physical picture explaining this, we expect a picture along the lines of section 6.3.2, where the interaction with the Chern-Simons gauge field has the effect of replacing free bosons or fermions by "free anyons".

This discussion can also be applied to the case of CS coupled to fundamental bosons. From [179] we know that the energy matrix, given in terms of CFT three-point functions, can be obtained from the fermionic theory by the replacement $\theta \to \theta + \frac{\pi}{2}$ when we consider the operator $\mathcal{O} \sim \phi^2$ of dimension $\Delta = 1$. More generally we can consider the answer (6.4.15) as giving the energy matrix of a large N theory with a slightly broken higher spin symmetry parametrized by θ.

6.4.2 3d Ising Model

As another example, we can apply our bounds to obtain predictions for three-point coefficients for the $3d$ Ising model. First let us parameterize the three-point coefficients of the energy-momentum tensor. Since this theory is parity preserving the coefficient N_{odd} in (6.4.1) is necessarily zero. The remaining two structures in $\langle TTT \rangle$ have recently been computed numerically using the conformal bootstrap in [168,181].

Explicitly[9]

$$N_B \approx .9334 \ , \qquad N_F \approx .0131 \ . \tag{6.4.16}$$

The Ising model has a $\mathbb{Z}_2$ global symmetry under which T is even. Therefore only $\mathbb{Z}_2$ even scalars participate in the bound. The lightest $\mathbb{Z}_2$ even and parity even scalar is the operator ε whose dimension is known

$$\Delta_\varepsilon \approx 1.4127 \ . \tag{6.4.17}$$

Therefore, in a normalization where the two-point function coefficient of ε is one, we can evaluate (6.4.12) and find the bound

$$|C_{TT\varepsilon}| \leq .0088 = (1.751)\, C_{\text{free}} \ , \tag{6.4.18}$$

where in the last equation we normalized the answer by the expression (6.3.15) for the value of the OPE coefficient in the free theory $C_{\text{free}} = |C_{TT:\phi^2:}|/\sqrt{C_{:\phi^2:}}$. Note that although $:\phi^2:$ saturates the bound in the free field theory, the dimension of ε is larger than that of $:\phi^2:$ and hence the OPE coefficient $C_{TT\varepsilon}$ may be larger than $C_{TT:\phi^2:}$.

We can obtain a stronger bound by including the operator ε' of dimension $\Delta_{\varepsilon'} \approx 3.8303$ in the sum of (6.4.12). Using the correct values for $f_{\text{even}}(\Delta)$ for these dimensions and normalizing by the $TT:\phi^2:$ OPE we obtain the constraint

$$0.3267|C_{TT\varepsilon}|^2 + 0.0063|C_{TT\varepsilon'}|^2 \leq C_{\text{free}}^2 \ . \tag{6.4.19}$$

[9] In making these estimates we use a value of $\theta \approx .014$. This is the central value of the calculation of [168] based on expectations for the parity odd scalar gap.

Since the operators ε and ε' are hermitian their OPE coefficients are real and the bound above defines the allowed region of OPE coefficients as the interior of an ellipse shown in Figure 6.3.

6.5 Bounds on TTJ in $d = 4$

As a final example, we consider states created by a linear combination of the energy-momentum tensor and a conserved vector current J in $d = 4$ spacetime dimensions. In this case the three-point function $\langle TTJ\rangle$ is controlled by a single OPE coefficient C_{TTJ} and is parity violating. This three-point function is presented in detail in Appendix B of [56].

One reason why this OPE coefficient is interesting is that it is equivalent to a non-trivial mixed anomaly between the flavor symmetry generated by J and the Lorentz symmetry generated by T [182]. In the presence of a background metric g, the current J is not conserved but instead obeys [183–185]

$$\langle \nabla^\mu J_\mu \rangle[g] = \frac{C_{TTJ}}{768\pi^2} \epsilon^{\mu\nu\rho\sigma} R_{\mu\nu\delta\gamma} R_{\rho\sigma}{}^{\delta\gamma} \ , \tag{6.5.1}$$

where $R_{\mu\nu\rho\sigma}$ is the Reimann tensor.

In the above, our normalization is such that the coefficient C_{TTJ} may be expressed as the net chirality of the charges of elementary Weyl fermions:

$$C_{TTJ} = \sum_{\text{Left Weyl } i} q_i - \sum_{\text{Right Weyl } j} q_j \ . \tag{6.5.2}$$

In particular, for the theory of a single Weyl fermion C_{TTJ} is one. In an abstract CFT without a Lagrangian presentation our normalization of the OPE coefficient is defined as follows. Fix complex coordinates (z, w). Then the OPE of operators restricted to

the $w = 0$ plane is

$$T_{ww}(z)T_{\bar{w}\bar{w}}(0) \sim \frac{C_{TTJ}}{4\pi^6|z|^6}\left(zJ^{\bar{z}} - \bar{z}J^{z}\right) \ . \tag{6.5.3}$$

We will also need the three-point function $\langle TJJ\rangle$. This correlator is controlled by two independent coefficients:

$$\langle TJJ\rangle = Q_{CB}^2\langle TJJ\rangle_{CB} + Q_{WF}^2\langle TJJ\rangle_{WF} \ . \tag{6.5.4}$$

Here the structures CB and WF are those found for the $U(1)$ current in a theory of free complex bosons (CB) or free Weyl fermions (WF). In a free field theory, these are expressed in terms of the charges of elementary fields as (see [174])

$$Q_{CB}^2 = \sum_{\text{complex scalars } i} q_i^2 \ , \qquad Q_{WF}^2 = \sum_{\text{Weyl fermions } i} q_i^2 \ . \tag{6.5.5}$$

In general, a single linear combination of these OPE coefficients is fixed by the Ward identity. We have

$$\langle JJ\rangle \propto C_J \equiv \frac{1}{3}\left(Q_{CB}^2 + 2Q_{WF}^2\right) \ . \tag{6.5.6}$$

The two-point function coefficient C_J can also be interpreted as a conformal anomaly. Indeed, in the presence of a non-trivial background gauge field that couples to J, the energy-momentum tensor acquires an anomalous trace. In our conventions this is

$$\langle T^\mu_\mu\rangle[A] = \frac{C_J}{4}F^{\alpha\beta}F_{\alpha\beta} \ . \tag{6.5.7}$$

We can bound the anomaly coefficient C_{TTJ} using the same methods described in earlier sections for scalar operators. We enforce positivity of the average null energy operator $\mathcal{E}$ in the state $|\Psi\rangle$ created by a linear combination of T and J

$$|\Psi\rangle = |T(q,\lambda_T)\rangle + |J(q,\lambda_J)\rangle. \tag{6.5.8}$$

The expectation values $\langle \mathcal{E} \rangle_{\lambda_T \cdot T}$ and $\langle \mathcal{E} \rangle_{\lambda_J \cdot J}$ have been computed in [160]. The matrix of energy expectation values in the states $|\Psi\rangle$ may again be decomposed in terms of the $SO(2)$ rotation symmetry about the vector n. The current operator J contributes states of charge $-1, 0, 1$. As in the review of section 6.2.2 we may express the null energy expectation value as $(qJ_i/4\pi)$ where i is the $SO(2)$ charge. One then finds

$$J_{\pm 1} = \frac{Q_{WF}^2}{C_J} \ . \tag{6.5.9}$$

By repeating the collider calculation we find that the new off-diagonal matrix element is given by

$$\langle T(q, \lambda_T) | \mathcal{E}(n) | J(q, \lambda_J) \rangle = \frac{q}{4\pi} \left(\sqrt{\frac{5}{\pi^4}} \frac{C_{TTJ}}{\sqrt{C_T C_J}} \varepsilon_{ijk} \lambda^*_{T,im} \lambda_{J,k} n^m n^j \right) \ . \tag{6.5.10}$$

Note that this structure is parity odd as expected. There are other allowed parity odd expressions in terms of λ_{ij} and n^i, but they do not arise in the null-energy matrix element. An important feature of (6.5.10) is that only those states of $SO(2)$ charge ± 1 can mix with the energy-momentum tensor. In particular, this means that bound will only involve the coefficient T_1 defined in (6.2.10).

Explicitly choosing appropriate polarization tensors we then find that positivity of the null energy matrix $\mathcal{E}$ leads to a single constraint on these OPE coefficients:

$$C_{TTJ}^2 \leq Q_{WF}^2 N_{WF} \ , \tag{6.5.11}$$

where $N_{WF} = N_F/2$ counts the effective number of Weyl Fermions in the $\langle TTT \rangle$ correlation function. This bound is saturated in the free field theory of Weyl fermions. This can be understood using the interference argument described in section 6.3.2.

6.5.1 Supersymmetry and the R-Current

As in our analysis of scalar operators, we can generalize these results to states created by multiple currents. This is particularly interesting in the case of supersymmetric theories.

In supersymmetric theories, there is always a current J_R contained in the same supermultiplet as T. In particular, since it resides in a different multiplet it can be distinguished from an ordinary flavor current J_F. We would like to improve our bound on the trace anomaly of J_F to account for the fact that the R-current J_R always exists. In order to do this we consider the state created by

$$|\Psi\rangle = v_1|T(q,\lambda_T)\rangle + v_2|J_R(q,\lambda_J)\rangle + v_3|J_F(q,\lambda_J)\rangle \ . \tag{6.5.12}$$

The new ingredient appearing in the calculation of the energy matrix corresponding to this state involves the three-point function $\langle TJ_RJ_F\rangle$. Using superconformal invariance we can fix this correlator completely. Since the details are not very illuminating we will outline the procedure. The number of parity even structures, two of them, coincides with the ones appearing in $\langle TJJ\rangle$, namely relaxing permutation symmetry does not add new structures [176]. Moreover, using supersymmetric Ward identities [186] one can check that no parity odd structure is allowed for $\langle TJ_RJ_F\rangle$.[10] Out of the two OPE coefficients characterizing $\langle TJ_RJ_F\rangle$, a linear combination of them is related to the two-point function $\langle J_RJ_F\rangle$, which vanishes due to superconformal invariance. This leaves $\langle TJ_RJ_F\rangle$ fixed by a single OPE coefficient. Finally, since J_R lies in the same multiplet as the stress tensor we can relate this number to C_{TTF}, the mixed anomaly generated by the flavor current.

Combining the results outlined in the previous paragraph, and the fact that there is no new structure involved in the collider calculation, it is straightforward to obtain

[10] This is not true for a three-point function of a stress tensor and two different conserved currents $\langle TJ_1J_2\rangle$ in a generic theory.

the off-diagonal matrix element

$$\langle J_R(q,\lambda_J)|\mathcal{E}|J_F(q,\lambda_J)\rangle = \frac{q}{4\pi}\left(\sqrt{\frac{20}{3\pi^4}}\frac{C_{TTF}}{\sqrt{C_T C_F}}\right), \tag{6.5.13}$$

where we chose $n = (1,0,0)$ and $\lambda_J = (0,1,i)$ for definiteness.

We can express parameters related to the R-current in terms of a and $c = C_T\pi^4/40$. The two-point function is related to C_T by a supersymmetry Ward identity as $C_R = \frac{16}{3}c$. Its mixed anomaly is also fixed by supersymmetry to $C_{TTR} = 16(c-a)$. Finally the energy one-point function is given by $J^R_{\pm 1} = \frac{a}{c}$ [160, 166]. Supersymmetry also fixes this parameter for flavor currents as $J^F_{\pm 1} = 1$. Taking these facts into account allows us to write down the energy matrix as a function only of a, c, C_{TTF} and C_F. We obtain

$$\langle\Psi|\mathcal{E}|\Psi\rangle = \frac{q}{4\pi}v^\dagger\begin{pmatrix} \frac{2c-a}{c} & \sqrt{3}\frac{c-a}{c} & \frac{1}{\sqrt{2c}}\frac{C_{TTF}}{\sqrt{C_F}} \\ \sqrt{3}\frac{c-a}{c} & \frac{a}{c} & \frac{1}{\sqrt{6c}}\frac{C_{TTF}}{\sqrt{C_F}} \\ \frac{1}{\sqrt{2c}}\frac{C_{TTF}}{\sqrt{C_F}} & \frac{1}{\sqrt{6c}}\frac{C_{TTF}}{\sqrt{C_F}} & 1 \end{pmatrix} v\ , \tag{6.5.14}$$

where for definiteness we have chosen $\lambda_J = (0,1,i)$ and a tensor polarization with the same $SO(2)$ spin.

Enforcing the positivity of this matrix yields several constraints. The leading two-by-two minor involving states $|T(q,\lambda_T)\rangle + |J_R(q,\lambda_J)\rangle$ gives the bound

$$\frac{1}{2} \le \frac{a}{c} \le \frac{3}{2}\ , \tag{6.5.15}$$

which coincides with those derived in [160]. This bound is saturated by a free chiral multiplet, $\frac{a}{c} = \frac{1}{2}$, or a free vector multiplet, $\frac{a}{c} = \frac{3}{2}$.

To constrain the gravitational anomaly coefficient we evaluate the determinant of the full three-by-three matrix (6.5.14). This gives the following bound on the mixed

anomaly for a flavor current

$$\left(\frac{a}{c}-\frac{1}{2}\right)\left(36c-24a-\frac{C_{TTF}^2}{C_F}\right)\geq 0\ . \tag{6.5.16}$$

For a free chiral multiplet the bound is automatically saturated, since the first term in the left hand side vanishes independently of C_{TTF}. Therefore we will assume that $\frac{a}{c}>\frac{1}{2}$. Then we obtain the following bound

$$\frac{C_{TTF}^2}{12C_F}\leq 3c-2a\ , \tag{6.5.17}$$

which is stronger than the one derived in the previous section, without the use of supersymmetry. Note also that this is consistent with the free vector multiplet. In that case the right-hand-side vanishes, but there are also no flavor currents.

To conclude this section, we can mention some contexts where such bound on the mixed anomaly is relevant. First of all, when we consider holographic CFT this anomaly is related to a 5d Chern-Simons term of the form $\int A\wedge R\wedge R$, where A is the gauge field dual to the current J (we will see in the next section how our bounds translate to bounds on the gravity couplings for the case of $TT\mathcal{O}$).

Finally, in the context of hydrodynamics and transport, quantum anomalies induce a special type of transport coefficients, see [187] and, in particular, for the mixed anomaly [188–190]. The coefficient bounded in this section C_{TTJ}, is related to the mixed anomaly recently observed experimentally in Weyl semimetals [191]. In the linear response regime, the mixed anomaly produces an energy current $\vec{j}$ given by [188–190]

$$\vec{j}=24C_{TTJ}T^2\vec{B}\ , \tag{6.5.18}$$

where we denote the temperature by T and the system is placed in a fixed magnetic field $\vec{B}$. This allows us to translate our results into concrete bounds for transport coefficients.

6.6 Bounds on Coefficients of the AdS Effective Action

If the d dimensional boundary theory has an AdS_{d+1} dual, then we would like to translate the bounds on $C_{TT\mathcal{O}}$ to bounds on the coefficients of the bulk effective action. We are imagining that the theory has a large N expansion. Then, to leading order, the bulk is given by a collection of free fields propagating on the AdS metric. The simplest interactions correspond to bulk three-point interactions. These lead to three-point functions in the boundary theory. For the case of gravitons we have a three-point interaction coming from the Einstein Lagrangian, but it is also necessary to include higher derivative terms, of the form W^2 and W^3, in order to get the most general structures for the tensor three-point function. It is possible to match the coefficients of the new structures to the coefficients of these higher derivative terms in the Lagrangian [160, 162].

Here we consider the same problem for the case of the $\langle TT\mathcal{O}\rangle$ correlator. The first observation is that in Einstein gravity this correlator is zero, since the action of any field, expanded around the minimum of its potential has an action without a linear term in the scalar field. Notice that this also implies that a massive scalar field cannot not decay into two gravitons. However, we can write the higher derivative term

$$S = M_{pl}^{d-1}\alpha \int d^{d+1}x\sqrt{g}\chi W^2 \tag{6.6.1}$$

in the action, where we normalized the χ field to be dimensionless.[11] This term enables the field χ to decay into two gravitons. In flat space there is only one structure for the on shell three-point function between a scalar and two gravitons, except in four dimensions where there is also a parity odd one, as we discuss later. Therefore the vertex (6.6.1) represents the general interaction that we can have in the theory. There can be other ways to write it which give the same three-point function as (6.6.1). It is possible to check that (6.6.1) gives rise to a $\langle TT\mathcal{O}\rangle$ three-point function with the coefficient

$$\frac{C_{TT\mathcal{O}}\sqrt{f(\Delta)}}{\sqrt{C_T}} = \frac{8\sqrt{2d}(d-1)\pi^{d/2}}{\sqrt{d+1}\Gamma(d/2)}\frac{\alpha}{R_{AdS}^2} \ . \tag{6.6.2}$$

At first sight, it seems surprising that the function $f(\Delta)$ appearing here is the same as the one that appears in the bound (6.3.10). This means that the Δ dependence disappears when we express the bound in terms of α. This is easy to understand when we derive (6.6.2) as follows.

First we notice that integrating the stress tensor along a null line, as in the definition of the energy measurement $\mathcal{E} = \int dx^- T_{--}(x^-, x^+ = 0, \vec{y} = 0)$, we produce a shock wave in the bulk that is localized at $x^+ = 0$. We can then imagine scattering a superposition of χ and a graviton through this shock wave. This leads to a time delay that is given by a matrix mixing the graviton and the scalar. An important point is that the propagation through the shock wave is given by integrating the wave equation in a small interval before and after $x^+ = 0$. Only the shock wave contributes to this short integral over x^+, but the scalar mass term does not contribute. Therefore the time delay matrix is independent of the mass of the scalar. We can determine the precise coefficient in (6.6.2) by doing this explicit computation for Einstein gravity plus (6.6.1). We then get a bound on α by requiring that the time delay is positive.

[11] Here M_{pl} is the reduced Planck mass in $d+1$ dimensions, defined so that the Einstein term is $S = \frac{M_{pl}^{d-1}}{2}\int d^{d+1}x\sqrt{g}R$. Similarly, the action of the scalar field is $S = \frac{M_{pl}^{d-1}}{2}\int[(\nabla\chi)^2 - m^2\chi^2]$.

Comparing this to the bound (6.3.10) we fix the coefficient to the one in (6.6.2). We explain this in more detail in Appendix 6.8.

This same shock wave method enables one to set even stricter bounds on α if one assumes that there is a gap to the higher spin particles,[12] as was discussed in [159] for the case of the graviton higher derivative interactions. A similar analysis can be done for the 5d Chern-Simons term coupling dual to the mixed anomaly [192].

In string theory, we expect that α is the order of α', the inverse string tension. If gravity is a good approximation, $\alpha' \ll R^2$, then we find that the bound on (6.6.2) is far from being saturated. The bound is saturated only as the string length becomes of the order of the radius of AdS. In particular, this implies that the bound is satisfied, and far from being saturated, for the Konishi operator of $\mathcal{N} = 4$ super Yang Mills at strong coupling. This operator is the lightest non-protected single trace operator which has a dimension growing like $\Delta \propto \lambda^{1/4}$ at strong coupling, $\lambda \gg 1$.

In the four dimensional case, we can also have a parity odd correlator with a corresponding coupling. In flat space this is related to the fact that the three-point functions with $++$ or $--$ graviton helicities are Lorentz invariant by themselves. (The $-+$ graviton helicities are forbidden by angular momentum conservation). We can then write the action as

$$S = M_{pl}^2 \int d^4x\sqrt{g}\left[\frac{1}{2}(R-2\Lambda) + \frac{1}{2}[(\nabla\chi)^2 - m^2\chi^2] + \int \alpha_e \chi W^2 + \alpha_o \chi W W^*\right] \quad (6.6.3)$$

where as above we have defined χ to be dimensionless.[13] In this normalization α_i has dimensions of length squared. They can be related to the coefficients of the three-point function as

$$\frac{C_{TT\mathcal{O}}^{\text{even}} h_{\text{even}}(\Delta)}{\sqrt{C_T}} = \frac{24}{\sqrt{2}}\frac{\alpha_e}{R_{AdS_4}^2}\ , \qquad \frac{C_{TT\mathcal{O}}^{\text{odd}} h_{\text{odd}}(\Delta)}{\sqrt{C_T}} = \frac{24}{\sqrt{2}}\frac{\alpha_o}{R_{AdS_4}^2}\ . \quad (6.6.4)$$

[12] We thank E. Perlmutter and D. Meltzer for discussions on this issue.

[13] We also define $(W^*)_{\mu\nu\rho\sigma} = \frac{1}{2}\epsilon_{\mu\nu\delta\gamma}W^{\delta\gamma}{}_{\rho\sigma}$.

The bounds in this case then read

$$\frac{\sqrt{\alpha_e^2+\alpha_o^2}}{R_{AdS_4}^2} \leq \frac{1}{12\sqrt{2}} \,, \tag{6.6.5}$$

in the case that there are no purely gravitational corrections to Einstein gravity. Of course, if there are three-point functions that lead to corrections to Einstein gravity, then the bound is corrected to those given in section 6.4.

6.7 Constraints for de-Sitter and Inflation

The physics of inflation might be our very best window into very high energy physics. The standard inflationary theory starts with a scalar field coupled to the Einstein action and includes all two (or less) derivative interactions. The universe undergoes a period of expansion that is governed by a nearly de-Sitter solution, characterized by a Hubble scale H that is nearly constant. The effective coupling of the gravitational sector is of order H/M_{pl} which is very small, less than 10^{-5}. However, it is possible that there are corrections to the two derivative action due to the presence of a light string scale. The value of the string tension could be fairly low $H^2 \lesssim T$. When the string tension becomes comparable to the Hubble scale, we expect significant corrections to the two derivative action. We do not have an explicit scenario where this happens. However, a similar situation happens in AdS space when we consider a gravity dual of a not so strongly coupled large N theory. Therefore it is natural to question whether something similar could happen in inflation and we can look for signatures of such a low string scale. It is important to find signatures that are as model independent as possible. Specially nice signatures are those that have a non-vanishing contribution in the de-Sitter approximation. These are not strongly suppressed by slow roll factors. In addition, their form is strongly constrained by the de-Sitter isometries. An example of such contributions are the three-point functions

of gravity fluctuations, where the higher derivative corrections were discussed in [193]. Another interesting case are the couplings of the form $f_e(\chi)W^2$ or $f_0(\chi)WW^*$. These two couplings are particularly interesting because their effects are visible at the two-point function level.

Let us discuss first the parity odd coupling, which leads to chiral gravity waves [194, 195]. Namely, we have different gravity wave two-point functions, hh_L, hh_R, for the left and right handed circularly polarization. We can define the asymmetry A as

$$A \equiv \frac{hh^L - hh^R}{hh^L + hh^R} = 4\pi \frac{\dot{f}_o(\chi)}{H} H^2 = \pm 4\pi \sqrt{2\epsilon} \left(\frac{\partial f}{\partial \chi} \right) H^2 \ , \qquad \chi = \frac{\phi}{M_{pl}} \ , \quad (6.7.1)$$

where χ is defined to be dimensionless and ϕ is the inflaton with canonical normalization. (The $\pm$ comes from going from $\dot{\chi}$ to $\sqrt{\epsilon}$, since the derivative of the scalar can have either sign). If we were in AdS_4 we would have a sharp bound on the coefficients via the condition (6.6.5), after we identify $\alpha_o = \frac{\partial f}{\partial \chi}$. It is reasonable to think that in the de-Sitter case too, there will be trouble is the bound is violated. Of course, we know that even near-saturation of the bound implies that the field theory approximation is breaking down.

In the de-Sitter case we do not have a sharp derivation of a bound from boundary theory reasoning. We do not have an analog of the null energy condition, discussed in section 6.4, for the boundary theory, since the boundary theory is purely spacelike. It would be nice to have a sharp derivation of a de-Sitter version of the bound. In de-Sitter, we can talk of a "quasi-bound", which we get by simply applying the same bound on the coefficients of the action that we had in anti-de-Sitter. This quasi-bound should be viewed simply as an educated guess, including numerical coefficients, for the validity of bulk effective theory. A near saturation of these quasi-bounds is a strong indication of a light string scale which could also have other manifestations such as indirect evidence of higher spin massive particles, etc [196]. In summary, in de-Sitter

also we have a quasi-bound on the coefficients similar to (6.6.5), with $1/R_{AdS} \to H$

$$\sqrt{\left(\frac{\partial f_e}{\partial \chi}\right)^2 + \left(\frac{\partial f_o}{\partial \chi}\right)^2} = \sqrt{\alpha_e^2 + \alpha_o^2} \leq \frac{H^2}{12\sqrt{2}} \ . \tag{6.7.2}$$

This bound, then implies a quasi-bound on the asymmetry (6.7.1) of the form

$$|A| \leq \frac{4\pi}{12}\sqrt{\epsilon} \ . \tag{6.7.3}$$

The allowed values by this quasi-bound seem to be smaller than the smallest possible measurable value from the CMB B-modes as analyzed in [197]. Conversely, this means that if chiral gravity waves through E-B mode correlators are measured, then we would need a higher derivative coupling with a coefficient so large that it violates (6.7.2).

Let us turn now to a discussion of the parity even coupling. This coupling gives rise to a violation of the consistency condition for the two-point function [198], even in the case that the speed of sound is close to one,

$$-8\frac{n_t}{r} = 1 + 8H^2\frac{H d_t f_e}{(d_t\chi)^2} = 1 \pm 8H^2\frac{\alpha_e}{\sqrt{2\epsilon}} \ , \tag{6.7.4}$$

where we assumed that the speed of sound for the scalar is close to one. Here n_t is the tensor spectral index and r the tensor to scalar ratio conventionally defined. Then the bound we had in (6.7.2) translates into the following constraint on the violation of the consistency condition

$$\left|-8\frac{n_t}{r} - 1\right| \leq \frac{1}{3\sqrt{\epsilon}} \ . \tag{6.7.5}$$

Finally we will comment on Scalar-Tensor-Tensor Three-Point Functions. The ϕW^2 higher derivative coupling between the scalar and the graviton also give rise

to new contributions to the scalar-tensor-tensor three-point function. This is a contribution, that is non-vanishing in the de-Sitter limit. More precisely, if we can approximate $\partial_\chi f_e(\chi(t))$ by a constant, then we get a contribution even in de-Sitter space. The standard Einstein gravity contribution, [199], is suppressed by a slow roll factor $\sqrt{\epsilon}$, if we assume that $\partial_\chi f$ is of order one. Of course, our bound constrains the size of this three-point function because it is constraining the size of the coefficient $\alpha_e \sim \partial_\chi f_e(\chi(t))$.

The three-point function for the parity odd coupling $f_o(\chi)WW^*$ was computed in [200], where it was found to be proportional to $\partial_\chi^2 f$. One might have naively expected a de-Sitter invariant contribution proportional to $\alpha_0 = \partial_\chi f_0$, when we approximate this by a constant. The explicit computation by [200] shows that there is no such contribution. This seems surprising at first sight because this parity odd coupling does indeed give a non-vanishing contribution to the three-point function in the AdS_4 case. The reason it vanishes in de-Sitter is that it gives a contribution to the de-Sitter wavefunction that is a pure phase, which disappears when we take the absolute value squared of the wavefunction. The same happens with the W^2W^* parity violating graviton three-point coupling [201]. The correlator proportional to $\partial_\chi^2 f$ found in [200] has an extra factor of $\dot{\phi}$ and is not expected to be de-Sitter invariant (though we did not check this explicitly).

It should be noted that the correction to the two-point function consistency condition (6.7.4) has the right form so that the consistency condition involving the soft limit of the three-point function [199, 202] is obeyed, though we have not explicitly checked the precise numerical coefficients. A similar remark applies in the parity odd case; the correction to the two-point function (6.7.1) is such that the soft limit of the three-point function in [200] obeys the consistency condition.

6.8 Appendix: Computing the Bound in the Gravity Theory

In this appendix we relate the OPE coefficient $C_{TT\mathcal{O}}$ to a coefficient, α, in the AdS_D effective action

$$S = \frac{M_{pl}^{D-2}}{2}\left[\int \sqrt{g}(R-2\Lambda) + (\nabla\chi)^2 - m^2\chi^2 + 2\alpha\chi W^2\right], \tag{6.8.1}$$

where D is the dimension of AdS_D and $\Lambda = -\frac{(D-1)(D-2)}{2R_{AdS}^2}$. χ is defined to be dimensionless and α has dimensions of length squared.

In principle we can compute the relation between α and $C_{TT\mathcal{O}}$ by computing the three point function between a scalar and the graviton produced by this cubic term in the Lagrangian, using Witten diagrams. Instead, we will follow a different route. We will directly compute the energy correlator in gravity and derive a bound on α by demanding its positivity. We then relate α and $C_{TT\mathcal{O}}$ by demanding that this gravity bound, in terms of α, matches the bound we obtained in terms of $C_{TT\mathcal{O}}$ in the field theory analysis.

We will rely on [160, 162] where the energy correlators were computed in gravity. An important point is that the insertion of T_{--} corresponds to a shock wave localized in a null plane. Furthermore, an operator insertion at the origin with definite energy-momentum gives rise to an excitation that crosses this null plane at a localized point. For this reason the computation of the bound boils down to analyzing the propagation of an excitation through a suitable gravitational shock wave in flat space. The AdS_D space is only relevant for determining the transverse profile of the shock wave, as we will see below.

For these reasons we consider a shock wave of the form

$$ds^2 = ds^2_{\text{flat}} + (dx^+)^2\delta(x^+)h(y)\ , \qquad ds^2_{\text{flat}} = -dx^+dx^- + dy^2\ . \tag{6.8.2}$$

Adding gravitons we get

$$ds^2 = ds^2_{\rm flat} + (dx^+)^2\delta(x^+)h(y) + dx^\mu dx^\nu \zeta_\mu\zeta_\nu e^{ip.x}G(p) + \text{h.c.}, \tag{6.8.3}$$

with $\zeta^2 = 0$, $\zeta^\mu p_\mu = 0$. Note that the graviton polarization is $\zeta_{\mu\nu} = \zeta_\mu\zeta_\nu$, and is normalized to one $\zeta.\bar{\zeta} = 1$. We can think of $G(p)$ and $\bar{G}(p)$ as complex numbers, which in the quantum theory will be related to a and $a^\dagger$. Inserting (6.8.3) into (6.8.1) we can derive the quadratic and cubic interaction terms.

$$\begin{aligned} S &= \frac{M_{pl}^{D-2}}{2}\int dx^+dx^-d^{D-2}y\left\{\left[p_+p_- + \delta(x^+)p_-^2h\right]\left[G(p)\bar{G}(p) + 4p_-p_+\chi(p)\bar{\chi}(p)\right] + \right. \\ &\left. +8p_-^2\alpha\zeta^{ij}\partial_i\partial_j h\delta(x^+)G(p)\bar{\chi}(p) + c.c.\right\}\ , \end{aligned} \tag{6.8.4}$$

where we only wrote the terms relevant for our computation, ignoring transverse derivatives in the kinetic terms. Momentarily setting the scalar field to zero, we see that we have the following equation for the graviton as it crosses the shock wave

$$\Delta h_{\mu\nu} \equiv h_{\mu\nu}|_{x^+=0^+} - h_{\mu\nu}|_{x^+=0^-} = ip_-hh_{\mu\nu}\ . \tag{6.8.5}$$

Exponentiating this, $h_{\mu\nu}(x^+ = 0^+) = e^{ip_-h}h_{\mu\nu}(x^+ = 0^-)$, we see that the time delay is simply given by h. This is as expected from (6.8.2) since we can shift x^- by h and make the term involving h disappear if we ignore its y dependence. So far, we considered the computation in flat space. An insertion of the null energy integrated along a ray in the boundary theory gives rise to a shockwave in AdS_D which is localized on a null direction. Its dependence on the transverse directions is the following. The transverse space is an H_{D-2}. This is easy to see in embedding coordinates where AdS_D is $\tilde{W}^+\tilde{W}^- + W^\mu W_\nu = -1$ (setting $R_{AdS_D} = 1$). The null plane is $\tilde{W}^+ = 0$. It contains the null direction parametrized by $\tilde{W}^-$ as well as the transverse space $W^\mu W_\mu = -1$. The profile of the wave is proportional to $h \propto (W^0 - W^i n^i)^{2-D}$ [160, 162], with a

positive coefficient. Here $\vec{n}^i$ is a vector on the sphere at infinity in the boundary Minkowski space. For (6.8.4) we need the derivatives at $W^i = 0$, which are given by

$$h \to h \ , \qquad \partial_i \partial_j h = [(\text{constant})\delta_{ij} + (D-2)(D-1)n_i n_j] h \frac{1}{R^2_{AdS_D}} \ , \tag{6.8.6}$$

where the constant does not matter because the graviton is traceless. If we take a localized shockwave instead then the result is the same replacing $R^2_{\rm AdS} \to b$, with b being the shockwave impact parameter.

The relevant component of the graviton is the one with polarization along n^i. This has the expression

$$\zeta_{ij} = \sqrt{\frac{D-2}{D-3}} \left[n^i n^j - \frac{\delta_{ij}}{D-2} \right] \ . \tag{6.8.7}$$

The expression for the time delay acting on a superposition of a graviton and a scalar is now a matrix proportional to

$$\begin{pmatrix} 1 & \gamma \\ \gamma & 1 \end{pmatrix} \ , \quad \gamma \equiv 4(D-1)\sqrt{(D-3)(D-2)} \frac{\alpha}{R^2_{AdS_D}} \ , \tag{6.8.8}$$

where the matrix is acting on a two dimensional space where one direction is the scalar and the other is the graviton with polarization (6.8.7). The unitarity bound comes from the restriction that the eigenvalues are non-negative, or $|\gamma| \leq 1$, which is

$$\frac{|\alpha|}{R^2_{AdS_D}} \leq \frac{1}{4(D-1)\sqrt{(D-3)(D-2)}} = \frac{1}{4d\sqrt{(d-2)(d-1)}} \ , \tag{6.8.9}$$

where d is the dimension of the boundary. Comparing this with the bound obtained in (6.3.8), with the non-Einstein-gravity structures set to zero, we obtain (6.6.2). Of course, once we get the proportionality constant between α and $C_{TT\mathcal{O}}$ for the Einstein gravity case, the same constant holds also if we add the purely gravitational higher

derivative terms that generate the other tensor structures for $\langle TTT \rangle$. We could add them to this computation, but we expect to reproduce the bounds we got in the general field theory analysis.

In the special case of the four dimensional theory, we actually have two couplings (6.6.3). This leads to a new interaction term in (6.8.4) of the form

$$\alpha \zeta^{ij} \partial_i \partial_j h \to \alpha_e \zeta^{ij} \partial_i \partial_j h + \alpha_o \zeta^{il} \epsilon_{lj} \partial_i \partial_j h \ , \tag{6.8.10}$$

where now ϵ_{ij} is the two dimensional epsilon symbol. This means that the scalar can now mix with the other graviton polarization component besides (6.8.7). Namely, defining (6.8.7) as $\zeta_\oplus$, it can also mix with $\zeta^{ij}_\otimes \equiv \epsilon^{il} \zeta^{lj}_\oplus$. Now the time delay is a a three by three matrix

$$\begin{pmatrix} 1 & \gamma & \beta \\ \gamma & 1 & 0 \\ \beta & 0 & 1 \end{pmatrix} \ , \qquad \gamma \equiv 12\sqrt{2} \frac{\alpha_e}{R^2_{AdS_4}} \ , \qquad \beta \equiv 12\sqrt{2} \frac{\alpha_o}{R^2_{AdS_4}} \ , \tag{6.8.11}$$

where the rows and columns correspond to the scalar and the two graviton polarizations. Now the bound is (6.6.5). Comparing this to (6.4.13), after setting the non-Einstein-gravity structures to zero, we get the precise mapping to the $C_{TT\mathcal{O}}$ coefficients (6.6.4).

Chapter 7

Conclusions

In this thesis we have studied several aspects of quantum chaos and near horizon scattering in black holes, related by gauge/gravity duality.

A lot of progress has been done after the discovery of holographic quantum mechanical systems such as the SYK model. These systems are characterized as being described in the IR by a pseudo-Goldstone mode that controls the breaking of conformal symmetry. This mode is directly related to the gravitational mode of dilaton gravity in (nearly) AdS_2. This connection explains the thermodynamics and chaos of SYK at low temperatures.

One of the results in this thesis, explained in chapter 2, has been to solve the Schwarzian/JT-gravity theory by finding the exact correlators (both time and out-of-time ordered). On the QM side this is interesting since exact answers for OTOC in non-trivial theories (specially maximally chaotic) are generally non tractable. Moreover this gives a solution to the Jackiw-Teitelboim model for quantum gravity. Of course this is still an expansion around large extremal entropy and is not useful to decide questions sensitive to the fine grained details of the black hole spectrum like the information paradox, but its still some progress.

As a by-product of this in chapter 3 we found a non-perturbative generalization of the Dray-'t Hooft S-matrix describing scattering near the black hole horizon. This is an interesting situation to study as we have explained in the Introduction. Even in the semiclassical analysis there are more to shockwaves than the Lyapunov exponent. In the eikonal approximation one can compute OTOC beyond the $t > \beta$ limit. In higher dimensions this is technically complicated but in near AdS_2 one can use it as a toy model for the more realistic situations.

It would be interesting to understand the fine-grained details of the spectrum responsible for the unitarization of the black hole evaporation. One option is to do numerics on the SYK model but the most interesting outcome would be understnading general lessons that could be applied to higher dimensions.

Another important open question is to identify a (possibly) string theory construction from which to derive the dual of the SYK model. Some evidence points into the belief that this should be a theory of strings in 2D, and not a reduction from higher dimensions. This would also help clarify the resolution of the information paradox in this simplified setting.

Other interesting question in holography for which $NAdS_2/NCFT_1$ might be helpful is to understand in which sense entanglement between disconnected QM systems *creates* the space time region connecting them. This is related to the belief that gravity and spacetime are closely connected to quantum information.

In chapters 4 and 5 we have extended some lessons from SYK to two dimensions. We have argued that a natural candidate for the theory describing the breaking of conformal symmetry is the theory of coadjoint orbits of the Virasoro group. This theory also controls the chaos exponent and gives maximal chaos. We have also found ways to create 2D field theories which share several of the prominent features with SYK.

Finally another interesting connection is between shockwaves and the recently proved averaged null energy condition (ANEC). In chapter 6 we have studied aspects of this connection in the context of the conformal collider. This produced mostly interesting bounds on general CFTs. For holographic CFTs this puts severe constrains on the low energy effective action for string theory. This would be interesting to study further and moreover if it has some connection with black holes and quantum chaos.

Bibliography

[1] J. D. Bekenstein, "Black holes and the second law," *Lett. Nuovo Cim.* **4** (1972) 737–740.

[2] S. W. Hawking, "Particle Creation by Black Holes," *Commun. Math. Phys.* **43** (1975) 199–220. [,167(1975)].

[3] S. W. Hawking, "Breakdown of Predictability in Gravitational Collapse," *Phys. Rev.* **D14** (1976) 2460–2473.

[4] A. Strominger and C. Vafa, "Microscopic origin of the Bekenstein-Hawking entropy," *Phys. Lett.* **B379** (1996) 99–104, `arXiv:hep-th/9601029 [hep-th]`.

[5] J. M. Maldacena, "The Large N limit of superconformal field theories and supergravity," *Int. J. Theor. Phys.* **38** (1999) 1113–1133, `arXiv:hep-th/9711200 [hep-th]`. [Adv. Theor. Math. Phys.2,231(1998)].

[6] T. Dray and G. 't Hooft, "The Gravitational Shock Wave of a Massless Particle," *Nucl. Phys.* **B253** (1985) 173–188.

[7] G. 't Hooft, "The Scattering matrix approach for the quantum black hole: An Overview," *Int. J. Mod. Phys.* **A11** (1996) 4623–4688, `arXiv:gr-qc/9607022 [gr-qc]`.

[8] P. C. Aichelburg and R. U. Sexl, "On the gravitational field of a massless particle," *General Relativity and Gravitation* **2** no. 4, (Dec, 1971) 303–312.

[9] G. T. Horowitz and A. R. Steif, "Space-Time Singularities in String Theory," *Phys. Rev. Lett.* **64** (1990) 260.

[10] K. Schwarzschild, "On the Gravitational Field of a Mass Point According to Einstein's Theory," *Abh. Konigl. Preuss. Akad. Wissenschaften Jahre 1906,92, Berlin,1907* (1916) .

[11] T. Dray and G. 't Hooft, "The Effect of Spherical Shells of Matter on the Schwarzschild Black Hole," *Commun. Math. Phys.* **99** (1985) 613–625.

[12] T. Dray and G. 't Hooft, "The Gravitational Effect of Colliding Planar Shells of Matter," *Class. Quant. Grav.* **3** (1986) 825–840.

[13] G. 't Hooft, "The black hole interpretation of string theory," *Nucl. Phys.* **B335** (1990) 138–154.

[14] W. K. Wootters and W. H. Zurek, "A single quantum cannot be cloned," *Nature* **299** (1982) .

[15] Y. Kiem, H. L. Verlinde, and E. P. Verlinde, "Black hole horizons and complementarity," *Phys. Rev.* **D52** (1995) 7053–7065, arXiv:hep-th/9502074 [hep-th].

[16] G. 't Hooft, "Dimensional reduction in quantum gravity," *Conf. Proc.* **C930308** (1993) 284–296, arXiv:gr-qc/9310026 [gr-qc].

[17] L. Susskind, "The World as a hologram," *J. Math. Phys.* **36** (1995) 6377–6396, arXiv:hep-th/9409089 [hep-th].

[18] E. Witten, "Anti-de Sitter space and holography," *Adv. Theor. Math. Phys.* **2** (1998) 253–291, arXiv:hep-th/9802150 [hep-th].

[19] S. S. Gubser, I. R. Klebanov, and A. M. Polyakov, "Gauge theory correlators from noncritical string theory," *Phys. Lett.* **B428** (1998) 105–114, arXiv:hep-th/9802109 [hep-th].

[20] M. A. Vasiliev, "Higher spin gauge theories: Star product and AdS space," arXiv:hep-th/9910096 [hep-th].

[21] J. M. Maldacena, "Eternal black holes in anti-de Sitter," *JHEP* **04** (2003) 021, arXiv:hep-th/0106112 [hep-th].

[22] E. N. Lorenz, "Deterministic nonperiodic flow," *Journal of the Atmospheric Sciences* **20** no. 2, (1963) 130–141.

[23] A. Larkin and Y. Ovchinnikov, "Quasiclassical method in the theory of superconductivity," *JETP* **28** (1969) 1200.

[24] R. A. Jalabert and H. M. Pastawski, "Environment-independent decoherence rate in classically chaotic systems," *Phys. Rev. Lett.* **86** (Mar, 2001) 2490–2493. https://link.aps.org/doi/10.1103/PhysRevLett.86.2490.

[25] J. Maldacena, S. H. Shenker, and D. Stanford, "A bound on chaos," *JHEP* **08** (2016) 106, arXiv:1503.01409 [hep-th].

[26] S. H. Shenker and D. Stanford, "Black holes and the butterfly effect," *JHEP* **03** (2014) 067, arXiv:1306.0622 [hep-th].

[27] S. H. Shenker and D. Stanford, "Stringy effects in scrambling," *JHEP* **05** (2015) 132, arXiv:1412.6087 [hep-th].

[28] I. R. Klebanov and A. M. Polyakov, "AdS dual of the critical O(N) vector model," *Phys. Lett.* **B550** (2002) 213–219, arXiv:hep-th/0210114 [hep-th].

[29] G. J. Turiaci and A. Zhiboedov, "Veneziano Amplitude of Vasiliev Theory," arXiv:1802.04390 [hep-th].

[30] A. Kitaev, " Talk given at the Fundamental Physics Prize Symposium." https://www.youtube.com/watch?v=0Q9qN8j7EZI, 2014.

[31] A. Kitaev, "A simple model of quantum holography." http://online.kitp.ucsb.edu/online/entangled15/kitaev/, 2015.

[32] W. G. Unruh, "Experimental black hole evaporation," *Phys. Rev. Lett.* **46** (1981) 1351–1353.

[33] L. J. Garay, J. R. Anglin, J. I. Cirac, and P. Zoller, "Black holes in Bose-Einstein condensates," *Phys. Rev. Lett.* **85** (2000) 4643–4647, arXiv:gr-qc/0002015 [gr-qc].

[34] B. Horstmann, B. Reznik, S. Fagnocchi, and J. I. Cirac, "Hawking Radiation from an Acoustic Black Hole on an Ion Ring," *Phys. Rev. Lett.* **104** (2010) 250403, arXiv:0904.4801 [quant-ph].

[35] F. C. Lombardo and G. J. Turiaci, "Decoherence and Loss of Entanglement in Acoustic Black Holes," *Phys. Rev. Lett.* **108** (2012) 261301, arXiv:1206.1351 [quant-ph].

[36] F. C. Lombardo and G. J. Turiaci, "Dynamics of an Acoustic Black Hole as an Open Quantum System," *Phys. Rev.* **D87** no. 8, (2013) 084028, arXiv:1208.0198 [quant-ph].

[37] A. Georges, O. Parcollet, and S. Sachdev, "Quantum fluctuations of a nearly critical heisenberg spin glass," *Phys. Rev. B* **63** (Mar, 2001) 134406. https://link.aps.org/doi/10.1103/PhysRevB.63.134406.

[38] S. Sachdev and J. Ye, "Gapless spin fluid ground state in a random, quantum Heisenberg magnet," *Phys. Rev. Lett.* **70** (1993) 3339, arXiv:cond-mat/9212030 [cond-mat].

[39] O. Parcollet and A. Georges, "Transition from overscreening to underscreening in the multichannel kondo model: Exact solution at large N," *Phys. Rev. Lett.* **79** (Dec, 1997) 4665–4668. https://link.aps.org/doi/10.1103/PhysRevLett.79.4665.

[40] O. Parcollet, A. Georges, G. Kotliar, and A. Sengupta, "Overscreened multichannel SU(N) Kondo model: Large-N solution and conformal field theory," *Phys. Rev.* **B58** no. 7, (1998) 3794, arXiv:cond-mat/9711192 [cond-mat.str-el].

[41] J. Polchinski and V. Rosenhaus, "The Spectrum in the Sachdev-Ye-Kitaev Model," *JHEP* **04** (2016) 001, arXiv:1601.06768 [hep-th].

[42] J. Maldacena and D. Stanford, "Remarks on the Sachdev-Ye-Kitaev model," *Phys. Rev.* **D94** no. 10, (2016) 106002, arXiv:1604.07818 [hep-th].

[43] R. Jackiw, "Lower Dimensional Gravity," *Nucl. Phys.* **B252** (1985) 343–356.

[44] C. Teitelboim, "Gravitation and Hamiltonian Structure in Two Space-Time Dimensions," *Phys. Lett.* **126B** (1983) 41–45.

[45] A. Almheiri and J. Polchinski, "Models of AdS_2 backreaction and holography," *JHEP* **11** (2015) 014, arXiv:1402.6334 [hep-th].

[46] K. Jensen, "Chaos in AdS_2 Holography," *Phys. Rev. Lett.* **117** no. 11, (2016) 111601, arXiv:1605.06098 [hep-th].

[47] J. Maldacena, D. Stanford, and Z. Yang, "Conformal symmetry and its breaking in two dimensional Nearly Anti-de-Sitter space," *PTEP* **2016** no. 12, (2016) 12C104, arXiv:1606.01857 [hep-th].

[48] J. Engelsoy, T. G. Mertens, and H. Verlinde, "An investigation of AdS_2 backreaction and holography," *JHEP* **07** (2016) 139, arXiv:1606.03438 [hep-th].

[49] J. Preskill, P. Schwarz, A. D. Shapere, S. Trivedi, and F. Wilczek, "Limitations on the statistical description of black holes," *Mod. Phys. Lett.* **A6** (1991) 2353–2362.

[50] D. J. Gross and V. Rosenhaus, "All point correlation functions in SYK," *JHEP* **12** (2017) 148, arXiv:1710.08113 [hep-th].

[51] T. G. Mertens, G. J. Turiaci, and H. L. Verlinde, "Solving the Schwarzian via the Conformal Bootstrap," *JHEP* **08** (2017) 136, arXiv:1705.08408 [hep-th].

[52] H. T. Lam, T. G. Mertens, G. J. Turiaci, and H. Verlinde, "Shockwave S-matrix from Schwarzian Quantum Mechanics," arXiv:1804.09834 [hep-th].

[53] G. J. Turiaci and H. Verlinde, "Towards a 2d QFT Analog of the SYK Model," *JHEP* **10** (2017) 167, arXiv:1701.00528 [hep-th].

[54] G. J. Turiaci and H. Verlinde, "On CFT and Quantum Chaos," *JHEP* **12** (2016) 110, arXiv:1603.03020 [hep-th].

[55] G. T. Horowitz and N. Itzhaki, "Black holes, shock waves, and causality in the AdS / CFT correspondence," *JHEP* **02** (1999) 010, arXiv:hep-th/9901012 [hep-th].

[56] C. Cordova, J. Maldacena, and G. J. Turiaci, "Bounds on OPE Coefficients from Interference Effects in the Conformal Collider," *JHEP* **11** (2017) 032, arXiv:1710.03199 [hep-th].

[57] G. J. Turiaci and M. Zaldarriaga, "Non-Gaussianities in Dissipative EFT of Inflation Coupled to a Fluid," arXiv:1310.4531 [gr-qc].

[58] F. C. Lombardo, F. D. Mazzitelli, A. E. R. Lopez, and G. J. Turiaci, "Nonequilibrium Lifshitz theory as a steady state of a full dynamical quantum system," *Phys. Rev.* **D94** no. 2, (2016) 025029, arXiv:1509.07459 [quant-ph].

[59] A. M. Levy and G. J. Turiaci, "Warm Ekpyrosis," *Phys. Rev.* **D94** no. 8, (2016) 083514, arXiv:1603.06608 [gr-qc].

[60] A. Lewkowycz, G. J. Turiaci, and H. Verlinde, "A CFT Perspective on Gravitational Dressing and Bulk Locality," *JHEP* **01** (2017) 004, arXiv:1608.08977 [hep-th].

[61] B. Le Floch and G. J. Turiaci, "AGT/$\mathbb{Z}_2$," *JHEP* **12** (2017) 099, arXiv:1708.04631 [hep-th].

[62] J. Polchinski, "Chaos in the black hole S-matrix," arXiv:1505.08108 [hep-th].

[63] A. Jevicki, K. Suzuki, and J. Yoon, "Bi-Local Holography in the SYK Model," *JHEP* **07** (2016) 007, arXiv:1603.06246 [hep-th].

[64] A. Jevicki and K. Suzuki, "Bi-Local Holography in the SYK Model: Perturbations," *JHEP* **11** (2016) 046, arXiv:1608.07567 [hep-th].

[65] E. Witten, "An SYK-Like Model Without Disorder," arXiv:1610.09758 [hep-th].

[66] M. Cvetic and I. Papadimitriou, "AdS_2 holographic dictionary," *JHEP* **12** (2016) 008, arXiv:1608.07018 [hep-th]. [Erratum: JHEP01,120(2017)].

[67] A. A. Kirillov, "Orbits of the group of diffeomorphisms of a circle and local Lie superalgebras," *Funktsional. Anal. i Prilozhen.* **15** (1981) .

[68] G. Segal, "Unitarity Representations of Some Infinite Dimensional Groups," *Commun. Math. Phys.* **80** (1981) 301–342.

[69] E. Witten, "Coadjoint Orbits of the Virasoro Group," *Commun. Math. Phys.* **114** (1988) 1.

[70] A. Alekseev and S. L. Shatashvili, "From geometric quantization to conformal field theory," *Commun. Math. Phys.* **128** (1990) 197–212. [,22(1990)].

[71] D. Bagrets, A. Altland, and A. Kamenev, "Sachdev-Ye-Kitaev model as Liouville quantum mechanics," *Nucl. Phys.* **B911** (2016) 191–205, arXiv:1607.00694 [cond-mat.str-el].

[72] D. Bagrets, A. Altland, and A. Kamenev, "Power-law out of time order correlation functions in the SYK model," *Nucl. Phys.* **B921** (2017) 727–752, arXiv:1702.08902 [cond-mat.str-el].

[73] D. Stanford and E. Witten, "Fermionic Localization of the Schwarzian Theory," *JHEP* **10** (2017) 008, arXiv:1703.04612 [hep-th].

[74] S. Jackson, L. McGough, and H. Verlinde, "Conformal Bootstrap, Universality and Gravitational Scattering," *Nucl. Phys.* **B901** (2015) 382–429, arXiv:1412.5205 [hep-th].

[75] B. Ponsot and J. Teschner, "Liouville bootstrap via harmonic analysis on a noncompact quantum group," arXiv:hep-th/9911110 [hep-th].

[76] J. Teschner, "Liouville theory revisited," *Class. Quant. Grav.* **18** (2001) R153–R222, arXiv:hep-th/0104158 [hep-th].

[77] J. Teschner and G. Vartanov, "6j symbols for the modular double, quantum hyperbolic geometry, and supersymmetric gauge theories," *Lett. Math. Phys.* **104** (2014) 527–551, arXiv:1202.4698 [hep-th].

[78] W. Groenevelt, "The Wilson function transform," *Int. Math. Res. Not.* **52** (2003) 2779–2817.

[79] W. Groenevelt, "Wilson function transforms related to Racah coefficients," *Acta Appl. Math. 91* **2** (2006) 133–191.

[80] A. Kitaev, "Talk given IAS chaos workshop," 2016.

[81] A. Comtet and P. J. Houston, "Effective Action on the Hyperbolic Plane in a Constant External Field," *J. Math. Phys.* **26** (1985) 185.

[82] G. Mandal, P. Nayak, and S. R. Wadia, "Coadjoint orbit action of Virasoro group and two-dimensional quantum gravity dual to SYK/tensor models," *JHEP* **11** (2017) 046, arXiv:1702.04266 [hep-th].

[83] J. J. Duistermaat and G. J. Heckman, "On the Variation in the cohomology of the symplectic form of the reduced phase space," *Invent. Math.* **69** (1982) 259–268.

[84] J. S. Cotler, G. Gur-Ari, M. Hanada, J. Polchinski, P. Saad, S. H. Shenker, D. Stanford, A. Streicher, and M. Tezuka, "Black Holes and Random Matrices," *JHEP* **05** (2017) 118, arXiv:1611.04650 [hep-th].

[85] L. McGough and H. Verlinde, "Bekenstein-Hawking Entropy as Topological Entanglement Entropy," *JHEP* **11** (2013) 208, arXiv:1308.2342 [hep-th].

[86] J. L. Cardy, "Boundary Conditions, Fusion Rules and the Verlinde Formula," *Nucl. Phys.* **B324** (1989) 581–596.

[87] V. Fateev, A. B. Zamolodchikov, and A. B. Zamolodchikov, "Boundary Liouville field theory. 1. Boundary state and boundary two point function," arXiv:hep-th/0001012 [hep-th].

[88] A. B. Zamolodchikov and A. B. Zamolodchikov, "Liouville field theory on a pseudosphere," arXiv:hep-th/0101152 [hep-th].

[89] S. Gukov and E. Witten, "Branes and Quantization," *Adv. Theor. Math. Phys.* **13** no. 5, (2009) 1445–1518, arXiv:0809.0305 [hep-th].

[90] B. Czech, L. Lamprou, S. McCandlish, and J. Sully, "Integral Geometry and Holography," *JHEP* **10** (2015) 175, arXiv:1505.05515 [hep-th].

[91] B. Czech, L. Lamprou, S. McCandlish, B. Mosk, and J. Sully, "A Stereoscopic Look into the Bulk," *JHEP* **07** (2016) 129, arXiv:1604.03110 [hep-th].

[92] H. Dorn and G. Jorjadze, "Boundary Liouville theory: Hamiltonian description and quantization," *SIGMA* **3** (2007) 012, arXiv:hep-th/0610197 [hep-th].

[93] J. Balog, L. Feher, and L. Palla, "Coadjoint orbits of the Virasoro algebra and the global Liouville equation," *Int. J. Mod. Phys.* **A13** (1998) 315–362, arXiv:hep-th/9703045 [hep-th].

[94] W. Fu, D. Gaiotto, J. Maldacena, and S. Sachdev, "Supersymmetric Sachdev-Ye-Kitaev models," *Phys. Rev.* **D95** no. 2, (2017) 026009, arXiv:1610.08917 [hep-th]. [Addendum: Phys. Rev.D95,no.6,069904(2017)].

[95] S. Forste and I. Golla, "Nearly AdS_2 sugra and the super-Schwarzian," *Phys. Lett.* **B771** (2017) 157–161, arXiv:1703.10969 [hep-th].

[96] D. Friedan, "NOTES ON STRING THEORY AND TWO-DIMENSIONAL CONFORMAL FIELD THEORY,".

[97] J. D. Cohn, "N=2 SUPERRIEMANN SURFACES," *Nucl. Phys.* **B284** (1987) 349–364.

[98] T. Fukuda and K. Hosomichi, "Super Liouville theory with boundary," *Nucl. Phys.* **B635** (2002) 215–254, arXiv:hep-th/0202032 [hep-th].

[99] C. Ahn, C. Rim, and M. Stanishkov, "Exact one point function of N=1 superLiouville theory with boundary," *Nucl. Phys.* **B636** (2002) 497–513, arXiv:hep-th/0202043 [hep-th].

[100] L. Hadasz, M. Pawelkiewicz, and V. Schomerus, "Self-dual Continuous Series of Representations for $U_q(sl(2))$ and $U_q(osp(1|2))$," *JHEP* **10** (2014) 91, arXiv:1305.4596 [hep-th].

[101] M. Pawelkiewicz, V. Schomerus, and P. Suchanek, "The universal Racah-Wigner symbol for $U_q(osp(1—2))$," *JHEP* **04** (2014) 079, arXiv:1307.6866 [hep-th].

[102] T. Eguchi and Y. Sugawara, "Modular bootstrap for boundary N = 2 Liouville theory," *JHEP* **01** (2004) 025, arXiv:hep-th/0311141 [hep-th].

[103] C. Ahn, M. Stanishkov, and M. Yamamoto, "One point functions of N = 2 superLiouville theory with boundary," *Nucl. Phys.* **B683** (2004) 177–195, arXiv:hep-th/0311169 [hep-th].

[104] H. Dorn and H. J. Otto, "Two and three point functions in Liouville theory," *Nucl. Phys.* **B429** (1994) 375–388, arXiv:hep-th/9403141 [hep-th].

[105] A. B. Zamolodchikov and A. B. Zamolodchikov, "Structure constants and conformal bootstrap in Liouville field theory," *Nucl. Phys.* **B477** (1996) 577–605, arXiv:hep-th/9506136 [hep-th].

[106] P. Gao, D. L. Jafferis, and A. Wall, "Traversable Wormholes via a Double Trace Deformation," *JHEP* **12** (2017) 151, arXiv:1608.05687 [hep-th].

[107] J. Maldacena, D. Stanford, and Z. Yang, "Diving into traversable wormholes," *Fortsch. Phys.* **65** no. 5, (2017) 1700034, arXiv:1704.05333 [hep-th].

[108] M. Hogervorst and B. C. van Rees, "Crossing symmetry in alpha space," *JHEP* **11** (2017) 193, arXiv:1702.08471 [hep-th].

[109] M. Hogervorst, "Crossing Kernels for Boundary and Crosscap CFTs," arXiv:1703.08159 [hep-th].

[110] H. Chen, A. L. Fitzpatrick, J. Kaplan, D. Li, and J. Wang, "Degenerate Operators and the $1/c$ Expansion: Lorentzian Resummations, High Order Computations, and Super-Virasoro Blocks," *JHEP* **03** (2017) 167, arXiv:1606.02659 [hep-th].

[111] Y. Gu, A. Lucas, and X.-L. Qi, "Spread of entanglement in a Sachdev-Ye-Kitaev chain," *JHEP* **09** (2017) 120, arXiv:1708.00871 [hep-th].

[112] I. Kourkoulou and J. Maldacena, "Pure states in the SYK model and nearly-AdS_2 gravity," arXiv:1707.02325 [hep-th].

[113] B. Le Floch, "S-duality wall of SQCD from Toda braiding," arXiv:1512.09128 [hep-th].

[114] S. Ribault, "Boundary three-point function on AdS2 D-branes," *JHEP* **01** (2008) 004, arXiv:0708.3028 [hep-th].

[115] D. J. Gross and V. Rosenhaus, "A Generalization of Sachdev-Ye-Kitaev," *JHEP* **02** (2017) 093, arXiv:1610.01569 [hep-th].

[116] M. Berkooz, P. Narayan, M. Rozali, and J. Simon, "Higher Dimensional Generalizations of the SYK Model," *JHEP* **01** (2017) 138, arXiv:1610.02422 [hep-th].

[117] Y. Gu, X.-L. Qi, and D. Stanford, "Local criticality, diffusion and chaos in generalized Sachdev-Ye-Kitaev models," *JHEP* **05** (2017) 125, arXiv:1609.07832 [hep-th].

[118] M. B. Green and J. H. Schwarz, "Covariant description of superstrings," *Physics Letters B* **136** no. 5, (1984) 367 – 370. http://www.sciencedirect.com/science/article/pii/0370269384920215.

[119] A. Quelle, C. M. Smith, T. Kvorning, and T. H. Hansson, "Edge majoranas on locally flat surfaces: The cone and the möbius band," *Phys. Rev. B* **94** (Sep, 2016) 125137. https://link.aps.org/doi/10.1103/PhysRevB.94.125137.

[120] V. G. Knizhnik, A. M. Polyakov, and A. B. Zamolodchikov, "Fractal Structure of 2D Quantum Gravity," *Mod. Phys. Lett.* **A3** (1988) 819.

[121] R. Dijkgraaf, *A geometrical approach to two-dimensional conformal field theory*. PhD thesis, Utrecht, 1989.

[122] H. L. Verlinde, "Conformal Field Theory, 2-D Quantum Gravity and Quantization of Teichmuller Space," *Nucl. Phys.* **B337** (1990) 652–680.

[123] E. Witten, "On Holomorphic factorization of WZW and coset models," *Commun. Math. Phys.* **144** (1992) 189–212.

[124] M. Blau and G. Thompson, "Derivation of the Verlinde formula from Chern-Simons theory and the G/G model," *Nucl. Phys.* **B408** (1993) 345–390, arXiv:hep-th/9305010 [hep-th].

[125] M. Fannes, B. Nachtergaele, and R. F. Werner, "FINITELY CORRELATED STATES ON QUANTUM SPIN CHAINS," *Commun. Math. Phys.* **144** (1992) 443–490.

[126] D. Perez-Garcia, F. Verstraete, M. M. Wolf, and J. I. Cirac, "Matrix Product State Representations," *eprint arXiv:quant-ph/0608197* (Aug., 2006) , quant-ph/0608197.

[127] S. Sachdev, "Bekenstein-Hawking Entropy and Strange Metals," *Phys. Rev.* **X5** no. 4, (2015) 041025, arXiv:1506.05111 [hep-th].

[128] S. Dubovsky, R. Flauger, and V. Gorbenko, "Solving the Simplest Theory of Quantum Gravity," *JHEP* **09** (2012) 133, arXiv:1205.6805 [hep-th].

[129] F. A. Smirnov and A. B. Zamolodchikov, "On space of integrable quantum field theories," *Nucl. Phys.* **B915** (2017) 363–383, arXiv:1608.05499 [hep-th].

[130] A. Cavaglia, S. Negro, I. M. Szecsenyi, and R. Tateo, "$T\bar{T}$-deformed 2D Quantum Field Theories," *JHEP* **10** (2016) 112, arXiv:1608.05534 [hep-th].

[131] L. McGough, M. Mezei, and H. Verlinde, "Moving the CFT into the bulk with $T\bar{T}$," arXiv:1611.03470 [hep-th].

[132] L. Freidel, "Reconstructing AdS/CFT," arXiv:0804.0632 [hep-th].

[133] G. Gur-Ari, M. Hanada, and S. H. Shenker, "Chaos in Classical D0-Brane Mechanics," *JHEP* **02** (2016) 091, arXiv:1512.00019 [hep-th].

[134] E. Perlmutter, "Bounding the Space of Holographic CFTs with Chaos," *JHEP* **10** (2016) 069, arXiv:1602.08272 [hep-th].

[135] P. Caputa, T. Numasawa, and A. Veliz-Osorio, "Out-of-time-ordered correlators and purity in rational conformal field theories," *PTEP* **2016** no. 11, (2016) 113B06, arXiv:1602.06542 [hep-th].

[136] Y. Gu and X.-L. Qi, "Fractional Statistics and the Butterfly Effect," *JHEP* **08** (2016) 129, arXiv:1602.06543 [hep-th].

[137] L. D. Faddeev and A. Yu. Volkov, "Hirota equation as an example of integrable symplectic map," *Lett. Math. Phys.* **32** (1994) 125–136, arXiv:hep-th/9405087 [hep-th].

[138] L. D. Faddeev, R. M. Kashaev, and A. Yu. Volkov, "Strongly coupled quantum discrete Liouville theory. 1. Algebraic approach and duality," *Commun. Math. Phys.* **219** (2001) 199–219, arXiv:hep-th/0006156 [hep-th].

[139] L. D. Faddeev and R. M. Kashaev, "Strongly coupled quantum discrete Liouville theory. 2. Geometric interpretation of the evolution operator," *J. Phys.* **A35** (2002) 4043–4048, arXiv:hep-th/0201049 [hep-th].

[140] L. D. Faddeev and L. A. Takhtajan, "Liouville model on the lattice," *Lect. Notes Phys.* **246** (1986) 166–179.

[141] A. Bytsko and J. Teschner, "The Integrable structure of nonrational conformal field theory," *Adv. Theor. Math. Phys.* **17** no. 4, (2013) 701–740, arXiv:0902.4825 [hep-th].

[142] D. Birmingham, I. Sachs, and S. N. Solodukhin, "Conformal field theory interpretation of black hole quasinormal modes," *Phys. Rev. Lett.* **88** (2002) 151301, arXiv:hep-th/0112055 [hep-th].

[143] D. Ruelle, "Resonances of Chaotic Dynamical Systems," *Phys. Rev. Lett.* **56** (1986) 405.

[144] A. Peres, "Ergodicity and mixing in quantum theory. I," *Phys. Rev.* **A30** (1984) 504–508.

[145] M. Feingold and A. Peres, "Distribution of Matrix Elements of Chaotic Systems," *Phys. Rev.* **A34** (1986) 591–595.

[146] J. M. Deutsch, "Quantum statistical mechanics in a closed system," *Phys. Rev.* **A43** (1991) 2046.

[147] M. Srednicki, "Chaos and quantum thermalization," *Phys. Rev.* **E50** (1994) 888.

[148] M. Srednicki, "The approach to thermal equilibrium in quantized chaotic systems," *J. Phys.* **A32** (1999) 1163.

[149] A. L. Fitzpatrick, J. Kaplan, and M. T. Walters, "Universality of Long-Distance AdS Physics from the CFT Bootstrap," *JHEP* **08** (2014) 145, arXiv:1403.6829 [hep-th].

[150] A. L. Fitzpatrick, J. Kaplan, and M. T. Walters, "Virasoro Conformal Blocks and Thermality from Classical Background Fields," *JHEP* **11** (2015) 200, arXiv:1501.05315 [hep-th].

[151] J. A. Teschner, *On quantization of Liouville theory and related conformal field theories*. PhD thesis, Hamburg U., 1995. http://lss.fnal.gov/archive/other1/desy-95-118.pdf.

[152] J.-L. Gervais and A. Neveu, "The Dual String Spectrum in Polyakov's Quantization. 1.," *Nucl. Phys.* **B199** (1982) 59.

[153] J.-L. Gervais and A. Neveu, "Dual String Spectrum in Polyakov's Quantization. 2. Mode Separation," *Nucl. Phys.* **B209** (1982) 125–145.

[154] J.-L. Gervais and A. Neveu, "New Quantum Treatment of Liouville Field Theory," *Nucl. Phys.* **B224** (1983) 329–348.

[155] K. Krasnov and S. N. Solodukhin, "Effective stringy description of Schwarzschild black holes," *Adv. Theor. Math. Phys.* **8** no. 3, (2004) 421–460, arXiv:hep-th/0403046 [hep-th].

[156] M. Rigol, V. Dunjko, and M. Olshanii, "Thermalization and its mechanism for generic isolated quantum systems," *Nature* **A52** (2008) 854–858.

[157] B. Czech, L. Lamprou, S. McCandlish, and J. Sully, "Tensor Networks from Kinematic Space," *JHEP* **07** (2016) 100, arXiv:1512.01548 [hep-th].

[158] D. Harlow, J. Maltz, and E. Witten, "Analytic Continuation of Liouville Theory," *JHEP* **12** (2011) 071, arXiv:1108.4417 [hep-th].

[159] X. O. Camanho, J. D. Edelstein, J. Maldacena, and A. Zhiboedov, "Causality Constraints on Corrections to the Graviton Three-Point Coupling," arXiv:1407.5597 [hep-th].

[160] D. M. Hofman and J. Maldacena, "Conformal collider physics: Energy and charge correlations," *JHEP* **05** (2008) 012, arXiv:0803.1467 [hep-th].

[161] J. de Boer, M. Kulaxizi, and A. Parnachev, "AdS(7)/CFT(6), Gauss-Bonnet Gravity, and Viscosity Bound," *JHEP* **03** (2010) 087, arXiv:0910.5347 [hep-th].

[162] A. Buchel, J. Escobedo, R. C. Myers, M. F. Paulos, A. Sinha, and M. Smolkin, "Holographic GB gravity in arbitrary dimensions," *JHEP* **03** (2010) 111, arXiv:0911.4257 [hep-th].

[163] T. Faulkner, R. G. Leigh, O. Parrikar, and H. Wang, "Modular Hamiltonians for Deformed Half-Spaces and the Averaged Null Energy Condition," *JHEP* **09** (2016) 038, arXiv:1605.08072 [hep-th].

[164] T. Hartman, S. Kundu, and A. Tajdini, "Averaged Null Energy Condition from Causality," *JHEP* **07** (2017) 066, arXiv:1610.05308 [hep-th].

[165] T. Hartman, S. Jain, and S. Kundu, "A New Spin on Causality Constraints," *JHEP* **10** (2016) 141, arXiv:1601.07904 [hep-th].

[166] D. M. Hofman, D. Li, D. Meltzer, D. Poland, and F. Rejon-Barrera, "A Proof of the Conformal Collider Bounds," *JHEP* **06** (2016) 111, arXiv:1603.03771 [hep-th].

[167] S. D. Chowdhury, J. R. David, and S. Prakash, "Constraints on parity violating conformal field theories in $d = 3$," arXiv:1707.03007 [hep-th].

[168] A. Dymarsky, F. Kos, P. Kravchuk, D. Poland, and D. Simmons-Duffin, "The 3d Stress-Tensor Bootstrap," arXiv:1708.05718 [hep-th].

[169] R. W. Fuller and J. A. Wheeler, "Causality and Multiply Connected Space-Time," *Phys. Rev.* **128** (1962) 919–929.

[170] H. Epstein, V. Glaser, and A. Jaffe, "Nonpositivity of energy density in Quantized field theories," *Nuovo Cim.* **36** (1965) 1016.

[171] J. L. Friedman, K. Schleich, and D. M. Witt, "Topological censorship," *Phys. Rev. Lett.* **71** (1993) 1486–1489, arXiv:gr-qc/9305017 [gr-qc]. [Erratum: Phys. Rev. Lett.75,1872(1995)].

[172] S. Balakrishnan, T. Faulkner, Z. U. Khandker, and H. Wang, "A General Proof of the Quantum Null Energy Condition," arXiv:1706.09432 [hep-th].

[173] Z. Komargodski, M. Kulaxizi, A. Parnachev, and A. Zhiboedov, "Conformal Field Theories and Deep Inelastic Scattering," *Phys. Rev.* **D95** no. 6, (2017) 065011, arXiv:1601.05453 [hep-th].

[174] H. Osborn and A. C. Petkou, "Implications of conformal invariance in field theories for general dimensions," *Annals Phys.* **231** (1994) 311–362, arXiv:hep-th/9307010 [hep-th].

[175] A. Zhiboedov, "On Conformal Field Theories With Extremal a/c Values," *JHEP* **04** (2014) 038, arXiv:1304.6075 [hep-th].

[176] M. S. Costa, J. Penedones, D. Poland, and S. Rychkov, "Spinning Conformal Correlators," *JHEP* **11** (2011) 071, arXiv:1107.3554 [hep-th].

[177] D. Pappadopulo, S. Rychkov, J. Espin, and R. Rattazzi, "OPE Convergence in Conformal Field Theory," *Phys. Rev.* **D86** (2012) 105043, arXiv:1208.6449 [hep-th].

[178] S. Giombi, S. Prakash, and X. Yin, "A Note on CFT Correlators in Three Dimensions," *JHEP* **07** (2013) 105, arXiv:1104.4317 [hep-th].

[179] J. Maldacena and A. Zhiboedov, "Constraining conformal field theories with a slightly broken higher spin symmetry," *Class. Quant. Grav.* **30** (2013) 104003, arXiv:1204.3882 [hep-th].

[180] E. Sezgin, E. D. Skvortsov, and Y. Zhu, "Chern-Simons Matter Theories and Higher Spin Gravity," *JHEP* **07** (2017) 133, arXiv:1705.03197 [hep-th].

[181] S. El-Showk, M. F. Paulos, D. Poland, S. Rychkov, D. Simmons-Duffin, and A. Vichi, "Solving the 3d Ising Model with the Conformal Bootstrap II. c-Minimization and Precise Critical Exponents," *J. Stat. Phys.* **157** (2014) 869, arXiv:1403.4545 [hep-th].

[182] J. Erdmenger, "Gravitational axial anomaly for four-dimensional conformal field theories," *Nucl. Phys.* **B562** (1999) 315–329, arXiv:hep-th/9905176 [hep-th].

[183] R. Delbourgo and A. Salam, "The gravitational correction to pcac," *Phys. Lett.* **40B** (1972) 381–382.

[184] T. Eguchi and P. G. O. Freund, "Quantum Gravity and World Topology," *Phys. Rev. Lett.* **37** (1976) 1251.

[185] L. Alvarez-Gaume and E. Witten, "Gravitational Anomalies," *Nucl. Phys.* **B234** (1984) 269.

[186] H. Osborn, "N=1 superconformal symmetry in four-dimensional quantum field theory," *Annals Phys.* **272** (1999) 243–294, arXiv:hep-th/9808041 [hep-th].

[187] D. T. Son and P. Surowka, "Hydrodynamics with Triangle Anomalies," *Phys. Rev. Lett.* **103** (2009) 191601, arXiv:0906.5044 [hep-th].

[188] A. Vilenkin, "Parity Nonconservation and Rotating Black Holes," *Phys. Rev. Lett.* **41** (1978) 1575–1577.

[189] K. Landsteiner, E. Megias, and F. Pena-Benitez, "Gravitational Anomaly and Transport," *Phys. Rev. Lett.* **107** (2011) 021601, arXiv:1103.5006 [hep-ph].

[190] K. Landsteiner, E. Lopez, and G. Milans del Bosch, "Quenching the CME via the gravitational anomaly and holography," arXiv:1709.08384 [hep-th].

[191] J. Gooth et al., arXiv:1703.10682 [cond-mat.mtrl-sci].

[192] A. Bhattacharyya, L. Cheng, and L.-Y. Hung, "Relative Entropy, Mixed Gauge-Gravitational Anomaly and Causality," *JHEP* **07** (2016) 121, arXiv:1605.02553 [hep-th].

[193] J. M. Maldacena and G. L. Pimentel, "On graviton non-Gaussianities during inflation," *JHEP* **09** (2011) 045, arXiv:1104.2846 [hep-th].

[194] A. Lue, L.-M. Wang, and M. Kamionkowski, "Cosmological signature of new parity violating interactions," *Phys. Rev. Lett.* **83** (1999) 1506–1509, arXiv:astro-ph/9812088 [astro-ph].

[195] S. Alexander and J. Martin, "Birefringent gravitational waves and the consistency check of inflation," *Phys. Rev.* **D71** (2005) 063526, arXiv:hep-th/0410230 [hep-th].

[196] N. Arkani-Hamed and J. Maldacena, "Cosmological Collider Physics," arXiv:1503.08043 [hep-th].

[197] S. Saito, K. Ichiki, and A. Taruya, "Probing polarization states of primordial gravitational waves with CMB anisotropies," *JCAP* **0709** (2007) 002, arXiv:0705.3701 [astro-ph].

[198] D. Baumann, H. Lee, and G. L. Pimentel, "High-Scale Inflation and the Tensor Tilt," *JHEP* **01** (2016) 101, arXiv:1507.07250 [hep-th].

[199] J. M. Maldacena, "Non-Gaussian features of primordial fluctuations in single field inflationary models," *JHEP* **05** (2003) 013, arXiv:astro-ph/0210603 [astro-ph].

[200] N. Bartolo and G. Orlando, "Parity breaking signatures from a Chern-Simons coupling during inflation: the case of non-Gaussian gravitational waves," *JCAP* **1707** no. 07, (2017) 034, arXiv:1706.04627 [astro-ph.CO].

[201] J. Soda, H. Kodama, and M. Nozawa, "Parity Violation in Graviton Non-gaussianity," *JHEP* **08** (2011) 067, arXiv:1106.3228 [hep-th].

[202] P. Creminelli and M. Zaldarriaga, "Single field consistency relation for the 3-point function," *JCAP* **0410** (2004) 006, arXiv:astro-ph/0407059 [astro-ph].